The Translocation Of CLIC5A To Membranes As A Peripheral Protein

by

Jong Suck Kim

A thesis submitted in partial fulfillment of the requirements for the degree of

Master of Science

Department of Medicine
University of Alberta

Abstract

Chloride intracellular channel (CLIC) proteins comprise six members CLIC1–CLIC6 in mammals and mediate functions not fully known. Their founding member was isolated from bovine kidney using the chloride channel inhibitor indanyloxyacetic acid-94, so CLICs were assumed to be typical anion channels. However, CLIC proteins possess several properties discordant with classical channels, and there are doubts regarding their capacity to form the integral transmembrane (TM) architecture of α- and β-type ion channels. Chief among such properties are their structural dimorphism. CLICs assume multiple conformational folds, and the transitions between them accompany their translocation to their diverse subcellular locales. Though several X-ray structures of their soluble form have been solved, the signaling pathways which mediate their transition in cells have not yet been identified, nor has any membrane-associated structure been solved.

In comparison to the diverse expression of most CLICs, CLIC5A is highly enriched in glomerular tissue within podocytes and endothelial cells and is frequently found in actin-rich projections of the plasma membrane (PM) in a highly polarized distribution. At the apical PM, CLIC5A is localized in clusters containing phosphatidylinositol-4,5-bisphosphate, where it promotes PM–actin cytoskeleton linkages by stimulating the activation of the cross-linking ezrin-radixin-moesin (ERM) proteins, in part by Rac1-induced activation of phosphoinositide kinases. Given that these signaling events are centralized at and near the PM, it is important to discern the cellular processes translocating CLIC5A from the cytosol to this site.

The primary focus of this thesis is to investigate the translocation process of CLIC5A using structural and cellular approaches, and to challenge widely-held notions that CLICs form

TM channels. NMR spectra of truncated *N*-terminal CLIC5A mutants containing the putative transmembrane domain were obtained to reveal that CLIC5A adopts multiple conformations in solution. Next, CLIC5A was assayed in transfected COS-7 cells under membrane permeabilizing and intact conditions, which revealed that this protein was detected only in the former condition, strongly suggesting CLIC5A is confined in the intracellular space with no appreciable extracellular domains. Furthermore, subcellular fractions extracted by differential detergent fractionation revealed that overexpressed CLIC1, CLIC4, and CLIC5A were predominantly cytosolic and not detectable in membrane fractions. However, Calyculin A-induced phosphatase inhibition significantly increased the retrieval of CLIC4, CLIC5A, and to a much lesser extent CLIC1, in membrane fractions. For CLIC5A, the phosphorylation-driven translocation to membranes was sensitive to Staurosporine, suggesting a protein kinase C (PKC) as a likely candidate mediating this process. Multifactorial prediction analyses reveal that CLIC5A is likely to be phosphorylated at two *C*-terminal Thr residues during this process.

Overall, this study demonstrates for the first time that CLIC4 and CLIC5A are translocated to membranes in a phosphorylation-driven process which for CLIC5A is mediated by a PKC. Further, our results corroborate earlier claims that CLIC5A does not form an integral TM protein and thus unlikely to function as a classical ion channel.

Dedication

"You keep it going, man! You keep those books rolling! You pick up those books you're going to read and not remember, and you roll, man!

You get that Associate's degree, okay? Then you get your Bachelor's. Then you get your Master's. Then you get your Master's Master's. Then you get your Doctorate; you go, man!

Then when everybody says, "quit!", You show them those degrees, man. When everybody says, "hey, you're not working, you're not making any money!"

You can say, "look at my degrees, and you look at my life! Yeah, I'm 52, so what? Hate all you want, but I'm smart. I'm so smart, and I'm in school. And these guys are out here making money all these ways, and I'm spending mine to be smart!

You know why? Because when I die, buddy, you know what's going to keep me warm? That's right—those degrees."

— *School Spirit (Skit 2)*,
from *The College Dropout* by Kanye West (2004)

Portions of this Thesis were written in the beautiful mountains of Banff, the vibrant metropolis of Toronto, and the pleasant coastline of Vancouver. Calgary and Edmonton are included in this list of places too.

Acknowledgments

First and foremost, I am indebted to both my supervisors, Dr Barbara Ballermann and Dr Peter Hwang, for their guidance and mentorship these past two years. Indeed, a Master's degree is physically, mentally, and emotionally challenging, but the support I received from both supervisors in the laboratory and beyond was essential to help me persevere. Both Dr Ballermann and Dr Hwang displayed leadership qualities above-and-beyond what is expected of a supervisor, which will undoubtedly raise my expectations of what I think leadership defines from now on. By respecting my intelligence in spite of my inexperience and validating the importance of my ideas, Dr Ballermann cultivated an environment essential for me to learn and develop as a scientist in-training. I am also extremely grateful for my supervisory committee members, Dr Michael Overduin and Dr Todd Alexander, for their guidance during my project.

The work presented in this thesis would not have been made possible without the training and supervision provided by Dr Laiji Li, the Lab Manager in the Ballermann Lab, and Philip Liu, the Laboratory Technician in the Hwang Lab. Dr Li generated the newly cloned FLAG-CLIC5A and most of the other plasmids used in this study. Philip Liu isolated a triple-labeled CLIC5A[1-99] construct, used in some of our NMR analyses. I also pass on my heartfelt gratitude to my colleagues, who together celebrated my victories and encouraged me in my downfalls: Dr Salah Aburahess, Mizan Rahman, and Dr Cindy Wang in the Ballermann lab, and Zabed Mahmud and Danmaliki Ibrahim in the Hwang lab. The companionship provided by my colleagues will be missed.

I would also like to thank my dearest appa 아빠 and umma 엄마 for the sacrifices they have made and continue to make for their children, and for encouraging me since I was a young boy to realize my ambitions and most importantly remain humble in my endeavours.

Last, but not least, I thank the Natural Sciences and Engineering Council of Canada (NSERC), as well as the Heart & Stroke Foundation of Canada, as the funding agencies supporting my project. Without the contribution from taxpayers, charities, and donors, my project and countless others undertaking breakthrough research would not be made possible.

Table of Contents

List of Tables

List of Figures

Abbreviations Used

A_{280}	Absorbance at 280 nm
ABC	ATP-binding cassette
amp	Ampicillin
ATPase	Adenosine triphosphatase
BSA	Bovine serum albumin
C-ERMAD	*C*-terminal ERM domain
cAMP	Cyclic adenosine monophosphate
CD	Circular dichroism
cDNA	Complementary DNA
CFTR	Cystic fibrosis transmembrane conductance regulator
ClC	Chloride Channel
ClCA	Calcium-activated chloride channel
CLIC	Chloride intracellular channel
DMEM	Gibco™ Dulbecco's Modified Eagle Medium
DOCA	Deoxycorticosterone acetate
DOPC	Dioleylphosphatidylcholine
DOPI(4,5)P_2	1,2-dioctanoyl-*sn*-glycero-3-phospho-(1'-myoinositol-4',5'-bisphosphate)
eDPC	Dodecylphosphocholine
DSS	4,4-dimethyl-4-silapentane-1-sulfonic acid
EPR	Electron paramagnetic resonance
ER	Endoplasmic reticulum
ERM	Ezrin-radixin-moesin
FBS	Fetal bovine serum
F-actin	Filamentous actin
FERM	Band 4.1-ezrin-radixin-moesin domain
FPLC	Fast protein liquid chromatography
FT	Flow-through
FRET	Fluorescence resonance energy transfer
GFP	Green fluorescent protein

GPCR	G-protein-coupled receptor
GPI	Glycosylphosphatidylinositol
GSH	Glutathione
GST	Glutathione-*S*-transferase
GTPase	Guanosine triphosphatase
HRP	Horseradish peroxidase
HSQC	Heteronuclear single quantum coherence
IAA-94	Indanyloxyacetic acid-94
IB	Immunoblot
IC_{50}	Half-maximal inhibitory concentration
IDP	Intrinsically-disordered protein
IF	Immunofluorescence
IPTG	Isopropyl β-D-1-thiogalactoyranoside
K_i	Inhibition constant
LB	Luria-Bertani
Lu-ECAM1	Lung-endothelial cell adhesion molecule 1
MAPK	Mitogen-activated protein kinase
MBP	Maltose-binding protein
MD	Molecular Dynamics
NCC27	Nuclear chloride channel-27 (CLIC1)
Ni^{2+}-NTA	Nickel nitriloacetic acid
NMR	Nuclear magnetic resonance
OD_{600}	Optical density at 600 nm
p-60	60-mm cell culture dish
p-100	100-mm cell culture dish
p-ERM	Phosphorylated ezrin-radixin-moesin
PC	Phosphatidylcholine
PBS	Phosphate-buffered saline
PDB ID	Protein Data Bank Identifier
PFP	Pore-forming protein
PH	Pleckstrin homology domain

$PI(3,4,5)P_3$	Phosphatidylinositol-3,4,5-triphosphate
$PI(4,5)P_2$	Phosphatidylinositol-4,5-bisphosphate
PI4P5K	Phosphatidylinositol-4-phosphate 5 kinase
PKA	Protein kinase A (cAMP-dependent protein kinase)
PKC	Protein kinase C
PLC	Phospholipase C
PM	Plasma membrane
POPC	Palmitoyloleoylphosphatidylcholine
POPE	Palmitoyloleoylphosphatidylethanolamine
PS	Phosphatidylserine
PTMD	Putative transmembrane domain
ROCK	Rho-associated kinase
ROS	Reactive oxygen species
SAGE	Serial analysis of gene expression
SDS	Sodium dodecyl sulfate
SDS-PAGE	Sodium dodecyl sulfate polyacrylamide gel electrophoresis
SRP	Signal recognition particle
TBS/T	TRIS-buffered saline with 1% TWEEN®
TC	Transporter Classification
TCL	Total cell lysate
TCEP	TRIS-2-carboxyethylphosphoine
TM	Transmembrane
TRP	Transient receptor potential
VDAC	Voltage-dependent anion channel
VGL	Voltage-gated-like

Symbols & Units Used

SI Prefixes:

kilo-	k-	10^{3}
milli-	m-	10^{-3}
micro-	μ-	10^{-6}
nano-	n-	10^{-9}
pico-	p-	10^{-12}

Units:

degrees Celsius	°C	**electric conductance**	$S = \Omega^{-1}$
second	sec	**molar mass**	g/mol
hour	hr	**molarity**	M = mol/L
gram	g	**Joule**	J
litre	L	**atomic mass unit**	Da = 1 g/mol
metre	m	**Angstrom**	Å = 10^{-10} m
moles	mol	**base pair**	bp

Standard Amino Acids:

Alanine	Ala	A
Cysteine	Cys	C
Aspartic acid	Asp	D
Glutamic acid	Glu	E
Phenylalanine	Phe	F
Glycine	Gly	G
Histidine	His	H
Isoleucine	Ile	I
Lysine	Lys	K
Leucine	Leu	L

Methionine	Met	M
Asparagine	Asn	N
Proline	Pro	P
Glutamine	Glu	Q
Arginine	Arg	R
Serine	Ser	S
Threonine	Thr	T
Valine	Val	V
Tryptophan	Trp	W
Tyrosine	Tyr	Y

Chapter 1: Introduction

1.1 Membrane Proteins

Beyond their roles in forming selective barriers and compartmentalization, biological membranes are, by their biochemical composition, dynamic organelles that mediate functions in signaling and energy transduction. The dynamic functions of biological membranes are conferred by their membrane proteins, which associate with them in various capacities. The earliest categorizations of membrane proteins broadly defined them as either intrinsic (integral) or extrinsic (peripheral) based on their mode of membrane association[1–5]. In these early definitions, integral membrane proteins were defined as permanent fixtures of the membrane continuum that penetrated bilayers through hydrophobic interactions, while peripheral membrane proteins temporarily associated to membranes by electrostatic forces[2,3]. In practice, this meant integral proteins were only retrievable in their native state with detergents, and largely partitioned into hydrophobic fractions during extraction. In contrast, peripheral proteins were defined as entities dissociable with mild treatments, such as salt or alkaline washes, and largely contained within aqueous fractions[1,3–7] (Table 1).

Table 1. Integral and peripheral proteins were defined by early operational definitions. Prior to the deeper molecular understanding and structural data obtained for membrane proteins, operational criteria were used to distinguish these proteins in the laboratory. [Reprinted with permission from Singer, S.J. 1974. The Molecular Organization of Membranes. *Annual Review of Biochemistry* 43:805-883. ©1974, Annual Reviews.]

Property	Peripheral membrane protein	Integral membrane protein
Requirements for dissociation from the membrane	Mild treatments: high ionic strength, metal ion chelating agents	Hydrophobic bond-breaking reagents: detergents, organic solvents, chaotropic agents
Association with lipids when solubilized	Usually soluble free of lipids	Usually associated with lipids when solubilized
Solubility after dissociation from membrane	Soluble and molecularly dispersed in neutral aqueous buffers	Usually insoluble or aggregated in neutral aqueous buffers

While such criteria remain practical today, the sheer diversity of membrane proteins has long warranted more precise definitions. For example, it is now recognized that many

integral proteins are routinely shuffled between different intracellular membranes[8,9], contradicting their designation as permanent fixtures of the membrane. Further still, peripheral proteins are now known to interact with membranes through forces other than electrostatic interactions, for instance hydrophobic interactions and covalent lipid modifications[10]. Due to the sheer diversity of membrane protein structures that have only recently begun to be unraveled, it has now become apparent that the distinction between integral and peripheral proteins do not define the method of attachment to membranes, but rather their relative strength of association[11]. Despite revising definitions, the dichotomy of integral and peripheral proteins largely remains useful today[12], and beyond semantics, the categorization of a membrane protein is essential to understanding its function.

The aim of the following chapter is to establish the physicochemical properties of lipid bilayers, followed by a discussion on how integral and peripheral membrane proteins associate within this continuum to establish the working definitions used in the explorations of this thesis.

1.1.1 Lipid Bilayers in Biological Membranes

1.1.1.1 Lipid Bilayers Are A Dynamic Heterogenous Continuum

The fluid mosaic model, which depicts cell membranes as a dynamic viscous lipid-protein mixture, has remained the dominant theory in delineating biological membranes for nearly half a century[1,12]. Within this framework, amphipathic phosopholipids are arranged in a bilayer to maximize thermodynamic stability by orienting their polar head groups to solvent and sequestering their non-polar acyl tails away from the aqueous surroundings[1,13,14].

Combined X-ray and neutron liquid-crystallography have determined with Angstrom-precision the thickness and atomic organization of fluid dioleoylphosphatidylcholine (DOPC) bilayers,[15–17] which serve as a good approximation to biological membranes since the lamellar phase behaviour of the DOPC lipid mimics the lamellar phase of biological membranes[18,19]. Due to the thermal motion contingent on bilayer fluidity, exact positions of a molecular unit cannot be calculated, so probability functions following a Gaussian distribution are reported instead[15–17], validated by molecular dynamics (MD) simulations[20]. Nevertheless, these probability distributions appeared to be contained within two discrete regions in the axis

normal to the bilayer. Bilayers are constructed with a 30 Å hydrocarbon core surrounded by a 15 Å interfacial region on either side[17]. A third region peripheral to the interfaces consisting of the water molecules hydrating the lipid headgroups are confined to a 'membrane network'[21]. Consequently, bilayers are more accurately viewed as a heterogenous dynamic continuum rather than an inert discrete hydrocarbon barrier[15,20–22].

The hydrocarbon core is composed primarily of fatty acyl chains and terminal methyl groups, with a molecular packing consistent with their corresponding liquid alkanes[16,20]. The hydrocarbon core is nearly, though not completely, devoid of water, and the represents a physicochemical barrier to hydrophilic and charged molecules[23]. In spite of dense packing, significant acyl tail-tail repulsions cause the core to be highly entropic and fluid, enabling bilayers to expand and contract in response to temperature, as well as conferring the dynamic motions of the membrane[20,21,24]. In contrast, the interface is chemically highly heterogeneous, representing a dynamic mixture of water, polar headgroups, carbonyl, and methylene groups, where these functional groups present an abundant source of dipole-based and electrostatic interactions with membrane proteins and other biomolecules[25]. Electrostatic interactions are mediated by the electric field originating from the charges and dipoles within the interface, which is maximal at the interface-hydrocarbon boundary before tapering off in the centre of the core[20,26]. The interfacial regions are also marked by a steep decline in polarity and electric field over short distances and thus signifies the boundary between the aqueous and hydrophobic phases[17,25,27].

1.1.1.2 Membrane Proteins Interact with Bilayers by Various Forces

The chemical heterogeneity described above dictates how membrane proteins interact with and fold in the membrane space. While soluble proteins fold primarily through the hydrophobic effect[28], the restraints of the bilayer favour van der Waals packing, intrachain hydrogen bonds, and salt-bridges as the dominant forces folding membrane proteins[29]. The differential propensity of particular amino acid residues to partition to the interface and core appear to have good correlation with the arrangement of membrane proteins in bilayers and is a driving force for membrane protein association[30–33]. For instance, the aliphatic sidechains Ala, Ile Val, and Leu have the greatest probability to be localized in the hydrocarbon core, while charged and polar residues appear more frequently at the interfacial regions[34]. The

aromatic residues Tyr and Trp appear most frequently at the interfacial regions[31] while positively-charged residues are most frequently on the cytoplasmic side of the interface in a phenomenon known as the positive-inside rule[32]. Indeed, site-directed mutagenesis studies have shown the importance of aromatic residues for stabilizing certain membrane proteins at the interface. For instance, substitution of Trp to non-aromatic amino acids dramatically reduces the affinity of the antimicrobial peptides tritrpticin to liposomes[35] and melittin to cell membranes[36]. Not only does the lipid bilayer affect the membrane proteins that associate with it, but proteins also affect the architecture of the bilayer's lipids[1,37].

Apart from chemical properties, mechanical forces also govern how membrane proteins interact with bilayers. As in typical oil-water interfaces, substantial pressure gradients of several hundred atmospheres in magnitude acting across the membrane, also termed lateral pressures, act at bilayer surfaces, and are caused by changes in free energy by the action of water molecules and electrostatic interactions[21,38]. Lateral pressures are largely positive at the water-headgroup boundary and negative at the headgroup–hydrocarbon boundary[20,38,39]. Positive lateral pressures are associated with repulsive intermolecular forces while negative values are attractive[39], mediating not only the aggregation of lipids to form ultrastructures[40], but also how membrane proteins interact with bilayers[19].

Thus, biological membranes form a highly dynamic and chemically heterogeneous continuum with a wide range of physicochemical properties, which enable membrane proteins to interact in a variety of modes contingent on both the chemical properties of the proteins and the physicochemical properties of the bilayer.

1.1.2 Integral Membrane Proteins

1.1.2.1 The Topology of Integral Proteins Describes their Orientation in Bilayers

Constituting 20–30% of the human proteome[41–44] and serving as over half of all drug targets[45,46], integral proteins are central to many biological processes. An early distinguishing feature of integral proteins are their inescapable affinity to lipids (Table 1), leading to the assumption that these proteins are strongly embedded within the hydrophobic interior of membranes by spanning the bilayer or protruding into the core[1,5,11]. The constraints of the bilayer establish expectations on how integral proteins arrange themselves. If integral proteins

were to intercalate so deeply within the hydrocarbon core where the hydrophobic effect is absent, and intramolecular hydrogen bonds and van der Waals forces dominate. It therefore stands to reason that such membrane-embedded regions would consist of predominantly hydrophobic segments with densely-packed secondary structures[29,47]. In this arrangement, any hydrophilic sections would be oriented outwards towards the solvent[5]. The number of times an integral protein spans the membrane refers to its topology, which can be classified as monotopic, bitopic, or polytopic (Figure 1)[48].

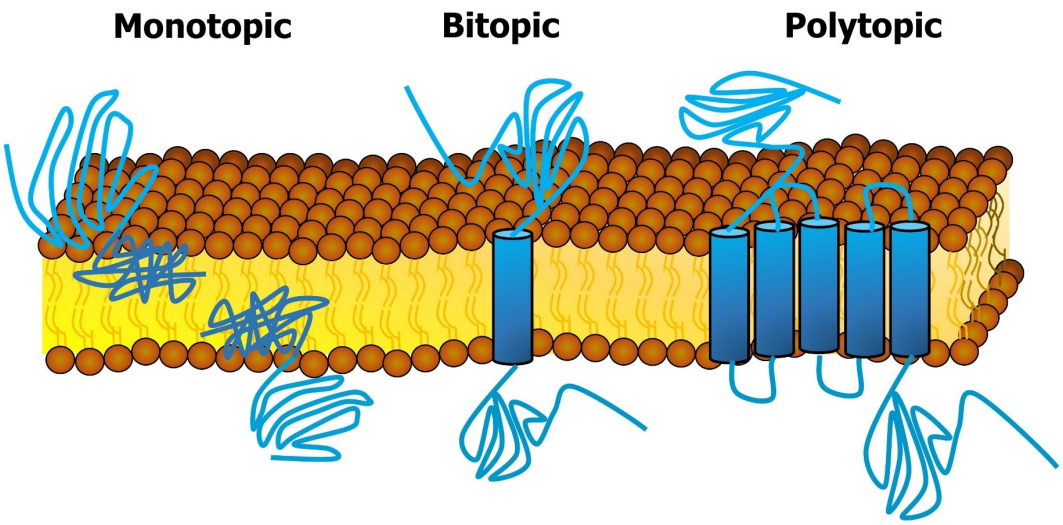

Figure 1. The topology of an integral protein defines the orientation of its membrane-embedded segments. Monotopic integral proteins are unilateral in that their hydrophilic domains face only one side of the bilayer. Such proteins are not transmembrane, in contrast to bitopic and polytopic integral proteins, which are bilaterally-oriented proteins that span the bilayer once and more than once respectively.

Monotopic integral proteins are unilateral in that their hydrophilic domain only face one side of the membrane, and that their hydrophobic segments do not span the entire bilayer. Bitopic and polytopic proteins are bilateral, exposing their hydrophilic segments on both sides of the bilayer. Such proteins are said to be transmembrane (TM) because they span the bilayer axis[48]. Most frequently, TM segments are α-helical structures, 17-25 hydrophobic residues in length[49], though TM β-strands are commonly found in bacteria and their endosymbiotic derivatives in mitochondria and chloroplasts[50,51]. The dominance of the α-helix in TM segments may be due to the tendency for helical structures to form in non-polar environments

to satisfy their hydrogen bond requirements[49]. Nevertheless, both α-helical and β-pleated TM segments fold to minimize the exposure of hydrophilic surfaces to the hydrophobic lipids[49,50]. To span the typical bilayer distance of 30 Å[15–17], an α-helix would need to contain 21 residues, though longer and shorter helices are accommodated by distortions in bilayer thickness, insertion at oblique angles, or oligomerization[49,52]. Hydrophobicity alone is not sufficient to predict TM segments due to the presence of amphipathic secondary structures, such as those lining the pore of channels[5,49]. Therefore, more accurate predictions incorporate statistical methods based on the availability of solved structures or known functions[49].

Polytopic integral proteins contain multiple TM helices, and are embedded so deeply within the bilayer that exposure of their soluble domains is minimal[53]. In comparison, bitopic integral proteins possess only a singular TM helix but possess one or more prominent soluble domains[54]. The number of TM segments within an integral protein appear to dictate whether the *N*- or *C*-terminal is oriented on exterior to or within the lumen of the bilayer: an odd number of TM helices have their *N*-terminals on the extracellular, lumenal, or cytoplasmic side and are termed Type I, while an even number of TM helices typically possess an inverse orientation and known as Type II[43]. Nearly half of all human TM proteins are bitopic, representing the most abundant and diverse of all TM proteins[42], though they are less well characterized than polytopic integral proteins[55].

1.1.2.2 The Topology of an Integral Protein Relates to Its Function

The topology of an integral protein has proven to be a good, though imperfect, predictor of function based on bioinformatic studies[43]. Monotopic proteins primarily serve enzymatic functions near the membranes and are specific for the compartment they are facing[56]. In contrast, the exposure of bi- and polytopic integral proteins on both sides of the bilayer enable them to fulfill more diverse roles, such as transducing signals or materials across membranes. Bitopic integral proteins function as non-G-protein-coupled receptors (GPCR) receptors and enzymes in the context of cell proliferation and differentiation, migration, apoptosis, and malignancy through their prominent hydrophilic domains[43,53]. Rather than serving as an inert membrane anchor, a sole TM α-helix mediates the differential targeting to membranes and serve as oligomerization sites for the assembly of protein complexes, signaling scaffolds, and

channels[55,57–59]. On the other hand, polytopic integral proteins function mostly as transporters, GPCR receptors, and structural cell-cell adhesion molecules in many biological contexts[43].

1.1.2.3 Integral Proteins Integrate to Bilayers Through Various Cellular Pathways

The integral proteins of all membranes initiate their integration into the bilayer at the endoplasmic reticulum (ER) in a process concerted with translation[60,61]. The extreme energetic costs of folding and unfolding within non-polar solvents force integral proteins to integrate into the bilayer with their secondary structures pre-formed[49]. For this reason, the ER is the site where the topology and three-dimensional structure of an integral protein are determined[60–62]. The initial step in the insertion of integral proteins to membranes is the recognition of the first hydrophobic segment emerging from the nascent polypeptide, which is an *N*-terminal signal sequence, an *N*-terminal stop-transfer sequence, or a downstream TM domain, by a targeting chaperone[63,64]. The targeting chaperone then promotes the insertion of the nascent polypeptide with complexes in the ER that mediate its integration into the bilayer. The sheer topological diversity of integral proteins necessitates the evolution of multiple integration pathways corresponding to specific topologies[65], as shown in Figure 2..

Most integral proteins insert into membranes via the secretory pathway[33], in which the signal recognition particle (SRP) binds to a signal sequence, which resembles a hydrophobic α-helix, to promote the association of the polypeptide with the SEC translocon to co-translationally insert the protein into the ER membrane with simultaneous cleavage of the signal sequence[61]. Integral proteins incorporated in this way assume a regular type II bitopic topology (Figure 2). Integral proteins with shorter, more hydrophilic TM domains tend to localize in earlier compartments of the secretory pathway while longer, more hydrophobic TM domains favour insertion at the plasma membrane (PM)[66]. Integral proteins encoding a stop-transfer sequence are also brought to the secretory pathway by the SRP, but do not have this region cleaved off; instead, it becomes incorporated as a part of its TM domains and result in a signal-anchored topology[63] (Figure 2). A minor proportion of integral proteins known as tail-anchored IMPs do not possess a signal sequence and are targeted to the ER for trafficking by an internal TM domain in an SRP- and translocon-independent pathway[63,65] (Figure 2). The relative hydrophobicity and hydrophilicity of this internal TM domain dictates which targeting chaperones are involved in this process and the eventual targeting of these proteins[67].

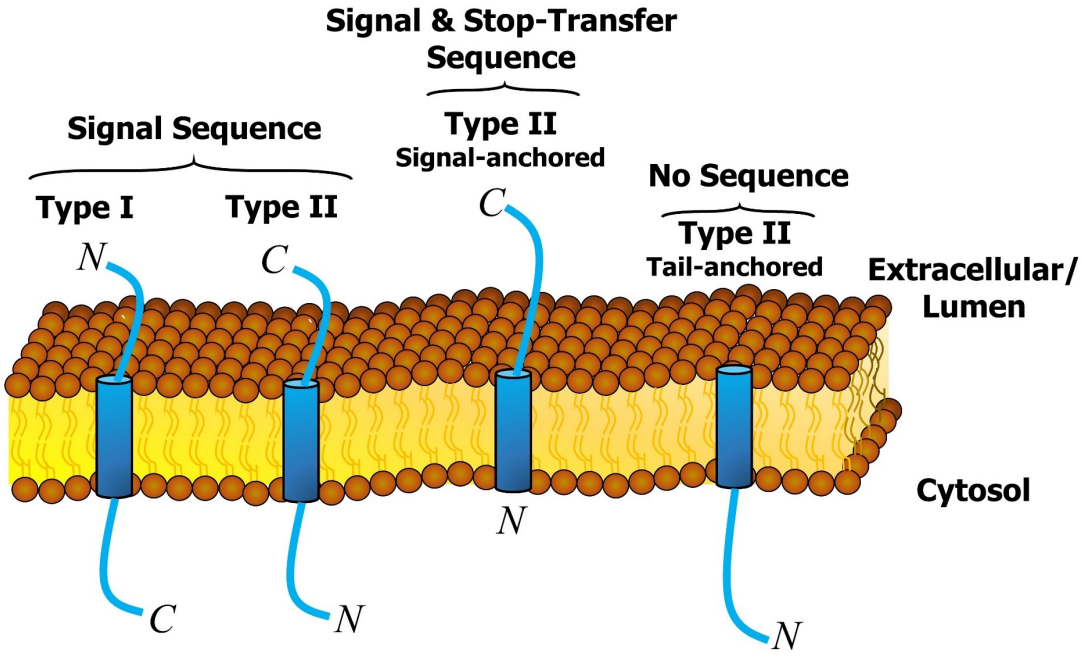

Figure 2. The topology of an integral protein is determined at the ER and is dependent on the sequence of specialized targeting motifs. Integral proteins with an *N*-terminal signal sequence insert into membranes as regular Type I or Type II proteins, which differ only in the orientation of their *N*- and *C*-termini, and are trafficked to their subcellular destination by the secretory pathway. Integral proteins with a dual signal and stop-transfer sequence insert as signal-anchored Type II proteins, and are also trafficked by the secretory pathway. A small portion of integral proteins do not possess either sequence, and insert into membranes as tail-anchored Type II proteins in a distinct trafficking pathway.

1.1.3 Peripheral Membrane Proteins

The defining characteristic of peripheral proteins are their weaker and thus reversible interactions with their membranes, enabling their extraction in detergent-free solutions[68] (Table 1). Peripheral proteins function as enzymes, electron carriers, toxins, adaptor proteins in the assembly of signaling complexes, and shuttling of membrane lipids in a variety of biological contexts including vesicle trafficking and retroviral assembly[69].

Peripheral proteins do not penetrate as deeply into bilayers as integral proteins and are exposed unilaterally. These proteins associate mostly with regions proximal to the interface of the membrane, where the chemical heterogeneity and lateral pressures of this region mediate intermolecular forces[70]. Cho & Stahelin defined three classes of peripheral proteins based on the extent of penetration in the interfacial region (Figure 3). S-type peripheral proteins do not

penetrate the lipid headgroup regions of the interface, while I- and H-type proteins do (Figure 3). H-type proteins are distinct from I-type proteins by their penetration into the hydrocarbon core. Peripheral proteins appear to interact with bilayers through at least four non-mutually exclusive interactions mediated by the interface: electrostatic, headgroup, and hydrophobic interactions, as well as post-translational modifications[10,70]. The extent of penetration into the interface determines the types of forces mediating the association of peripheral proteins with the bilayer. S-type peripheral proteins interact solely with headgroups while I- and H-type proteins interact with both the headgroups and the hydrocarbon core[70].

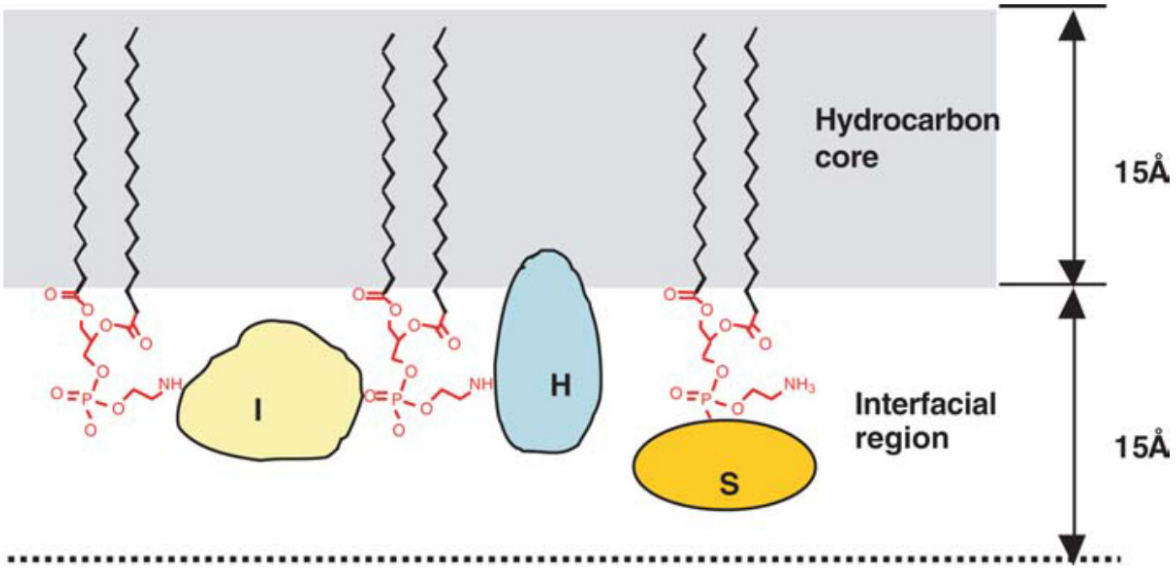

Figure 3. Peripheral proteins associate at the interfacial regions of membranes with varying degrees of penetration. All peripheral proteins associate at regions proximal to the interface of membranes. I-type and H-type peripheral proteins penetrate the regions occupied by the lipid headgroups, with H-type proteins inserting partially, but not fully, into the hydrocarbon core. In contrast, S-type proteins do not penetrate to the headgroup or hydrocarbon core regions significantly, and instead associate strongly with the network of water molecules proximal to the interface. [Reprinted with permission from Cho, W. & Stahelin, R.V. 2005. Membrane-protein Interactions In Cell Signaling and Trafficking. *Annual Review of Biophysics and Biomolecular Structure* 24:119-151. ©2005, Annual Reviews.]

1.1.3.1 Peripheral Proteins Associate with Membranes in a Two-Step Process

Charged lipid headgroups of the interface from lipids such as phosphatidylserine (PS) and phosphoinositides generate electric fields, mediating long-range Coulombic forces[26]. By charge complementarity to anionic surfaces of membranes, cationic peripheral proteins are

recruited nonspecifically to the interfacial regions[10]. Proteins with well-defined conserved polycationic cluster motifs, such as those of the small guanosine triphosphatase (GTPase) family, appear to bind with some degree of specificity, particularly to phosphatidylinositol-4,5-bisphosphate [$PI(4,5)P_2$] and phosphatidylinositol-3,4,5-triphosphate [$PI(3,4,5)P_3$][71]. Of course, not all peripheral proteins are cationic, and not all bilayer surfaces are equally anionic due to differential lipid composition[72]. Nevertheless, all membrane surfaces contain anionic lipid headgroups and most peripheral proteins contain cationic surfaces, so electrostatic interactions are expected to be a ubiquitous mode of peripheral protein association[70]. Though electrostatic adsorption is generally nonspecific, this interaction is regulated. For instance, phosphorylation of cationic clusters in the peripheral proteins PTEN[73] and MARCKS[74] dramatically reduces their membrane affinity, presumably by attenuating their positive charge.

By themselves, electrostatic interactions are not sufficient to anchor peripheral proteins to membranes, but they are essential for targeting and biological activity[75]. The initial adsorption of a peripheral protein to the bilayer surface increases its local concentration by up to 1000-fold, thereby reducing the 'dimensionality of space' and enhancing the interactions of peripheral proteins with other bilayer components, whereby processes such as the interaction with specific lipids and/or hydrophobic interactions stabilize and confer specificity[70,75,76]. Interface-partitioning aromatic residues[31] on peripheral proteins may induce penetration into the headgroup region while hydrophobic residues may promote penetration into the core[70,77,78]. Thus, the association of most peripheral proteins is a two-stage process first involving weak nonspecific electrostatic adsorption followed by stronger, more specific interactions[70].

1.1.3.2 Peripheral Proteins Can Associate with Membranes by Lipid Clamp Domains

A significant number of peripheral proteins contain modular domains sometimes known as lipid clamps that are specialized to bind to specific lipids by typical protein-ligand interactions[70]. At present, 11 distinct lipid-clamp domains have been identified[79] (Table 2) and include the protein kinase C (PKC) conserved 1 (C1)[80], PKC conserved 2 (C2)[80], pleckstrin homology (PH)[81], Fab1-YOTB-Vac1-EEA1 (FYVE)[82], Phox (PX)[83], epsin amino-terminal homology (ENTH)[84], AP180 amino-terminal homology (ANTH)[85], band 4.1-ezrin-radixin-moesin (FERM)[86], Bin/amphihysin/Rvs (BAR)[87], and tubby domains[88]. Many peripheral

Table 2. Several lipid clamp domains, along with their lipid targets, have been described in peripheral proteins. Lipid clamp domains are specialized domains in some, but not all, membrane-associated peripheral proteins. The specificity to their lipid targets range from strong to poor, and there is a significant overlap in lipid specificity. Some peripheral proteins contain multiple lipid clamps acting in concert to stabilize membrane interactions.

Domain	Lipid Target	Example
C1	Diacylglycerol (DAG) / phorbol esters	PKC
C2	Ca^{2+}-dependent lipid binding	PKC
PH	Various phosphoinositides	PLCδ
FYVE	Phosphatidylinositol-3-phosphate [PI(3)P]	Vps7p
PX	Various phosphoinositides	$p47^{phox}$
ENTH	$PI(3,4)P_2$, $PI(4,5)P_2$	CALM
ANTH	$PI(4,5)P_2$	AP180
FERM	$PI(4,5)P_2$	Ezrin
BAR	Anionic curvatures of the bilayer	Bin
Tubby	$PI(4,5)P_2$, $PI(3,4)P_2$, and $PI(3,4,5)P_3$	Tub

proteins contain multiple lipid clamps acting synergistically to stabilize membrane association. For example, the conventional PKCα contains both a C1 and C2 domain[80].

The lipid clamp domains of peripheral proteins assume a variety of folds ranging from the zinc finger in the C1 domain[89] to the β-sandwich in the PH domain[81], and bind their ligands through various mechanisms with specificities ranging from poor to strong. Notably, the majority of solved structures to date reveal that the β-sandwich or helical bundle is the predominant lipid clamp fold, though there is no detectable sequence similarity amongst these folds[90]. Among the best-studied of the lipid-clamp domains is the C1 domain (Table 2). The X-ray structure of PKCδC1 in a complex with phorbol-13-acetate (PDB ID 1PTR) shows a V-shaped polar binding pocket flanked on both sides by cationic residues in the middle and hydrophobic residues at the top[89]. While the cationic residues nonspecifically adsorb the protein to the membrane and position the ligand for binding[91], ligand-binding facilitates membrane insertion by capping the V-pocket to form a continuous hydrophobic surface[89,92].

In contrast, PH domains lack any discernable lipid-binding pockets and instead interact with their various phosphoinositides by nonspecific electrostatic adsorption, with specificity being coordinated by the loops within its β-sandwich fold[81,93]. Interestingly, the same domain expressed in different proteins displays differential specificities and affinities to lipids. For example, the C1 domain in conventional and novel PKCs bind to diacylglycerol (DAG) and its phorbol ester analogues, but not when expressed in atypical PKCs or other proteins[92]. Likewise, the PH domain in phospholipase C-δ (PLCδ) binds $PI(4,5)P_2$[94] but to $PI(3,4)P_2$ and $PI(3,4,5)P_3$ when expressed in protein kinase B[95] (Table 2).

1.1.3.3 Some Peripheral Proteins Associate with Membranes by Hydrophobic Interactions

Either contingent to or independent of lipid binding, peripheral proteins may penetrate partially into the bilayer core by insertion of a hydrophobic or amphipathic α-helix or loop, or by virtue of a post-translational lipid modification (see below)[10,70]. The formation of non-bilayer lipids such as phosphatidylethanolamine, which are non-lamellar due to their non-cylindrical geometries[96], also plays a critical role in peripheral protein binding. The production of non-bilayer lipids decreases packing density at the interfacial region, decreasing the localized lateral pressure to insert peripheral proteins by attractive mechanical forces[19]. Since such hydrophobic surfaces are typically buried in proteins, a conformational change must occur to expose these surfaces for membrane association[85]. Binding to either cofactors or lipids and phosphorylation appear to be two dominant mechanisms regulating the conformational change of peripheral proteins. For example, phosphorylation of the NADPH oxidase subunit $p47^{phox}$ at multiple *C*-terminal sites dissociates the intramolecular grip of its phosphoinositide-binding PX domain (Table 2) from its SH3 domain, facilitating binding to $PI(3,4)P_2$ and phosphatidic acid and enabling penetration of the bilayer through its hydrophobic lipid-binding pockets[97,98]. Other mechanisms, such as the binding of DAG/phorbol ester to C1 domains as described above, form hydrophobic surfaces without a drastic conformational change[89].

The post-translational addition of a lipid moiety to proteins, referred to as lipidylation, is a ubiquitous mode of peripheral protein insertion into bilayers. At least five lipid classes including fatty acids, isoprenoids, sterols, phospholipids, and glycosylphosphatidylinositol (GPI) anchors conjugate to proteins through amide, thioether, and thioester linkages depending

on the residue cross-linked to (Table 3)[99]. The conjugation of a lipid moiety is catalyzed by a distinct lipidyltransferase and modifies the function and localization of a protein in a protein-specific manner[99]. The effects conferred by lipidylation are considered reversible in that lipid conjugation does not permanently alter function, though myristate and isoprenoid moieties cannot be hydrolyzed off their proteins[99]. In most cases, lipidylation promotes the association of peripheral proteins with membranes by direct insertion of lipid carbons into the bilayer core[78], but they may also promote intra- and intermolecular protein-protein interactions, conformational switching, and sorting of integral proteins into lipid rafts[99–101]. Lipidylation alone is insufficient for membrane binding[102]. Consistent with the two-stage model of peripheral protein association, lipidylation acts in concert with other mechanisms to promote stable membrane association such as electrostatic adsorption[103], ligand-binding[104], proteolytic

Table 3. A number of lipid anchors are conjugated to specific residues on target proteins to enable membrane association or to confer other functions. Each lipid moiety is conjugated to a target protein by a distinct lipidyltransferase, and confers, among other functions, targeting to specific subcellular compartments. Depending on the residue a moiety is conjugated to, a different covalent bond may form. These bonds may or may not be hydrolyzable.

Lipid Moiety	Lipid Class	Lipid-protein bond	Residue	Targets	Hydrolyzable moiety?
Myristate	Fatty acid	Amide	Gly	Cytosol, PM, cytoskeleton	No
Palmitate (*S*-palmitoylation)	Fatty acid	Thioester	Cys	PM	Yes
Palmitate (*N*-palmitoylation)	Fatty acid	Amide	Cys	Secretory pathway	Yes
Farnesyl	Isoprenoid	Thioether	Cys	PM, Golgi, nuclear envelope	No
Geranylgeranyl	Isoprenoid	Thioether	Cys	PM, Golgi, intracellular vesicles	No
Cholesterol	Sterol	Ester	-COOH	Outer PM leaflet	Unknown
GPI anchor	Glycophos-pholipid	Amide	-COOH	Outer PM leaflet	Yes

cleavage[105], or concomitant post-translational modifications including multiple lipidylations[103] and phosphorylation[74].

The diversity of lipid moieties likely evolved to differentially sort peripheral proteins to various subcellular destinations, or to either leaflet of the PM (Table 3). Targeting specificity may occur through 'bilayer trapping', in which a singly-lipidylated protein is non-discriminately recruited to any bilayer surface, but persists only where it can interact with its target lipidyltransferase, which would then conjugate an additional lipid moiety to stabilize the interaction[106]. The localization of secretory products, for instance the various acetylcholine-esterases, to the outer leaflet of the PM occurs through GPI-anchors[107]. Such proteins possess a *C*-terminal sequence in addition to their *N*-terminal signal sequence which directs them for GPI-anchoring and subsequent anchoring to the outer PM[108]. The conjugation of a cholesterol moiety is thought to be an alternative route to anchor secretory products to the outer PM[99].

Despite the sheer abundance of peripheral proteins, most appear to utilize common themes unified in fairly predictable ways established by the unique environmental constraints of the bilayer, particularly at the interfacial regions. In the next section, a distinct category of membrane proteins sharing properties with both integral and peripheral proteins, known as amphitropic proteins, will be discussed.

1.1.4 Amphitropic Proteins

1.1.4.1 The Reversibility of Amphitropic Proteins Serve Biological Functions

In 1988, Burn classified a novel class of proteins distinct from either integral or peripheral proteins, termed amphitropic proteins[109]. Amphitropic proteins exist in both soluble and membrane-bound states and thus possess properties of soluble, integral, and peripheral proteins[109]. While all peripheral proteins possess relatively weak interactions that are, by their nature, reversible[1,5,68], amphitropic proteins reversibly interact with membranes in biologically relevant contexts[109–111]. At the membrane, amphitropic proteins may interact as either peripheral or integral proteins**.** Such reversible membrane associations are thought to meet the dynamic needs of the cell when required and are implicated in regulating enzymatic function, assembling signaling complexes in response to stimuli, providing regulated access to substrates, and to regulate membrane-cytoskeletal interactions[111]. For instance, recruitment of

lipid-transfer proteins, which shuttle membrane lipids from one membrane to another, and various phospholipases places these enzymes in proximity to their substrates when turnover capacity is high[112,113]. Vinculin, a component of focal adhesions, is one protein that links membranes to the actin cytoskeleton, and its dissociation from the membrane is essential in stress fibre remodeling[114]. The ezrin-moesin-radixin (ERM) proteins couple the actin cytoskeleton to the PM in a similar fashion[115]. Similarly, bacterial pore-forming toxins are kept in their soluble, inert state by dimerization or production as a proprotein within the host, and convert to their cytotoxic membrane-associated form only upon reaching a target cell[116].

1.1.4.2 The Reversibility of Amphitropic Proteins Is Regulated

Since reversibility of the membrane association is central to their function, it is not surprising that amphitropic proteins are regulated through two dominant mechanisms, namely conformational changes in the protein, and changes in membrane lipid composition[111].

As discussed above, conformational changes are required to expose hydrophobic membrane-targeting regions from the core of membrane-associating proteins. For example, calcium-binding to the EF-hand domains of the retinal protein recoverin results in large-scale structural changes that ultimately releases its buried myristoyl group to anchor to the membrane[117]. Conformational changes may occur in more subtle ways, such as in the actin-binding protein hisactophilin, which associates with membranes when its polyhistidine cluster is protonated near pH 6 to confer a net positive charge for electrostatic adsorption[103]. Phosphorylation is another common means to regulate membrane association of proteins, as in the case of PTEN and MARCKS discussed above. Phosphorylation of cAMP-dependent protein kinase (also known as protein kinase A, PKA) results in the expulsion of its myristoyl from its hydrophobic cleft to promote membrane association[118]. The *Bacillus anthracis* anthrax protective antigen is a pore-forming toxin that associates with membranes upon exposure of some key hydrophobic residues following proteolytic cleavage of its *N*-terminal domain, presumably by a cell surface protease on a target cell[119].

By virtue of their affinity to specific lipids, amphitropic proteins with lipid clamp domains are sensitive to changes in the abundance of specific membrane lipids[120]. Often, these membrane lipids are messengers central to signaling pathways, and among the most well-

defined are DAG and polyphosphoinositides such as $PI(4,5)P_2$[111]. The levels of lipid messengers are tightly regulated to orchestrate signaling events by recruiting proteins to bilayers. For instance, the canonical GPCR pathway mediated by the $G_{\alpha(q/11)}$ isoform activates PLCγ to hydrolyze $PI(4,5)P_2$, yielding DAG and recruiting PKCα to membranes by virtue of its C1 domain[121]. Other lipids with the capacity to function as messengers include ceramide, phosphatidylserine (PS), phosphatidic acid, lysophosphatidic acid, and arachidonic acid, though they do not operate through lipid-clamp domains[110,122]. For instance, blood clotting factors are secretory proteins that bind specifically to PS without lipid clamp domains[123]. Changes in mechanical properties of the bilayer, such as curvature and packing density, are another mode of recruiting amphitropic proteins to membranes. To illustrate, the rate-limiting enzyme in phosphatidylcholine (PC) synthesis CTP:phosphocholine cytidyltransferase is recruited to areas of the membrane with low headgroup density and high curvature, where the lateral pressure is high, to mediate insertion of its amphipathic α-helix[124–126]. Notably, negative curvature stress induced by phosphatidylethanolamine production is a means by which several phosphatidic acid-binding proteins are recruited to membranes[127].

In closing, amphitropic proteins form an essential mechanism by which the dynamic demands of the cell can be met, and add a layer of complexity on how cells orchestrate their events by exploiting their reversible association to membranes to fulfill their functional roles. This amphitropism will be revisited in the context of certain ion channels known as pore-forming proteins, following a discussion on what defines ion channels.

1.2 Transporters & Anion Channels

The emergence of membranes is considered to be one of the earliest events in evolution[128,129], yet their formation would have presented significant constraints to prototypical organisms. A lipid bilayer presents impermeable barrier and hinders the acquisition of key molecules from the environment, thus creating a problem for these early life forms. It turns out that the universal expression of the F_0F_1-ATPase[130] and SecY[131] transporters in all living organisms makes these among the most conserved genes[132] and illustrates how these organisms adapted to emergence of membranes. It is therefore not surprising that transporters are essential for a wide variety of biological processes, given the early roots in the evolutionary tree of life. The biological role of transporters is fulfilled by two fundamental

effects of their activity—the selective import and export of materials across the bilayer, and the resulting effects of their asymmetrical distribution. The import and export of materials is required for nutrient acquisition[133], toxin and drug clearing[134], secretion of bioactive compounds such as messengers[133], and the promotion of genetic diversity by DNA export[135], while the electrochemical gradients through the asymmetrical distribution of materials is a key component for energy transduction and signal transmission[136,137].

1.2.1 Transporter Classification

Most transporters are integral proteins, which may function alone or in concert with signaling, energy-coupling, or regulatory proteins[133]. In humans, at least 77% of all transporters are polytopic integral proteins possessing more than six TM helices[43]. Single-spanning integral proteins exist, such as the mitochondrial pore-forming Bcl-2 family, but they possess transporter activity only upon oligomerization[138].

1.2.1.1 Transporters Are Classified as Channels or Carriers

The transporter classification (TC) system categorizes transporters based on their mode of transport and energy-coupling source, broadly dividing transporters into two broad groups, channels or carriers[133] (Figure 4). Channels transit their solutes through an internal trans-bilayer passage that may be hydrophilic or amphipathic, depending on the solute transported[133]. In contrast, carriers lack a trans-bilayer passage and instead bind their solutes by typical protein-ligand interactions on one side of the membrane, with translocation achieved through conformational changes of the carrier[139]. This conformational change has remained elusive to structural studies, but MD simulations[140] and some X-ray structures, such the mitochondrial ADP/ATP translocase[141] (PDB ID 1OKC), support this hypothesis. Channels are usually oligomeric and transport their solutes at fast rates, while carriers are typically monomeric and possess significantly lower rates of transport[133]. While carriers are capable of both facilitated diffusion and energy-coupled active transport, channels are restricted to only the former[133]. Both channels and carriers are highly modulated by cellular and physicochemical regulators.

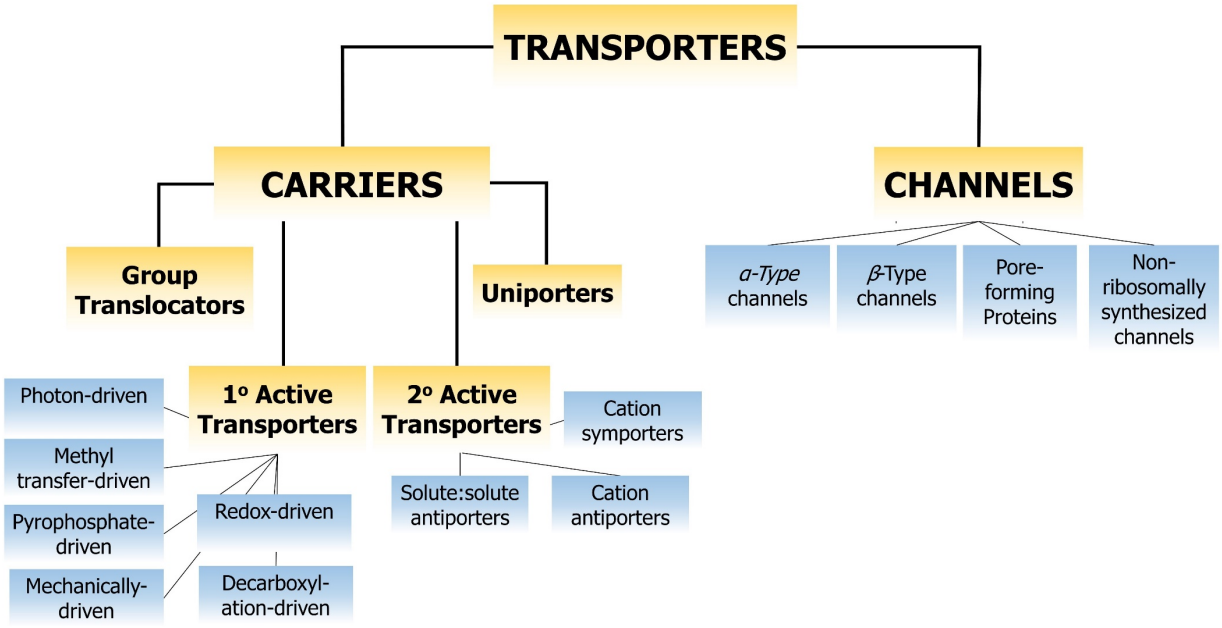

Figure 4. The Transporter Classification (TC) system classifies transporters as Carriers or Channels. Transporters are broadly defined as carriers or channels. Carriers mediate facilitated or active transport and have typically slow kinetics. Carriers can be further classified by their mode of active transport, such as group, primary, or secondary active transport. In contrast, channels transport their solutes only by facilitated diffusion and have higher rates of transport. Channels are further classified as α-helical (α-type), β-pleated (β-type), pore-forming proteins, or non-ribosomally synthesized channels. See text for details.

1.2.1.2 Channels are Further Classified as Four Types

Channels are divided into four categories (Figure 4). α-type channels are ubiquitously-distributed channels composed primarily of α-helices. β-barrel channels, also known as porins, are found only in the outer membranes of Gram-negative bacteria, mitochondria, and chloroplasts. The remaining two classes conduct their solutes in atypical ways. Pore-forming proteins (PFPs) are amphitropic proteins or peptides produced across several phyla that generate large nonspecific pores upon their translocation to membranes[142]. Non-ribosomally synthesized channels are formed by lipopeptides and non-polypeptide biomolecules produced in fungi and bacteria that cause ion-conductance in context of biological warfare[143,144].

1.2.2 α- and β-type Channels

Even before their structures were solved, the arrangement of α-type channels were correctly predicted based on the thermodynamic constraints of membranes[4]. When amph-

ipathic TM subunits associate, their hydrophilic portions sequester from the hydrocarbon core by facing each other, creating a hydrophilic or ionic pore formed at the junction of the subunits[145]. Indeed, this arrangement comprises what is today known as the barrel-stave motif (Figure 5A,B)[146]. Multimeric assemblies of tetramers, pentamers, and hexamers have been described, and the number of subunits creating the pore is roughly related to its size and solute specificity[147]. To illustrate, tetrameric K^+ channels form small pores meticulously specific for K^+ ions[148], yet hexameric gap junctions form large pores with little specificity[149]. The barrel-stave motif is not ubiquitous among channels, nor are all channels oligomers. For instance, the pore of certain Cl^- channels and aquaporins are not formed at the multimeric interface, but are embedded within each individual subunit (Figure 5C,D)[150,151]. In addition, the cystic fibrosis conductance regular (CFTR) channel is monomeric[152] with a solute-conducting pore formed by two internal TM α-helices[153].

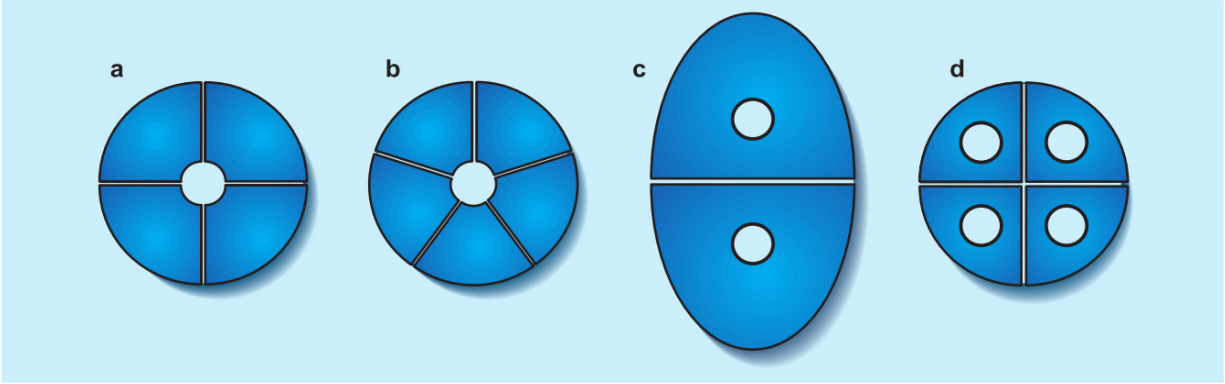

Figure 5. The pores of some channels are formed at the interface of oligomeric subunits. [A] Hexameric and [B] pentameric assemblies form a barrel-stave motif, in which a solute-conducting hydrophilic pore is formed at the junction of multiple subunits. Barrel-stave motifs are archetypical of cation channels, but the ClC chloride channel features the [C] double-barrel motif, in which the solute-conducting pore is not formed at the multimeric interface but rather within each subunit of the homodimeric complex. This structural motif is also similar for [C] aquaporins, which are tetratmeric. [Reprinted by permission from RightsLink Permissions Springer Customer Service Centre GmbH: *Springer Nature*. *Nature*. Chloride Channels Are Different. Jentsch, T. ©2002]

When β-barrels were first proposed[154], their geometrical constraints suggested that their hydrophilic cores would be significantly larger than those of α-helical channels[155]. Decades later, the first X-ray structures of β-barrel transporters, termed porins, corroborated

these claims[156–158]. While β-barreled proteins are structurally diverse as a whole, porins are homotrimeric assemblies of amphipathic and antiparallel β-strands joined together to form a large central hydrophilic core[159]. Whether they be α-helical or β-barreled, the key characteristic of these channels is the formation of a polar or amphipathic trans-bilayer passage through which solutes are conducted.

1.2.2.1 Channels Are Gated

With the exception of constitutively open TRP channels[160,161], nearly all channels convert between open and closed states through a process known as gating. Ligand-gated channels possess conserved ligand-binding domains and utilize the free energy of ligand-binding to interconvert between its states[162]. pH-gated channels lack any such conserved structural motifs and are gated by ionizable residues that are clustered by the pore[163,164]. Channels may also be gated by voltage, tension, curvature, fluid flow rate, and temperature, using sensors which operate through diverse mechanisms that may or may not be defined by conserved structural domains[165]. For instance, while most voltage-gated channels possess a conserved voltage-sensing domain[166], two-pore domain K^+ leak channels do not[167].

The intricate atomic maneuvers that occur during gating have been revealed by structures of channels "trapped" in their various conformations. In the nicotinic acetylcholine receptor, for example, electron microscopy of its open and closed conformations reveals that ligand-binding causes a 60 Å rotation of its TM helices to open its pore[168]. K^+ channels across all domains of life share a conserved Gly which functions as a 'hinge', succeeded by a Glu or Ala five residues downstream to ensure a wide path for ions through the pore[169].

1.2.2.2 Channels are Selective for their Solutes by Structural Features

As previously mentioned, most channels achieve selectivity ranging from extremely precise to indiscriminate. Channels possess a myriad of structural motifs known as selectivity filters which contribute to their selective solute transport. The structural arrangement, degree of conservation, and mechanism of selectivity differ between channels, but is somewhat solute-specific. For instance, the selectivity filter is defined by a highly conserved TVGYG sequence amongst all K^+ channels[170], but defined by a DEKA ring formed at the juncture of four inter-helical loops in all mammalian Na^+ channels[171]. The selectivity filter in the ClC Cl^- channel is

even more complex, comprised of four conserved sequences at the *N*-termini of four separate TM helices, which generate a helical dipole of positive charge facilitating anion binding[150]. In contrast, porins are notoriously unselective and pass solutes restricted only by a size exclusion limit of 600 Da[172]. The structure of Omp32 complexed with a periplasmic peptide (PDB ID 1E54) reveals a significant positively-charged cavity which likely functions as a crude selectivity filter for anions[173].

Generally, selectivity filters function by providing complementary electrostatic surfaces to their solutes and excluding those that do not occupy the binding site well[174]. The K^+ selectivity filter, for instance, contains four ion-binding sites which coordinate its ions through the partial negative charges on carbonyl oxygens of the polypeptide backbone[175]. The ion permeation process defines the stoichiometry and binding mechanisms of ions as they conduct through the pores. The exact process is largely channel and solute-dependent and ranges from a "knock-on" mechanism in which ions are dehydrated and conducted single-file, as in K^+ channels[176,177], to one in which multiple ions and their solvation spheres are co-transported, as in Na^+ channels[178]. The permeation process for Cl^- channels is not as precisely defined, though evidence suggests a mechanism distinct from cation channels[151].

1.2.3 Pore-Forming Proteins

1.2.3.1 Pore-forming Proteins Associate with Membranes Following Structural Changes

Pore-forming proteins (PFPs) and non-ribosomally synthesized channels conduct their solutes across membranes in less typical ways than in α- and β-type channels. These channels generate nonspecific pores to disturb membrane integrity as toxins[179], immune modulators[180], and as stimulators of apoptosis[181]. Other functions are also achieved by this process including signaling, metabolism, and the transport between different membranes[90].

PFPs are nearly ubiquitous and have been described in bacteria, cnidaria, plants, and mammals[182]. PFPs are synthesized as soluble proteins which undergo dramatic structural transitions to reveal amphipathic surfaces[183]. These amphipathic surfaces then spontaneously insert into membranes to generate pores consisting of transmembrane α-helices or β-barrels[183–185]. Because these amphipathic structures are not sufficient for stable membrane association, structural transitions of PFPs usually involve other large-scale transformations[90]. Among the

best-studied of these is the hemolytic toxin cytolysin A from *Escherichia coli*, in which the β-tongue of its soluble form transforms into an elongated α-helix in its transmembrane form[186]. Two discontinuous α-helices in the bacterial toxin perfringolysin refold in the membrane as β-hairpins which constitute the transmembrane β-barrel[187–189], and it is postulated that members of the MACPF superfamily of the complement system in innate immunity undergoes similar structural transitions, based on structural similarity[190]. LL37, a human antimicrobial peptide, adopts a random coil in solution, but transforms to completely α-helical in the presence of lipid vesicles[191] to form transmembrane pores[192]. The dramatic structural transformations of PFPs classify them as metamorphic proteins, defined as proteins with multiple conformational folds (described in Section 1.4)[193].

The majority of PFPs associate with specific components of membranes to initiate their structural transitions to prevent autoactivation within host cells. For instance, MACPF proteins of the complement system are kept inactive by binding to the regulatory protein CD59[194,195]. Diphtheria toxin interacts with cell surface receptors to initiate receptor-mediated endocytosis and proteolytic processing[196], and cholesterol-dependent cytolysins interact specifically with cholesterol to stabilize their membrane interactions[197]. The pore-forming action of some PFPs appears to be regulated, as illustrated by the proapoptotic Bcl-2 member Bad. *In vitro* ion conductance measurements in planar bilayers demonstrated that recombinant Bad is able to form pores only when polyphosphorylated[198].

The association of many PFPs with membranes appears be pH-dependent, with greater association at acidic conditions. In the case of the *E. coli* toxin colicin A, its overall secondary structure as assessed by circular dichroism (CD) spectroscopy remains constant between pH 2.0–7.0[199]. However, dramatic changes occur in the near-ultraviolet region, suggesting that aromatic residues are solvent-exposed at pH 2.0 instead of buried in the hydrophobic core[199]. The conservation of secondary structure with hydrophobic residues inverted outward is strongly suggestive of a pH-induced 'molten globule' state[200]. The loose tertiary structure of the molten globule promotes the exposure of hydrophobic surfaces, thereby lowering the energetic barrier required for insertion into membranes[184]. The local pH of a lipid surface differs drastically than the bulk, strongly suggesting that a pH-induced molten globule could form as an intermediate in the insertion of colicin A to membranes[199]. This acid-destabilizing

process has been demonstrated several pore-forming toxins[184], though proteins with defined soluble and membrane conformations such as Bcl_{XL} may not adopt a molten globule intermediate, and instead insert to membranes by the protonation of certain side chains[201].

1.2.3.2 The Pores Made by Pore-Forming Proteins are Usually not Defined Structures

When a sufficient PFP-to-lipid ratio is reached, concentration-driven events result in the creation of flexible pores by two routes. In the first, PFP protomers self-oligomerize by lateral protein-protein interactions to create a barrel-stave pore reminiscent of α- and β-type channels[202]. In the toroidal pore model, a sufficient concentration of PFPs in the membrane perturb the local curvature of bilayers to generate a transbilayer pore[202]. In most cases, the pores generated by PFPs do not assume well-defined structures and are transient. MD simulations have shown that the supramolecular organization of membrane-active peptides as membrane pores is dependent on an interplay of peptide sequence, lipid composition, peptide-to-lipid ratio, and other factors[203]. The hemolytic toxin α-hemolysin (PDB ID 7AHL) from *Staphylococcus aureus* is highly unusual among PFPs in that it forms a well-structured pore with a fixed stoichiometry as a homoheptamer (Figure 6)[204]. The pores generated from PFPs range from 10 – 150 Å in diameter and is largely dependent on the stoichiometry of protomeric units joining to form the pore[188,205,206].

1.2.3 Anion Channels: ClC, CFTR, & Ligand-Gated GABA/Glycine Receptors

Anion channels, often called Cl^- channels given that Cl^- is the most abundant anion in cells[207], are ubiquitous ion channels which perform diverse roles including the regulation of membrane potentials, cell volume regulation, trans-epithelial salt transport, and acidification[208]. Most anion channels are α-type, though a notable β-type channel is the voltage-dependent anion channel (VDAC) porin of the mitochondrial outer membrane[209]. Perhaps the most obvious sites for anion channels is the PM, though the functions and maintenance of organelles would not be made possible without these intracellular anion channels[207]. Intracellular anion channels are required for the extrusion of anions from degradative and biosynthetic compartments[210], acidification of intracellular organelles in conjunction with H^+ transporters, the maintenance of organellar volume to combat swelling[211], and to enhance the activity of transporters by the neutralization of excess positive charge[212].

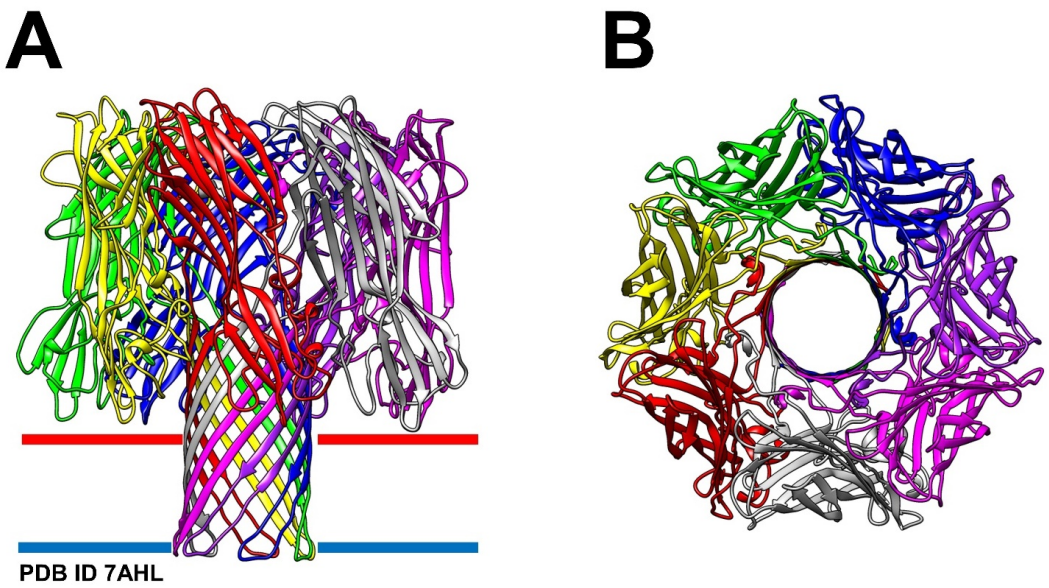

Figure 6. The pore-forming protein α-hemolysin from *S. aureus* forms a homoheptameric ion channel upon membrane localization. α-hemolysin is unusual among pore-forming proteins because it forms stable ion channels with a defined stoichiometry of seven subunits. [A] Side view of α-hemolysin in its membrane-associated form, with each subunit of the heptameric ring bearing a different colour. The lipid bilayer is depicted by solid lines. [B] Top view of α-hemolysin from the extracellular face.

Given the importance of these roles, it should not be surprising that dysfunctions of chloride channels is implicated in diseases widely classified as chloride channelopathies, the most notable among them being cystic fibrosis due to CFTR dysfunction[213].

The astounding diversity of anion channels with respect to their selectivity, gating, and conductance make classification difficult. At present, there is no official consensus regarding the classification of anion channels[208], but at least three well-established gene families of Cl^- channels have been defined including the ClC, CFTR, and ligand-gated GABA/glycine receptors[207]. As stated above, the phylogenetic relationships among and between anion channels are not completely clear, though it has been suggested that anion channels evolved independently of cation channels[214]. Within each family, Cl^- channels are gated by similar mechanisms and display broad tissue expression and cellular localization.

1.2.3.1 ClC Channels are the Archetypical Anion Channels

The ClC gene family consists of nine members localized at the PM or in endosomes[215], though they are shuttled between subcellular locations under certain conditions[216]. While most

ClC members are classical ion channels, ClC-4 and ClC-5 function as carriers with Cl^-/H^+ antiporter activity[217]. ClC channels are localized at the PM and primarily function in trans-epithelial transport and the generation of resting membrane potential, while ClC carriers are bound in endosomes to acidify organellar compartments[218]. The majority of ClCs possess the anion selectivity order of $SCN^- > Cl^- > Br^- > NO_3^- > I^-$[219–221], with selectivity critically dependent on an essential Ser residue at the centre of the pore[222]. Its members are mostly, but not always, voltage-gated, with further regulation by anion concentrations, pH[207], and phosph-orylation[223,224]. All ClC proteins described to date are homodimeric, with a self-contained pore within each subunit forming the previously mentioned 'double-barreled' motif'[150] (Figure 5C). An *N*-terminal signal sequence has been identified in ClC4 and is generalizable for most ClCs, which directs it to the ER for conventional co-translational membrane integration[225].

1.2.3.2 The CFTR is an ABC Carrier with Channel Activity

The CFTR Cl^- channel holds the unique distinction of being the sole channel of the ABC carrier family, meaning it possesses a cytosolic nucleotide-binding domain (NBD) with intrinsic ATPase activity[226]. CFTR is localized at the apical epithelial membranes of the lungs, pancreas, sweat glands, intestines, and brain[227], and primarily functions in transepithelial anion transport, though it also regulates other transporters, a function for which it was initially given its name[228]. From whole cell patch experiments, an anion selectivity order of $Br^- \geq Cl^- > I^- > F^-$ was reported[229], though CFTR is relatively nonselective among anion channels and allows the permeation of other monovalent anions such as SCN^-, NO_3^-, HCO_3^-, and HCO_2^- [230]. In contrast to ClC channels, the CFTR is not gated by voltage, but rather by interactions with ATP with its NBD. The precise gating cycle has yet to be resolved, though patch-clamp studies in HeLa cells reveal that ATP-binding opens the channel, leaving either ATP hydrolysis or dissociation to close the channel[231]. The CFTR is unique among the ABC carriers in that it possesses an additional cytosolic regulatory domain which must become phosphorylated by PKA to enable ion conductance[232].

CFTR has been demonstrated in living cells as monomeric[152], with a solute-conducting pore formed at the cationic interface of two internal helices among its total 12 TM helices[153]. The insertion of CFTR into membranes is complex and occurs by both co-translational and post-translational ER insertion, mediated by the signal sequence within its first and second TM

segment[233]. Interestingly, promotion of the conventional co-translational pathway by mutating certain residues abolished anion conductance in a heterologous expression system and may be associated with channel dysfunction[234].

1.2.3.3 Ligand-Gated GABA/Glycine Receptors are Cys-Loop Channels

The last of the well-established anion channel gene families discussed here are the ligand-gated GABA/glycine receptors, which are members of Cys-loop channel superfamily, named after a conserved 13-amino acid long *N*-terminal sequence flanked by cysteines on each side[235]. GABA/glycine receptors are typically situated on neuronal PMs at synapses, where ligand-binding opens the pores of the channels to allow an influx of anions into the cytosol and hyperpolarizing neurons[207]. Both glycine and GABA receptors display the general anion selectivity series of $SCN^- > I^- > Br^- > Cl^- > F^-$[235], though the kinetics and regulation are remarkably different between the two receptors.

Other Cys-loop proteins include the acetylcholine, serotonin, and zinc-activated ion channels, of which all are thought to have evolved from a common ancestor[235,236]. Despite this, Cys-loop members have divergent functionalities. For instance, of the three GABA receptor classes, $GABA_A$ and $GABA_C$ are Cl^- channels[237], while $GABA_C$ functions as a GPCR[238]. Cys-loop proteins form pores at the interface of five subunits as a typical barrel-stave (Figure 5B), and oligomerize as hetero- or homopentamers[239]. Sequencing of the $GABA_A$ and glycine receptors reveal a conventional *N*-terminal signal sequence for membrane insertion[237,240].

1.2.4 Other Anion Channels

In the 1980s, the development of specific and potent pharmacological ligands enabled many transporters to be discovered in what is known today as the "transporter explosion", yet in this era, most of the Cl^- channels discovered were known only by their function[219]. For instance, several candidates including P-glycoprotein, Icln, and the Band 3 anion exchanger failed to account for the volume-activated currents for the supposed volume-activated Cl^- channel[241]. These currents are now considered more likely to be mediated by multiple channels[241]. Without the acquisition of a molecular target and cloned genes, studies of these putative Cl^- channels remain theoretical. Amongst these orphan channels are two extensive gene families formerly and tentatively classified as Cl^- channels, yet due to sparse and

conflicting evidence, are not always considered as such[207]: the calcium-activated Cl^- channel (ClCA) and the chloride intracellular channel (CLIC) families.

1.2.4.1 ClCAs Were Discovered as Putative Chloride Channels

In 1991, Ran & Benos isolated a 38 kDa protein from bovine tracheal membranes which demonstrated [$^{125}I^-$] uptake that was blocked by the anion channel inhibitor DIDS when reconstituted into PC/cholesterol liposomes[226]. When separated by native PAGE, bands enriched at 62–64 kDa and 140 kDa were observed, suggesting that this anion-conducting protein could form disulfide-bonded tetramers[242]. Consistent with this notion, reconstitution of the 140 kDa protein into planar bilayers under reducing conditions abolished [$^{125}I^-$] uptake[243], and currents produced by this protein could be increased by calcium ions[244]. Its complementary DNA (cDNA) was cloned from a bovine cDNA library and named ClCA for its proposed role as a calcium-activated Cl^- channel[244]. Its cDNA sequence identified the bovine lung-endothelial cell adhesion molecule 1 (bLu-ECAM-1), independently discovered by another group in the same year[245], as a ClCA homologue[246], and this gene was re-named ClCA2. Reports of the role of ClCA2 in tumor cell adhesion and metastasis[247] were puzzling in light of their initial classification as ion channels. Nevertheless, four genes in humans *hClCA1 – 4* and several others in cow, mouse, rat, and horse were subsequently identified by homology screens, establishing the basis of a distinct gene family[248].

Further evidence for ion conductance was gained by heterologous overexpression of various ClCAs from several species in HEK293 human embryonic kidney cells. For many but not all ClCAs, their overexpression increased the total cell current, though the contribution of Cl^- or anions to the total current was not established in these expression systems, nor were background currents assessed[249]. Nevertheless, these currents were blocked by DIDS and DDT for human, murine, and bovine ClCA1[246,250,251], as well as human ClCA2[252], consistent with early reconstitution studies. Patch-clamp studies in whole cells[250,253] and single-channels[251] in hClCA1-transfected HEK293 cells demonstrated a calcium-induced ion flow at 2 mM and 1 mM concentrations respectively, concentrations that far exceed physiological ranges.

1.2.4.2 ClCAs Have Structural Characteristics Inconsistent with Ion Channels

Early topology studies on ClCA proteins showed conflicting results. By *c*-myc epitope insertion and hydropathy plot analyses, four TM domains were predicted in ClCA2 following an *N*-terminal signal sequence[251], but this early model was problematic for two reasons. First, this arrangement predicted a TM region within the conserved von Willebrand factor type-A soluble domain, which would require domain-disrupting rearrangements to become TM[249]. To support this idea, a model was generated in which the von Willebrand factor type-A domain was intact, resulting in a singular TM topology of ClCA2[254]. Second, insertion of recombinant tags for topology screening in ClCAs impair its conformation-dependent proteolytic processing[255–257]. The tags therefore seem to have altered the ClCA conformation giving misleading results. Third, the topology of other ClCA members provides no unifying consensus on which to base their structure. Glycosylation scanning and protease protection assays suggested that hClCA2 spans the membrane five times[252], while cloning of hClCA3 reveals that it is expressed as a truncated *N*-terminal domain lacking any TM segments[253]. On the basis of these structural inconsistencies, weak evidence for Cl^- conductance, and divergent functions not attributable to ion conductance, experts in the field raised doubt that ClCAs form true membrane-spanning ion channels, instead suggesting that ClCAs were activators of endogenous Cl^- channels[253,258,259].

Revised models of ClCAs using improved sequence analysis, and revised experiments now depict these proteins as soluble secretory proteins[260,261], though some members associate with the PM by a single *C*-terminal TM α-helix[262] or a GPI anchor[263]. Therefore, the ClCAs lack the structural requirements to form true TM ion channels, and this gene family is no longer considered a class of Cl^- channels, despite their initial discovery as such[249,261].

As a whole, much less is known about anion channels than their cation channel counterparts[151]. Progress in this field has been hampered by insufficient availability of three-dimensional structures[219]. The progression of the ClCA family's status as a Cl^- channels to that of an unspecified function is not unique to this family, and in the next chapter, the CLIC family of proteins with similar problems will be discussed to establish the background of this thesis.

1.3 Chloride Intracellular Channel (CLIC) Proteins

CLIC proteins form a conserved family of proteins in most eukaryotes[264], and recent findings of a bacterial CLIC homolog establish an ancient lineage of this gene family[265]. In vertebrates, six conserved paralogs CLIC1–CLIC6 have been identified through homology screening and isolation from tissue[207]. The defining feature of CLICs is an approximately 240 residue 'CLIC module' which is structurally homologous to the Ω-class glutathione *S*-transferase (GST) superfamily[266]. Its homology to GST is based more structure than sequence, though several residues involved in gluthathione (GSH) binding or catalytic activity are well conserved[266]. Recently, enzymatic activity of several CLICs has been demonstrated, so CLICs may function as catalytically active enzymes in various signaling pathways[267]. CLICs vary immensely with respect to their tissue distribution and subcellular localization, with some members displaying extremely specialized tissue expression. Despite their discovery and initial classification as ion channels, the function of CLICs described in various cellular processes including cell cycle regulation[268], differentiation[269], cytoskeletal remodeling[270], membrane trafficking[271,272], and apoptosis[273] is not obviously attributable to ion conductance. In fact, their initial classification as ion channels has biased many studies to treat them as channels without regard to their true functional behaviour[274], similar to the now questionable classification of ClCA proteins as ion channels.

1.3.1 Discovery of the CLIC (p64) Gene Family

1.3.1.1 p64 Is the Founding Member of the CLIC Family

The search for novel Cl^- channels in the 1980s was hindered by the scarcity of good pharmacological ligands. In a search for inhibitors, Landry *et al.* identified indanyloxyacetic acid-94 (IAA-94) as a potent Cl^- channel blocker with an inhibition constant K_i of 1 μM[275]. An affinity resin based on IAA-94 was subsequently used to isolate a 64 kDa protein in a mixture with others from bovine kidney cortex vesicles. This protein conferred [$^{36}Cl^-$] uptake when reconstituted into liposomes and planar bilayers[276]. The p64 protein was purified and shown to be the sole protein responsible for the observed Cl^- conductance after reconstitution into phospholipid vesicles[277]. Furthermore, Cl^- currents in bovine kidney microsomes were abolished by antibodies against p64, thereby establishing p64 as a putative Cl^- channel[277]. The *p64* gene was eventually cloned from a bovine kidney cDNA library and found to encode a

437-residue protein with two putative TM regions across all species tested[278]. It was extracted from microsomal fractions of a *Xenopus laevis* oocyte overexpression system, and so was designated as an intracellular anion channel[278].

1.3.1.2 Additional CLICs Were Discovered by Cloning & Interaction Studies

Genes homologous to *p64* were found in various rat tissues[279] and raised the possibility that p64 could form the basis of a novel gene family. A homologue, *p64H1,* was cloned from rat brain and found to encode a smaller protein consisting of 253 amino acids, notably lacking the *N*-terminal region of p64[280]. Similarly, the first cloned human homologue, named the nuclear chloride channel-27 (NCC27) on the basis of its nuclear localization by immunofluorescence (IF) staining and nuclear fractionation[281] also lacked the N-terminal domain of p64. Upon the cloning of another human p64 homologue *XAP121*, the nomenclature as the chloride intracellular channel (CLIC) was proposed in 1997, and NCC27 was renamed CLIC1 and XAP121 as CLIC2[282].

Unlike CLIC1 and CLIC2, human CLIC3 was identified in a yeast two-hybrid screen using the *C*-terminal tail of the mitogen-activated protein kinase (MAPK) member ERK7 as bait, thus identifying the first known interaction between this putative ion channel and a MAPK signaling protein[283]. Like CLIC1, CLIC3 was found to have nuclear localization by IF staining of FLAG-CLIC3-transfected CV-1 cells, and conferred a Cl^--associated current in CLIC3-transfected LTK cells[283]. The human homologue of p64H1 was cloned from a retinal cDNA library[284] and eventually re-named CLIC4[285]. By immnohistochemical staining and immunoblot analysis, CLIC4 was shown to associate with endocytic vesicles and cytoskeletal components[284]. The mouse homologue *mtCLIC* was cloned from keratinocytes in the same year with 98% sequence identity to CLIC4 and had both mitochondrial and cytoplasmic localization, as demonstrated by IF staining and subcellular fractionation[286].

The 32 kDa CLIC5 protein was discovered from human placental microvilli extracts[287], which were affinity purified using a GST-conjugated *C*-terminal sequence of the membrane-cytoskeletal linking protein ezrin[115]. It turns out that this protein, named CLIC5A, is an alternatively spliced variant of p64 (CLIC5B). Given that CLIC5A is the central focus of this thesis, its identification will be described in further detail in section 1.5.1.

The latest CLIC member CLIC6 was discovered in a search for phosphoproteins in [^{32}P]-loaded rabbit gastric glands in response to acid secretion[288]. A phosphoprotein which translocated from the cytosol to membrane-rich fractions during acid secretion was cloned a year later from a rabbit cDNA library, and was identified as a CLIC due to its 75.3% identity with the *C*-terminus of bovine p64[289]. The gene coded for a 637 amino acid protein with a predicted relative molecular mass of 65 kDa, and since it was enriched in parietal and choroid cells, was given the name parchorin[289]. By IF staining, green fluorescent protein (GFP)-CLIC6-transfected LLC-PK1 cells displayed a diffuse cytoplasmic localization that was translocated to the PM when the cell medium was replaced with a Cl^--free medium[289]. Human CLIC6 was eventually cloned three years later, and truncated GFP-CLIC6 mutants appeared to localize in the cytoplasm based on IF staining in COS-7 cells[290].

In summary, six mammalian *CLIC* genes, with several isoforms produced by alternative splicing, have been discovered (Table 4). These CLICs vary widely in tissue distribution and subcellular localization, with no members being exclusively localized to one compartment. Many CLICs appear to translocate between subcellular sites, and this translocation, discussed in detail below in Section 1.3.3.5, seems to relate to their function.

CLICs are highly conserved in both nucleotide and protein sequence (Figure 7). CLIC5B and CLIC6 are unique in the gene family in that they possess much longer *N*-terminal domains than other CLICs, which are not homologous to each other or to any other known gene family. Aside from those exceptions, within the human CLIC family, paralogues show between 53 – 67% sequence identity. It is also worth noting that the number of paralogues differ between vertebrate species. For instance, fish and lizard species do not express CLIC1, and teleost fish express a second copy of CLIC5[274]. CLIC proteins have also been discovered in invertebrate and prokaryotic organisms. These include the invertebrate CLICs in the fruit fly *Drosophila melanogaster* as *Dm*CLIC[291], and in the roundworm *Caenorhabditis elegans* as in EXC4 and EXL1[292]. In addition, four plant homologues *At*DHAR1–4, have been identified *Arabidopsis thaliana,* as well as SspA in Gram-negative bacteria[265]. Its discovery in prokaryotes and homology to GSTΩ proteins may indicate that higher-order CLICs evolved from bacteria, and this lineage shares a common ancestor with the GSTΩ family[265].

Table 4. Six mammalian CLIC paralogues have been discovered to date. The name of the CLIC and alternative names, such as the original designation prior to the unifying CLIC nomenclature, are given. All molecular weights (M_W) and lengths are reported for human CLICs. Molecular weights are calculated based on the amino acid (aa) sequence deposited on UniProt[293]. Tissue distributions were obtained from a review by Signh[264], with additional sources being cited in the Table. Subcellular localizations were reported specific to the cell lines or tissues studied, as shown in square brackets.

Name	M_W (kDa)	Length (aa)	Tissue Distribution	Subcellular Localization
CLIC1 (NCC27)	27	241	Broad; absent in brain, low in skeletal muscle	Cytoplasm, plasma membrane, endocytic vesicles [T84, Panc-1][294], nuclear envelope [CHO-K1[281]], ER [rat cardiomyocytes[295]]
CLIC2	28	247	Adult muscles, fetal liver	Cytoplasm, nucleus, plasma membrane [HEK293][296]
CLIC3	26	236	Placenta, heart, lung, kidney, pancreas, skeletal muscle	Cytoplasm, nucleus [LC-V1][283], secreted [Various][297]
CLIC4 (p64H1)	29	253	Brain, liver, testis, kidney, lungs, skeletal muscle	Cytoplasm & plasma membrane [human placenta][287], endocytic vesicles & cytoskeleton [rat hippocampal neurons][284], ER & outer mitochondrial membrane [mouse keratinocytes[273], L929, rat cardiomyocytes[298]], nucleus [BAE, COS-1, HeLa, JEG-3, MDCK[299], mouse & human keratinocytes[300,301]]
CLIC5A	28	251	Heart, kidney, lung, placenta, skeletal muscle, overexpressed in hepatocellular cancer cells[302]	Cytoplasm, plasma membrane, & cytoskeleton [human placenta[287], JEG-3[303], HepG2[302]], inner mitochondrial membrane [rat cardiomyocytes][298]
CLIC5B (p64)	46	410	Heart, cortex, skeletal muscle; absent in lung and kidney[304]	Cytoplasm & Golgi [HCA-7[305]], secretory vesicles[264], inner mitochondrial membrane [rat cardiomyocytes][304]
CLIC6 (parchorin)	73	704	Choroid plexus, gastric mucosa	Cytoplasm [LLC-PK1[289], COS-7[290]], plasma membrane [LLC-PK1[289], HEK293[306]]

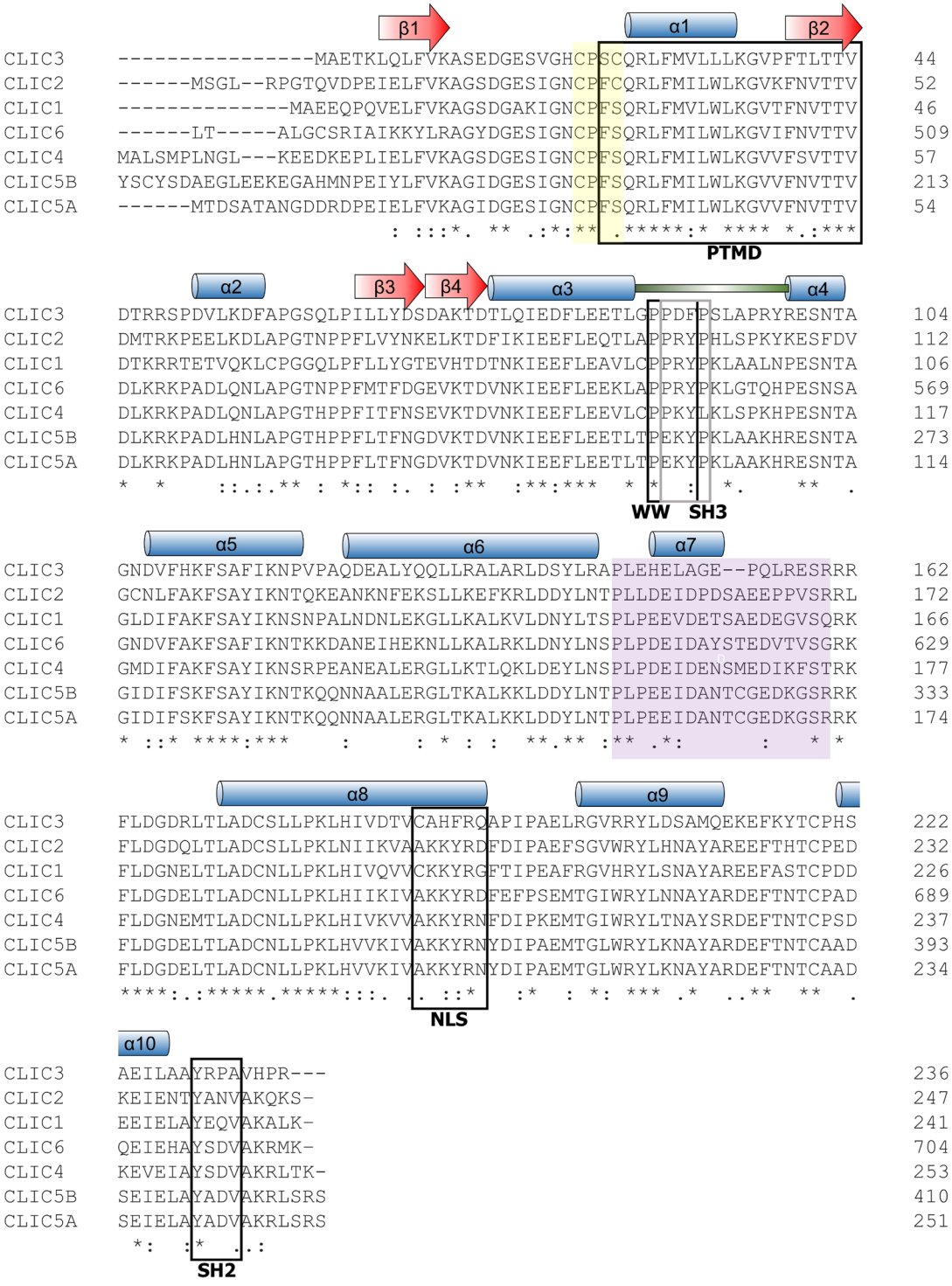

Figure 7. CLIC proteins are highly conserved. Secondary structures are depicted above the sequence with α-helices as cylinders, β-strands as arrows, and the interdomain linker as a green box. A conserved motif within the thioredoxin domain homologous to GSTΩ containing a reactive cysteine is highlighted yellow, and the anionic foot loop of the *C*-terminal domain in magenta. Boxed are the putative transmembrane domain (PTMD) and the speculated WW [PPXY], SH2 [PYXX(V/I)], and SH3 [PXXP] domain binding motifs, as well as the nuclear localization signal (NLS) as defined for CLIC4.

1.3.2 The Ion Conductance of CLICs

1.3.2.1 CLIC1 has the Most-Studied Ion Currents In the CLIC Family

Given the initial discovery of the founding p64 as a Cl^- channel[277,278], all subsequent CLIC proteins identified on the basis of homology were methodically screened for Cl^- channel activity[274]. Yet even in the early beginnings of the CLIC family, their status as Cl^- channels was met with scepticism[207] for reasons discussed below. Nevertheless, ion channel activity has been demonstrated for most CLIC proteins, and scrupulous studies over two decades have firmly established that CLICs do indeed conduct currents, at least *in vitro*[264].

The first indication that CLICs form intracellular channels[278] prompted researchers to employ methods specific to intracellular, rather than PM, ion channels. Generally, such methods bring intracellular channels to a surface where they can be measured by reconstitution into artificial bilayers or liposomes, overexpression, or engineered targeting sequences[264]. The ion conductance of bovine p64, for instance, was studied by reconstituting crude kidney microsome fractions into PC liposomes[277]. Because these preparations are impure, the specificity of ion conductance must be demonstrated by an antibody or inhibitor, as was demonstrated by the IAA-94- and anti-p64-abrogation of ion current[277]. Ion conductance was demonstrated by NCC27 (CLIC1) through whole-cell and nuclear patch clamp in a CHO-K1 overexpression system[281] and later in untransfected CHO-K1 cells[268]. Notably, CLIC1 conductance at the PM was almost undetectable in untransfected cells, which illustrates the potential of creating artefactual channel activity by overexpression[268,281]. These experiments established an anion selectivity order of $SCN^- > F^- > Cl^- > NO_3^- > I^- = HCO_3^- > CH_3COO^-$ for CLIC1, and showed that these currents were IAA-94-sensitive, though only at concentrations exceeding 10 μM[281]. It remains probable that CLIC1 is a modulator of endogenous anion channels, since whole-cell currents were similar across three untransfected cell lines[307].

Studies using purified recombinant protein demonstrated that CLIC1 could confer ion conductance in the absence of any other protein. Reconstitution of pure recombinant CLIC1 to isolectin vesicles conferred Cl^- efflux that was IAA-94-sensitive, though once again only at a high concentration of 50 μM[308]. Reconstitution of pure CLIC1 into PC bilayers by tip-dip resulted in currents nearly identical to CLIC1-transfected CHO cells[309,310]. However, these currents could not be reproduced when CLIC1 was reconstituted into planar PC bilayers, and

only displayed conductance when a 4:1:1 lipid mixture of palmitoyloleoylphosphatidylcholine (POPC)-to-palmitoyloleoylphosphatidylethanolamine (POPE)-to-cholesterol was used[311], corroborating earlier reports that CLIC1 requires specific lipids for channel activity[312]. These findings were further supported by observations that although CLIC1 can readily insert into monolayers of various lipids, channel activity was only minimal unless they were supplemented with cholesterol[311]. Curiously, this study reported a different anion selectivity order than was reported previously, this time displaying little to no anion selectivity[311]. Overall, single-channel conductance values have ranged from 6–120 pS for CLIC1[264], which show considerable variation but is within the typical range of an ion channel[313]. This variation has been attributed to differences in lipid composition, redox conditions, or pH, all of which are known modulators of CLIC1 function and ion conductance[264].

1.3.2.3 The Ion Conductance Of Other CLICs Have Also Been Studied

To date, ion conductance has been demonstrated in CLIC2, CLIC4, CLIC5A, and CLIC5B, as well as in the invertebrate homologues *Dm*CLIC and *Ce*EXC4[264] and the prokaryotic homologue *Ec*SspA[265], by various methods. Like CLIC1, CLIC4 was immediately tested for ion conductance on the basis of its homology to p64. The first study to demonstrate its ion conductance reconstituted crude microsomal fractions containing CLIC4 into planar POPC/POPS bilayers, which resulted in a small current, though it was poorly selective for anions and was neither IAA-94 nor DIDS-sensitive[280]. On the other hand, reconstitution using purified recombinant CLIC4 into planar bilayers containing POPS:POPE:cholesterol in a 4:1:1 mixture, based on earlier observations that CLIC4 localized to cholesterol-rich caveolae[285], showed a similar lack of selectivity between anions, though it established that CLIC4, like CLIC1, could be regulated by redox conditions[314].

The ion conductance of CLIC5A was first investigated by reconstituting the recombinant protein into isolectin vesicles, which established a Cl^- efflux that was CLIC5A-concentration-dependent and IAA-94-sensitive at 50 μM[303]. Later, reconstitution into planar POPC:POPE:cholesterol bilayers showed that CLIC5A displayed even poorer selectivity than either CLIC4 or CLIC1, being unable to even discriminate between anions and cations[315]. Strangely, the reconstituted CLIC5A in this study displayed multiple conductances, ranging from 3–116 pS under the same conditions[315]. One theory posits that each conductance

corresponds to a different multimeric state, but these claims remain untested[307]. In another study, the ion conductance of CLIC1 and CLIC5A, but not CLIC4, was inhibited by pure filamentous-actin (*F*-actin) added to the 'cytosolic side'[315], suggesting these proteins may be regulated by actin similarly to CFTR[316], though no actin-binding elements were observed.

Therefore, it is currently accepted that most CLICs can induce ion channel activity, at least *in vitro*, although conflicting reports and variable conductance rates and selectivities need to be consolidated. Notably, overexpression of CLIC6 in HEK293 cells had no effect on ion conductance[306], nor is there evidence that CLIC3 possesses anion channel activity. The channel activity of CLICs is strongly lipid, pH, and redox-dependent, and varies considerably between CLICs. Most CLICs are poorly selective for anions, with CLIC5A being unable to discriminate between anions and cations, prompting some to recommend a change in nomenclature to distinguish them from true anion channels[264,315]. Ion channel activity has yet to be proven *in vivo*, but CLICs are still tentatively classified as anion channels[207,264,274,317].

1.3.3 Biochemical Features of CLICs

1.3.3.1 CLICs Are Structurally Inconsistent with Ion Channels

Much like the ClCA family of proteins whose function as ion channels has been disproven, CLIC proteins do not fulfill expectations established for conventional ion channels. Even before the acquisition of structures, hydropathy analyses of bovine p64 predicted only two putative transmembrane domains (PTMDs)[278], and as more CLICs were cloned, this number fell to one, located in the *N*-terminus[314] (Figure 7). A singular TM segment is highly unusual among ion channels, though this does not exclude the possibility of pores being formed at the interface of oligomers, as proposed by Singh & Ashley[314]. The importance of the *N*-terminus for membrane association was established by reconstituting an *N*-terminal truncated CLIC4 mutant in planar bilayers, which was still able to confer conductance[314]. Strangely, the non-homologous *N*-terminal region of CLIC5B appears to confer PM localization, while its conserved *C*-terminal domain prevents it, as revealed by truncation mutants[307]. This phenomenon has not been explored in other CLIC proteins.

Furthermore, CLICs are much smaller than typical ion channels, with molecular weights ranging from 26–73 kDa. Notably, another small protein thought to form ion channels,

the 8.4 kDa phospholemman, was eventually found to be a modulator of endogenous channels rather than a channel itself[318]. Sequence analysis further reveals that CLICs lack a signal sequence, raising the question of how CLICs insert into membranes in the first place[307]. The first X-ray structure of the CLIC family, CLIC1 (PDB ID 1K0M), was obtained as a soluble, globular protein and confirmed the sequence-based predictions that CLICs bore similarity to GSTO1[319] with a GSTΩ-like structure consisting of an *N*-terminal mixed helical-pleated thioredoxin-like domain, and an all-helical *C*-terminal domain[309] (Figure 8). GSTO1 is a soluble protein with no reports suggesting that they form ion channels[319]. Comparison of GFP-tagged GSTO1 and *Ce*EXC4 reveal that the former is strictly cytoplasmic while the latter readily localized to membranes, suggesting that membrane association is a property specific to CLICs rather than the GSTΩ-like superfamily[292].

The X-ray structure of CLIC1 demonstrated that the PTMD actually spans α-helix 1 (α_1) and β-strand 2 (β_2), and is situated within the conserved thioredoxin motif[309]. Thus, in order to expose this region to associate with membranes, domain-disrupting conformational changes would be required in a fashion similar to amphitropic or pore-forming proteins, as discussed above[307]. To date, X-ray structures of CLIC1 (PDB ID 1K0M)[274], CLIC2 (PDB ID 2R5G)[320], CLIC3 (PDB ID 3KJY)[321], and CLIC4 (PDB ID 2D2Z)[322], as well as homologues in, *Yp*SspA (PDB ID 1YYV), *Dm*CLIC (PDB ID 2YV7) and *Ce*EXC-4 (PDB ID 2YV9)[291] have been solved, and all show folds similar to GSTO1 (Figure 8)[323]. Interestingly, the asymmetric units in these structures ranged from dimeric in hCLIC1 to trimeric in hCLIC4, though the biological quaternary state for most CLICs appears to be monomeric. Notably, the presence of multiple conductance levels in reconstituted CLIC5A, as well as the variability of conductance measurements between different CLICs, is hypothesized to be a function of distinct multimeric states[264,307], though this hypothesis has not been tested so far.

1.3.3.2 CLICs are Dimorphic and assume at least two stable forms

While the X-ray structures above would lead one to reason that CLICs are typical soluble proteins, extensive ion channel studies (see above), in addition to cellular and biophysical methods have firmly established that CLICs associate with membranes. For instance, microsomal fractions retained recombinant CLIC4, resistant to alkali washes and

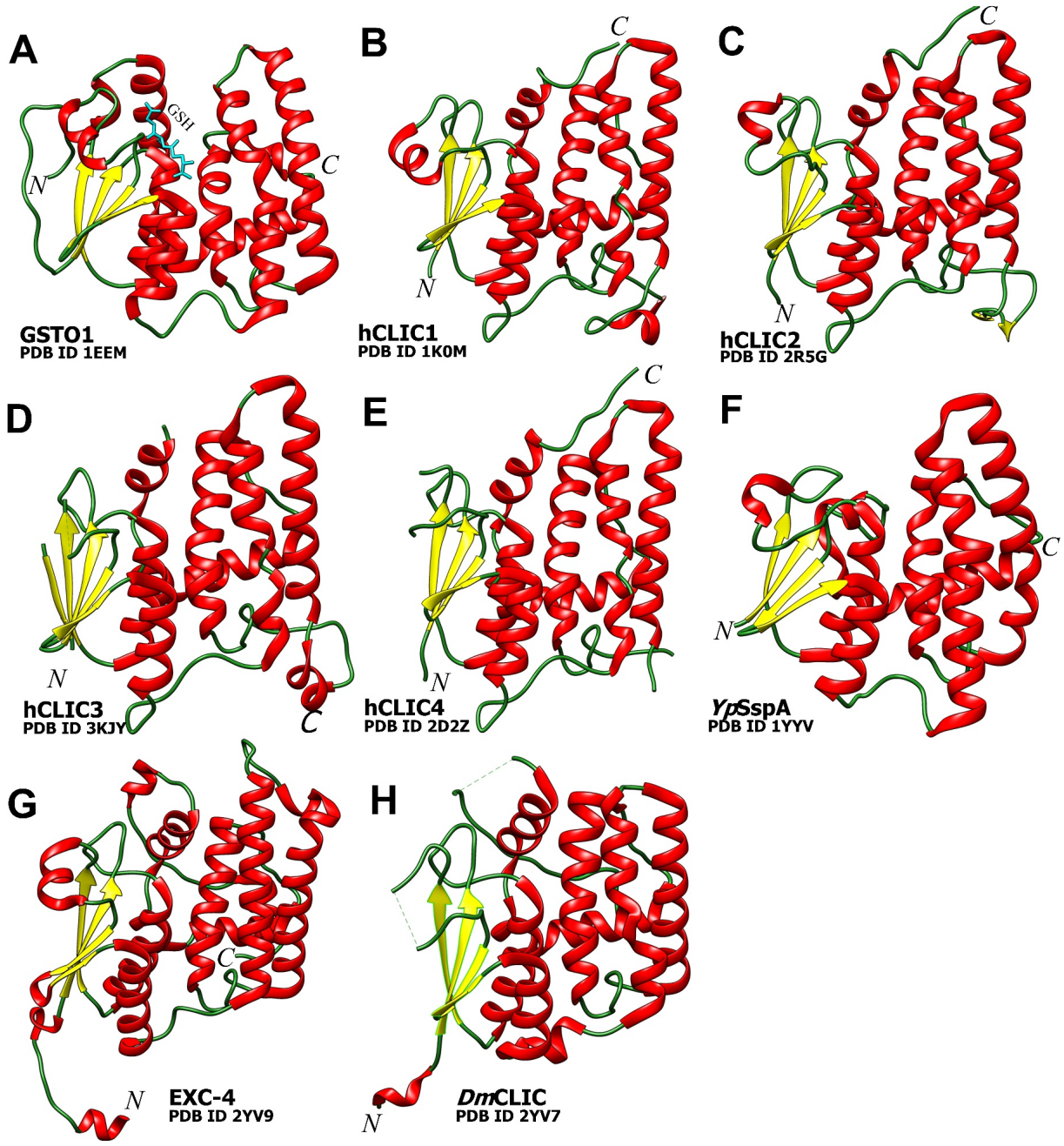

Figure 8. CLIC proteins are defined by an *N*-terminal module which is structurally homologous to GSTΩ. To date, X-ray structures of human CLIC1 – CLIC4 and homologues in *Y. pestis* as *Ys*SspA, *C. elegans* as EXC-4, and *D. melanogaster* as *Dm*CLIC, have been solved. All CLICs are structurally homologous to the GSTΩ member GSTO1, shown here complexed with its glutathione (GSH) ligand, by sharing a mixed helical/pleated *N*-terminal domain joined by an all-helical *C*-terminal domain. The CLIC putative transmembrane domain is situated within the *N*-terminal domain of the GST fold, and spans across an α-helix and β-strand across all structures.

protected from proteolytic hydrolysis, suggesting that CLIC4 forms TM associations with bilayers[280]. Furthermore, in GFP-CLIC4-transfected SP1 keratinocytes both endogenous and exogenous CLIC4 was observed in membrane fractions, though significant amounts were also retrieved in cytoplasmic fractions[286]. Patch-clamp measurements of FLAG-epitope tagged CLIC1[324] and CLIC4[325] in transfected CHO-K1 and HEK293 cells respectively displayed a reduced current when targeted with anti-FLAG in outside-out, but not inside-out configurations, suggesting these proteins were transmembrane with their *N*-terminus oriented outward. Biophysical methods have also demonstrated association of CLICs with lipid bilayers. Purified CLIC1 was found to associate with PC-cholesterol liposomes in a pH-dependent fashion[310]. CLIC1 has also been demonstrated to insert into artificial hemibilayers containing POPC or equimolar POPC/POPE as measured by membrane expansion under constant lateral pressure[311], and a similar association has been recently measured by X-ray and neutron scattering in POPC and POPS monolayers in a phosphatidylserine (PS) and cholesterol-dependent manner[326]. Similarly, pure CLIC4 bound to artificial PC liposomes in a concentration-dependent manner as detected by surface plasmon resonance[327]. The membrane localization of CLICs have also been demonstrated *in vivo* by immunogold electron microscopy for CLIC5B in avian osteoclast tissue[328] and for CLIC5A in mouse podocyte and glomerular endothelial cells[329].

The sequence and structural homology to GSTΩs led researchers to investigate if CLICs could be modified by redox. Cys-24 in CLIC1 was of particular interest because it was situated within a CxxC thioredoxin active site motif (CPFS in CLIC1), which mediates the formation, isomerization, and reduction of disulfide bonds in their native redox proteins[330]. Indeed, the X-ray structure of CLIC1 reveals that it covalently binds to GSH through a disulfide bond with Cys-24, though this site is more open with fewer GSH interactions than in GSTΩs[309]. CLIC1 reversibly dimerized in 2 mM H_2O_2 and 50 mM DTT respectively, as demonstrated by gel filtration. A high-resolution X-ray structure of the oxidized form was solved (PDB ID 1RK4) under the same H_2O_2 concentration in a dimerized state[331] (Figure 9). Intriguingly, several large-scale structural transformations occur in CLIC1 when oxidized by H_2O_2. While the *C*-terminal domain remains intact, the *N*-terminal domain containing the PTMD converts from a mixed helical/pleated structure to completely helical, with slight extension of helix 2. Alongside, Cys-24 forms a disulfide bond with Cys-59, which is normally

kept 13.1 Å apart when reduced (Figure 9). The importance of these residues in dimerization was shown by point mutations at these sites, which abrogated dimerization as assessed by gel filtration[331]. The dimerization interface is formed between sheets of helices and is predominantly hydrophobic[331].

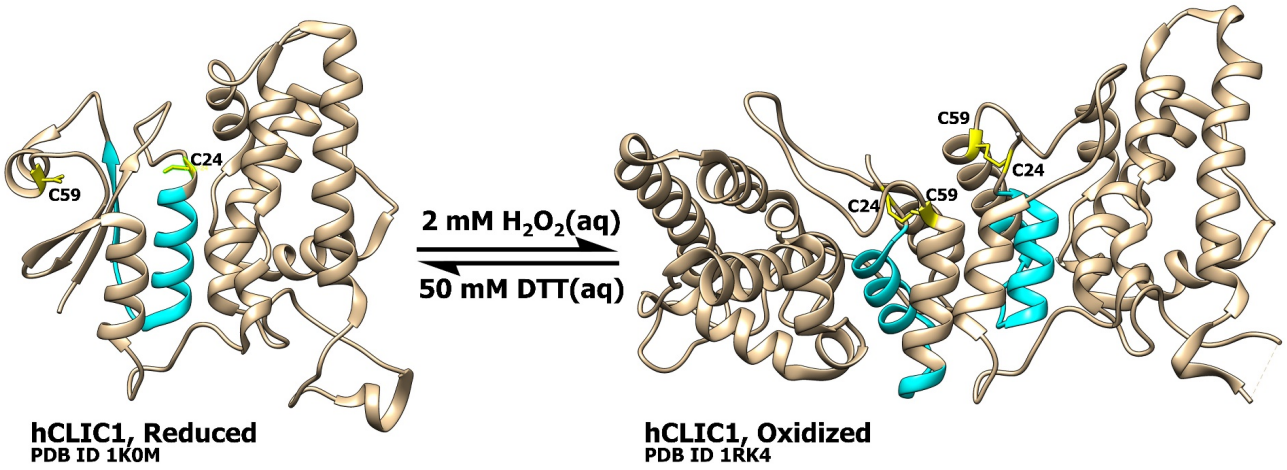

Figure 9. CLIC1 can be oxidized *in vitro* to undergo dramatic structural transitions. X-ray structures of CLIC1 under reducing [Left] and oxidizing conditions with 2 mM H_2O_2 [Right] reveal large-scale structural rearrangements that are mediated by the formation of a disulfide bond between Cys-24 and Cys-59 (yellow) to form an entirely helical dimer. Gel filtration studies suggest that this dimerization is be reversible by 50 DTT. The putative *N*-terminal transmembrane domain is coloured cyan.

Based on these structures, the authors postulated that in the presence of lipids, a conformational change targets a conformationally-altered oxidized form not isolated in this study, while the absence of lipids facilitates this dimeric form[331]. While appealing, this model is problematic for at least three reasons. First, Cys-59 is notably missing in other CLICs, which makes a disulfide-mediated conformational change less likely as a universal mechanism of membrane insertion[264]. Nevertheless, Cys-24 is well-conserved among CLICs and is implicated in the redox-regulation of CLIC1, CLIC4, and CLIC5A[264]. The invertebrate *Ce*EXC4 lacks a Cys-24 at a homologous site and is thus not under redox control[291]. Further, a C24A CLIC1 mutation eliminated the redox sensitivity in conductance measurements, though it still formed functional channels[311]. Secondly, Cys-24 and Cys-59 are situated on opposite sides of the PTMD and thus would be unable to form disulfide bonds. Finally, the H_2O_2 concentrations of 2 mM used in these studies far exceed those of physiological limits,

which is dynamic and ranges from 1–10 μM corresponding to oxidative eustress and stress, respectively[332].

Until a three-dimensional structure of a membrane-associated form is solved, the exact conformational changes mediating membrane binding of CLICs remain elusive. Nevertheless, the structures have provided the first evidence that CLIC1 and likely other CLICs exist in more than one stable state, supporting their classification as metamorphic proteins within the class of dimorphic proteins[274], an unusual trait for ion channels. Metamorphic proteins are discussed in Section 1.4. The elusive membrane-bound structure of CLIC1 has been predicted in PC:cholesterol liposomes using fluorescence energy transfer (FRET) and electron paramagnetic resonance (EPR) studies designed to measure interatomic distances in fluorophore- and EPR-labeled cysteines[333]. This model predicts that in a membrane-bound state, the *C*-terminal domain separates from the *N*-domain to reside on the surface of the bilayer, favoring predictions that the PTMD is buried (Figure 10). During the transition, the *N*-terminal domain was predicted to refold into an all-helical domain, similar to the X-ray structure of oxidized CLIC1.

1.3.3.3 The Association of CLICs to Membranes Is Redox- and pH-Mediated

Based on the findings that CLIC1 could be oxidized, the effect of redox was widely investigated to define the significance of redox control of CLIC protein function. Indeed, the *N*-terminal cysteine within its thioredoxin-like motif is conserved among all mammalian CLICs (Figure 7) and its reactivity has been demonstrated by Cys-labeling studies in CLIC1, CLIC4, and CLIC5A[334]. While the notion that CLICs possess enzymatic functions is gaining recognition[267], what remains unclear is whether the redox reactivity is associated with the dimorphic conformational switch in CLICs. As described above, H_2O_2 treatment formed CLIC1 dimers by gel filtration[331]. In PC:cholesterol liposomes, dimeric CLIC1 resulted in significantly higher Cl^- efflux than the monomeric form, though comparable conductances were seen for both states when reconstituted in PC monolayers absent in cholesterol[331]. Using PC:cholesterol liposomes in fluorescence quenching assays, it was shown that monomeric CLIC1 more readily associates with vesicles in response to 2 mM H_2O_2 than dimeric CLIC1, suggesting the dimerized form of CLIC1 is not the form that associates with membranes[335]. Moreover, this study suggests a membrane-associated form is likely oxidized

in some way. These findings are further supported by a recent study utilizing tethered bilayers made with PC-like lipids and cholesterol, which demonstrated higher conductance measurements for monomeric CLIC1 than dimeric CLIC1[336]. Notably, the presence of CLIC1 at plasma and nuclear membranes was enhanced in Alzheimer's disease models, a disease state associated with elevated reactive oxygen species (ROS) levels[337], which also coincided with an increase in overall total conductance in these cells[338,339]. Recent studies have established

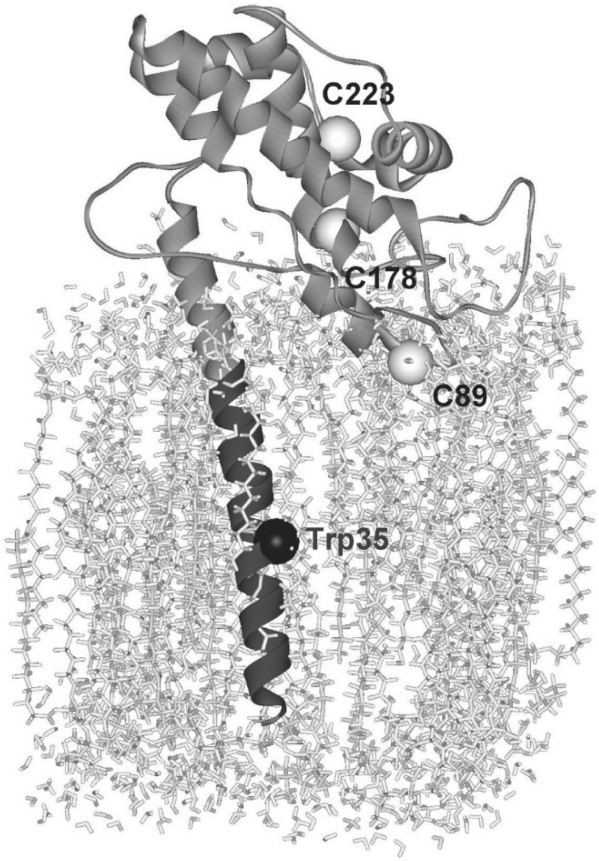

Figure 10. The membrane-bound structure of CLIC1 was modeled using distances obtained from FRET and EPR. In their study, Goodchild and colleagues substituted all cysteines in human CLIC1 except for one to alanine across multiple constructs in order to generate singly-reactive cysteines for labeling. For FRET analysis, the fluorophore IAEDANS (5-iodoacetamidoethyl-aminonapthalene-1-sulfonic acid) was used as a FRET donor, and Trp-35 as the FRET acceptor. Similar measurements were also made using the EPR label MTSSL (3-methylthiosulfonyl-1-oxyl-2,2,5,5-tetramethyl-3-pyrroline). Measurements were performed using purified CLIC1 in liposomes composed of soybean phosphatidylcholine and cholesterol in a 10:1 ratio to obtain interatomic distances, which were used to create this model. [Reprinted with permission from Goodchild, S.C., *et al.* 2010. Metamorphic Response of the CLIC1 Chloride Intracellular Channel Ion Channel Protein Upon Membrane Interaction. *Biochemistry* 59:5278–5289. ©2010, American Chemical Society.]

that the enzymatic activity of CLIC1 is mediated through its conserved thioredoxin Cys-24, and is inhibited by IAA-94[336,340].

Unlike CLIC1, CLIC4 remains monomeric with H_2O_2 treatment, which is predictable since it lacks the homologous Cys-59 of CLIC1 to form a disulfide bond[327]. However, in the presence of H_2O_2 there was a dramatic increase of CLIC4 association with PC liposomes detected by surface plasmon resonance, and under reducing conditions with DTT treatment, its channel activity in planar PC bilayers was abrogated, suggesting that CLIC4 was also under some form of redox control[327]. The X-ray structure of CLIC2 (Figure 8) shows a disulfide bond between the two cysteines of its thioredoxin motif, Cys-30 and Cys-33, but since CLIC2 has no Cys residues at a position homologous to Cys-59 it did not dimerize with H_2O_2 treatment[320]. Interestingly, even when Cys was introduced in CLIC2 at a position homologous to Cys-59 in CLIC1, dimerization was not observed, strongly suggesting that dimerization is unique to CLIC1. Nevertheless, channel activity was eliminated in planar PC bilayers with DTT treatment, necessitating the role of a disulfide for ion conductance, at least *in vitro*[320].

Similarly, an intramolecular disulfide bond was seen within the thioredoxin motif of CLIC3 in its oxidized form (PDB ID 3FY7), mediated by its Cys-22/Cys-25[321]. But the structure with disulfide bond was practically identical to that in the reduced state (PDB ID 3KJY), further supporting that CLIC1 dimerization is a specific, not general, trait (Figure 11)[321]. The authors reported that CLIC3 crystals nucleated more readily under oxidizing conditions, though functional studies akin to the other CLICs were not done in this study[321]. Like CLIC1, CLIC3 possesses enzymatic activity through its conserved thioredoxin cysteine, and its physiological substrate was identified as transglutaminase-2, and has been identified as a secreted protein *in vitro* and *in vivo*[297]. To date, no studies have investigated the effects of redox on CLIC5A, CLIC5B, or CLIC6, apart from demonstrating that the thioredoxin Cys is reactive to a Cys-labeling reagent in CLIC5A[334]. However, nigericin-induced activation of the NLRP3 inflammasome, which is downstream of ROS activation[341], results in translocation of CLIC1, CLIC4, and CLIC5A to membrane fractions in marrow-derived macrophages[342].

On the basis of its low isoelectric point of 5.1[343], CLIC1 was predicted to be pH-sensitive. Indeed, the incorporation of recombinant CLIC1 into PC:cholesterol liposomes was significantly enhanced at pH 6.5 compared to pH 7.4, and this corresponded with a faster onset

of channel activity in planar PC bilayers[310]. Because many pore-forming proteins insert to membranes by an acid-destabilizing process due to a low local pH proximal to bilayers, CLIC1 was investigated to see if it might associate with the bilayer as a molten globule[184]. CD spectroscopy and fluorescence measurements indicated that while the secondary structure of CLIC1 remains intact at low pH[310], CLIC1 did not assume features of molten

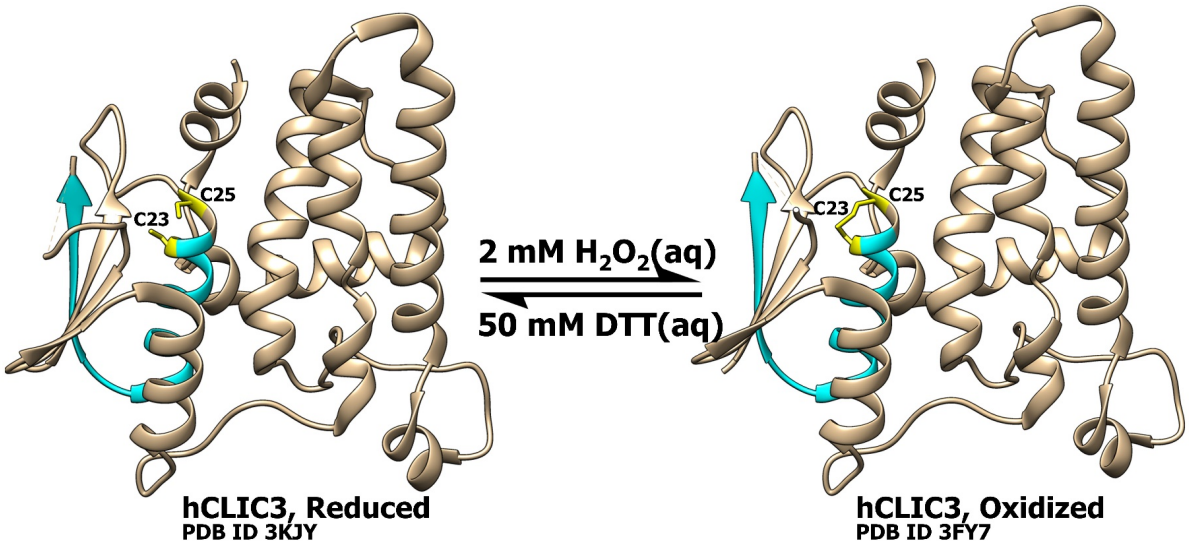

Figure 11. CLIC3, unlike CLIC1, does not undergo dramatic structural transformations when oxidized. As shown by their X-ray structures, CLIC3 forms a disulfide bond between the two Cys residues located within its thioredoxin motif (yellow), however unlike CLIC1 this is not accompanied by dimerization or large-scale structural transitions. The putative membrane-associating region is coloured cyan.

globules[344]. Instead, CLIC1 assumes a destabilized unfolded intermediate conformation at an acidic pH, as suggested by denaturation studies[344]. Hydrogen-deuterium exchange studies further demonstrated that acidic conditions destabilize the *N*-terminal domain significantly more than the *C*-terminal domain, suggesting that this domain could potentially refold to expose its PTMD as a method of membrane insertion[345]. Mutagenesis studies subsequently identified His-74 and His-185 as mediators of this pH-induced destabilization[346], though only the latter is conserved in CLICs (Figure 7). Overall, these studies offer an appealing pH-mediated mechanism of membrane insertion for CLIC1 that does not involve oxidation, though it remains to be studied in other CLICs. CLIC4-induced Cl^- efflux showed a partial dependence

on pH though not as significantly as CLIC1[327], and similar reports exist for CLIC2, *Dm*CLIC, and *Ce*EXC4[274], though none have been studied to the same extent as CLIC1.

1.3.3.4 CLICs Require Certain Lipids To Associate With Membranes

The first indication that CLICs require a particular lipid environment to bind to membranes was revealed when pure CLIC1 could elicit Cl^- efflux only when reconstituted into liposomes supplemented with the anionic phospholipids PS and phosphatidic acid[312]. Similarly, ion conductance was greater for CLIC4 when reconstituted into brain microsomes than in pure PC planar bilayers[280,311]. Consistent with the observation that CLIC4 frequently localized to cholesterol-enriched caveolae[285], CLIC1 was only able to generate anion currents when reconstituted into bilayers supplemented with cholesterol, though cholesterol had an inhibitory effect on conductance for reasons not explored[311]. An impedance spectroscopy study revealed that CLIC1-mediated membrane conductance was directly proportional to the cholesterol content of tethered bilayers[347], with similar behaviours in monolayers[347,348]. With the discovery of a GXXXG motif as a cholesterol-binding site in the amyloid precursor protein[349], it was speculated that this sequence, notably conserved in all CLICs (Figure 7), was responsible for the cholesterol dependence of CLIC1 binding. The HIV glycoprotein fusion protein binds with a distinct cholesterol-binding motif LWYIK[350], which is conserved in all CLICs except CLIC3 which contains the LWLKG variant (Figure 7), thus representing another possible motif. Unexpectedly, CLIC1 bound more readily to tethered bilayers made with the fungal steroid ergosterol than cholesterol at similar concentrations[336].

Recently, the interaction of CLIC1 with monolayers of several phospholipids in the presence and absence of cholesterol was determined with specular X-ray and neutron reflectometry, enabling the depth of insertion to be determined at the nanometre scale[326]. In the absence of cholesterol, no significant acyl chain insertion was measured, though insertion into the interfacial headgroup region was observed[326], suggesting the adsorption of CLIC1 to the monolayer surface akin to a peripheral protein. The presence of cholesterol increased acyl chain and interfacial insertion to 25.7 Å, with 30.6 Å remaining in the solvent[326]. Notably, this study demonstrates for the first time that CLIC1 can associate in multiple membrane-bound states: a membrane-adsorbed and membrane-inserted form[326]. Based on these findings, the authors proposed a two-step mechanism in which cholesterol enhances the adsorption of

CLIC1 to membranes through a recognition motif, and cholesterol subsequently stimulates conformational changes[326].

Despite the abundance of high-resolution structures, the precise conformational changes occurring during the association of CLICs with membranes is still not clear. What is known, however, is that CLICs exist in distinct soluble and membrane-associated states, which convert between each other through large-scale transitions, including the rearrangement of their unstable *N*-terminal domain. Despite these findings, the biological triggers inducing these structural changes have yet to be identified[264].

1.3.3.5 CLICs Display Differential Subcellular Localization

Corresponding to their dimorphism, CLIC proteins display differential subcellular localization that depends, at least partly, on cell type (Table 4). For instance, CLIC1 is expressed at the apical membranes of polarized columnar epithelial cells[294], diffusely in the cytoplasm of placental trophoblasts[287], and within intracellular organelles of cerebellar granule neurons[264]. The cellular status of the cell may also play a role, since the PM localization of CLIC1 is cell-cycle dependent, as indicated by channel activity which was only detectable in cells that are dividing or recently divided[281]. Similarly, the localization of CLIC1 in the human endometrium changes between the proliferative and secretory phases[351]. Their diverse localizations may be related to the wide variety of functions CLIC proteins may execute. For instance, the localization of CLIC1 in apical membranes of polarized cells could contribute to endocytosis or membrane recycling[294], and the nuclear localization of CLIC4 enhances TGFβ signaling by interacting with nuclear proteins[352].

Overexpression may disrupt the normal localization of these proteins, since channel activity is only detected in the nuclei of untransfected CHO-K1 cells, yet constitutively at the PM in transfected cells[281]. Similarly, while endogenous CLIC4 in HEK293 cells is primarily cytosolic, overexpressed CLIC4 localizes to intracellular membranes and the PM[325]. This overexpression-induced translocation may be associated with metastatic potential, as CLIC5A is overexpressed in hepatocellular cancer biopsies, and its binding partners ezrin and podocalyxin show irregular localization[302]. Further, the differentiation state of the cell may affect the localization of some CLICs. CLIC1 is notably absent in the nuclei of rat cardio-

myocytes, a terminally differentiated cell line[353], and CLIC4 is nuclear predominantly only in differentiating human and mouse keratinocytes[301].

Presumably, the diverse subcellular locales in which CLICs reside is the result of their translocation between different compartments which act in concert with interacting proteins, post-translational modifications (see below) and/or structural transformations. An X-ray structure of the CLIC4 nuclear localization peptide in a complex with the nuclear import protein α-importin establishes the importance of this motif for nuclear import[354]. Notably, this sequence is conserved across most CLICs (Figure 7), though not all CLICs show nuclear localization (Table 4), nor has this sequence been studied in other CLICs. Certain stimuli have been linked with the translocation of CLICs. Co-expression of CLIC1 with CFTR and activation of cAMP dependent pathways resulted in a redistribution of CLIC1 from soluble to membrane fractions in *Xenopus* oocytes, suggesting a cross-talk between CFTR and CLIC1[355]. Stimulation of BV2 microglial cells with Aβ peptides in an Alzheimer's disease model enhanced anion currents and was associated with the translocation of soluble CLIC1 to the PM accompanied with NADPH oxidase-mediated ROS production[338]. CLIC1 was also translocated to actin-enriched projections of the PM of invadopodia when these cells were cultured on a fibronectin matrix[356].

Both endogenous and GFP-CLIC4 rapidly translocated to the nuclei of mouse keratinocytes forced to undergo apoptosis in an *N*-terminal PTMD and *C*-terminal nuclear localization sequence-dependent manner[300]. Rapid translocation was observed in serum-starved GFP-CLIC4-transfected human cancer cell lines of soluble CLIC4 to the PM when treated with 1 μM lysophosphatidic acid (LPA), a GPCR agonist[357]. Both YFP-CLIC2 and YFP-CLIC4 mobilized from the cytosol to the PM of cell-cell junctions of HEK293 cells stimulated with various GPCR agonists, including LPA, strongly involving GPCR signaling in the translocation of these proteins[296]. However, CLIC4 also translocates to the nucleus upon lipopolysaccharide (LPS) stimulation in murine macrophages, which is coupled with the Toll-like receptor rather than GPCR pathway[358]. Lastly, CLIC6 has been shown to translocate to the PM from the cytosol in response to Cl^- depletion in the medium[289].

Thus, CLIC proteins are dynamic with respect to their subcellular localization, in keeping with functions extending beyond ion conductance. Indeed, differential localization to

this degree is highly unusual for ion channels and a cytosolic distribution would be highly unusual for an ion channel. What remains to be investigated are the cellular triggers that induce CLIC translocations, which may be mediated by post-translational modifications of CLICs[317].

1.3.3.6 CLICs Are Post-Translationally Modified

The first indication that CLICs could be phosphorylated came from the first study of bovine p64, which showed that currents mediated by p64-containing bovine microsomes were attenuated by ATP, suggesting an inhibitory effect of phosphorylation[275]. When p64 was sequenced, consensus sites for PKC, casein kinase-II, and a tyrosine kinase phosphorylation were predicted in its *N*-terminal region at sites not homologous with other CLICs, with a single PKA site in its conserved *C*-terminal domain[278]. p64 was eventually immunoprecipitated from [γ -^{32}P]ATP-labeled sheep thyroid parafollicular cells showing that p64 could be directly phosphorylated in a hormone- and Ca^{2+}-dependent manner[359]. Intriguingly, p64 phosphorylation in that study increased anion conductance, contrasting with the earlier claim that phosphorylation was inhibitory[275]. It was therefore proposed that p64 contained multiple phosphorylation sites that were either inhibitory or stimulatory[359]. However, inhibition of its predicted kinases had no discernable effect on anion conductance, suggesting some other kinase was mediating its phosphorylation. Subsequent studies concretely established that CLIC5B (p64) is tyrosine phosphorylated on an *N*-terminal residue, though this region is not applicable to other CLICs as it resides in the non-conserved region[360]. Nevertheless, CLICs contain consensus sequences for tyrosine phosphorylation and SH2 domains in their *C*-terminal domains[264,307], thus paving the way for others to investigate CLIC phosphorylation.

Multiple consensus phosphorylation sites were also predicted for CLIC4, and it was shown to be phosphorylated *in vitro* by recombinant PKC, as indicated by migration on immunoblot[280]. Karoulias & Ashley claim that CLIC4 is tyrosine phosphorylated in cells, and by casein kinase-II and PKA *in vitro* in unpublished work[307]. In a similar fashion, recombinant CLIC1 and CLIC4 was shown to be phosphorylated by recombinant PKCα, β, γ, and δ *in vitro*, suggesting a lack of specificity among CLICs as PKC substrates[301]. Care should be taken to interpret *in vitro* phosphorylation assays, as they may not reflect phosphorylation in living cells. In the same study, for instance, the authors found no detectable phosphorylation of

CLIC4 in keratinocytes[301]. Rather, the authors identified CLIC4 as a downstream target of PKCδ that was not directly phosphorylated.

A yeast two-hybrid screen using a portion of protein kinase A-anchoring protein-350 (AKAP350), a scaffolding protein that anchors PKA and other signaling effectors, as bait identified CLIC1 and CLIC5B as direct binding partners[305]. Furthermore, a pan-CLIC antibody reactive to CLIC4, CLIC5A, and CLIC6 pulled down AKAP350 by coimmunoprecipitation, suggesting that all CLICs are scaffolded by AKAP350[305]. Indeed, it was shown that CLIC4 and AKAP350 colocalize by immunofluorescence staining[299], supporting this prediction. Given that AKAP350 associates with PKA and that CLIC4 can be PKA-phosphorylated *in vitro*, it is conceivable that CLIC4 could be a PKA substrate in cells, though no further studies have demonstrated this in cells[307].

Other post-translational modifications have also been proposed to modulate CLICs. Concomitant with its nuclear translocation in mouse macrophages stimulated with LPS, CLIC4 is *S*-nitrosylated, a reversible covalent attachment of a nitric oxide group onto a cysteine residue[301]. Large-scale mass spectrometry proteomics studies have also identified that CLICs are ubiquitinylated[361] and palmitoylated[362] in murine tissue, though the functional significance of these modifications have not yet been established.

In closing, much of what has been described in CLIC proteins mirrors that of the ClCA family of proteins, now known not to function as ion channels. Chief among their unique properties and most discordant with their classification as ion channels are their metamorphic nature and their extent of intracellular translocation. The dimorphism of CLICs warrants a discussion of metamorphic proteins in general, as discussed in the next Section.

1.4 Metamorphic and Intrinsically-Disordered Proteins

A central dogma of biochemistry holds that a polypeptide sequence holds all the information necessary to generate its three-dimensional fold[363]. In other words, one sequence defines one fold. While the dogma holds up very well with some modification today, many proteins defy this expectation and assume more than one conformational fold per sequence. For instance, the folding intermediates of proteins, once thought to be merely transient

byproducts of the folding process, are now known to possess distinct functions[364]. Misfolded proteins involve an irreversible transition into an alternative fold that may or may not result in dysfunction[364]. Additionally, metamorphic proteins reversibly transition between multiple conformational folds, and each may possess distinct functions[365]. Similarly, intrinsically-disordered proteins (IDPs) do not assume a singular defined secondary structure and instead resemble random coils or an ensemble of transient secondary structures[364].

1.4.1 Metamorphic Proteins

While the term metamorphic protein was first coined in 2008 by Murzin[365], it was known that certain protein sequences could adopt multiple secondary structures since the 1980s[193]. Since then, several terms have been proposed for such proteins, such as morpheein, moonlighting protein, and transformer[366]. A 1998 PDB survey found that the longest continuous stretch of amino acids that could adopt either a helical or sheeted conformation was seven[367]. Since then, it has been recognized that longer sequences can restructure, up to eight continuous residues[193]. Undoubtedly, this structural plasticity complicates the task of structural prediction immensely, as there are currently no sequence-based methods to predict metamorphic proteins[193]. The energy landscape of protein folding does permit a multiple thermodynamically stable folds[368], though the kinetics of interconversion *in vivo* and the possibility of semi-stable folds complicates the feasibility of predicting metamorphic proteins. To satisfy these claims, it is proposed that interconversion between two states does not involve a fully unfolded intermediate[365]. It is theorized that certain elements of the primary sequence possess stabilizing and destabilizing properties[369] which act in concert with 'gatekeeper residues'[370] to help restrict the number of possible folds from infinity. Furthermore, environmental factors such as the bilayer acid-induced destabilization (see 1.2.3.1) or buffer conditions may catalyze a process and enable the selection of certain folds over others[371]. While these issues have not yet been completely resolved, what is clear is that both intrinsic and extrinsic factors mediate the structural transitions of metamorphic proteins.

The different folds of many metamorphic proteins are involved with distinct interacting partners, functions, or both, with structural transformations ranging from large whole-domain conformational flips to subtler localized changes. The *C*-terminal region of the *N*-terminal domain in the bacterial antiterminator protein RfaH adopts two distinct states: an all-helical

'closed state' (PDB ID 2OUG) and an all-pleated 'open state' (PDB ID 2LCL)[372]. In the former state, RfaH binds to an RNA polymerase to inhibit transcription termination, while in its latter state, it binds to a ribosomal protein to promote translation[372] (Figure 12). While the structural details of this transition have been well established, the physiological triggers mediating this change has yet to be studied, though transcriptional pause sequences which halt the progression of DNA-binding proteins were suggested to allow RfaH to bind to its partners[373].

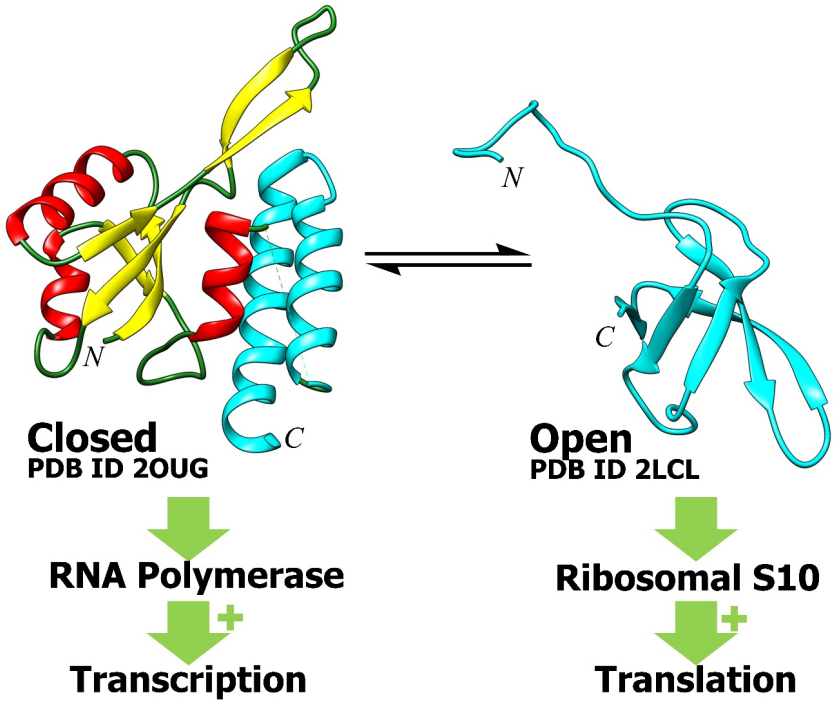

Figure 12. The metamorphic protein RfaH has differential functionalities between its its two conformations. RfaH is a bacterial antiterminator protein whose *C*-terminal region of its *N*-terminal domain adopts two conformations: an all-helical form in its Closed state, and an all-pleated form in its Open state. Its structural transition is induced by some unidentified factor, and each form preferentially binds to a different partner to confer distinct functions. In its Closed state, RfaH binds to an RNA polymerase to inhibit termination while binding to a ribosomal S10 protein in its Open state to promote translation.

Oligomerization is a common route facilitating the structural transitions of metamorphic proteins. For instance, the chemotactic chemokine lymphotactin exists in a dynamic equilibrium of monomers consisting of three β-strands and one α-helix, and completely β-stranded dimers, which show differential affinity for certain surface receptors[374]. As monitored by nuclear magnetic resonance (NMR) spectroscopy, lymphotactin is predominantly

monomeric under high salt and low temperatures, but is dimeric at low salt and high temperatures[374]. Site-directed mutagenesis studies have established that specific cysteine residues promote dimerization, which occur by forming intradomain disulfide bonds[375] in a similar fashion to the oxidative dimerization of CLIC1 (Figure 9) . Metamorphic proteins may also adopt higher-order oligomers in their structural transitions, such as the structural transformation of the pore-forming toxin cytolysin A, in which the β-tongue of its soluble form completely transforms into an elongated α-helix in its homododecameric TM form[186].

1.4.2 Intrinsically-Disordered Proteins

Like metamorphic proteins, IDPs, or the intrinsically-disordered regions within them, defy the one-sequence-one-fold dogma by adopting an ensemble of structures, as opposed to a singular fold[364]. These structures may resemble a random coil or represent a simultaneous adoption of multiple albeit transient secondary structures[364]. IDPs are highly flexible, enabling the fulfilment of several roles as structural flexible linkers that mediate the dynamic motions of a protein, linear motifs which mediate protein interactions, and promiscuous binding sites for partner swapping[376]. It is predicted that up to 35–50% of eukaryotic genomes encode proteins with significant disordered regions[377], cementing their importance in the repertoire of biological function and bearing their classification as one of the four archetypes of proteins alongside globular, membrane, and fibrous proteins[378].

Many IDPs assume a stable structure upon binding with a protein or ligand[376]. For instance, the bacterial iron-sulfur cluster scaffolding IscU interconverts between a disordered and structured conformation, both of which are functional, by total isomerization of its four Pro residues upon binding to a peptidylpropyl isomerase[379]. Further, IDPs can assume different conformations when bound to different partners. The α-domain of the disordered hypoxia-inducible factor HIF-1α assumes a helical conformation when bound to the cAMP-response element binding protein, but becomes extended when bound to an enzyme that catalyzes its hydroxylation[377]. However, many IDPs retain high conformational entropy throughout their entire existence and form heterogeneous complexes when bound to their partners[376].

Proteins may contain varying amounts of disordered regions, whose sequences are typically enriched in polar and ionic residues such as Ser, Gly, Pro, Asn, Gln, Lys, Arg, Glu,

and Asp with very few hydrophobic amino acids that could form the hydrophobic core[377]. Knowledge of which sequences confer disorder in a protein's region is invaluable in sequence-based prediction methods, and several algorithms have been proposed[377].

The inherent flexibility of IDPs are best studied by NMR spectroscopy, which enable dynamic motions to be measured[376]. However, the high disorder poses problems in NMR signal acquisition, frequently resulting in a lack of signal dispersion of ^{1}H resonances and severe signal overlap[376]. Nevertheless, certain methods are routinely used to overcome these limitations including obtaining higher-dimensional spectra and employing heteronuclear ^{1}H–^{13}C and ^{1}H–^{15}N[376] methods. More often than not, a multifactorial approach employing other methods such as FRET, electron paramagnetic resonance spectroscopy, small-angle X-ray scattering is required to fully characterize IDPs[376]. X-ray crystallography may not be well-suited for studying proteins with significant intrinsically-disordered regions, as they frequently fail to crystallize or potentially generate misrepresentative conformations due to crystal packing forces[380]. Electron density-deficient regions in X-ray structures may indicate an intrinsically-disordered region, among other things[380].

Clearly, the presence of metamorphic and IDP structures presents new challenges on the frontier of structural biology, and sheds light to the complexity of that evolution has conferred proteins. It is likely that current methods employed in structural studies are biased to detect just one metamorphic fold[381] or one of many conformations of IDPs, raising the urgency to re-evaluate the current repository of structures[193]. Reports that structural predictions by homology modeling and computational algorithms approached 80% accuracy[382] should make one hopeful that these anomalous structures may one day become predictable too.

1.5 The Chloride Intracellular Channel 5A

Similar to other CLICs, CLIC5A was first reported in the literature as a Cl^- channel[303] whose conductance was regulated by actin[315]. Yet its localization in actin-rich ensembles in placental microvilli[287,303], inner ear hair cell stereocilia[383], and glomerular podocyte foot processes[329,384] as well as its association with members of the plasma membrane-cytoskeletal linker ezrin-radixin-moesin (ERM) proteins[287,303,383] suggested functions beyond Cl^- conductance, as has been found for other CLICs. Furthermore, although recombinant CLIC5A

conferred channel activity *in vitro*, these channels are not selective for anions over cations and displayed multiple conductance levels under the same conditions[315], raising significant doubt about the function of CLIC5A as a legitimate ion channels. The literature suggests strongly that CLIC5A possesses other functions not attributable to ion conductance.

1.5.1 Discovery, Tissue Distribution, & Subcellular Localization of CLIC5A

1.5.1.1 CLIC5A Was First Isolated from Placental Microvilli In A Cytoskeletal Complex

The 32 kDa CLIC5 protein was initially isolated from human placental microvilli extracts subjected to affinity purification using a GST-conjugated *C*-terminal sequence of the plasma membrane-cytoskeletal linker protein ezrin along with other prominent cytoskeletal proteins including actin, *α*-actinin, gelsolin, and IQGAP1[287]. Its gene was cloned and was determined to be 76, 52, 66, and 63% homologous with CLIC4, CLIC3, CLIC2, and CLIC1 respectively[287]. Strikingly, CLIC5 was 91% identical to residues 197–437 of bovine p64, suggesting that CLIC5 shared a more recent ancestor with p64 than with other CLICs[287]. Indeed, immunoblot analysis of HCA-7 human colon cancer cell lysates with a pan-CLIC antibody revealed a novel 46 kDa CLIC protein that was cross-reactive with a CLIC5 antibody[305]. By searching with the 5' coding sequence from bovine p64 against genomic bacterial artificial chromosomes containing human CLIC5 cDNA, an alternative initiation site 65 kbp upstream of the CLIC5 initiation site was found, revealing that CLIC5 was an alternative splice product of p64 which differ only in the first exon. Thus, CLIC5 was renamed CLIC5A and human p64 was renamed CLIC5B[305].

1.5.1.2 CLIC5A mRNA Is Enriched In Particular Tissues

Northern blot analysis using a probe for full-length CLIC5A revealed that a major 6.4 kbp transcript was detected at highest levels in heart and skeletal muscle of human tissue, with modest expression in kidney, lung, and placenta[287] (Table 4). After it was discovered that CLIC5 existed as two splice variants, a more specific probe now including the 5' untranslated region and the unique first exon of CLIC5A found greatest expression in the lung, with lower levels in heart, kidney, and skeletal muscle than reported previously[287], with trace amounts in the colon and placenta[305]. In contrast to CLIC5A, the authors reported that CLIC5B was only detectable in the small intestine[305], though further studies reported that CLIC5B is also

expressed in heart, renal cortex, and skeletal muscle[264,385] (Table 4). RT-PCR analysis of wild-type and jitterbug (*jbg*) mutant mice, which exhibit progressive deafness and vestibular defects, revealed that CLIC5A was additionally expressed in the inner ear and was deficient in *jbg* mice[383], suggesting a role for CLIC5A in auditory and vestibular function. Subsequent genetic analysis of a Turkish family with autosomal recessive non-syndromic hearing impairment identified a homozygous nonsense mutation of the *CLIC5* gene in two affected siblings[386], which implicated this protein in human disease. A 2009 study assessing the abundance of mRNA transcripts in human glomeruli by serial analysis of gene expression (SAGE), which accurately quantifies the amount of mRNA transcripts *in situ*[387], revealed that CLIC5A was enriched in excess of 800-fold in glomeruli compared to other tissues[388]. Microscopy of mouse kidney sections subsequently revealed that CLIC5A is predominantly expressed in actin-based foot processes of podocytes and glomerular endothelial cells[329,384].

Further studies have identified the expression of CLIC5A in tissues not detected by transcriptome analyses. CLIC5A was expressed in the livers of rats and humans in a study of hepatocellular carcinoma, though significantly upregulated in tumor relative to non-tumor livers[302]. Recently, CLIC5A was detected in the lens of mice, and its expression was absent in a cataract model, which suggest a previously unidentified role of CLIC5A in vision[389].

1.5.1.3 CLIC5A Localizes Within Actin-Rich Projections of The Plasma Membrane

Like other CLICs, CLIC5A has been described in diverse subcellular localizations (Table 4). To date, CLIC5A has been described at the plasma membrane, inner mitochondrial membrane, and cytoplasm both *in vitro* and *in vivo*[264,270,287,298,329,384]. Consistent with these observations, CLIC5A was retrieved in cytosolic, membrane, and cytoskeletal fractions of fractionated placental tissues[287]. CLIC5A displays a polarized localization in cells, being concentrated at the base of stereocilia, which are actin-based projections from the apical domain of inner ear sensory hair cells[383], and at the apical plasma membrane in podocyte foot processes[329,384] (Figure 13A-B). CLIC5A consistently localizes to actin-based projections of the plasma membrane including microvilli[287,303], inner ear hair bundles[383], podocyte foot processes[329,384], and structures resembling cilia in the lens of the mouse[389]. Its association with cytoskeletal proteins relates to its physiological functions, as described below. Within the plasma membrane, its distribution appears to be clustered rather than dispersed, where it co-

localizes with PI(4,5)P_2[270] (Figure 13C). Phospholipase C-γ (PLCγ) activation redistributes CLIC5A from these PI(4,5)P_2 clusters to the cytosol, which suggest a possible dependence on phosphoinositides for membrane binding[270] (Figure 13C). Additionally, both *N*- and *C*-terminal CLIC5A deletion mutants of 20–50 residues completely abolishes membrane association, suggesting that membrane association requires more than just its *N*-terminal putative transmembrane domain[270] (Figure 7). To date, the particular signaling pathways involved in the translocation of CLIC5A between its cellular locations have not been described, though CLIC5A is overexpressed in a hepatocellular carcinoma model and undergoes dramatic shifts in subcellular localization[302].

Apart from its description in the inner mitochondrial membrane[298], CLIC5A has not yet been found to localize in other subcellular compartments. In isolated mouse cardiomyocytes, CLIC5A showed negligible co-localization with ER membrane markers whereas CLIC1 and CLIC4 were abundant[295]. Intriguingly, both wild-type CLIC5B and a truncated mutant corresponding to exons 2–6 shared between CLIC5A and CLIC5B was targeted to the Golgi, where it co-localized with AKAP350[305], though no reports of a full-length CLIC5A at the Golgi have since been reported.

1.5.1.3 Both CLIC4 and CLIC5A Co-localize With ERM Proteins

Consistent with its co-localization with ezrin and cytoskeletal proteins[287] and frequent localization in actin-based projections of the plasma membrane, CLIC5A and CLIC4 interact with the ERM proteins ezrin, radixin, and moesin. ERM proteins possess dual *N*-terminal PI(4,5)P_2 and C-terminal filamentous actin (*F*-actin) binding abilities by virtue of their FERM (Table 2) and C-ERMAD domains respectively, thus enabling these proteins to form connections between the plasma membrane and the actin cytoskeleton[390]. ERM proteins also exist as autoinhibited cytosolic forms in which N- and C-terminal domains bind each other. A conserved Thr phosphorylation by several kinases, including PKCs[391] and Rho-associated kinases (ROCKs) in the C-ERMAD enable these proteins to cross-link the plasma membrane to the cytoskeleton[390]. At the plasma membrane, ERM proteins bind directly to PI(4,5)P_2, and the cytosolic domains of integral membrane proteins[390]. ERM proteins coordinate their functions in concert with other signaling proteins, most notably the Rho GTPases, by producing PI(4,5)P_2 through phosphatidylinositol-4-phosphate 5 kinase (PI4P5K) activation[86].

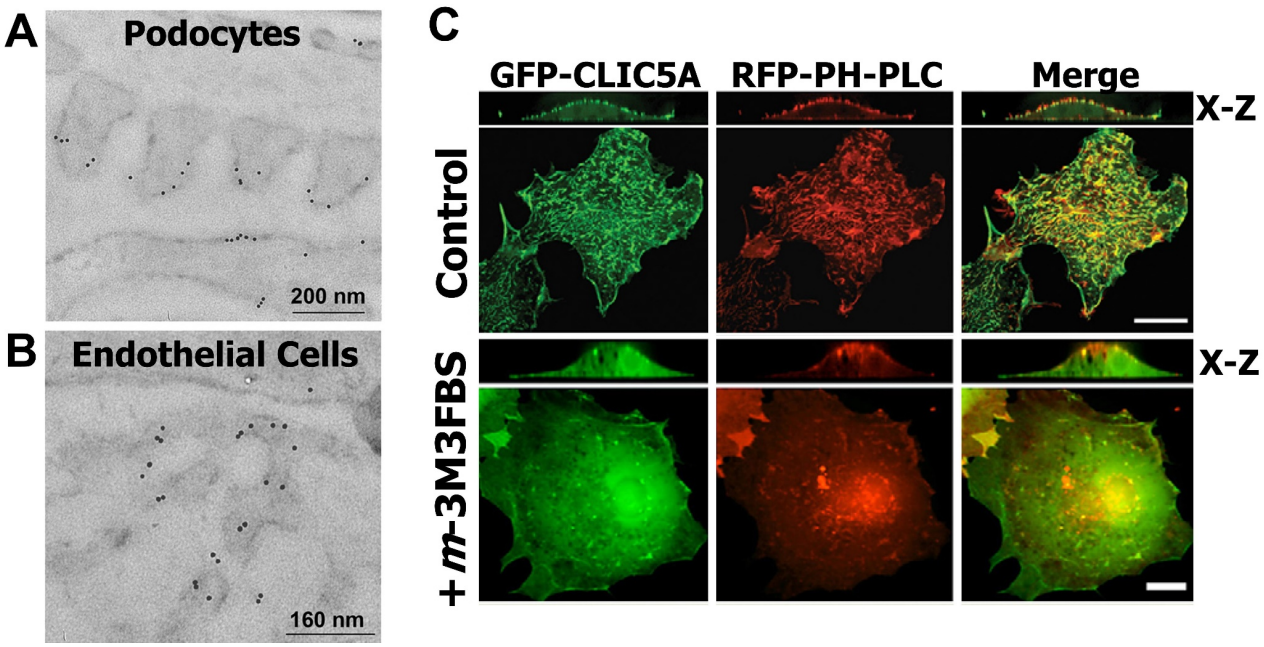

Figure 13. CLIC5A localizes to the apical plasma membrane of polarized cells and displays a clustered membrane distribution with PI(4,5)P_2. Immunogold transmission electron microscopy was performed in [A] podocytes and [B] endothelial cells using anti-CLIC5A (black dots) in mouse kidney sections. [C] Live-cell imaging of GFP-CLIC5A-transfected COS-7 cells co-transfected with the PI(4,5)P_2 marker RFP-PH-PLC. Images were obtained by spinning-disk confocal microscopy of cells under no treatment (Control) or treated with the PLCγ activator *m*-3M3FBS (800 µM) for 5 minutes. Cross-sections (X-Z) of the dorsal (apical) plasma membrane are depicted in boxes. Scale bar: 10 µm. [Figures A & B reprinted with permission from Wegner, B., *et al.* 2010. CLIC5A, a component of the ezrin-podocalyxin complex in glomeruli, is a determinant of podocyte integrity. *American Journal of Renal Physiology* 298:1492-1503. ©2010, American Physiological Society. Figure C modified and reprinted with permission from Al-Momany, A., *et al.* 2014. Clustered PI(4,5)P_2 accumulation and ezrin phosphorylation in response to CLIC5A. *Journal of Cell Science* 127:5164-5178. ©2014, Company of Biologists Ltd.]

Though CLIC5A was retrieved in a pulldown using the *C*-terminal sequence of ezrin, it remained possible that CLIC5A was interacting with a number of the proteins co-retrieved in the pulldown, which included actin, α-actinin, gelsolin, and IQGAP1[287]. A more direct association with ezrin was concluded when dissociation of *F*-actin prior to the pulldown did not decrease its retrieval from tissue[303]. Furthermore, this study showed for the first time that CLIC5A co-localized in the apical region of choriocarcinoma JEG-3 cells with ezrin[303]. The extent of CLIC5A-ezrin interaction remains to be defined. Since ezrin is only weakly detected by coimmunoprecipitation of GFP-CLIC5A using anti-GFP antibodies[392], the interaction may be indirect or transient.

CLIC5A also colocalizes with radixin in the stereocilia of the cochlea and vestibule in the bullfrog and mouse, and in the utricle of chicken[383]. CLIC5A also colocalizes with ezrin and moesin in mouse podocytes[329,384,393]. Confocal microscopy and coimmunoprecipitation assays also revealed that CLIC5A colocalizes with the integral sialoglycoprotein podocalyxin, an ezrin binding partner, in the ezrin-podocalyxin complex[329,384]. CLIC4 was eventually found to colocalize with ezrin and moesin in a similar fashion to CLIC5A in endothelial cells of mouse kidneys[393], as well as in the microvilli of the mouse retinal pigment epithelium[394]. The colocalization with ERM proteins and frequent observations in actin-rich projections is not merely coincidental and is central to enable CLIC5A (and CLIC4) to mediate its functional properties, which will be explored in the next section.

1.5.2 Physiological Roles of CLIC5A

1.5.2.1 CLIC5A Activates ERM Proteins to Remodel and Strengthen Actin-Based Projections

Two independent studies in 2010 using wild-type and CLIC5A-deficient mice revealed that ezrin and podocalyxin expression were dependent on CLIC5A, since CLIC5A-deficient mice displayed lower levels of these proteins[329,384]. Confocal microscopy images of whole mouse glomeruli revealed that active phospho-ERM (pERM) abundance was decreased in CLIC5A-deficient mice, which was attributed to a reduction in total ezrin[329,384]. These lower p-ERM levels were cell-type specific, as p-ERM reduction was primarily observed in podocytes and not in endothelial cells[329]. A subsequent study found that CLIC4 can substitute for CLIC5A in ERM phosphorylation. Since CLIC4 is abundantly expressed by endothelial cells, but not by podocytes, this finding explains why CLIC5A-deficiency resulted in a reduction in p-ERM levels only in podocytes and not in glomerular endothelial cells[393]. The authors found that podocyte foot processes in CLIC5A-deficient mice, which are actin-rich projections modulating renal filtration[395], were significantly shorter, more irregular[384], and less dense[329], resulting in greater proteinuria[384] and an increased susceptibility to glomerular injury by adrimycin[329] and hypertension[396]. For reasons not yet known, podocyte injury by adriamycin also decreases CLIC5A and pERM expression levels, and this phenotype is rescued by cAMP treatment, suggesting a previously unexplored link between cAMP signaling and CLIC5A expression[397]. Overall, these studies indicate that CLIC4 and CLIC5A stimulate

ERM phosphorylation, and in podocytes, CLIC5A is involved in the formation or maintenance foot processes through its effects on ezrin expression.

Studies in cell culture further showed that CLIC5A transfection enhances the association of pERM with cytoskeletal fractions, in addition to forming cell surface projections and ruffles alongside an enhancement of actin polymerization[270]. Curiously, total ezrin levels in were unchanged with CLIC5A transfection, unlike in mouse glomeruli[329,384], though CLIC5A was once again shown to enhance ERM phosphorylation in a PKC-dependent manner[270]. This study also revealed CLIC5A colocalizes with $PI(4,5)P_2$ in discrete clusters at the plasma membrane (Figure 13C), alongside its generating enzyme PI4P5Kα[270], later shown to be activated by the CLIC5A-mediated stimulation of the Rho GTPase Rac1[396]. Given that the generation of $PI(4,5)P_2$ by phosphoinositide kinases and ERM phosphorylation are two steps in their activation[390], a functional role of CLIC5A in the formation of actin-based

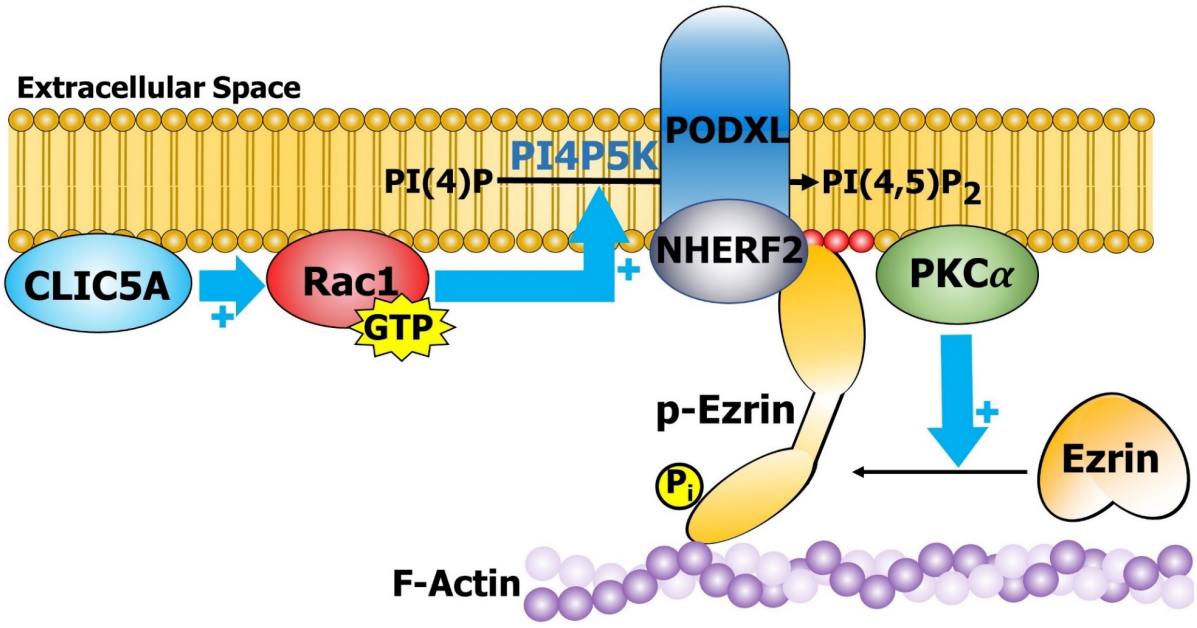

Figure 14. At the apical plasma membrane, CLIC5A stimulates Rac-1-induced phosphatidylinositol-4,5-bisphosphate production to enhance ezrin stimulation. CLIC5A stimulates Rac-1-GTP to enhance phosphatidylinositol-4,5-bisphosphate $PI(4,5)P_2$ production, likely by stimulating a phosphatidylinositol-4-phosphate 5 kinase (PI4P5K). The conformational change of ezrin from its soluble to membrane-associated form requires both $PI(4,5)P_2$ and a *C*-terminal Thr phosphorylation by PKCα. Once at the plasma membrane, ezrin couples the transmembrane glycoprotein podocalyxin (PODXL) to cortical F-actin through the adaptor protein NHERF2.

projections of the plasma membrane was proposed, as shown in Figure 14. In podocytes, this process is involved in the proper formation and/or maintenance of foot processes, which are actin-based projections forming part of the blood-urine barrier in the glomerulus[396].

Similar reports of the CLIC5A-mediated effect in the formation or maintenance of actin-based projections have been described in other cell types. The ezrin-podocalyxin-CLIC5A complex is significantly upregulated in rat liver tumors, while inhibiting CLIC5A or podocalyxin expression was observed with a reduction in metastatic invasion and migration[302]. CLIC5A also stabilizes plasma membrane–cytoskeletal linkages in stereocilia[392], and a deficiency in the lens confers defects in lens fibre cell extension and organization[389,398]. These reports suggest that CLIC5A performs similar functions in as-of-yet unexplored cell types, though its activation of ERM proteins.

1.5.2.2 CLIC5A Knockouts in Mice Potentiate Glomerular Injury In Hypertension

In addition to the natural *jbg* mutation in mice whose phenotype involves vestibular dysfunction, studies on mice with a global deletion in *CLIC5* on the C57BL/6J background implicate CLIC5A in renal health. Uninephrectomized *CLIC5*$^{-/-}$ mice subjected to hypertensive stress by deoxycorticosterone acetate (DOCA) and salt treatment lacked the hypertension-induced increase in phosphorylated ERM and p21-activated kinase (Pak) proteins[396]. Further, the reduction of podocalyxin in response to hypertension was significantly greater in *CLIC5*$^{-/-}$ mice than in wild-type mice[396]. Evaluation of glomerular tissue sections of *CLIC5*$^{-/-}$ mice showed a significant reduction in endothelial fenestrae in response to hypertension, and these mice had fewer and broader foot processes in both normotensive and hypertensive states[396]. Remarkably, *CLIC5*$^{-/-}$ mice had a 2-fold greater proportion of glomeruli with microaneurysms than their wild-type littermates, and these mice had substantially higher levels of albuminuria both in normotensive and hypertensive states[396]. Overall, these studies indicate that CLIC5A plays a protective role in renal injury by maintaining glomerular structures including podocyte foot processes and endothelial fenestrae, both dependent on ERM and Pak phosphorylation.

1.6 Hypotheses & Goals Of The Thesis

CLIC5A and other CLICs possess properties discordant with classical ion channels that conduct ions through well-defined pore structures as integral transmembrane proteins. And

while the functions of most CLIC proteins have yet to be established, the functions that have been uncovered, such as the activation of ERM proteins by CLIC4 and CLIC5A, are not attributable to ion channel activity. Their controversial status as chloride intracellular channels propagates a misunderstanding in the literature, resulting in many often confusing and misinformed reports and investigations today. Perhaps among the most unique characteristics of CLICs is their status as dimorphic proteins, which may be related to their capacity to translocate to various subcellular locales. The translocation of CLICs from the cytoplasmic compartment to their target sites is important to fulfill their roles in signaling (Figure 14). To understand how CLICs function in the cell, it is of paramount importance to elucidate the stimuli, triggers, and processes that mediate this process at both the cellular and biochemical level.

Thus, we hypothesize that CLIC5A—and most likely all other CLICs—are not integral proteins and thus not transmembrane. Instead, we posit that CLIC5A is a peripheral protein that binds to the intracellular leaflet of the plasma membrane. Furthermore, we hypothesize that CLIC5A and other CLICs translocate from the cytoplasm to their target membranes by a phosphorylation-driven process, and within this process, the putative *N*-terminal transmembrane domain becomes exposed in a large-scale structural transformation.

The objectives of this study focus on CLIC5A, but aim to be generalizable for all CLIC proteins.

1. ***Uncover the major structural changes occurring during the translocation of CLIC5A to membranes by NMR spectroscopy.*** At present, no three-dimensional structure exists for CLIC5A. Further, all the structures solved for CLICs have used X-ray crystallography, thus leaving the structural dynamics of CLICs largely unstudied. Given that CLICs are metamorphic and undergo large-scale transitions during their activity, much can be learned about this aspect. Thus, we aimed to determine the atomic structural changes that occur using a truncated CLIC5A *N*-terminal mutant in response to its interaction with detergents using NMR spectroscopy. This is the main objective of Chapter 3.

2. ***Challenge the claim that CLIC5A is an integral and transmembrane protein, and show that CLICs are unlikely to form classical ion channels.*** Many reports claim that CLICs possess the capacity to form legitimate ion channels. We aimed to disprove that CLIC5A

is an integral transmembrane protein. While the ion conductance of CLICs have been well-demonstrated, we sought to demonstrate that their ion conductance cannot be ascribed to classical ion channel activity. This is the major objective of Chapter 4.

3. ***Determine the biological triggers that mediate the translocation of CLIC1, CLIC4, and CLIC5A to membranes in cells.*** While it is now well-established that CLIC proteins translocate to their subcellular destinations under a variety of conditions and stimuli, the precise signaling pathways and the effectors mediating these transitions are not yet clear. Thus, we aimed to determine the signaling effectors that translocate CLICs to membranes. This is the major objective of Chapter 5.

Chapter 2: Materials & Methods

2.1 Reagents & Antibodies

All chemicals used in this study were reagent-grade and purchased from Sigma-Aldrich (Oakville, ON) unless otherwise stated. Rabbit anti-*N*-Cadherin, rabbit anti-GAPDH, and rabbit phospho-CREB antibodies were purchased from Cell Signaling Technology (Danvers, MA, USA). Mouse anti-β-Actin and mouse anti-FLAG M2 antibodies were purchased from Sigma-Aldrich (Oakville, ON). Rabbit anti-p-ERM and rabbit anti-phospho-PAK1/2/3 antibodies were purchased from Abcam, Inc. (Cambridge, MA, USA). Rabbit anti-CLIC5A antibodies were purchased from Aviva Systems Biology (San Diego, CA, USA), while rabbit anti-CLIC1, rabbit anti-CLIC4, and rabbit anti-Rac1 antibodies were purchased from Santa Cruz Biotechnology (Dallas, TX, USA). Horseradish-peroxidase (HRP) conjugated with streptavidin was purchased from Cell Signaling Technology, and HRP-conjugated donkey-anti-rabbit and goat-anti-mouse antibodies. Fluorescent secondary antibodies donkey_anti-rabbit and goat anti-mouse secondary antibodies labeled with Alexa Fluor 594 were purchased from Thermo Fisher (Waltham, MA, USA).

2.2 Cloning & Generation of FLAG-CLIC5A Constructs

Since the anti-CLIC5A antibody used in our study is notoriously cross-reactive for CLIC4[393], we generated an *N*-terminal FLAG-epitope (DYKDDDDK) tagged CLIC5A to enhance the specificity in our immunoassays. The full-length cDNA of human CLIC5A encoding the entire open reading frame was amplified by PCR using the forward primer 5'–GCAGGTCG**ACCATG**CGCAAATGGGCGGTAGGCGTGGTCTGGGACGTCGTATGG GTAACAGACTCGGCGACAGCTAAC–3' and the reverse primer 5'–CCGGGATCCTCAG GATCGGCTGAGGCGTTTGGC–3' from cDNA generated by our laboratory[270] (University of Alberta). A Kozak consensus sequence (bold) and FLAG epitope (underlined) were added to the 5' terminus of the forward primer ahead of the first 21 nucleotides of the CLIC5A sequence. Inserts were then cloned into a pTARGET mammalian expression vector (Promega, Madison, WI, USA) by restriction digestion and ligation according to the manufacturer's instructions. Sequences were verified by restriction digest and full-insert sequencing, and plasmids were reproduced in *E. coli* strain DH5α using the QIAgen MaxiPrep kit (Germantown, MD, USA) according to the supplied instructions.

2.3 Cell Culture & Transfection

The simian fibroblast-like COS-7 cells, derived from kidneys of the African grivet monkey *Cercopithecus aethiops*[399] and transformed with the SV40 virus[400], were purchased from Thermo Fisher. Cells were cultured in Gibco™ Dulbecco's Modified Eagle Medium (DMEM; Thermo Fisher) supplemented with 10% *v*/*v* fetal bovine serum (FBS; Life Technologies, Burlington, ON) and 1% *v*/*v* pencillin/streptomycin (Life Technologies) in an incubator at 37°C humidified with 5% CO_2. Two days later, cells were split using a Gibco™ 0.05% *w*/*v* tryspin-EDTA solution (Life Technologies) into either 100-mm (p-100) or 60-mm (p-60) dishes in a 1:2 and 1:6 split ratio respectively. The following day, medium was replaced with FBS-supplemented DMEM without antibiotics and transfected using 7 μg plasmid and 15 μL Lipofectamine™ 2000 (Life Technologies) dispersed in the reduced serum medium OPTI-MEM™ (Life Technologies) for p-100 cultures, or 2 μg plasmid and 6 μL Lipofectamine™ 2000 for p-60 cultures. Media was replaced with antibiotic-supplemented medium the next day, and experiments were performed 48 hrs post-transfection.

2.4 Biotinylation Surface Protein Capture

To determine the surface accessibility of CLIC5A, surface proteins in control vector- and CLIC5A-transfected cells cultured in p-100 dishes were labeled with synthetic, membrane-impermeable sulfo-NHS-SS-biotin, and biotinylated proteins were captured on a streptavidin-like column using the Pierce™ Cell Surface Protein Isolation Kit (Thermo Fisher) according to the manufacturer's instructions with minor modification. A total of three independent experiments were performed.

In brief, cells were washed twice with ice-cold phosphate-buffered saline (PBS; 137 mM NaCl, 2.7 mM KCl, 10 mM Na_2HPO_4, 2 mM KH_2PO4, pH 7.4) and incubated with 10 mL of 272 μM sulfo-NHS-SS-biotin in PBS by gentle agitation on an orbital shaker in 4°C for 30 min. Labeling was terminated with a proprietary Quenching Solution, and cells were harvested by scraping into 10 mL PBS and centrifugation at 500 × *g* for 3 min in 4°C. Pellets were washed with PBS, lysed with 500 μL of a propriety Lysis Buffer for 30 min on ice with intermittent vortexing, and cellular debris was sedimented by a spin at 10,000 × *g* for 2 min in 4°C. Columns of 500 μL NeutrAvidin, a deglycosylated preparation of egg white avidin that reduces nonspecific biotin binding[401], was prepared in a 1.5-mL collection tube as a slurry.

Lysate supernatants were applied to columns and equilibrated at room temperature for 60 min with end-over-end mixing on a rotary shaker. Flow-through (FT) was obtained for immunoblot (IB) analysis by spinning columns at 1,000 × *g* for 1 min, and columns were washed four times with a proprietary Wash Buffer supplemented with 1× protease inhibitor cocktail (Thermo Fisher). In our procedure, this Wash Buffer was further supplemented with 300 mM NaCl to reduce nonspecific binding.

Bound proteins were eluted by incubation with 400 μL 2× Laemmli buffer (4% *w*/*v* sodium dodecyl sulfate, SDS, 20% *v*/*v* glycerol, 120 mM TRIS-HCl, 0.02% *w*/*v* bromophenol blue, pH 6.8) with 50 mM dithiothreitol for 60 min by rotary shaking to reduce the disulfide bonds linking biotinylated proteins to the Neutravidin column. Eluted proteins were retrieved by centrifugation at 1,000 × *g* for 1 min, and collected fractions were analyzed by IB analysis.

2.5 Protease Protection Assay

A trypsin degradation assay was performed in intact and permeabilized FLAG-CLIC5A-transfected COS-7 cells to determine the accessibility of surface and intracellular proteins to trypsin in a protocol adapted and modified from Nguyen and colleagues[402]. Cells were grown on p-100 plates, washed with ice-cold PBS, and harvested by scraping in 10 mL PBS and centrifugation at 350 × *g* for 5 min in 4°C. Pellets were washed and resuspended in 1 mL PBS for equal distribution into eight 1.5-mL microfuge tubes prior to a second spin in the same conditions. Pellets were resuspended in PBS with various concentrations of digitonin (EMD Millipore, Danvers, MA, USA), a mild detergent which forms complexes with cholesterol, which represents up to 40% in PMs, to generate pores[72,403,404]. Except for the control, trypsin-EDTA (Life Technologies) was added to 0.02 mg/mL in a total volume of 200 μL, and cells were incubated on ice for 30 min. Trypsin degradation was terminated using 1× protease inhibitor cocktail and incubation for a further 10 min on ice. Cells were pelleted by centrifugation at 1,500 × *g* for 10 min in 4°C and solubilized in Laemmli buffer for IB analysis. Three independent experiments were performed.

2.6 Non-permeabilizing immunofluorescence & confocal microscopy

To assess whether the FLAG epitope of FLAG-CLIC5A is confined in the extracellular or intracellular space, immunofluorescence (IF) imaging was performed in intact or

permeabilized FLAG-CLIC5A-transfected COS-7 cells. Cells were grown on p60 plates for 24 hours and split in a 1:6 ratio onto glass coverslips in 6-well plates. Cells were grown for a further 24 or 48 hours followed by staining for FLAG-CLIC5A or control GAPDH and *N*-Cadherin. For immunofluorescence labeling, cells were washed with ice-cold PBS and fixed with 1% paraformaldehyde (Life Technologies) at room temperature for 15 min. Fixing agent was washed away with two washes with ice-cold PBS, and membranes were either kept intact in PBS or permeabilized with 0.05% *v*/*v* Triton X-100 in PBS for 10 min on ice. Cells were then blocked with 5% *w*/*v* bovine serum albumin (BSA) in PBS for 1 hr. at room temperature and incubated with rabbit anti-*N*-Cadherin at 1:200, rabbit anti-GAPDH at 1:100, or mouse anti-FLAG M2 at 1:200 concentrations overnight in 4°C.

The next day, antibodies removed by washing six times in 1% *w*/*v* BSA followed by incubation with Alexa Fluor 594-labled donkey anti-rabbit or goat anti-mouse IgG at a dilution of 1:400 for 45 min in the dark at room temperature. The secondary antibodies were washed away with four rinses in 1% BSA and mounted overnight using frosted microscope slides and the ProLong® Diamond (Thermo Fisher) mounting medium. Images were acquired with a Zeiss LSM710 laser-scanning confocal microscope and processed using ZEN (v 2.3) software. In total, three independent experiments were performed.

2.7 Differential Detergent Fractionation & Inhibitor Treatments

The membrane localization of CLIC5A and FLAG-CLIC5A was determined by differential detergent fractionation, in which cell proteins are sequentially extracted with detergents of increasing strength[405]. Cells were first treated with digitonin to create pores in the plasma membrane (PM) releasing soluble, cytoplasmic components, followed by Triton X-100 to release proteins in plasma membrane and organellar lipid bilayers. Cytoskeletal and nuclear components remain insoluble and were sedimented by centrifugation. Digitonin complexes with cholesterol in PM, though cholesterol content varies between cell lines[406,407]. Therefore, we initially screened for optimal digitonin concentrations in cytoplasmic extraction buffer (40 mM PIPES, 1.2 M sucrose, 400 mM NaCl, 12.5 mM $MgSO_4 \cdot H_2O$, 5 mM EDTA, 1× protease inhibitor cocktail, 50 nM Calyculin A, pH 6.8) for COS-7 and HeLa lines. As determined by IB analysis and the resolution of the intracellular marker GAPDH from Triton-

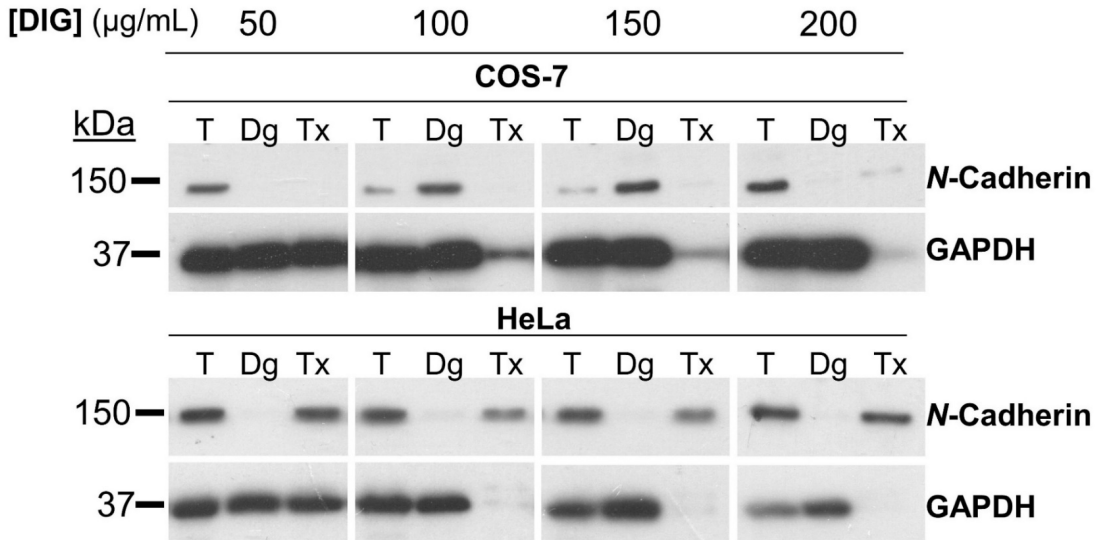

Figure 15. The efficiency of digitonin permeabilization is cholesterol-dependent. Since cell lines vary in plasma membrane cholesterol content, a digitonin (DIG) concentration screen was done in COS-7 and HeLa cells to establish optimal working concentrations. From a differential detergent fractionation procedure, digitonin- (Dg) and Triton-soluble (Tx) fractions were yielded from total cell lysate (T).

soluble fractions, we determined working concentrations of 200 μg/mL and 100 μg/mL digitonin for COS-7 and HeLa cells respectively (Figure 15).

Using the established working concentrations, cells were washed twice with ice-cold PBS and harvested by scraping in 4 mL PBS and centrifugation at 350 × *g* for 5 min in 4°C. Pellets were rinsed, thoroughly resuspended in 400 μL cytoplasmic extraction buffer containing 200 μg/mL digitonin and 1× protease inhibitor cocktail, and incubated by end-over-end rotary shaking for 10 min 4°C. A sample was obtained as total cell lysates, and the mixture was centrifuged at 2,000 × *g* for 10 min in 4°C to yield cytoplasmic contents in the supernatant (Figure 16). Pellets were rinsed with ice-cold PBS, spun the same conditions, then resuspended in 350 μL membrane extraction buffer (50 mM HEPES, 150 mM NaCl, 5 mM EDTA, 1× protease inhibitor cocktail, 50 nM Calyculin A, pH 7.4) containing 0.5% *v*/*v* Triton X-100. Contents were incubated for 30 min on ice with intermittent vortexing, and membrane/organellar fractions were retrieved in the supernatant by centrifugation at 6,000 × *g* for 10 min in 4°C, with debris sedimented as the pellet (Figure 16). All fractions were solubilized in Laemmli buffer and prepared for IB analysis. The volume of each fraction was

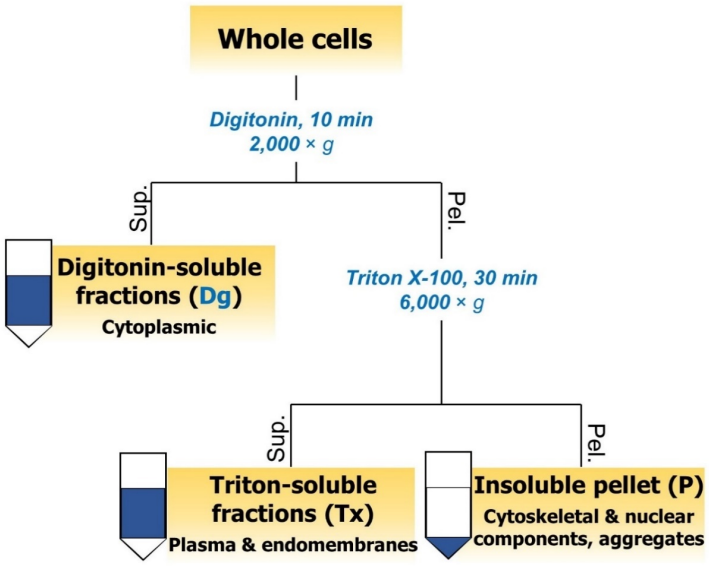

Figure 16. Differential detergent fractionation extracts subcellular fractions by treating cells in-series with detergents of increasing strength. Whole cells are first treated with the mild detergent digitonin, and digitonin-soluble components (Dg) containing cytoplasmic proteins are separated in the supernatant (Sup.) by centrifugation. In the next step, pellets (Pel.) are treated with the stronger detergent Triton X-100 to yield Triton-soluble fractions (Tx) containing plasma and endomembranes in the Sup., leaving behind insoluble debris containing cytoskeletal, nuclear, and aggregates in the Pel.

made to reflect the volume of the initial digitonin extraction volume, so that protein quantity between fractions can be compared.

In some studies, we treated the living cells with phosphatase and kinase inhibitors prior to fractionation to determine the response of FLAG-CLIC5A and CLIC5A localization. For phosphatase inhibition studies, cells were treated with 50 nM of the marine sponge toxin[408] and Ser/Thr phosphatase inhibitor[409] Calyculin A (Santa Cruz Biotechnology) for 15 or 20 min at room temperature. For kinase inhibition studies, cells were treated with the broad kinase inhibitor[410,411] Staurosporine at 20 or 2 nM for 3 hr, the PKA inhibitor[412] H-89 at 30 μM for 1 hr, or the PAK inhibitor[413] IPA-at 15 μM for 6 hr in 37°C. Thereafter, all cells were treated with 50 nM Calyculin A for 20 min at room temperature before fractionations, as above.

2.8 SDS-PAGE, Immunoblot, & Statistical Analysis

All samples subject to IB analysis were prepared by heat denaturation at 95°C for 10 min and centrifugation at 13,000 × *g* for 1 min. Proteins were separated by sodium dodecyl

sulfate polyacrylamide electrophoresis (SDS-PAGE) according to standard methods[414] and transferred onto polyvinylidene fluoride membranes by electroblotting. Transferred proteins were stained with Amido black (Thermo Fisher), destained with 20% *v*/*v* acetic acid and 20% *v*/*v* methanol and washed with TRIS-buffered saline (20 mM TRIS-HCl, 150 mM NaCl, pH 7.5) with 1% *v*/*v* TWEEN® (TBS/T; Sigma-Aldrich) prior to blocking with proprietary Western Blocking Reagent (Sigma-Aldrich) for 1 hr at room temperature. Membranes were washed with TBS/T, then incubated with rabbit anti-*N*-Cadherin at 1:1,000, rabbit anti-GAPDH at 1:8,000, rabbit anti-CLIC1 at 1:15,000, rabbit anti-CLIC4 at 1:4,500, rabbit anti-CLIC5A at 1:9,000, rabbit anti-pERM at 1:7,000, mouse anti-β-Actin at 1:15,000, or mouse anti-FLAG M2 at 1:9,000 dilutions in Western Blocking Reagent overnight in 4°C. The following day, the appropriate donkey anti-rabbit-HRP or goat anti-mouse-HRP antibodies at 1:10,000 or 1:100,000 dilution were applied for 1 hr at room temperature, and membranes were exhaustively washed with TBS/T. Images were developed using enhanced chemiluminescence (GE Amersham, Baie d'Ure, QC) exposed onto Fuji medical X-ray film (Super Rx, Fujifilm, Edison, NJ, USA).

Band density was quantified by densitometry using ImageJ2[415] (v 1.51) using *N*-Cadherin as the loading control in Triton-soluble fractions, which contained membrane proteins. For quantification, three independent experiments were performed, using comparison of two groups using a paired Student's *t*-test.

2.9 Expression & Purification of Recombinant CLIC5A in *E. coli*

Expression plasmids were purchased from GenScript (Piscataway, NJ, USA) or ATUM (Newark, CA, USA), reproduced in *E. coli* strain DH5*α*, and isolated with the QIAprep Spin MiniPrep Kit (Germantown, MD, USA) according to the supplier's instructions. Two constructs were prepared for NMR spectroscopy: wild-type CLIC5A (CLIC5A WT) fused with to the *N*-terminal cleavable solubility tag maltose-binding protein (MBP), as well as *N*-terminal truncated mutants CLIC5A[1-99] and CLIC5A[1-112], which differ in the inclusion of few *C*-terminal residues of the loops connecting the *N*- and *C*-terminal domains.

E. coli strain BL21(DE3), which are Lon and OmpT protease deficient and possess a *lac*-inducible T7 RNA polymerase gene derived from a bacteriophage *λ*[416], were made competent

by $MgCl_2$ treatment according to standard methods[417]. Bacteria were transformed with 1 μg plasmid by heat shock at 42°C for 60 sec, and transformants were selected on Luria-Bertani (LB) agar made with 5% *w*/*v* ampicillin (amp) overnight in 37°C. The next day, five transformant colonies were used to inoculate a starter culture of 20 mL LB broth with 0.5% *w*/*v* amp to an optical density at 600 nm (OD_{600}) of 1, at which point the starter culture was diluted into 1 L LB broth supplemented with 0.5% *w*/*v* amp. For nuclear magnetic resonance (NMR) spectroscopy, CLIC5A[1-99] was triple-labeled with ^{2}H, ^{15}N, and ^{13}C by inoculating the starter culture into 1 L M9 minimal media (8 g Na_2HPO_4, 2.2 g KH_2PO_4 per 0.9 L D_2O) supplemented with 1 g [^{15}N]-NH_4SO_4 and 3 g [^{13}C]-glucose. Cells were cultured to an OD_{600} of ~0.6, corresponding to mid-log phase, and protein expression was induced by 1 mM isopropyl β-D-1-thiogalactoyranoside (IPTG) for 3-4 hrs in 37°C.

Cells were harvested by centrifugation at 5,000 rpm for 20 min at 4°C, then resuspended in resuspension buffer (50 mM TRIS-HCl, 10 mM $MgSO_4$, 0.05 mg/mL DNAse A, 1 mM β-mercaptoethanol, pH 8.0). Lysates were prepared by chemical and mechanical treatment using 20 mg lysozyme, 200 mg deoxycholate, and manual homogenization. Insoluble debris was sedimented by centrifugation at 10,000 rpm for 15 min in 4°C, and the supernatant containing soluble proteins was clarified in a 0.45-μm Millex filter before application to a nickel nitriloacetic acid (Ni^{2+}-NTA) agarose column with a 30 mL capacity, equilibrated with binding buffer (20 mM TRIS, 300 mM NaCl, 10 mM imidazole, 1 mM β-mercaptoethanol, pH 7.90). The column was rinsed with two volumes of the same buffer containing 80 mM imidazole and eluted with the same buffer containing 250 mM imidazole with a flow rate of 1 mL/min. Collected fractions were assessed for total protein by the absorbance at 280 nm (A_{280}) by spectrophotometry, and eluates of the highest intensity were pooled. For MBP-CLIC5A, the MBP fusion tag was cleaved off by incubation with TEV protease in a 1:100 ratio of total protein by end-over-end rotary mixing in 4°C for 48 hr (Figure 17), and dialyzed in 3,000 Da-cutoff Spectra/Por membranes (Repligen, Waltham, MA, USA) in 4°C for 24 hr prior to a second purification on a Ni^{2+}-NTA column under the same conditions to separate hexahistidine-tagged MBP in the Eluates from CLIC5A in the wash fractions. Eluates were again dialyzed in Spectra/Por membranes (Repligen, Waltham, MA, USA) against 10 mM NH_4HCO_3, pH 7.6 in 4°C for 48 hr, then lyophilized overnight or concentrated using centrifugal filters. A summary of the purification of MBP-CLIC5A is shown in Figure 18.

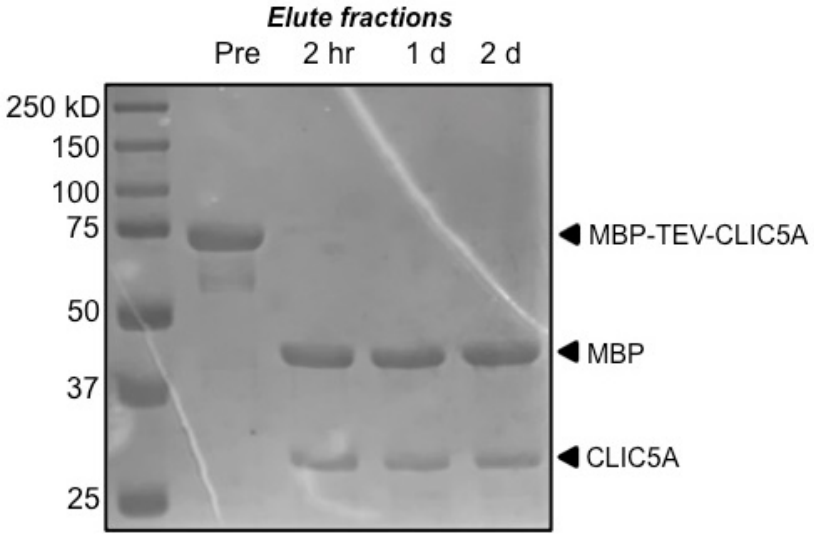

Figure 17. The MBP solubility fusion tag of MBP-CLIC5A was cleaved by TEV protease. Following Ni-NTA chromatography, wash fractions and elute fractions—which both contained significant amounts of target protein—were pooled in separate fractions (Pre). The total protein concentration was estimated to be ~31 μM (Wash) and ~36 μM (Elute) based on UV-VIS spectroscopy, and TEV protease was added to a ratio of 100:1 of protein-to-protease. TEV proteolysis was performed at 4˚C for the specified time period.

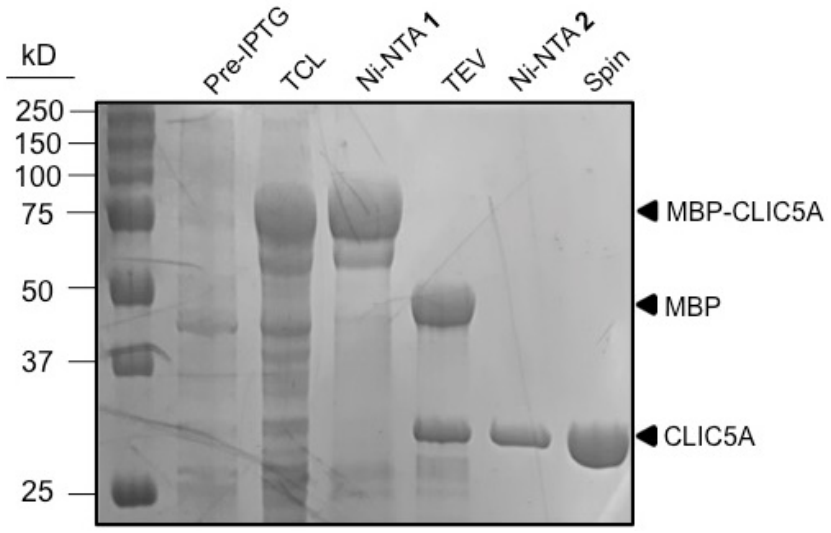

Figure 18. Recombinant MBP-CLIC5A was purified in a multistep procedure. *E. coli* BL21(DE3) cultures were grown in 2 L of LB medium to mid-log phase prior to induction with 1 mM IPTG (Pre-IPTG), and MBP-CLIC5A was expressed in 37˚C for 3.5 hr. Cells were lysed using 1 mg/mL lysozyme, 1 mg/mL deoxycholate, and mechanical homogenization to yield total cell lysate (TCL). MBP-CLIC5A was isolated by Ni-NTA affinity chromatography (Ni-NTA 1), and the His-MBP fusion tag was cleaved by TEV protease (TEV). Cleaved protein was applied to a second round of Ni-NTA chromatography (Ni-NTA 2) to separate CLIC5A from MBP, which was then concentrated by centrifugal filters (Spin).

2.10 Gel Filtration Chromatography

Gel filtration chromatography was run using purified CLIC5A WT and CLIC5A[1-99] to determine their quaternary structure. A Superdex® 200 10/300 GL (GE Life Sciences, Pittsburgh, PA, USA) column of a 23.5 mL capacity was in a ÄKTA™ Pure fast protein liquid chromatography (FPLC) system was equilibrated using one column volume of equilibration buffer (0.05 M NaH_2PO_4, 0.05 M NaCl, pH 7.0) applied at a flow rate of 0.4 mL/min, followed by equilibration with two column volumes of equilibration buffer containing 0.15 M NaCl. CLIC5A[1-99] and CLIC5A WT was dissolved in equilibration buffer to 0.5 mg/mL, clarified by a brief spin, and applied onto the column in a total volume of 0.5 mL and a flow rate of 0.5 mL/min. Protein was eluted using 1 column volume of equilibration buffer.

2.11 NMR Spectroscopy

For NMR spectroscopy, lyophilized protein samples were dissolved to 1.5–10 mg/mL in 100 mM KCl, 1 mM EDTA, 20 mM DTT, 5% D_2O, 0.005% sodium azide, and 10 mM imidazole at pH 6.49 – 6.70, employing 0.25 mM 4,4-dimethyl-4-silapentane-1-sulfonic acid (DSS) as a standard. Stock solutions of 10 – 50 mM 7-cyclohexyl-1-heptylphosphocholine, also known as cyclofos-7 (Anatrace Products, Maumee, OH, USA) or 1,2-dioctanoyl-*sn*-glycero-3-phospho-(1'-myoinositol-4',5'-bisphosphate) (DOPI(4,5)P_2, Avanti Polar Lipids, Alabaster, AL, USA) were prepared for titration into NMR samples. NMR spectra for CLIC5A WT, CLIC5A[1-99], and CLIC5A[1-112] were obtained on a Varian INOVA 500 MHZ spectrometer at 30°C unless otherwise stated, which were equipped with triple-resonance probes and pulse-field gradient technology.

2.12 Circular Dichroism (CD) Spectroscopy

The secondary structure of CLIC5A WT and CLIC5A[1-99] was estimated by circular dichroism (CD) spectroscopy. Protein samples were dissolved to 0.77 mg/mL, dialyzed in Spetra/Por membranes, dissolved in 1 mM TRIS-2-carboxyethylphosphine (TCEP), 50 mM TRIS, 1 mM EDTA, pH 7.00. CD spectra were obtained using a Jasco J-810 spectrometer at a temperature range from 25°C – 95°C at 5°C intervals, scanning for 260 nm – 190 nm.

2.13 Phosphorylation Prediction Methods

Phosphorylation sites were predicted for CLIC5A in a multifactorial process utilizing sequence, structural, and proteomic data. Sequence prediction in a neural network strategy was done by querying the sequence onto the NetPhos (v 3.1) sever[418,419], and least probable sites were eliminated by using a threshold of 0.50. Putative phosphorylation sites were assessed among all CLICs by multiple sequence alignment using ClustalW2[420], and homologous sites were mapped onto the X-ray structure of CLIC1[309] (PDB ID 1K0M) and subjectively assessed for surface-exposure using PyMOL[421] (v 2.0) or UCSF Chimera[422] (v 1.12) visualization software, which was also used to obtain images for Figures used within this thesis. Proteomic data for phosphorylation sites were obtained on the PhosphoSitePlus server[423], which is a database for mammalian post-translational modifications compiled using proteomic and site-specific data, for CLIC5B, CLIC1, and CLIC4. A combination of these data was used to select the most likely phosphorylation sites in CLIC5A.

Chapter 3: Structural Studies on CLIC5A

3.1 Introduction

Since their discovery using the potent Cl^- antagonist indanyloxyacetic acid-94 (IAA-94)[275,276], the CLIC gene family proteins were believed to be ion channels which conduct their solutes as integral membrane proteins, typical of other mammalian ion channels[207]. Yet doubts to their capacity to form legitimate ion channels were raised when the genes were cloned to reveal only one putative transmembrane domain (PTMD)[278,314]. Further puzzling was the first X-ray structure of a CLIC member, CLIC1 (PDB ID 1K0M), which showed the protein as a globular soluble protein with structural homology to GSTΩ[309]. This structure and that of all other CLICs (Figure 8) reveal that the PTMD spans its first α-helix and β-strand, and thus a disruption of this motif would be necessary to expose the putative transmembrane segment. Nevertheless, given that ion conductance activity of CLICs is well-established[264], it is conceivable that CLICs likely possess at least two distinct forms, which earns them designation as metamorphic proteins[364]. In this regard, CLICs would be similar to pore-forming proteins (PFPs), which also translocate from the cytosol to membranes by structural transitions[142].

The majority of structural studies on CLICs thus far have focused on CLIC1, and no three-dimensional structure has been solved for CLIC5A. On the other hand, cellular studies indicate that CLIC5A stimulates the activation ezrin-moesin-radixin (ERM) proteins at plasma membrane-cytoskeletal junctions to remodel actin-rich projections of the plasma membrane [270,329,384,385,392,393,396]. Notably, CLIC5A activates ERM proteins in part by enhancing phosphatidylinositol-4,5-bisphosphate [(PI(4,5)P_2] generation through a Rac-1-coupled interaction with a phosphatidylinositol-4-phosphate 5 kinase (PI4P5K)[270,396], and PI(4,5)P_2 hydrolysis by phospholipase C-γ (PLCγ) activation redistributes CLIC5A from the plasma membrane to the cytosol, suggesting a dependence on phosphoinositides for membrane association not shared with other CLICs.

In the following chapter, structural analyses on wild-type (WT) recombinant CLIC5A and a truncated *N*-terminal CLIC5A[1-99] and CLIC5A[1-112] were conducted by NMR and circular dichroism (CD) spectroscopy in the absence and presence of detergents to induce structural transitions. We anticipated changes in structural signals during this transition, though we learned that recombinant CLIC5A possesses unusual properties by these methods.

3.2 Results

3.2.1 CLIC5A[1-99] and Intact WT CLIC5A Were Analyzed By Gel Filtration

Recombinant CLIC constructs were assessed for quaternary structure by gel filtration chromatography. Molecular weight standards were not run concurrently with these samples instead, standard curves published by the manufacturer were used for comparison. The chromatogram of CLIC5A[1-99] ran on a Superdex® 75/600 column eluted at what appeared to be a singular peak at ~50 mL, though this peak was not symmetrical in shape (Figure 19A). Comparison to standard curves published by the manufacturer showed that human IgG at 158 kDa elute at this volume, which is nearly 10-fold greater than the expected molecular weight of CLIC5A[1-99]. Given the asymmetrical peak of the curve and a molecular weight much greater than expected, CLIC5A[1-99] was most likely forming aggregates in solution, despite behaving as a soluble protein during its purification.

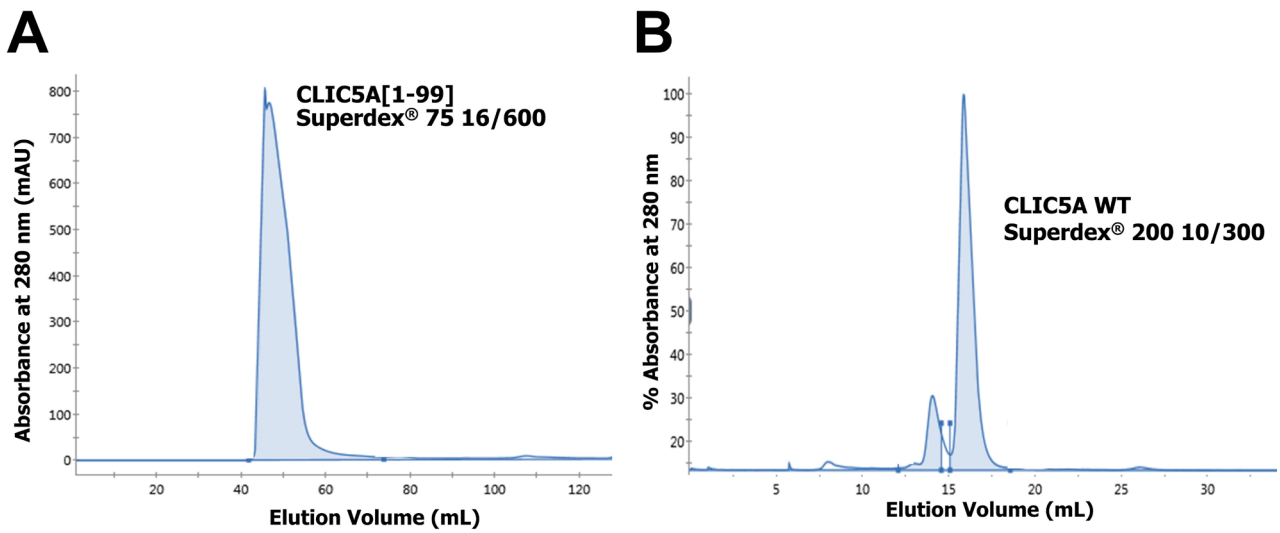

Figure 19. While CLIC5A WT is monomeric and properly folded in solution, CLIC5A[1-99] forms significant aggregates. [A] CLIC5A[1-99] and [B] wild-type CLIC5A WT were ran on gel filtration chromatography to determine their quaternary structure in a Superdex® 75 16/600 GL and 200 10/300 GL column respectively equipped onto an AKTA FPLC apparatus.

WT CLIC5A run on a Superdex® 200 10/300 column showed a minor peak at ~14 mL and a major peak at ~ 16 mL (Figure 19B). Unlike the peak obtained for CLIC5A[1-99], the shape of these peaks was symmetrical. Comparison to the manufacturer's standard curves

indicate that peaks at 14 and 16 mL are closest to conalbumin and carbonic anhydrase at 75 and 29 kDa respectively. Thus, elution of CLIC5A WT as a major peak at 16 ml corresponds to its known molecular weight of 28 kDa. Therefore, unlike CLIC5A[1-99], WT CLIC5A does not aggregate significantly in solution, though the minor peak at 75 kDa could represent some oligomerization.

3.2.2 CLIC5A WT and CLIC5A[1-99] Adopts Multiple Conformations In NMR

We performed NMR spectroscopy in hopes of observing the structural transitions occurring during membrane association by the titration with certain detergents. Without detergent, $^{1}H–^{15}N$ heteronuclear single quantum coherence (HSQC) spectra of ^{15}N-labeled CLIC5A[1-99], which details N-H correlations of the amide backbone and sidechains, showed a very clear absence of peaks (Figure 20A), hindering the possibility for spectral assignment and structural elucidation. The absence of peaks could suggest aggregation, unfolding, or rapid conformational exchange. Since this construct eluted at a molecular weight much higher than

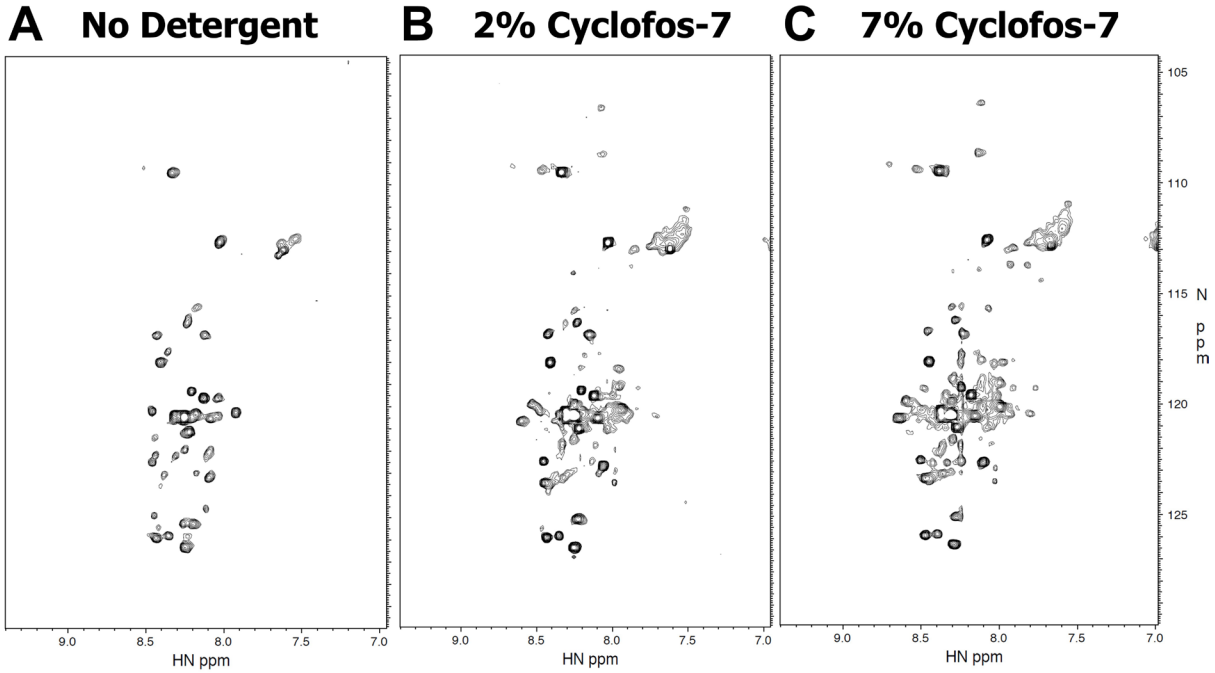

Figure 20. Cyclofos-7 induces the appearance of few peaks in the ^{1}H-^{15}N HSQC spectrum of CLIC5A[1-99]. [A] 7.2 mg/mL ^{15}N-labeled CLIC5A[1-99] in buffer containing 10 mM imidazole, pH 6.49, 100 mM KCl, 20 mM DTT, 5% D_2O, 0.25 mM DSS, and 0.005% sodium azide at 30°C. The detergent cyclofos-7 was titrated to these samples at 2% at 30°C [B] and at 7% at 40°C [C].

expected (Figure 19A), it is probable that aggregation played a significant factor to the paucity of peaks. Nevertheless, given that CLIC proteins are metamorphic and possess multiple conformational states, it remained possible that addition of detergent could induce a singular predominant state that could be studied in solution by NMR. Titration of up to 2% cyclofos-7 induced the appearance of many peaks, though these signals were poorly dispersed (Figure 20B). Titration to 7% cyclofos-7 and raising the temperature by 10°C induced a few more poorly-dispersed signals in the backbone amide region (Figure 20C).

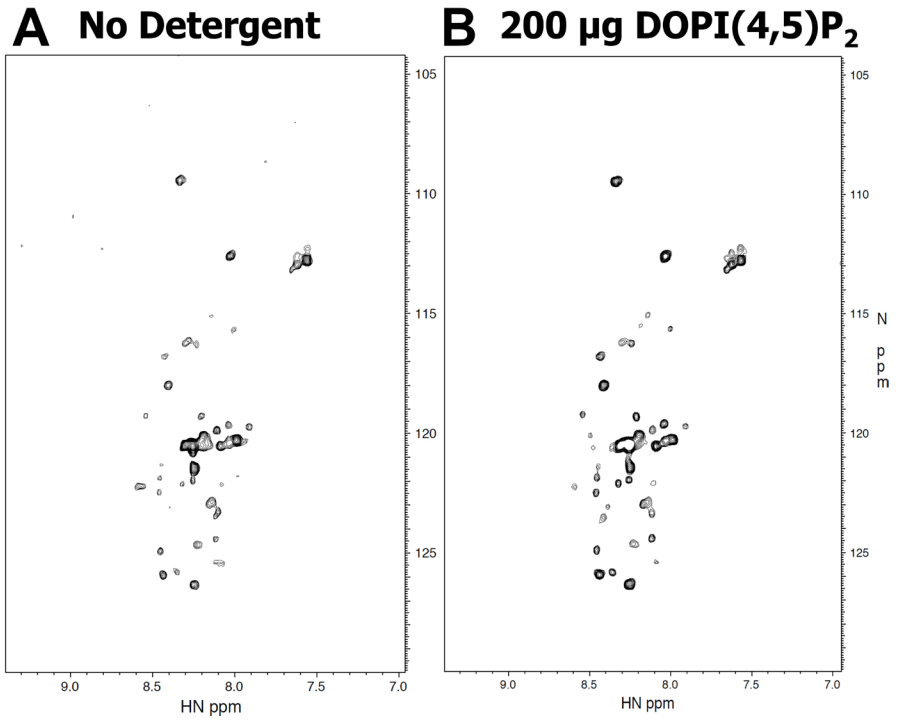

Figure 21. Relative to cyclofos-7, DOPI(4,5)P_2 confers less changes in the ^{1}H-^{15}N HSQC spectrum of CLIC5A[1-112]. [A] HSQC spectrum of 1.5 mg/mL ^{15}N-labled CLIC5A[1-112] in buffer containing 10 mM imidazole, pH 6.70, 100 mM KCl, 20 mM DTT, 5% D_2O, 0.25 mM DSS, and 0.005% sodium azide at 30°C. [B] Addition of 200 μg of the PI(4,5)P_2 analogue 1,2-dioctanoyl-*sn*-glycero-3-phospho-(1'-myo-inositol-4',5'-bisphosphate) DOPI(4,5)$_2$.

Studies in transfected cells indicate that GFP-CLIC5A localizes at the apical region of the plasma membrane in discrete clusters containing PI(4,5)P_2[270], suggesting CLIC5A may require phosphoinositides to assume a correct membrane-associated conformation. To explore this, we added 200 μg of the PI(4,5)P_2 analogue 1,2-dioctaoyl-*sn*-glycero-3-phospho-(1'-myo-

inositol-4',5'-bisphosphate) DOPI(4,5)P_2, an *N*-terminal truncated mutant CLIC5A[1-112] with additional *N*-terminal loop residues (Figure 21). Without detergent, the HSQC spectrum of ^{15}N-labeled CLIC5A[1-112] was nearly identical to that of CLIC5A[1-99] (Figure 21A). DOPI(4,5)P_2 did not result in a significant change in the overall spectrum, and certainly to a much lesser degree` than by cyclfos-7 titration, suggesting CLIC5A had no discernable affinity to this reagent.

Intact WT CLIC5A was also analyzed by NMR. Like CLIC5A[1-99] and CLIC5A[1-112], it also displayed very few peaks (Figure 22). Because gel filtration indicates that WT CLIC5A elutes as a singular peak at the expected molecular weight, it was unlikely to aggregate to the same degree as the truncated *N*-terminal mutants. Therefore, the absence of peaks in this spectrum was likely due to conformational exchange. Overall, the absence of peaks shown in our NMR spectral analyses could suggest CLIC5A adopts multiple conformations in solution, hindering our ability to study these constructs by this method.

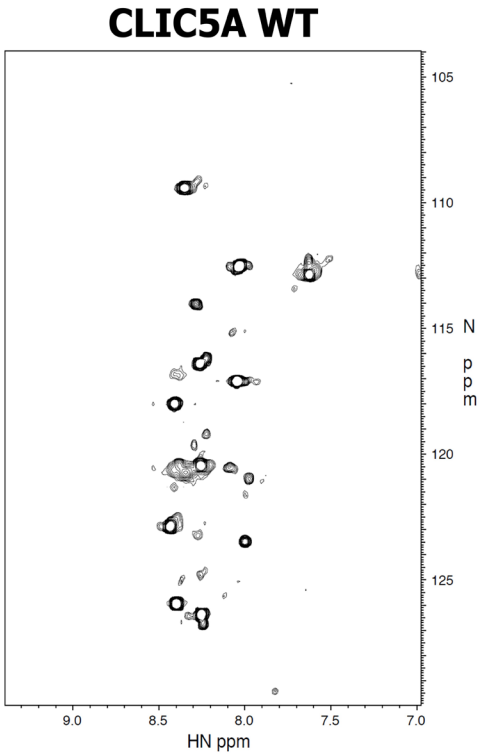

Figure 22. Similar to CLIC5A[1-99], the ^{1}H-^{15}N HSQC spectrum of CLIC5A WT yields few peaks that are poorly dispersed. HSQC spectrum of 10 mg/mL ^{15}N-labeled CLIC5A WT in buffer containing 10 mM imidazole, pH 6.70, 100 mM KCl, 10 mM DTT, 1 mM EDTA, 5% D_2O, 0.25 mM DSS, and 0.005% sodium azide at 30°C.

3.2.3 The Secondary Structure of WT CLIC5A and CLIC5A[1-99] Was Evaluated By CD Spectroscopy

The secondary structure of both CLIC5A constructs were next assessed by circular dichroism (CD) spectroscopy. For WT CLIC5A, a maximum peak occurred at ~190 nm, which is suggestive of a folded structure with α-helical and/or β-pleated elements rather than a random coil, in which case negative ellipticity values would be seen at this wavelength (Figure 23A). Analysis of the spectrum using the CD analysis software CAPITO[425] predicted that CLIC5A WT had 1% α -helical, 52% β-pleated, and 55% irregular secondary structure, which is inconsistent with the X-ray structures obtained for any other CLIC (Figure 8), which are all predominantly α-helical. However, intense CD signals from turns, β-sheets, and Trp residues can heavily alter the shape of a CD spectrum, and so secondary structure calculations may become unreliable, which likely occurred in the case of WT CLIC5A.

Next, the stability of WT CLIC5A was assessed by an estimation of its melting

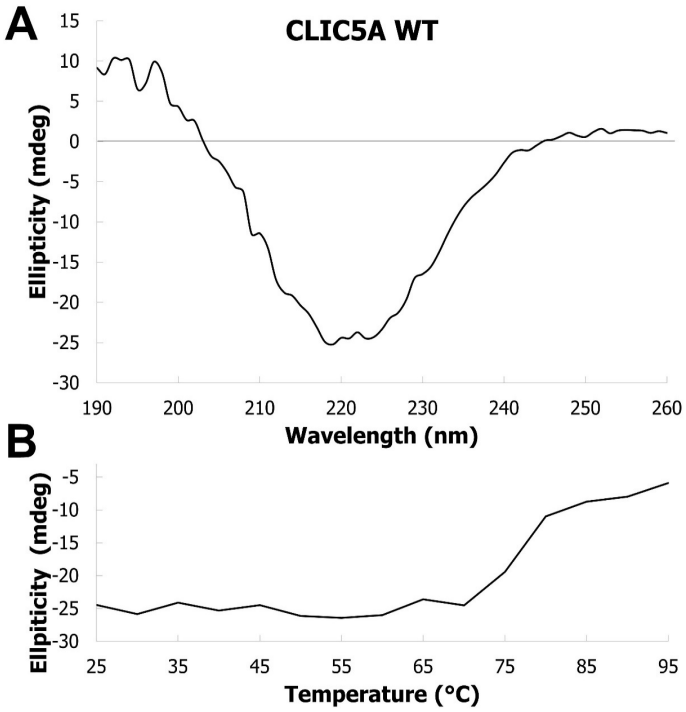

Figure 23. CD spectra show that CLIC5A WT in solution is mostly β-pleated and irregular, with an estimated melting temperature of 75°C. Circular dichroism (CD) spectra were obtained on CLIC5A WT at 0.77 mg/mL in 1 mM TCEP, 50 mM TRIS, 1 mM EDTA, pH 7.00 using a Jasco J-180 spectrometer. A temperature scan from 25°C to 95°C was done to determine its melting temperature. [A] CLIC5A WT at 25°C, and [B] ellipticity at the 220 nm minimum as a function of temperature.

temperature by CD spectra. A dramatic shift in ellipticity was observed at 75°C using the minimum obtained at 220 nm, serving as a rough estimation of its melting temperature (Figure 23B). Because these values are within the expected range of a folded protein, these results further suggest that recombinant WT CLIC5A was indeed properly folded, strengthening the validity of our NMR results of this construct.

In a similar fashion, CD spectra for CLIC5A[1-99] was obtained (Figure 24). Positive ellipticity values were observed at ~195 nm while negative values were obtained from 208 – 222 nm, as would be expected for a properly folded protein. However, the smaller magnitude of the positive ellipticity at 195 nm in comparison to WT CLIC5A suggests a higher proportion of CLIC5A[1-99] assumes a random coil structure. Taken together with its gel filtration, which was suggestive of aggregation, these results suggest that CLIC5A[1-99] is at least partially misfolded, thus making it prone to aggregation and hindering our ability to observe its spectra by NMR.

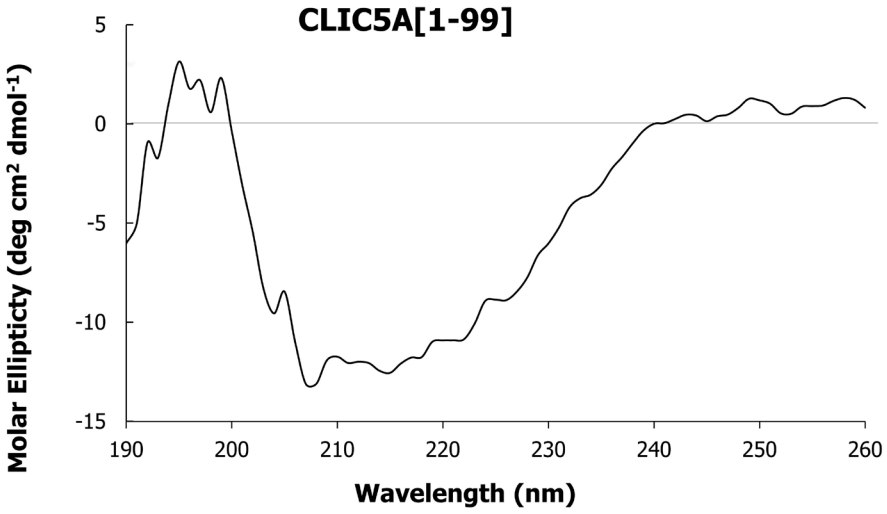

Figure 24. The CD spectra of CLIC5A[1-99] differs from CLIC5A WT. Circular dichroism (CD) spectra were obtained for CLIC5A[1-99] at 0.77 mg/mL in 1 mM TCEP, 50 mM TRIS, 1 mM EDTA, pH 7.00 using a Jasco J-180 spectrometer.

3.3 Discussion

To date, X-ray structures of human CLIC1–CLIC4 have been solved (Figure 8), all of them depicting CLIC proteins as globular soluble proteins. However, several studies have

firmly established that CLIC proteins do indeed associate with membranes. Ion conductance studies of recombinant proteins further demonstrate that CLICs are capable of generating ion currents, at least *in vitro*[264]. Given that CLIC proteins are metamorphic, it is conceivable that their translocation from the cytosol to target membranes is accompanied by structural changes. Indeed, given that its PTMD is buried within the globular core of these X-ray structures, such changes would be necessary for these soluble proteins to associate with membranes.

We embarked on this study hoping to observe a soluble-to-membrane switch by NMR spectroscopy. Unfortunately, the HSQC spectra obtained for CLIC5A[1-99] (Figure 20), CLIC5A[1-112] (Figure 21), and WT CLIC5A (Figure 22) yielded spectra unsuitable for resonance assignment and further structural elucidation, primarily due to a lack of signals. The HSQC spectrum of a well-folded protein with no significant subconformations would display more abundant and well-dispersed signals, as illustrated by the HSQC spectra of cardiac troponin C, shown in Figure 25 for reference. In contrast, an intrinsically-disordered protein

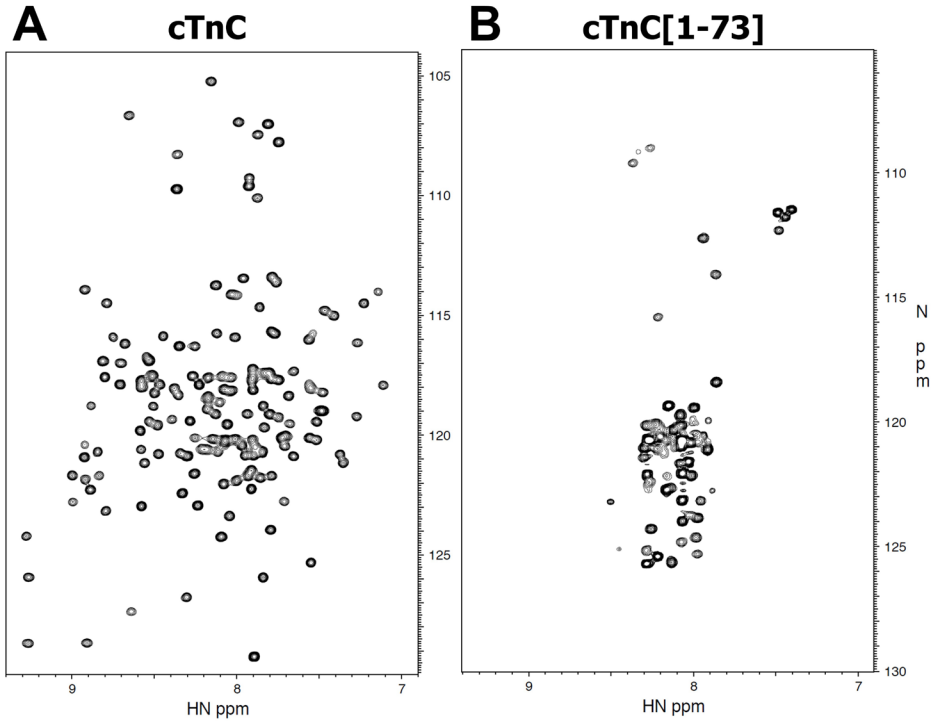

Figure 25. The HSQC spectrum of cardiac troponin C illustrates a well-structured protein in NMR. [A] ^{1}H-^{15}N HSQC NMR spectrum of 0.4 mM ^{15}N-labeled cardiac troponin C in buffer containing 10 mM imidazole, pH 6.25, 100 mM KCl, 10 mM CaCl2, 5% D_2O, 0.25 mM DSS, and 0.005% sodium azide, in 30°C. [B] 0.8 mM ^{15}N-labeled cardiac troponin I, residues 1-73, in buffer containing 10 mM imidazole, pH 6.25, 100 mM KCl, 20 mM CaCl2, 5% D_2O, 0.25 mM DSS, 0.005% sodium azide, in 40°C.

displays narrow but poorly dispersed signals, as shown by the spectrum of a truncated *N*-terminal cardiac troponin C mutant (Figure 25B). Our attempts to enhance the signals by triply-labeling CLIC5A[1-99] with ^{1}H, ^{13}C, and ^{15}N did not improve the signals by any considerable means (data not shown), nor did our titrations with cyclofos-7 and addition of DOPI(4,5)P_2 micelles, though cyclofos-7 appeared to result in the appearance of more peaks than DOPI(4,5)P_2. Notably, the concentration of cyclofos-7 used in our experiments exceeded its critical micelle concentration whereas the 200 μg of DOPI(4,5)P_2 used did not. Proper micellar formation would greatly enhance the solubility of membrane proteins, which could explain why DOPI(4,5)P_2 had no effect.

It is highly probable that the structural dimorphism of CLIC proteins complicates our spectral analyses and results in the sparsely-populated spectra we obtained. In comparison, the X-ray structures obtained by crystallization would capture the conformation most predominant in solution and further favoured by interactions present in other CLIC homologues, crystal packing forces, or the cold temperatures used to collect diffraction data. Thus, discrepancies in our NMR spectra with the crystal diffraction patterns is not entirely unexpected.

In vitro reconstitution and membrane-binding studies using recombinant CLIC1 and CLIC4 reveal that CLIC proteins require a specific lipid environment for proper membrane association. The reconstitution of CLIC1 into pure phosphatidylcholine (PC) liposomes did not yield ion currents, and ion conductance was only observed when these liposomes were supplemented with the anionic lipids phophatidylserine and phosphatidic acid[312]. Similarly, CLIC1 could only elicit ion conductance in artificial bilayers supplemented with cholesterol[311,347,348] and ergosterol[336], and specular X-ray/neutron reflectivity measurements reveal that in the absence of cholesterol, CLIC1 merely adsorbs to the surface of lipid monolayers, but penetrates into monolayers when cholesterol is present[326]. Thus, a possible reason we could not observe significant signals in our detergent titrations could be the multifactorial dependence on a complex lipid environment for proper membrane association, though a Cl^- efflux assay with recombinant CLIC5A in pure PC liposomes was able to elicit ion conductance[303]. Indeed, recombinant CLIC4 displayed greater ion conductances when reconstituted into brain microsomes than in pure PC bilayers[280,311], and the earliest report of CLIC1 ion currents was conducted in isolectin vesicles, which contain a mixture of various

phospholipids[308]. It is curious that the PI(4,5)P_2 analogue induced the appearance of fewer peaks than even cyclofos-7, given that cell culture studies suggest that CLIC5A associates in PI(4,5)P_2-enriched domains at the plasma membrane[270]. It is thus highly probable that CLIC5A, like CLIC1 and CLIC4, also requires a more specific lipid environment to bind to membranes.

To date, no structure has been solved for the membrane-associated form of any CLIC protein, though a model generated using distances from FRET and EPR labeling suggest that the α-helix and β-strand of the *N*-terminal PTMD reorganizes into an elongated α-helix, which inserts into the membrane[333] (Figure 10). Based on studies suggesting that the *N*-terminal domain of CLIC1 is less stable than the *C*-terminal domain, a conformational change of this kind is conceivable, though more work must be done in order to demonstrate this hypothesis.

Overall, our structural studies on CLIC5A were hindered by the poor quality of spectra obtained by NMR spectroscopy, and we could not gain significant insight in the soluble-to-membrane transition occurring of CLIC5A.

Chapter 4: The Transmembrane Topology of CLIC5A

4.1 Introduction

Although ion conductance has been demonstrated for most of its members, CLIC proteins are unlikely to form classical α- or β-type ion channels (Figure 4), both integral transmembrane proteins[207], for the following reasons. First, the molecular weights of CLIC proteins, ranging from 26 – 73 kDa (Table 4), is less than typical ion channels, though the smallest known ion channel at present, the *Chlorella* virus Kcv K^+ channel, is an exception at ~10 kDa[426]. Second, CLIC proteins contain just one putative transmembrane domain (Table 4) as predicted by hydropathy analysis, whereas even the miniature Kcv K^+ channel has two[426]. This is highly unusual for ion channels, which usually span lipid bilayers multiple times[207]. Additionally, CLIC proteins lack a signal sequence[307], unlike the ClC[219], CFTR[233], or ligand-gated GABA/glycine receptor[237,240] anion channels, thus making the coordinated insertion of CLIC proteins into membranes a questionable process. Finally, the dimorphism of CLICs as metamorphic proteins distinguishes this family from classical ion channels. The X-ray structures of all CLICs solved to date show that in their soluble form, CLICs assume a compact globular fold with its putative transmembrane domain (PTMD) sequestered within its hydrophobic core (Figure 8). This structure would necessitate a large-scale structural change, including a disruption of the conserved GSTΩ fold, to achieve membrane insertion. In this regard, CLIC proteins resemble pore-forming proteins, not classical ion channels, and have been classified as such by Fiel and colleagues[142].

Nevertheless, their initial discovery as ion channels have led researchers to establish CLICs as transmembrane proteins analogous to classical α-type ion channels. Microsomal vesicles retained recombinant CLIC4 after alkali washes and protected CLIC4 from protease degradation[280], leading the authors to conclude that CLICs were integral membrane proteins. Furthermore, FLAG antibodies abolished electric currents in FLAG epitope-tagged CLIC1 and CLIC4 reconstituted into artificial membranes when oriented in outside-out configurations, suggesting the *N*-terminus was oriented to the extracellular or lumenal space[324,325]. However, these models were generated with the assumed bias that CLICs assumed a topology typical of ion channels and failed to address the possibility of CLICs associating with membranes in non-transmembrane configurations.

Considering the unusual structural properties of CLIC proteins as ion channels, we hypothesized that CLIC5A does not assume a transmembrane configuration. In this chapter, we investigated this hypothesis by employing a number of methods distinguishing transmembrane proteins from intracellular soluble and peripheral proteins, utilizing the cell adhesion molecule *N*-Cadherin[427] and the glycolytic enzyme glyceraldehyde-3-phosphate dehydrogenase (GAPDH)[428] as controls respectively.

4.2 Results

4.2.1 CLIC5A Is Not Retrieved By Biotinylation Surface Protein Capture

To determine whether CLIC5A spans the plasma membrane, control vector- and CLIC5A-transfected COS-7 cells were labeled with a membrane-impermeant biotin derivative, which covalently bonds with the primary amines on *N*-termini and lysine residues[429] exposed on surface proteins. The biotinylated proteins were then captured on an avidin affinity column followed by elution. The control transmembrane *N*-Cadherin was detected in abundance in the avidin column eluate but CLIC5A was not captured and was instead retrieved as unbound proteins in the flow-through (Figure 26A), similar to the soluble cytoplasmic control, GADH. This finding suggested that CLIC5A was not biotinylated. To confirm, the same fractions were stained with streptavidin-HRP and analyzed by immunoblot (Figure 26B). Not observable increase in signal in any of the fractions was observed between vector- and CLIC5A-transfected cells in the molecular weight range corresponding to CLIC5A at ~29 kDa, indicating that CLIC5A was not biotinylated.

4.2.2 The FLAG-CLIC5A Epitope Is Confined To The Intracellular Space

Previous studies suggest that if CLICs were transmembrane, its *N*-terminus would be oriented in the extracellular space at the PM, or within the lumen of organelles[324,325]. But in vivo and in cultured cells, CLIC5A localizes to the apical membrane of epithelial cells and podocytes, suggesting that the N-terminus should be extracellular. To determine whether epitopes of control N-Cadherin or GAPDH, and FLAG-epitope tagged CLIC5A are accessible to antibodies when cells are impermeable, intact and Triton X-100 permeabilized COS-7 cells were incubated with primary and flurophore-conjugated secondary antibodies and visualized by confocal microscopy (Figure 27). The transmembrane protein *N*-Cadherin was detected in

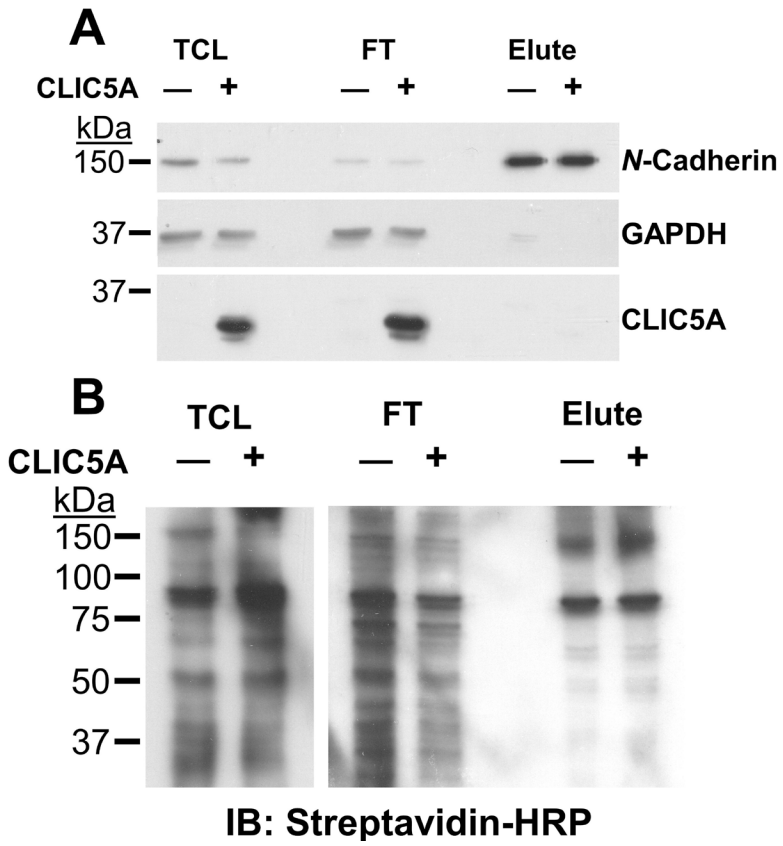

Figure 26. CLIC5A is not retrievable by biotin tagged surface protein capture. Intact control vector- (—) and CLIC5A-(+) transfected COS-7 cells were labeled with a membrane-impermeant biotin derivative to tag surface proteins, then biotinylated proteins were captured and eluted off an avidin-based column from total cell lysate (TCL). Uncaptured proteins were retrieved as the flow-through (FT), and all fractions were analyzed by immunoblot (IB) to detect [A] CLIC5A, the intracellular control GAPDH, and the surface protein control *N*-Cadherin, and [B] biotinylated proteins by streptavidin-HRP.

both, intact and permeabilized cells, whereas the intracellular control GAPDH as well as FLAG-CLIC5A were only detected in permeabilized cells, suggesting the *N*-terminal FLAG epitope of FLAG-CLIC5A is confined in the intracellular space.

4.2.3 FLAG-CLIC5A Resists Proteolytic Degradation

In a similar approach, we reasoned that if CLIC5A was not an integral transmembrane protein, it should resist proteolytic degradation in intact cells, but become vulnerable in permeabilized cells. To this effect, we permeabilized FLAG-CLIC5A-transfected COS-7 cells with varying digitonin concentrations, which creates pores at the PM in a concentration-dependent manner[406], and treated cells with 0.1 mg/mL trypsin. As indicated by immunoblot

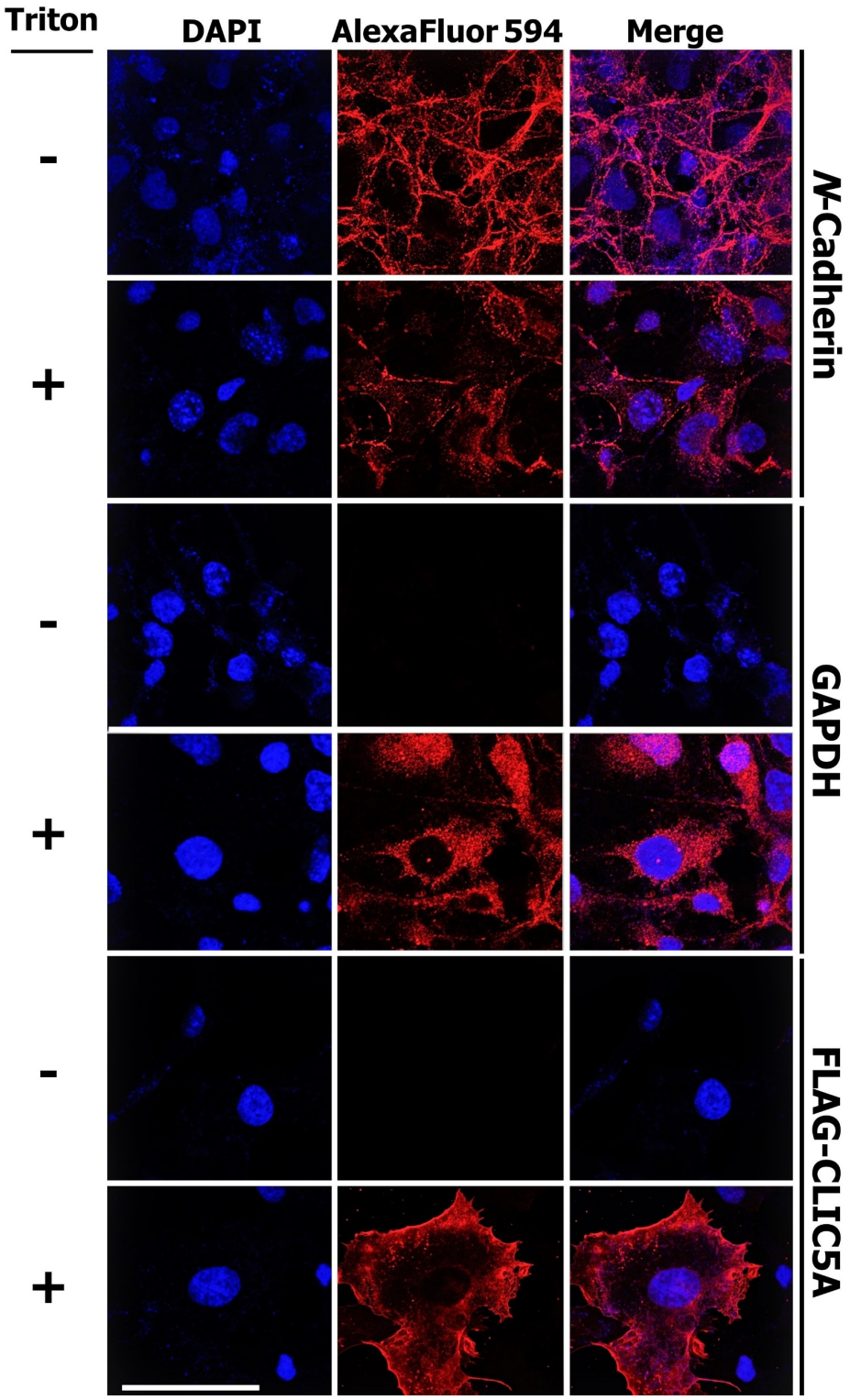

Figure 27. The *N*-terminal FLAG epitope of FLAG-CLIC5A is confined intracellularly. COS-7 cells expressing a CLIC5A with an *N*-terminal FLAG tag were fixed and stained for the indicated proteins with either intact (-) or Triton X-100-permeabilized (+) membranes. Nuclei are stained in blue (DAPI), and proteins are stained in red with the AlexaFluor® 594 dye. Images were obtained by confocal microscopy. Scale bar = 50 μm.

analysis, we observed proteolysis of *N*-Cadherin independent of permeabilization while FLAG-CLIC5A, like GAPDH, was only degraded in permeabilized cells (Figure 28). Antibodies toward to the *N*-terminal FLAG and *C*-terminal CLIC5A epitope of FLAG-CLIC5A displayed similar degradation patterns (Figure 28), suggesting a degradation of total CLIC5A rather than just an extruded segment.

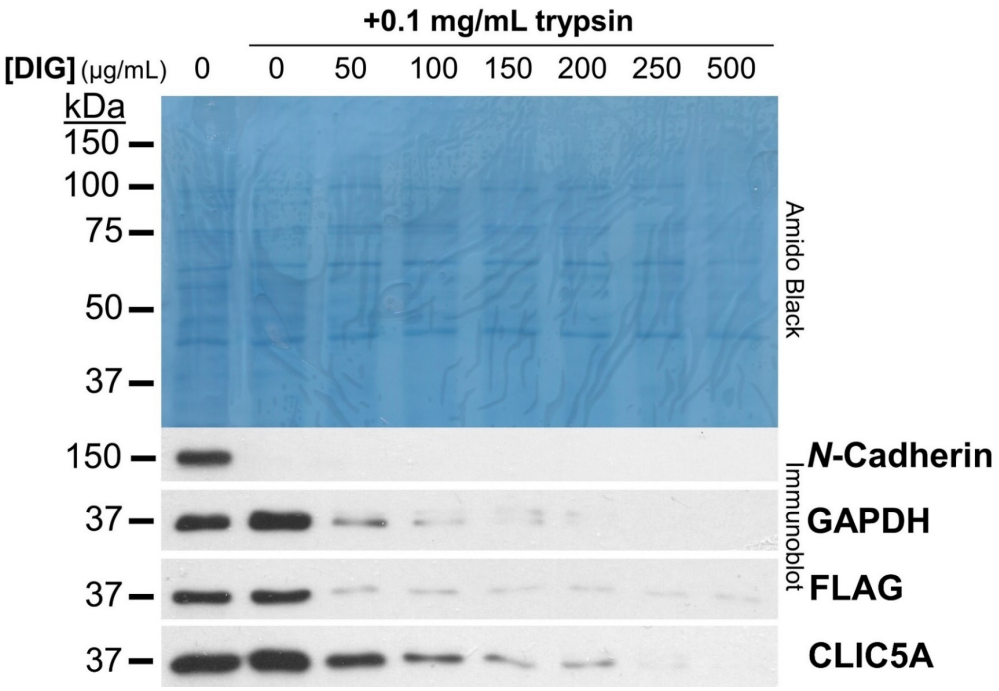

Figure 28. FLAG-CLIC5A is protected from proteolytic degradation. FLAG-CLIC5A expressing COS-7 cells were kept intact or permeabilized with the detergent digitonin (DIG) at increasing concentrations to permeabilize cells at different extents. Cells were then treated with 0.1 mg/mL trypsin for 30 min on ice to determine the accessibility of these substrates to proteolytic degradation. PVDF membranes were stained for total protein using Amido Black and for specific proteins by immunoblot analysis. Both the *N*-terminal FLAG epitope and a *C*-terminal CLIC5A epitope for FLAG-CLIC5A were stained and showed similar results.

4.2.4 CLIC1, CLIC4, & CLIC5A Are Predominantly Cytosolic In Differential Detergent Fractionation

As the final test of its transmembrane topology, transfected cells were subjected to differential detergent fractionation, in which subcellular fractions are obtained by sequential treatment with detergents of increasing strength[430]. Similar to the cytosolic marker GAPDH, CLIC5A was predominantly retrieved in digitonin-soluble (Dg) fractions containing cytosolic

proteins and absent from Triton-soluble (Tx) fractions containing PM and endomembrane proteins, opposite to the findings for the integral transmembrane protein control *N*-Cadherin, which was enriched in Tx fractions and not observed in the Dg fractions (Figure 29). Consistent with its amphitropism, PKCα was retrieved in both Dg and Tx fractions, though to a much lesser extent in the latter. This behavior is consistent with dissociation of the peripheral protein PKCα from the membrane by the high ionic strength of the extraction buffers (Figure 29). All proteins except GAPDH were retrieved in insoluble pellets enriched in cytoskeletal proteins (Figure 29), likely due to tethering of membrane proteins to the cytoskeleton[12]. CLIC5A was also detected in the pellets, which contain protein aggregates and the detergent-insoluble cytoskeleton. These results signify that CLIC5A, which is observed at the PM by imaging in living cells, must associate with the PM through very weak interactions reminiscent of a peripheral protein, and that it is not an integral transmembrane protein.

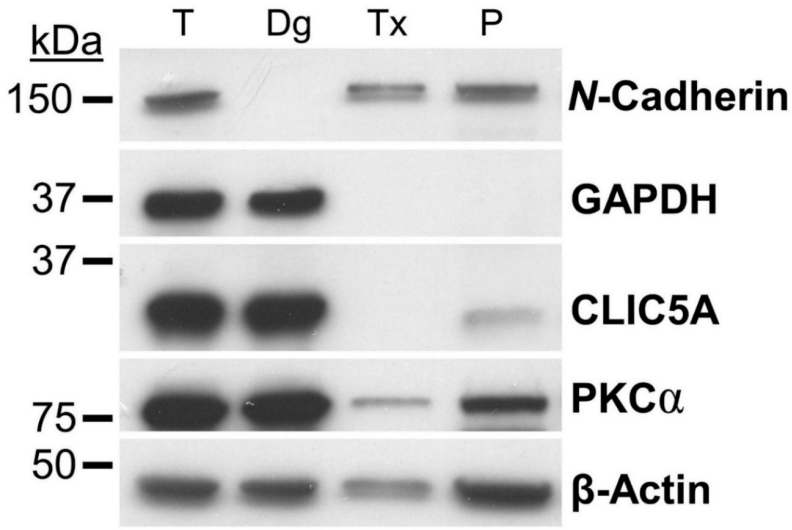

Figure 29. CLIC5A is predominantly retrieved in cytosolic fractions by differential detergent fractionation. Subcellular fractions were obtained from CLIC5A-transfected-COS-7 cells (T) by differential detergent fractionation to yield cytosolic proteins in digitonin-soluble (Dg) fractions, plasma membrane and endomembrane proteins in Triton-soluble (Tx) fractions, and cytoskeletal, nuclear, and aggregated proteins sedimented in the insoluble pellet (P).

To determine if CLIC1 and CLIC4 share the weak membrane interaction with CLIC5A, untransfected COS-7 cells, which express both these proteins at baseline, were fractionated. Like CLIC5A, CLIC1 and CLIC4 were predominantly retrieved in Dg fractions and absent

from Tx fractions, though neither protein was detectable in pellets (Figure 30). These results suggest that CLIC1, CLIC4, and CLIC5A interact with membranes with weak interactions akin to peripheral proteins. However, because digitonin complexes with cholesterol[403,404], to which CLIC1 and perhaps other CLICs bind[311,326,336,347,348], it is also possible that the cytoplasmic distribution of CLIC1, CLIC4, and CLIC5A in these experiments is due to cholesterol depletion.

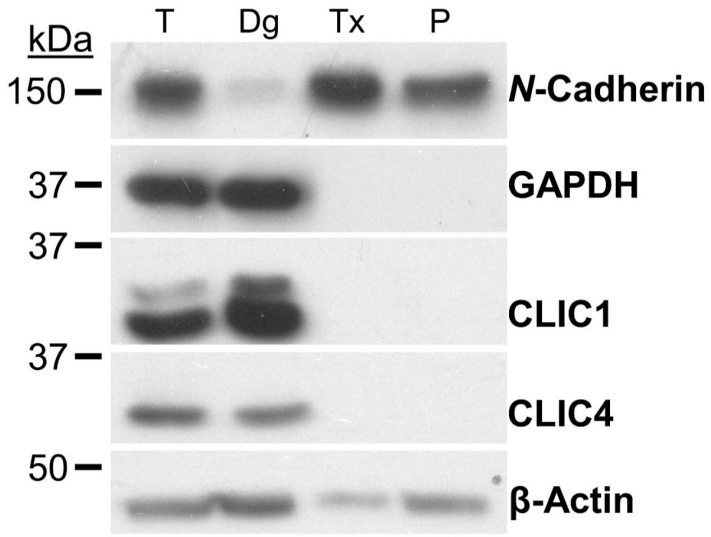

Figure 30. CLIC1 and CLIC4, like CLIC5A, is predominantly retrieved in cytosolic fractions by differential detergent fractionation. Untransfected COS-7 cells, which express CLIC1 and CLIC4 at baseline, were fractionated by differential detergent fractionation as before to yield cytosolic proteins in digitonin-soluble (Dg) fractions, plasma membrane and endomembrane proteins in Triton-soluble (Tx) fractions, and cytoskeletal, nuclear, and aggregated proteins sedimented in the insoluble pellet (P).

4.3 Discussion

Since their discovery, CLIC proteins have been assumed to be integral transmembrane proteins based on their ability to confer ion conductances in artificial lipid bilayers *in vitro*. Yet these claims were not supported by solid evidence, and skepticism about their ability to form legitimate ion channels has been voiced[207,290,306,383]. Nevertheless, ion conductance has been demonstrated for nearly all CLICs[264] apart from CLIC3 and CLIC6[306], though these reports are doubtful for several reasons. First, anion selectivity ranges from no selectivity between anions in CLIC1[311] and CLIC4[314], or an inability to discriminate between anions and

cations at all in CLIC5A[315]. Perhaps more disconcertingly, ion conductance measurements are highly variable both within and between CLICs[264], even under identical conditions for the same protein[315]. While differences in experimental set-up, lipid composition, redox conditions, or pH could explain the variability between studies[264], they cannot account for the variation under the same experimental setup. One hypothesis posits that the variable conductances could be attributable to different multimeric states[307], suggesting that pores mediating these currents are not well-defined structures but rather, nonspecific pores dependent on a complex interplay of the protein-to-lipid ratio, sequence, and stoichiometry of units joining to form the pore, similar to pore-forming proteins[188,205,206]. Since all ion conductance studies for CLICs were done *in vitro* with artificial membranes, it is probable that these measurements may simply be a reflection of the ability of CLICs to translocate to, and perturbing lipid bilayers *in vitro*[142], thus necessitating the urgency to demonstrate ion conductance *in vivo*.

Our present study challenges the claims that CLICs form legitimate ion channels typical of classical α- and β-type channels[133]. CLIC5A was neither retrieved by biotinylation surface protein capture from intact cells, nor biotinylated (Figure 26), suggesting no portion of CLIC5A has an extracellular region that is surface-exposed. Further, its *N*-terminal FLAG epitope, predicted to be outward-facing in a transmembrane configuration[324,325], remained confined to the intracellular space as visualized by IF imaging (Figure 27). Also, both the *N*-terminal FLAG and *C*-terminal CLIC5A epitope of FLAG-CLIC5A resisted proteolytic degradation in intact cells (Figure 28), and only became sensitive to trypsin at concentrations of digitonin sufficient to permeabilize the plasma membrane of COS-7 cells (Figure 15). Finally, membrane protein-containing fractions obtained by differential detergent fractionation revealed that CLIC5A (Figure 29), as well as CLIC1 and CLIC4 (Figure 30), are largely cytoplasmic and not membrane-associated. Overall, these findings indicate that CLIC5A lacks the biochemical characteristics of integral membrane proteins, and thus could not be transmembrane. Given that the association of CLICs with membranes have been extensively demonstrated *in vitro*[280,286,310,311,326,327] and *in vivo*[328,329], we posit that CLIC5A associates with the inner leaflet of the PM as a peripheral protein and not as an integral transmembrane protein.

Biotin conjugates with primary amines on *N*-termini and lysines[429], raising the possibility that the lack of retrieval of CLIC5A in eluates or its biotinylation (Figure 26) could

be due to a lack of primary amines on a surface-exposed segment, steric hindrance, or both. Nevertheless, because a transmembrane configuration of CLIC5A would theoretically orient its *N*-terminus outwards, we would expect a greater retrieval if it were indeed transmembrane. An earlier study reported that recombinant CLIC4 was resistant to proteolytic degradation when reconstituted into rat brain microsomes, similar to our study (Figure 28), though the authors interpreted these findings to suggest that the majority of CLIC4 was intracellular in a transmembrane configuration, based on the assumption that CLICs formed typical ion channels[280]. Considering our findings, we instead interpret these results to suggest that CLIC5A is entirely intracellular and that its location at the PM in imaging studies and its association with lipid bilayers in vitro are due to a peripheral association with the inner leaflet of the plasma membrane.

The present study did not identify the mechanism by which CLIC5A binds to membranes if it is a peripheral protein. All peripheral proteins bind in a two-step process, in which electrostatic forces nonspecifically adsorb the protein to the bilayer surface, at which point other more specific forces such as lipidylation or the exposure of a hydrophobic anchor dominate[70]. Structural predictions based on FRET and EPR labeling assume the PTMD becomes helical structure upon membrane insertion[333], which could serve as a hydrophobic anchor. Yet given that X-ray structures of all CLICs to date are of their soluble globular form, with the PTMD hidden in the hydrophobic core and spanning across an α-helix and a β-strand (Figure 8), large-scale structural transformations would be necessary to expose its PTMD. Proteomic data indicate that CLICs may be palmitoylated[362], which could also serve as a method of membrane association, though lipid tags do serve functions other than membrane targeting. Further study must be done to determine the mechanism of membrane association.

Differential detergent fractionation is a cheap, reproducible, and easy-to-employ procedure. Cytosolic proteins are extracted by permeabilizing the plasma membrane using digitonin, which creates pores by complexing with cholesterol[403,404]. CLIC proteins require a specific lipid environment to bind to membranes including acidic lipids such as phosphatidyl-serine and phosphatidic acid, and thus show greater ion conductance and membrane association in mixed rather than homogeneous artificial membranes[280,311,312]. Additionally, CLIC1 displays ion conductance only in bilayers supplemented with cholesterol[311,336,347,348].

Specular X-ray and neutron reflectometry, which enables the depth of protein insertion into membranes to be measured, reveal that in the absence of cholesterol, CLIC1 adsorbs to the monolayer surface, while it penetrates the headgroup and acyl chain region by a sum of 25.7 Å in the presence of cholesterol[326], notably less than the ~60 Å length of biological membranes[15–17]. Not only do these biophysical measurements suggest that CLIC1 is also not transmembrane, but they also establish the importance of cholesterol for membrane binding. Given that cholesterol may play a role in the membrane association of CLIC1, and that its putative cholesterol-binding motifs, shared with the amyloid precursor protein[349] and the HIV fusion glycoprotein[350], are conserved among nearly all CLICs (Figure 7), our results showing a solely cytoplasmic distribution of CLIC1, CLIC4, and CLIC5A (Figure 29–Figure 30) could be attributed to cholesterol depletion by digitonin. Regardless, the dissociation of CLICs from membranes would not be expected for integral proteins, and do not contradict our conclusions that CLIC5A is not transmembrane.

Among its role in regulating the fluidity of biological membranes, cholesterol is a structural component of lipid rafts[431] and caveolae[432], both of which are microdomains of the membrane. Given that CLICs may associate with cholesterol in cells, our fractionation studies (Figure 29–Figure 30) suggest that these proteins could sort within these microdomains at the plasma membrane. Rafts and caveolae differ in their leaflet distribution: rafts are exoplasmic while caveolae are situated in the inner leaflet[432]. Thus, given that CLIC5A appears to be confined in the intracellular space, it may, in addition to CLIC1 and CLIC4, associate in caveolae microdomains based on the following lines of evidence. First and most obvious is the localization of CLIC4 in caveolae[285]. Second, cross-sectional IF images of GFP-CLIC5A at the plasma membrane suggest that like $PI(4,5)P_2$, CLIC5A is distributed in what appears to be clustered rather than diffuse localization[270], similar to that of cholesterol[433]. Third, NHERF2, which is in the CLIC5A pathway[396], is postulated to mediate the dimerization and sorting of podocalyxin into rafts and other microdomains[434,435]. Intriguingly, CLIC5A also interacts with a number of proteins that associate with membrane microdomains such as ezrin, which is a raft protein[436] and Rac1 which is found in caveolae[437,438], supporting this hypothesis. If CLIC5A were indeed to associate with lipid microdomains, it would support the notion that CLIC5A participates in membrane-reorganizing processes, including the formation of

podocyte foot processes[396]. Since our study did not prove cholesterol binding of CLIC5A, this hypothesis remains to be explored.

In summary, CLIC5A lacks many of the biochemical features expected of transmembrane and thus integral membrane proteins. We can therefore safely conclude that it cannot function as a classical ion channel. Instead, CLI5A likely is a peripheral protein bound to the inner leaflet of the plasma membrane, and potentially sorted to cholesterol-containing microdomains, possibly caveolae. It is still possible that CLIC5A and other CLICs could function as pore-forming proteins, which do not require the characteristics of transmembrane channels. In the next chapter, a process translocating CLIC5A to the membranes is explored.

Chapter 5: The Translocation of CLIC5A to Membranes

5.1 Introduction

Of the six mammalian CLICs, not one member localizes to a singular subcellular location (Table 4). For instance, CLIC5A has been found to localize to the cytoplasm, PM, and cytoskeleton with recent reports of an inner mitochondrial membrane distribution in rat cardiomyocytes[302,303,329,353]. In line with their broad subcellular locales, CLICs appear to translocate to specific sites under certain conditions such as the differentiation state of the cell[301,353] and exogenous stimuli such as cAMP[355], fibronectin[356], and Aβ peptide[338]. Given that CLICs are metamorphic and assume at least two distinct folds[424], it is conceivable that the translocation of CLICs to membranes is accompanied by structural transitions between a soluble and membrane-associated form in a similar fashion as pore-forming proteins[183].

The association of CLICs with membranes appears to be redox- and pH-regulated, with membrane association promoted under oxidizing and acidic conditions in CLIC1[310,335,424] and CLIC4[327]. A particular lipid environment dependent on acidic phospholipids[312] and cholesterol[336], is also required for the binding of CLICs to membranes. CLIC4 localizes to cholesterol-enriched caveolae[285], and CLIC1 generates ion conductance proportional to the cholesterol content in artificial membranes[311,347,348]. Two consensus sequences, both situated within the *N*-terminal CLIC module, are hypothesized to enable its interaction with cholesterol (Figure 7), though further studies are required to necessitate this claim. Nevertheless, specular X-ray and neutron reflectometry measurements indicate that while CLIC1 readily adsorbs to the surface of monolayers containing acidic phospholipids, insertion into the membrane only occurs when cholesterol is present[326], signifying the importance of cholesterol for the membrane association of CLICs.

While the structural dimorphism and translocative property of CLICs have been studied in detail, the biological triggers and signaling pathways involved have not yet been identified for most CLICs. Certain post-translational modifications, such as phosphorylation, have been detected *in vitro* for CLIC1 and CLIC4[280,301,307], but fail to account for its biological activity in cells, though CLIC4 has been identified to be *S*-nitrosylated during LPS-induced nuclear translocation[301]. Given the sparsity of identified biological triggers inducing the translocation of CLICs to membranes, we aimed to identify a potential signaling pathway that

translocates CLIC5A to membranes by method of differential detergent fractionation in transfected COS-7 cells treated with various kinase and phosphatase inhibitors, as well as hydrogen peroxide.

5.2 Results

5.2.1 CLIC5A Translocates To Membranes In A Phosphorylation-Driven Process

Given that CLICs contain multiple putative phosphorylation sites[307] and can be phosphorylated *in vitro* by both conventional and novel PKCs[301], we investigated whether phosphorylation could affect the translocation of CLIC5A to different subcellular locations. FLAG-CLIC5A transfected COS-7 cells were pre-treated with the Ser/Thr phosphatase inhibitor Calyculin A[409] at 50 nM for 15 and 20 min prior to fractionation. As before, CLIC5A was only faintly detectable in Triton-soluble fractions but its abundance in this fraction increased after Calyculin A treatment in what appeared to be a time-dependent manner (Figure 31A). p-ERM levels, which increase by PKCα-mediated threonine phosphorylation[391], were elevated, confirming that phosphatase inhibitor treatment was effective (Figure 31A). Densitometry quantification by anti-FLAG in three independent experiments confirmed that Calyculin A treatment significantly increased CLIC5A in Triton-soluble fractions (Figure 31B,D), though time-dependence did not reach significance. This increased association of CLIC5A was not due to upregulation of CLIC5A levels (Figure 31C). These results suggest that a Ser/Thr phosphorylation-mediated process translocates CLIC5A to membranes.

5.2.2 Staurosporine Inhibits The Phosphorylation-Driven Translocation of CLIC5A To Membranes

We next aimed to identify the particular Ser/Thr kinase mediating the Calyculin A-driven translocation of CLIC5A to membranes. CLIC5A-transfected COS-7 cells were pre-incubated with either Vehicle or the broad kinase inhibitor Staurosporine[410,411] prior to Calyculin treatment. Staurosporine treatment abolished the Calyculin A-induced elevation of CLIC5A in Triton-soluble fractions at a concentration of 20 nM (Figure 32A). Densitometry quantification in three independent experiments confirm that Staurosporine at 20 but not 2 nM abolishes the effect of Calyculin A (Figure 32B,D). Curiously, the amount of

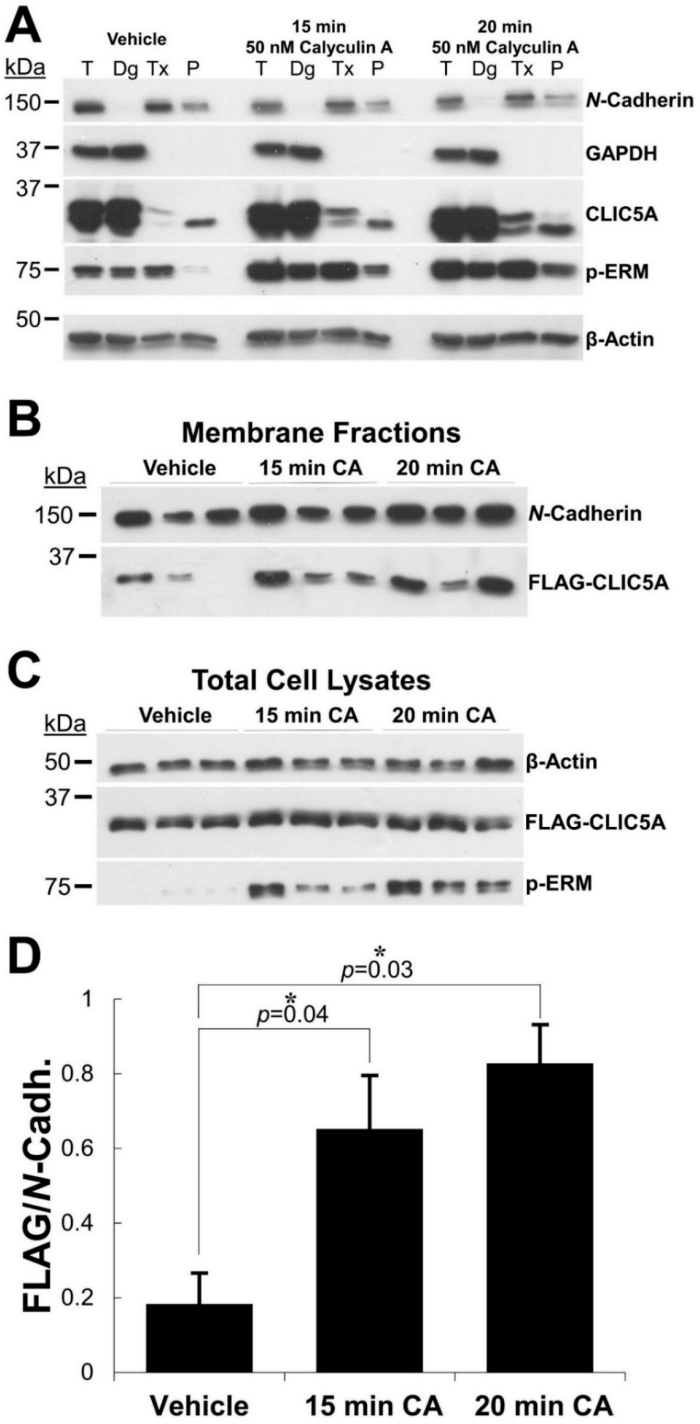

Figure 31. CLIC5A stably associates with Triton-soluble fractions in response to phosphatase inhibition by Calyculin A. [A] FLAG-CLIC5A-transfected COS-7 cells were treated with either Vehicle or 50 nM Calyculin A (CA) for 15 or 20 min at room temperature. Subcellular fractions of cytosolic and membrane proteins were then retrieved in digitonin-soluble (Dg) and Triton-soluble (Tx) fractions respectively from the total cell lysate (T). Insoluble aggregates were sedimented in the pellet (P). [B] Triton-soluble membrane fractions and [C] total cell lysates from three independent experiments. [D] The ratio of FLAG-to-*N*-Cadherin in Triton-soluble fractions as quantified by densitometry (mean ± SEM; $n = 3$ independent experiments; $^*P < 0.05$).

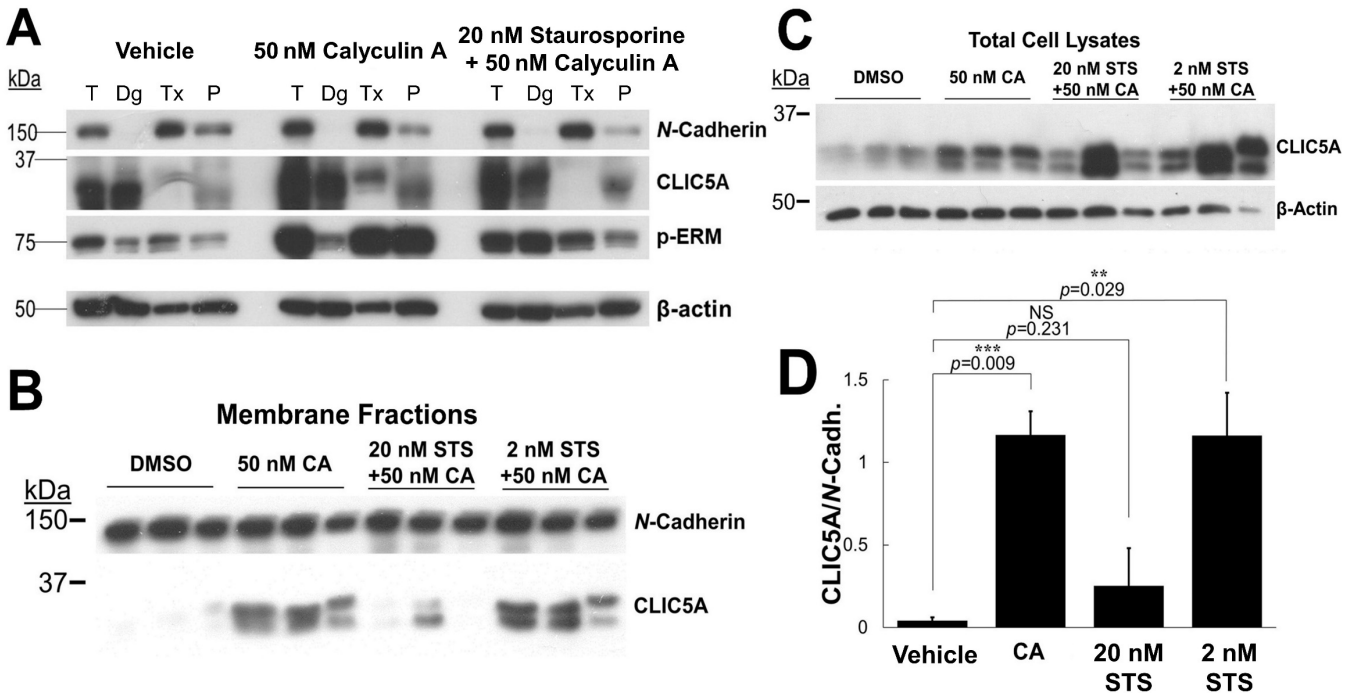

Figure 32. The Calyculin A-induced enrichment of CLIC5A in Triton-soluble fractions is abolished by Staurosporine. [A] CLIC5A-transfected COS-7 cells were pre-treated with either Vehicle or 20 nM Staurosporine (STS) for 3 hrs in 37°C prior to treatment with 50 nM Calyculin A (CA). Subcellular fractions of cytosolic and membrane proteins were then retrieved in digitonin-soluble (Dg) and Triton-soluble (Tx) fractions respectively from the total cell lysate (T). Insoluble aggregates were sedimented in the pellet (P). [B] Triton-soluble membrane fractions and [C] total cell lysates from three independent experiments. [D] The ratio of CLIC5A-to-*N*-Cadherin in Triton-soluble fractions, quantified by densitometry (mean ± SEM; $n = 3$ independent experiments; $^{*}P < 0.05$).

CLIC5A in total cell lysates were lower in Vehicle-treated cells when compared to Calyculin A treatment (Figure 32A). To determine if this reduction was due to a downregulation of CLIC5A, the experiments were repeated using FLAG-CLIC5A-transfected COS-7 cells and quantified using anti-FLAG instead of anti-CLIC5A (Figure 33 & Figure 35). As shown by densitometry, the amount of FLAG-CLIC5A did not change with Calyculin A treatment (Figure 35C), suggesting the apparent reduction in CLIC5A seen in Figure 32C could be due to a differential sensitivity of the antibody during immunoblot analysis, perhaps by masking of its *C*-terminal epitope provoked by a conformational change of CLIC5A.

Though potent, staurosporine is a nonspecific kinase inhibitor, inhibiting PKCα, δ, γ, and η with IC_{50} values of 2, 20, 5, and 4 nM respectively[439] in addition to several others

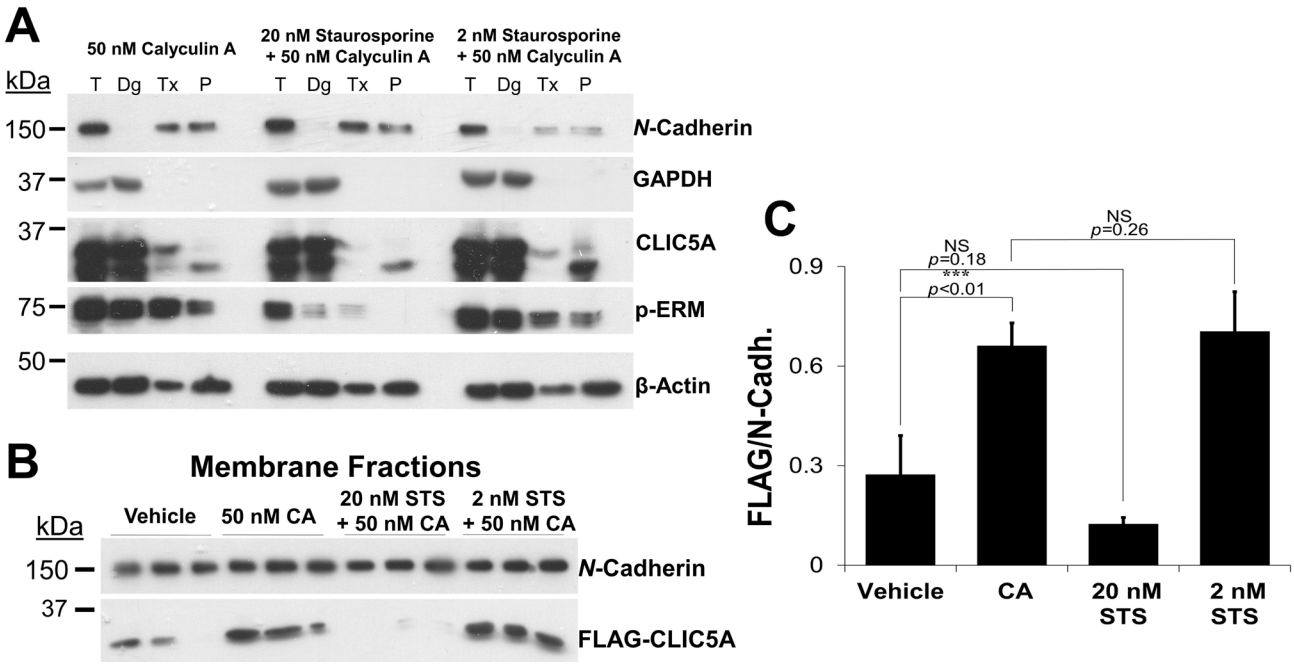

Figure 33. The Calyculin A-induced enrichment of CLIC5A in Triton-soluble fractions is abolished by Staurosporine. [A] FLAG-CLIC5A-transfected COS-7 cells were pre-treated with Vehicle or either 2 or 20 nM Staurosporine (STS) for 3 hrs in 37°C prior to treatment with 50 nM Calyculin A (CA). Subcellular fractions of cytosolic and membrane proteins were then retrieved in digitonin-soluble (Dg) and Triton-soluble (Tx) fractions respectively from the total cell lysate (T). Insoluble aggregates were sedimented in the pellet (P). [B] Triton-soluble membrane fractions from three independent experiments. [C] The ratio of FLAG-to-*N*-Cadherin in Triton-soluble fractions, quantified by densitometry (mean ± SEM; $n = 3$ independent experiments; $*P < 0.05$).

including PKA (15 nM), myosin light chain kinase (1.3 nM), and Ca^{2+}/calmodulin-dependent protein kinase (20 nM)[440]. Given that CLIC5A interacts with the PKA-scaffolding protein AKAP350[305], as well as its involvement with Rac-1-induced PAK1-3 stimulation[396], we investigated using more specific inhibitors whether these kinases mediated the translocation to membranes in CLIC5A (Figure 34) and FLAG-CLIC5A-transfected COS-7 cells (Figure 35). Unlike staurosporine at 20 nM, neither H-89 nor IPA-3 for PKA and PAK1-3 inhibition, respectively, reduced CLIC5A in membrane fractions, suggesting neither kinase is involved in the translocation process.

Overall, these results indicate that despite the depletion of cholesterol in the differential detergent fractionation procedure, a phosphorylation-driven process which is sensitive to staurosporine is sufficient to stably associate CLIC5A to membranes. Theoretically, this stable

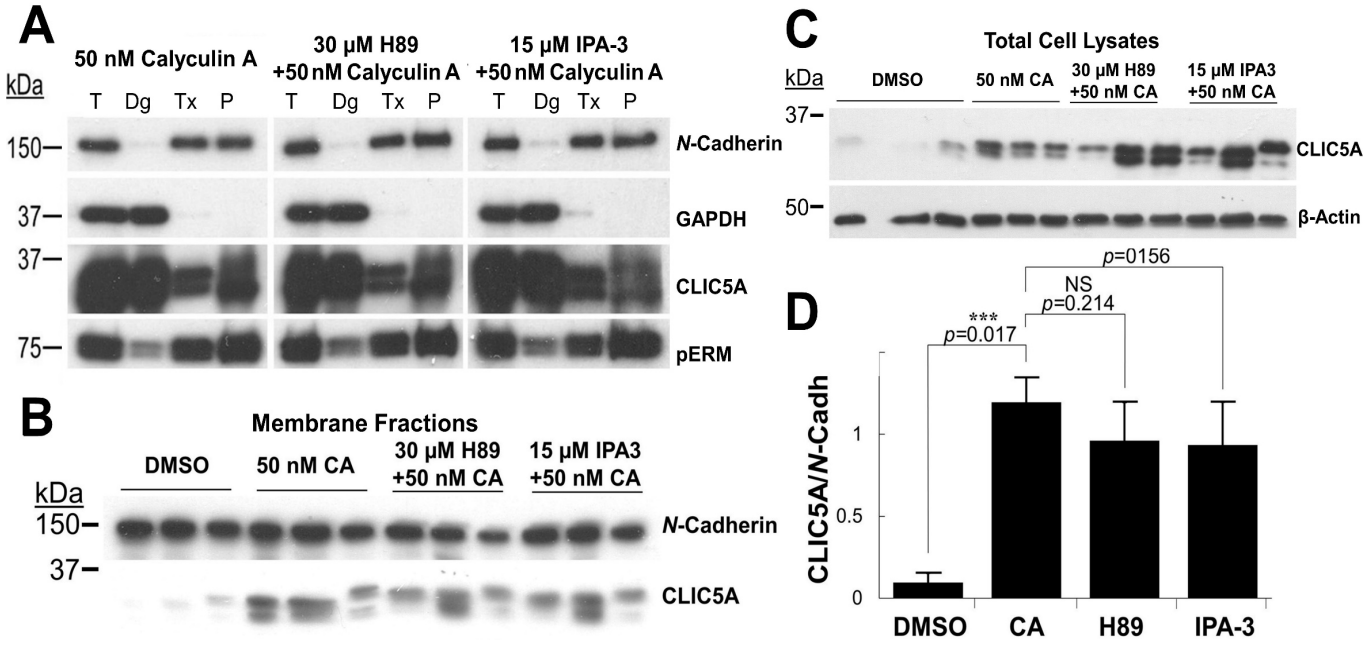

Figure 34. PKA and PAK1-3 inhibitors do not abolish the Calyculin A-induced enrichment of CLIC5A in Triton-soluble fractions. [A] CLIC5A-transfected COS-7 cells were pre-treated with Vehicle, the PKA inhibitor H89 (30 μM, 1 hr, 37°C), or the PAK1-3 inhibitor IPA-3 (15 μM, 5 hr, 37°C) prior to treatment with 50 nM Calyculin A (CA). Subcellular fractions of cytosolic and membrane proteins were then retrieved in digitonin-soluble (Dg) and Triton-soluble (Tx) fractions respectively from the total cell lysate (T). Insoluble aggregates were sedimented in the pellet (P). [B] Triton-soluble membrane fractions and [C] total cell lysates from three independent experiments. [D] The ratio of CLIC5A-to-*N*-Cadherin in Triton-soluble fractions quantified by densitometry (mean ± SEM; n = 3 independent experiments; $^*P < 0.05$).

association could occur due to a structural transition into an integral protein form in a fashion similar to pore-forming proteins, or due to the promotion of protein-protein interactions, which remains to be investigated.

5.2.3 CLIC4, But Not CLIC1, Also Translocates To Membranes In A Phosphorylation-Driven Process

As CLIC1 and CLIC4 are highly homologous to CLIC5A, we investigated whether these proteins share the phosphorylation-driven translocation process demonstrated in CLIC5A. Differential detergent fractionation was carried as before in CLIC1 and CLIC4-transfected cells, though since our pilot studies indicated that neither CLIC1 nor CLIC4 was sensitive to Calyculin A treatment at 15 or 20 min, we extended the time course to include 20

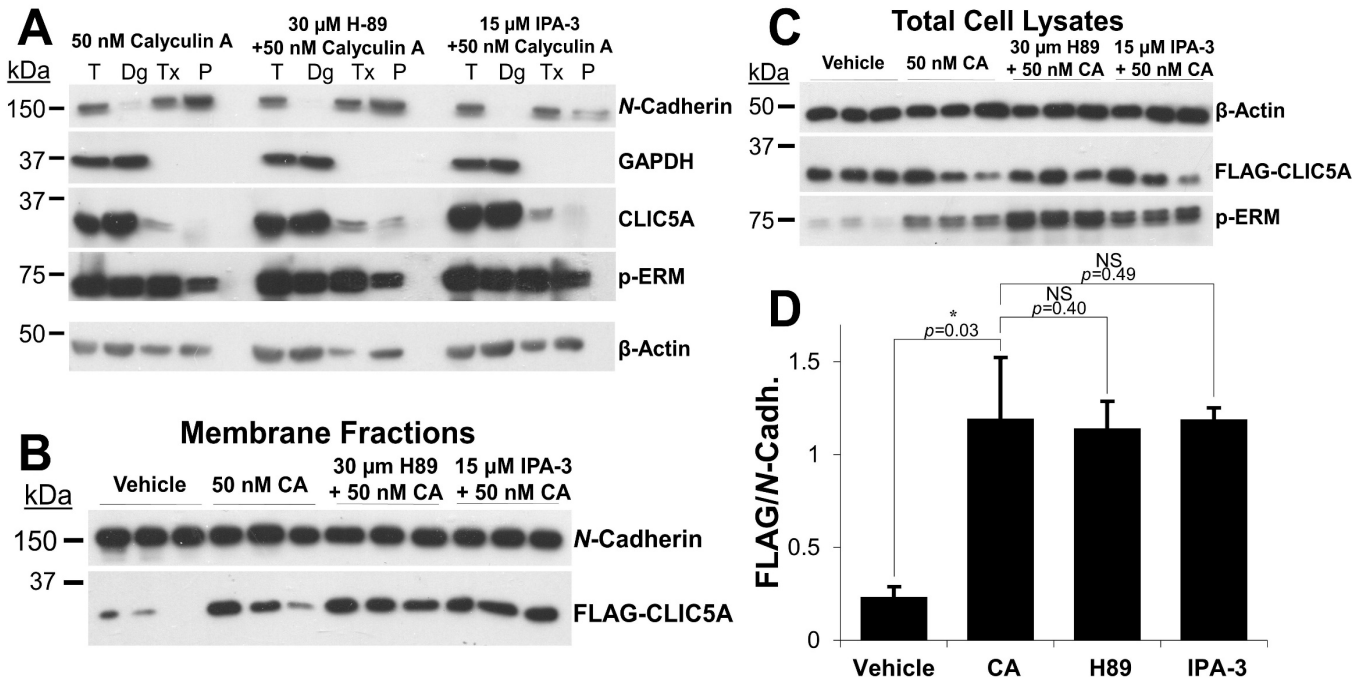

Figure 35. PKA and PAK1-3 inhibitors do not abolish the Calyculin A-induced enrichment of CLIC5A in Triton-soluble fractions. [A] CLIC5A-transfected COS-7 cells were pre-treated with Vehicle, the PKA inhibitor H89 (30 μM, 1 hr, 37°C), or the PAK1-3 inhibitor IPA-3 (15 μM, 5 hr, 37°C) prior to treatment with 50 nM Calyculin A (CA). Subcellular fractions of cytosolic and membrane proteins were then retrieved in digitonin-soluble (Dg) and Triton-soluble (Tx) fractions respectively from the total cell lysate (T). Insoluble aggregates were sedimented in the pellet (P). [B] Triton-soluble membrane fractions and [C] total cell lysates from three independent experiments. [D] The ratio of FLAG-to-*N*-Cadherin in Triton-soluble fractions as quantified by densitometry (mean ± SEM; n = 3 independent experiments; *P < 0.05).

and 30 min. CLIC1, unlike CLIC5A, did not translocate to membranes with Calyculin A treatment to significance (Figure 36), whereas CLIC4 did (Figure 37). However, when performing the same experiment in native, untransfected cells, neither protein was detectable in membrane fractions (results not shown), suggesting that membrane translocation by overexpression could be artefact, or our assay was not sensitive enough to detect endogeouns CLIC4 or CLIC1 proteins in membrane fractions.

5.2.4 Phosphorylation Status Does Not Convert CLIC5A To A Transmembrane Form

During phosphorylation-driven membrane translocation, it is probable that CLIC5A could convert to an integral transmembrane protein state, as predicted by EPR and FRET

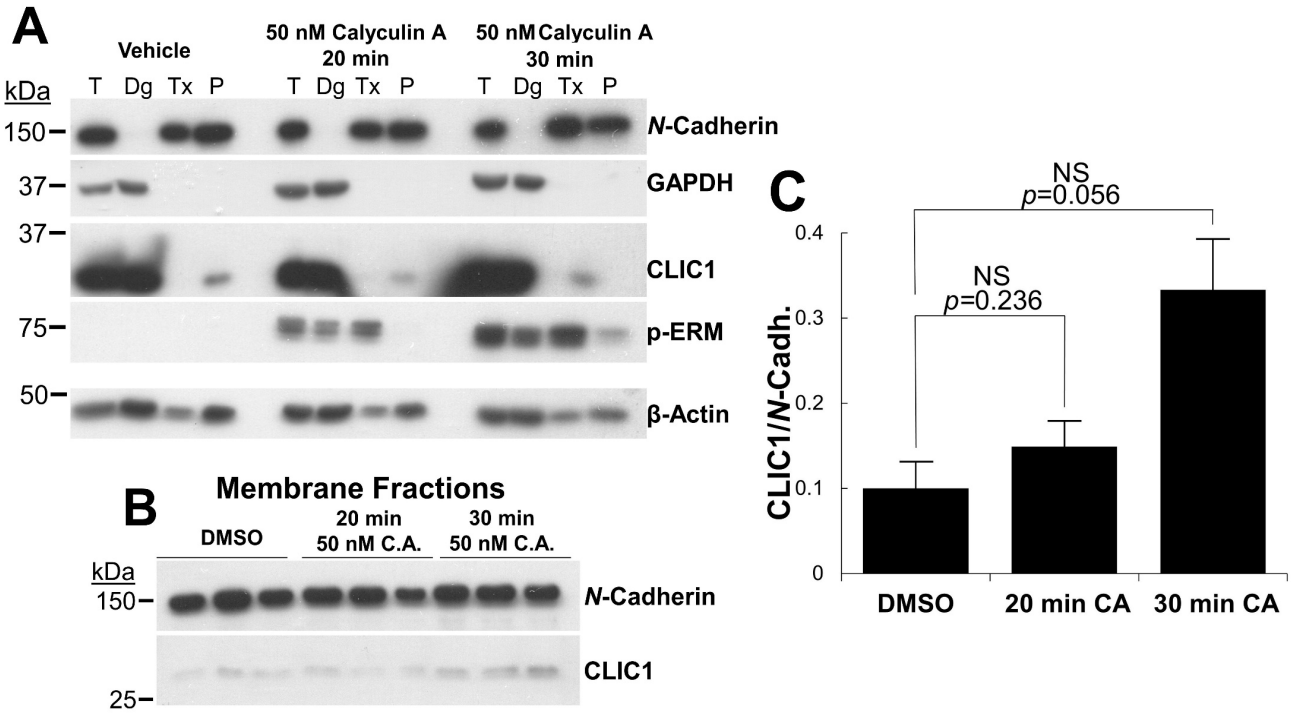

Figure 36. CLIC1 does not translocate to membranes in a phosphorylation-driven process. [A] CLIC1-transfected COS-7 cells were pre-treated with 50 nM Calyculin A for the indicated times. Subcellular fractions of cytosolic and membrane proteins were then retrieved in digitonin-soluble (Dg) and Triton-soluble (Tx) fractions respectively from the total cell lysate (T). Insoluble aggregates were sedimented in the pellet (P). [B] Membrane fractions from three independent experiments. [C] The ratio of CLIC1-to-*N*-Cadherin in Triton-soluble fractions as quantified by densitometry (mean ± SEM; $n = 3$ independent experiments; $^{*}P < 0.05$).

labeling studies[333]. To explore this possibility, we repeated the biotinylation surface protein capture assay with Calyculin A treatment. CLIC5A was retrieved predominantly in the flow-through with minimal detection in eluates regardless of Calyculin A treatment (Figure 38), suggesting that CLIC5A does not become transmembrane in response to phosphorylation.

5.2.5 CLIC5A Has Several Phosphorylation Sites Predicted By Sequence, Structure, & Proteomic Data

Given that CLICs have multiple predicted Ser, Thr, and Tyr phosphorylation sites based on consensus sequence analysis[307], we investigated whether CLIC5A could be directly phosphorylated. Phosphorylation sites were predicted based on sequence data for CLIC5A using the NetPhos (v 3.1) software[418,419] at a threshold of 0.50 to screen for the more probable

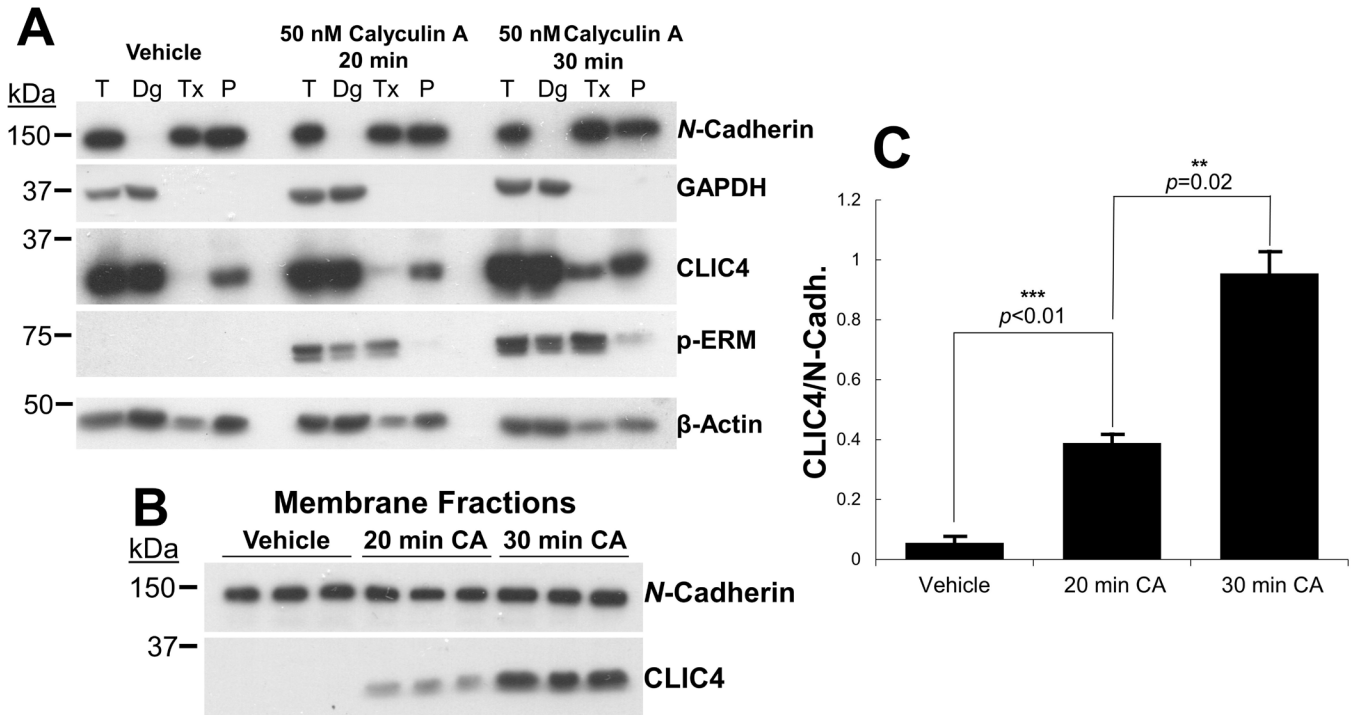

Figure 37. CLIC4, like CLIC5A, translocates to membranes in a phosphorylation-driven process. [A] CLIC4-transfected COS-7 cells were pre-treated with 50 nM Calyculin A for the indicated times. Subcellular fractions of cytosolic and membrane proteins were then retrieved in digitonin-soluble (Dg) and Triton-soluble (Tx) fractions respectively from the total cell lysate (T). Insoluble aggregates were sedimented in the pellet (P). [B] Membrane fractions from three independent experiments. [C] The ratio of CLIC4-to-*N*-Cadherin in Triton-soluble fractions as quantified by densitometry (mean ± SEM; $n = 3$ independent experiments; $*P < 0.05$).

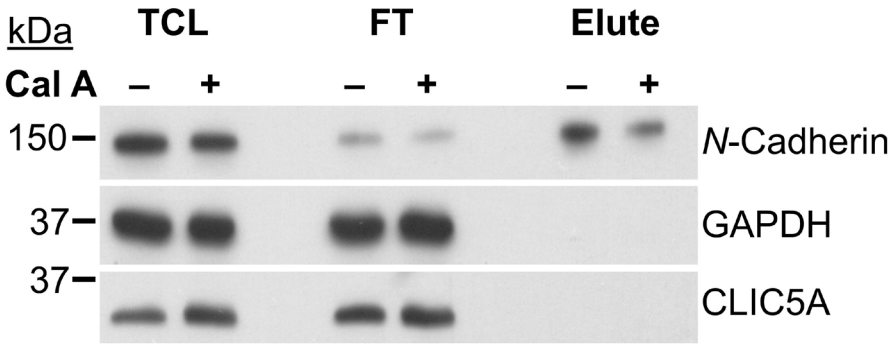

Figure 38. The phosphorylation-driven translocation of CLIC5A to membranes is not accompanied by conversion to a transmembrane state. Calyculin A (Cal A; 50 nM, 20 min, room temperature) or Vehicle-treated CLIC5A-transfected COS-7 cells were labeled with a membrane-impermeant biotin derivative to tag surface proteins, and biotinylated proteins were captured then eluted from an avidin column from total cell lysate (TCL). Uncaptured proteins were retrieved as the flow-through (FT) and analyzed by immunoblot analysis.

sites (Table 5). Multiple sequence alignments obtained by ClustalW2[420] among all CLICs (Figure 7) reveal that a significant number of these predicted sites were conserved, signifying a possible evolutionary importance. Furthermore, mapping the predicted sites of CLIC5A onto a homologous site on the X-ray structure of CLIC1 (PDB ID 1K0M) reveal that a striking

Table 5. Several phosphorylation sites are predicted for CLIC5A by NetPhos (v 3.1), and a striking number of these sites are conserved across CLICs and surface-exposed. Sequence-based phosphorylation sites were generated by inputting the sequence of CLIC5A onto the NetPhos (v 3.1) server. Multiple sequence alignment showed that many of these sites were conserved (: for similar residues and * for identical residues) across all CLICs. Candidate sites were mapped onto a homologous site for the X-ray structure of soluble CLIC1 (PDB ID 1K0M), and many of these were also found to be surface-exposed.

Residue in CLIC5A	Residue in CLIC1	Surface-exposed	Proximal Sequence in CLIC5A	Conservation
Ser-28	Lys-20	—	… GIDGE**S**IGN …	:
Ser-35	Ser-27	—	… CPF**S**QRLFM …	:
Thr-83	Thr-75	Yes	… GDVK**T**DVNK …	*
Thr-95	Val-87	Yes	… FLEE**T**LTPEK …	:
Thr-97	Cys-89	—	… FLEETL**T**PEK …	—
Tyr-101	Tyr-93	Yes	… TPEK**Y**PKLAA …	*
Ser-111	Ser-103	Yes	… HRE**S**NTAG …	*
Ser-120	Ala-112	—	… DIF**S**KFS …	*
Tyr-125	Tyr-117	—	… KFSA**Y**IKNT …	*
Tyr-151	Tyr-143	—	… KLDD**Y**LNTP …	*
Thr-154	Ser-146	Yes	… DYLN**T**PLPE …	*
Thr-164	Ser-156	Yes	… DAN**T**CGED …	:
Ser-171	Ser-163	Yes	… DKG**S**RRKFL …	*
Thr-182	Thr-174	—	… GDEL**T**LADC …	*
Tyr-222	Tyr-214	—	… LKNA**Y**ARDE …	:
Tyr-230	Thr-222	—	… DEFTN**T**CAA …	*
Tyr-241	Tyr-233	—	… IELA**Y**ADVAK …	*
Ser-249	Lys-241	Yes	… VAKRL**S**RS …	:
Ser-251	—	Yes	… VAKRLSR**S** …	—

number of these predicted sites are also surface-exposed and thus accessible as a kinase substrate (Table 5). A total of eight residues were both conserved and surface-exposed and thus strongly predicted to be phosphorylated including Thr-83, Thr-95, Tyr-101, Ser-111, Thr-154, Thr-164, Ser-171, and Ser-249 (Table 5).

To narrow the number of potential phosphorylation sites, we probed for experimental data compiled on PhosphoSitePlus, a database for mammalian post-translational modifications based either on mass spectrometry and site-specific data[423]. Although there were no entries for CLIC5A in the database, there was a query for CLIC5B, which we used in our analysis. One site, Thr-113 in CLIC5A, was not predicted by NetPhos but showed one mass spectrometric phosphorylation hit in CLIC5B (Table 6). To expand our search, we searched for homologous residues on PhosphoSitePlus entries for CLIC1 and CLIC4. Thr-154 and Thr-164 in CLIC5A showed mass spectrometry hits in homologous residues across both CLIC1 and CLIC4 (Table 6), thus making these the most likely sites based on sequence, structural, and proteomic data. All phosphorylation sites predicted by our analysis are depicted on Figure 39.

5.2.6 Hydrogen Peroxide Translocates CLIC1 and CLIC5A To Membranes

Because H_2O_2 promotes the association of CLIC1 and CLIC4 to membranes[335] *in vitro*, we investigated if CLIC5A also shares this property in cells. As expected, CLIC1 translocated to membranes with 100 μM H_2O_2 treatment at 30 min in 37°C (Figure 40). Similarly, CLIC5A also translocated to membranes under the same conditions, in what appears to be a time-dependent manner (Figure 41). Our results show, for the first time, the H_2O_2 -driven membrane association occurs in cells for CLIC1 and CLIC5A.

5.3 Discussion

Save for a few cases, such as the internalization of some surface proteins to nuclear membranes[9], integral proteins are more or less permanent fixtures of membranes[12,145] in direct contrast to peripheral proteins, which are bound to membranes by weaker, reversible interactions [12,145]. Amphitropic proteins form a sometimes distinct[109–111] class of membrane proteins sharing properties with integral, peripheral, and soluble proteins whose

Table 6. PhosphoSitePlus data on site-specific (LTP) and proteomic (HTP) predictions of putative phosphorylation sites. Based on phosphorylation prediction by sequence and structure by NetPHOS (v 3.1) and assessment of surface exposure, the most likely residues to be phosphorylated in CLIC5A were queried on PhosphoSite, a database compiling experimental data on post-translational modifications. The most likely sites in CLIC5A were compared with their homologous residues in CLIC1 and CLIC4, and the compiled data were tabulated in the table below.

CLIC5B Residue	CLIC5A Residue	LTP/HTP	CLIC1 Residue	LTP/HTP	CLIC4 Residue	LTP/HTP	Con.
Thr-242	Thr-83	—	Thr-75	—	Thr-86	—	*
… GDVK**T**DVNK …							
Thr-254	Thr-95	—	Val-87	—	Val-98	—	:
… FLEE**T**LTPEK …							
Tyr-267	Tyr-101	—	Tyr-93	0/1	Tyr-104	—	*
… LTPEK**Y**PKLA …							
Ser-270	Ser-111	0/1	Ser-103	0/3	Ser-114	—	*
… LNPE**S**NTAG …							
Thr-272	Thr-113	0/1	Thr-105	—	Thr-115	—	*****
… PESN**T**AGIDI …							
N.B.: not predicted by NetPhos							
Thr-313	Thr-154	—	Ser-146	0/8	Ser-157	0/1	:
… DDYLN**T**PLPE …							
Thr-323	Thr-164	—	Ser-156	0/5	Ser-167	0/7	:
… DAN**T**CGED …							
Ser-330	Ser-171	—	Ser-163	0/8	Ser-174	—	*
… DKG**S**RRKFL …							
Ser-408	Ser-249	—	Lys-241	—	Thr-252	—	:
… VAKRL**S**RS …							
Ser-410	Ser-251	—	—	—	—	—	—
… VAKRLSR**S** …							

reversible interaction with membranes is critical for their function[109–111]. The selective recruitment of such proteins to membranes enables cells to meet their needs. For instance, enzymes can be recruited to membranes only when turnover capacity is high, or membrane-disrupting

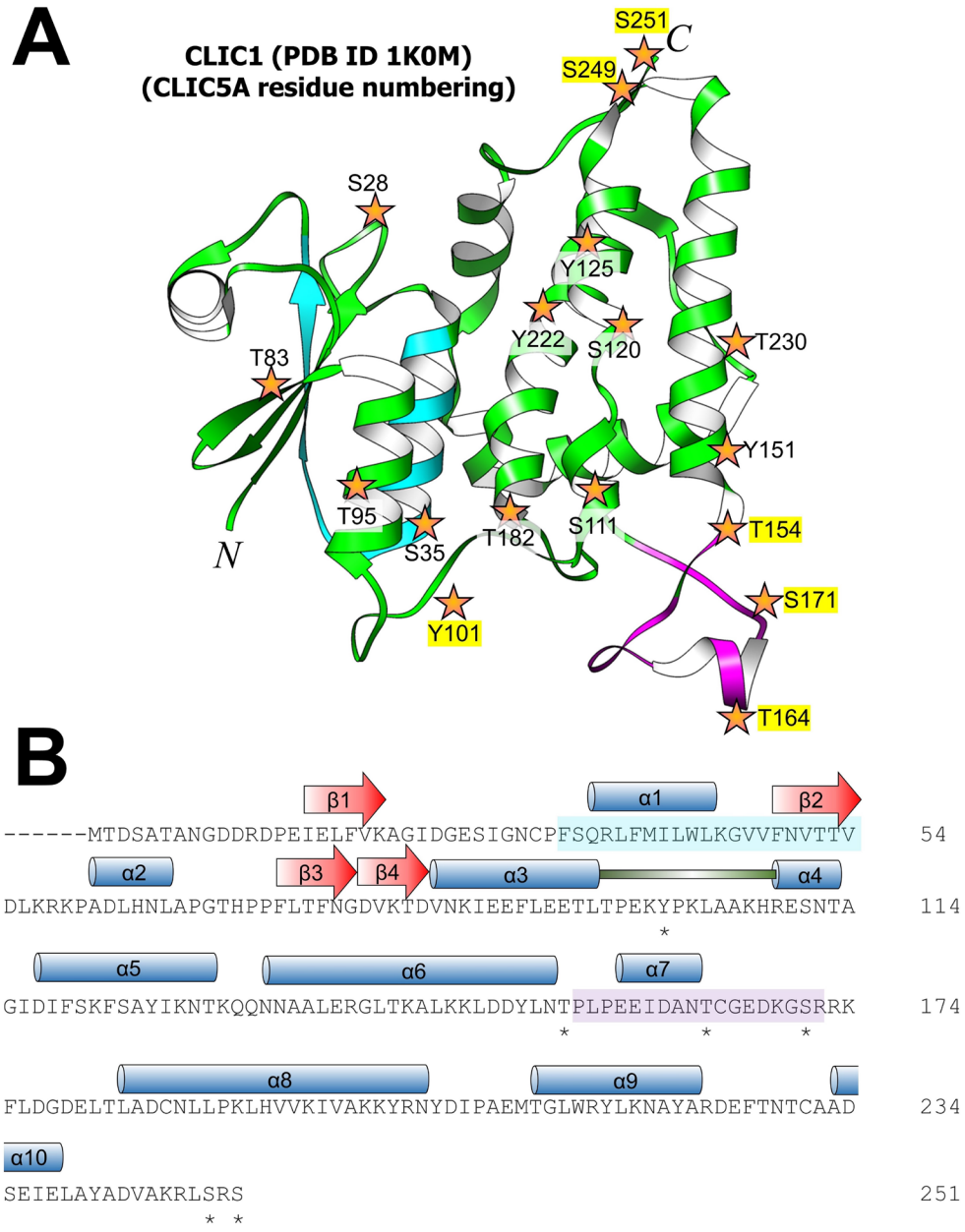

Figure 39. Using sequence, structural, and proteomic data, the most likely sites of phosphorylation in CLIC5A were predicted. [A] Sequence analysis for CLIC5A based on phosphorylation consensus sites by NetPhos (v 3.1) returned several predicted phosphorylation sites on serine, threonine, and tyrosine residues. These sites were then mapped onto homologous locations on the crystal structure of CLIC1 (PDB ID 1K0M) to assess for surface-exposure to kinases. Residues that were most surface-exposed are highlighted in yellow. [B] The most likely phosphorylation sites are indicated on the primary sequence of CLIC5A as asterisks (*). The secondary structure of CLIC1 are indicated above the sequence with α-helices depicted as cylinders and β-strands as arrows. The interdomain linker is depicted as a green line. In both [A] and [B], the putative transmembrane domain is coloured cyan, and the anionic foot loop is coloured magenta.

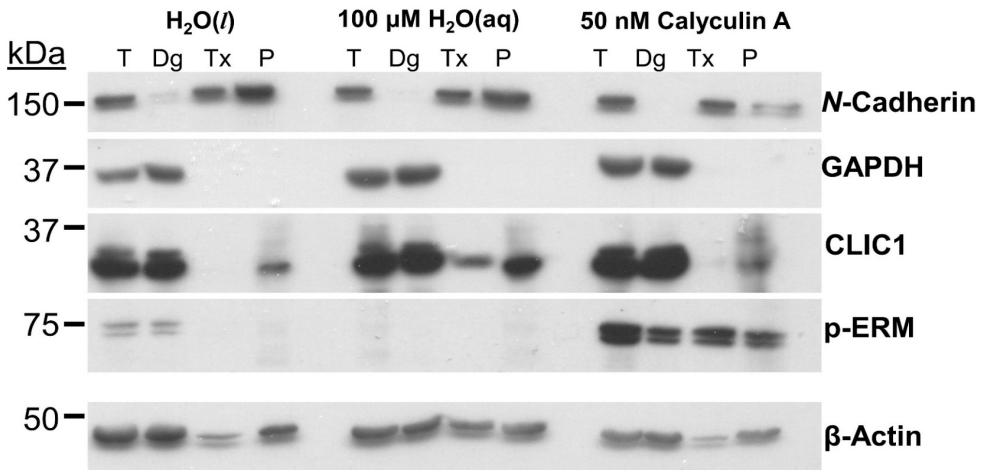

Figure 40. Hydrogen peroxide, but not Calyculin A, translocates CLIC1 to membranes. CLIC1-transfected COS-7 cells were pre-treated with either 100 μM H_2O_2 for 30 min or 50 nM Calyculin A for 20 min in 37°C. Subcellular fractions of cytosolic and membrane proteins were then retrieved in digitonin-soluble (Dg) and Triton-soluble (Tx) fractions respectively from the total cell lysate (T). Insoluble aggregates were sedimented in the pellet (P).

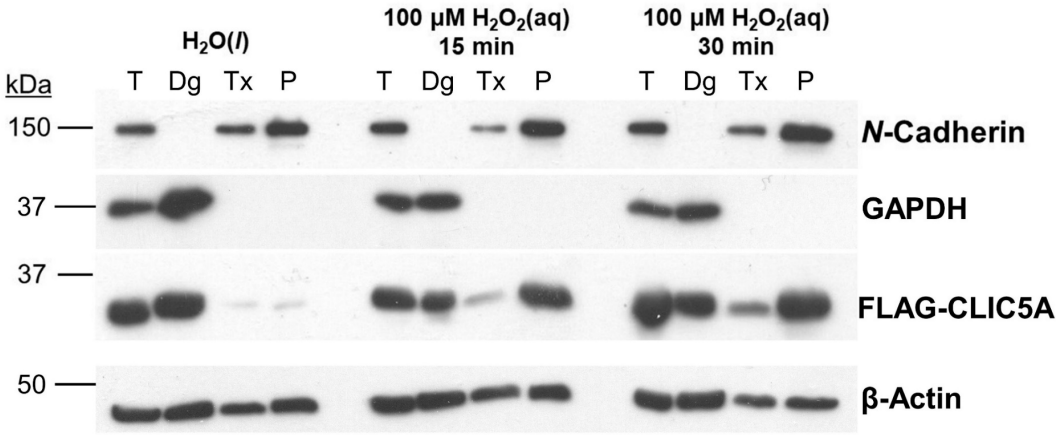

Figure 41. CLIC5A stably associates within Triton-soluble fractions in response to hydrogen peroxide treatment. FLAG-CLIC5A-transfected COS-7 cells were pre-treated with water or 100 μM H_2O_2 for the indicated time intervals in 37°C. Subcellular fractions of cytosolic and membrane proteins were retrieved in digitonin-soluble (Dg) & Triton-soluble (Tx) fractions respectively from the total lysate (T). Insoluble proteins were sedimented in the pellet (P).

disrupting pore-forming proteins (PFPs) can be kept inactive until needed[116,138]. Given the diverse subcellular locales CLICs occupy (Table 4) and their observed translocation in response to differentiation status[298,301] and certain stimuli[289,338,355,356], CLICs seem to share this amphitropic property with PFPs.

While the biological stimuli and signaling pathways facilitating the translocation of CLICs have not been identified for most members, our study shows for the first time that phosphorylation status (Figure 31) promotes the translocation of CLIC5A and CLIC4 (Figure 37) to membranes, and CLIC1 to a lesser extent (Figure 36). For CLIC5A, this process is sensitive to the kinase inhibitor staurosporine (Figure 32–Figure 33). Staurosporine is potent, but nonspecific, and at the 20 nM concentration we used inhibits PKCα, δ, γ, η[439], PKA, myosin light chain kinase, and Ca^{2+}/calmodulin-dependent kinase[440]. H-89 did not abolish the phosphorylation-driven translocation to membranes (Figure 34–Figure 35), thus ruling out PKA as a driving force in this process. In their activation, ERM proteins are phosphorylated on a *C*-terminal Thr residue chiefly by PKCs and Rho-associated kinase (ROCK)[441], and the CLIC4- and CLIC5A-stimulation of ERM phosphorylation[393,396] is similarly sensitive to staurosporine, suggesting PKC as the main kinase involved in this process. Therefore, given that both CLIC5A and PKC are associated with ERM phosphorylation, and that staurosporine similarly inhibits the phosphorylation-driven translocation of CLIC5A to membranes, it is probable that a PKC may be mediating this process too. In further support of this, *in vitro* kinase assays with purified recombinant CLIC1 and CLIC4 showed that it was a substrate for the α. βII, γ, δ, and ε PKC isoforms[301].

PKCδ has been previously shown to mediate the nuclear translocation of CLIC4 in differentiating keratinocytes, though it was not a direct substrate for phosphorylation[301]. On the other hand, CLIC6 was isolated as a phosphoprotein that translocated to membrane-rich fractions of rabbit gastric glands during acid secretion[289]. While the direct phosphorylation of CLIC5A is highly probable given our multifactorial prediction analysis (Figure 39) and supported by previous predictions[305,307], we cannot not establish this with certainty, and further work is required to test this hypothesis. Our predictions yielded Thr-154 and Thr-164 as the most likely sites for phosphorylation, though Ser-249 has been previously predicted as a PKA site in CLIC5A and CLIC5B[287]. Phosphorylation is the most common post-translational modification, and it has been estimated that between one-third and two-third of an organism's proteome could be modulated by this process[442]. Therefore, it would not be unconceivable that CLIC5A is directly phosphorylated.

CLICs possess multiple stable folds and are considered metamorphic proteins[364]. While all three-dimensional structures obtained so far are of CLICs in their soluble globular state (Figure 7), and no membrane-bound structures have been reported, apart from a predictive model based on FRET and EPR distances[333], denaturation studies show that under acidic conditions similar to proximal membrane surfaces [199], CLIC1 assumes a destabilized unfolded intermediate[344]. Furthermore, hydrogen-deuterium exchange studies show that this acid-induced intermediate destabilizes the *N*-terminal domain more than the *C*-terminal domain[345], thus offering a potential mechanism for this domain to unfold and expose its PTMD for membrane insertion. Indeed, this conformational maneuver is common among peripheral and amphitropic proteins, including PFPs, which frequently sequester their hydrophobic membrane-associating motifs in their core until recruitment[85], and phosphorylation is a regulator for this process. For instance, phosphorylation of the NADPH oxidase subunit $p47^{phox}$ at multiple *C*-terminal sites exposes its phosphoinositide PX domain (Table 2) to insert into membranes[97,98]. Additionally, the PFP and proapoptotic factor Bad only forms pores in artificial membranes when phosphorylated[198]. While we did not demonstrate that CLIC5A is directly phosphorylated, a conformational change promoted by some phosphorylation-related cascade seem plausible, since anti-FLAG and anti-CLIC5A antibodies by immunoblot analysis show differential sensitivities (Figure 34C compared to Figure 35C). Further studies must be done to evaluate this. Nonetheless, we can conclude that phosphorylation status does not convert CLIC5A to a transmembrane form since phosphatase inhibition, which causes membrane association, did not increase the retrieval of CLIC5A in the biotin surface protein capture assay (Figure 38). Whichever transitions occur during this phosphorylation-driven process, it is sufficient to stabilize the association of CLIC5A to membranes even with the depletion of cholesterol by digitonin during differential detergent fractionation.

In addition to direct effects from phosphorylation, it is also probable that this cascade confers indirect effects promoting CLIC5A's translocation to membranes. Complement system proteins of the immune response are kept cytosolic and inactive by binding to a regulatory protein CD59, and dissociation from these factors promotes membrane association[194,195]. Similarly, phosphorylation of a protein other than CLIC5A could promote or destabilize protein-protein interactions, which then translocate CLIC5A to membranes.

While the direct phosphorylation of CLIC5A is appealing given our predictions (Figure 39), our experiments show that H_2O_2 also induces translocation of CLIC1 (Figure 40) and CLIC5A (Figure 41) to membranes, and therefore cannot be discounted as a possible biologically relevant pathway. Once thought to be primarily involved in pathology, reactive oxygen species (ROS) are now appreciated as signaling molecules that regulate several normal physiological processes, most notably gene activation, growth and differentiation, and inflammation[443,444]. Our study is the first to examine a redox effect on CLIC5A in cells. Ever since the seminal study first cementing CLICs as metamorphic proteins, in which H_2O_2 caused significant structural transformations in recombinant CLIC1[424] (Figure 9), several studies since then have investigated the effect of dimerization and oxidation in membrane translocation. Indeed, H_2O_2 has been frequently demonstrated to promote the interaction of CLICs to membranes, though evidence thus far has been strictly *in vitro*[327,335,336]. However, CLIC1 is translocated to plasma and nuclear membranes in Alzheimer's disease models[338,339], a disease state associated with ROS[337]. Additionally, nigericin treatment, which activates the NLRP3 inflammasome, induces translocation of CLIC1, CLIC4, and CLIC5A to the membrane fractions of bone-marrow-derived macrophages[342]. Since H_2O_2 results in NLRP3 activation, this would be consistent with sredox signaling as a mechanism of CLIC translocation[341]. The recent detection of CLIC5A and CLIC5B in the inner mitochondrial membrane of rat cardiomyocytes[353], a centre for ROS production[445], also strengthens this hypothesis.

By the action of intracellular oxidoreductases, intracellular H_2O_2 concentrations have been estimated to be between 7–10-fold[446] to 100-fold[332] and even 65-fold[447] lower than in the extracellular space. If we assume a modest depression of 100, the 100 μM concentrations used in our fractionations would be near 1 μM, corresponding to oxidative distress in which damage to biomolecules occur by free radicals[332]. What is known, however, is that we were able to detect membrane translocation at far lower concentrations than those of former *in vitro* studies, which typically used 2 mM H_2O_2. These fractionations could be repeated using lower H_2O_2 concentrations to aim for the range of oxidative eustress (1–10 nM)[332] to strengthen this as a plausible biologically-relevant pathway.

What remains to be answered if H_2O_2 is the pathway translocating CLIC5A to membranes in living systems is whether CLICs become oxidized during this process. During

oxidative eustress, H_2O_2 mediates its roles by the reversible oxidation of Cys and Met residues, and certain lipids as well[332]. Several *in vitro* studies focused on the probable structural transitions occurring in response to oxidation, though an oxidized dimeric CLIC1 is likely not the one that inserts into membranes, since monomeric CLIC1 more readily associates with membranes[335,336], and dimerization is unique to this protein among CLICs[320,321,327]. Despite this, H_2O_2 treatment does promote the association of CLICs to membranes *in vitro*, suggesting that a membrane-bound form is directly affected by oxidation in some way[327,335]. Furthermore, while other CLICs may not dimerize by oxidation, DTT extinguishes the ion conductance of CLIC1[335,336], CLIC4[327], and CLIC2[320] in artificial membranes, further suggesting the membrane association of CLICs are under some form of direct redox control. Given that the conserved thioredoxin cysteine (Cys-32 in CLIC5A) is reactive to cysteine-labeling reagents for CLIC1, CLIC4, and CLIC5A[334], and that this cysteine forms intramolecular disulfide bonds *in vitro* in CLIC2 and CLIC3[320,321], this strengthens the possibility that CLICs are oxidized.

So far, our results indicate that phosphorylation and/or oxidation are biologically relevant candidates that stimulate the translocation of CLIC5A and other CLICs to membranes. It is curious that while CLIC4 and CLIC5A translocate to membranes by phosphatase inhibition, CLIC1 does not respond to this stimulus at appreciable levels. CLIC1 and CLIC4 are homologous to CLIC5A by 63% and 76% respectively[287], and thus consensus-based phosphorylation sites would be similar. What would differ more between these proteins may be the proteins they interact with. Therefore, it is also possible that that phosphorylation-driven translocation promotes or hinders certain protein interactions. Again, further studies must be performed to demonstrate which pathway is biologically relevant.

Chapter 6: Conclusions & Future Directions

6.1 Conclusions

CLIC5A is a peripheral protein, not an integral transmembrane protein. The findings in this thesis confirm many earlier doubts about the capacity of CLIC5A and other CLICs to generate ion currents as classical ion channels. Both α- and β-type channels are integral transmembrane proteins, yet the assays we performed distinguishing surface integral proteins from fully intracellular proteins fail to detect CLIC5A at the cell surface (Figure 26–Figure 30). From these assays, CLIC5A possesses more characteristics of intracellular soluble proteins than integral membrane proteins. In fact, if the association of CLICs with membranes *in vitro*, by direct lipid bilayer - CLIC interaction, and *in vivo*, by live cell imaging and immunogold labeling, had not yet been firmly established, our findings could be interpreted to indicate that CLIC5A is a soluble protein, in keeping with the X-ray structures of all CLICs that all describe soluble proteins (Figure 8). To bring our results in line with the well-established membrane association of CLICs, we propose that CLIC5A is a peripheral protein which binds to the inner leaflet of the plasma membrane, or associates with a protein partner or complex that associates with the inner leaflet of the plasma membrane.

CLIC5A is amphitropic and associates with membranes through a phosphorylation-dependent process. The membrane association of CLIC1, CLIC4, and CLIC5A may require cholesterol. Differential detergent fractionations in the absence of any chemical pre-treatment reveal that CLIC1, CLIC4 (Figure 30), and CLIC5A (Figure 29) are predominantly retrieved in cytosolic rather than membrane fractions. Since the digitonin used in this procedure complexes with cholesterol to permeabilize cells and given that CLIC1 and CLIC4 require cholesterol for membrane association, these results may be explained by the depletion of a crucial membrane-binding element of CLICs by digitonin. Nevertheless, phosphatase inhibition is sufficient to support stable association of CLIC5A (Figure 31) and CLIC4 (Figure 37), but not CLIC1 (Figure 36), with membranes, even in the presence of digitonin. In fact, these interactions were strong enough to withstand PBS washes of significant ionic strength, suggesting the forces enabling this interaction are stronger than simple electrostatic adsorption. What our study demonstrates is that this may not be due to a conversion of CLIC5A to a

transmembrane integral form (Figure 38). Instead, we propose that phosphorylation status either facilitates a conversion exposing its hidden putative transmembrane domain to anchor into membranes, or certain protein interactions become promoted or hindered.

CLIC5A is likely phosphorylated by a PKC. By employing a methodical approach using sequence, structural, and proteomic data (Figure 39), it seems highly probable that CLIC5A is directly phosphorylated, most likely on Thr-154 and Thr-164, during the membrane translocation process. Given that this translocation is specifically inhibited by staurosporine (Figure 32–Figure 35), and that CLIC5A shares signaling pathways with PKCα through its effects on ERM phosphorylation, we posit that CLIC5A may be a PKCα substrate, and that its phosphorylation results in the translocation to membranes. We therefore propose a revised model of the CLIC5A signaling pathway, depicted in Figure 42, in which PKCα phosphorylates CLIC5A and ezrin in a shared pathway to translocate both proteins to the membrane.

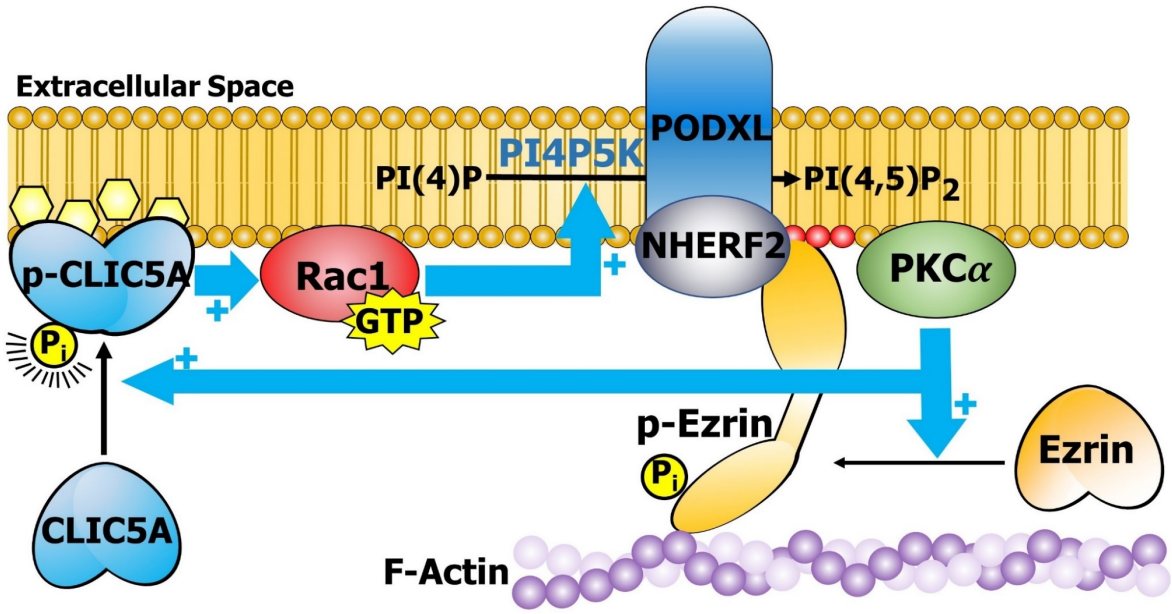

Figure 42. In our revised model, CLIC5A is phosphorylated by PKCα to translocate to membranes, where it sorts within cholesterol-enriched microdomains. We posit that the phosphorylation of CLIC5A, which is mediated by PKCα, results in its translocation to membranes, where it sorts into cholesterol-enriched microdomains (yellow hexagons) of the inner leaflet, perhaps within caveolae rather than lipid rafts since the latter is situated mostly on the exoplasmic leaflet. At the membrane, CLIC5A signals to stimulate Rac-1-induced stimulation of ezrin phosphorylation, likely by activation of a phosphoinositide kinase (PI4P5K).

H_2O_2 may also be a biologically-relevant stimulus translocating CLIC1 and CLIC5A to membranes. Consistent with a multitude of studies implicating oxidation in the membrane association of CLICs, we demonstrate for the first time that H_2O_2 treatment stimulates the translocation of both CLIC1 and CLIC5A to membranes (Figure 40–Figure 41) in living cells at concentrations closer to physiologically relevant limits than the 2 mM concentration used in several previous *in vitro* studies. Given that our work also identified phosphorylation as a potential route for membrane translocation, we postulate that either pathway, or both, could be be physiologically relevant for membrane translocation of CLIC proteins.

6.2 Future Directions

Firmly establish whether CLIC5A and other CLICs associate with cholesterol-enriched membrane microdomains. Our theory that CLIC5A and other CLICs associate with cholesterol in lipid membranes, while supported by a wealth of *in vitro* studies and localization data, requires validation. We reasoned that the behaviour of CLIC1, CLIC4 (Figure 30), and CLIC5A as fully soluble proteins during differential cell fractionation (Figure 29) could be due to cholesterol depletion by digitonin. However, it is also possible that the interaction of these CLIC proteins with lipid bilayers in vivo is so weak that they appear as soluble proteins in this assay. In any case, the possibility that the association of CLICs with membranes is cholesterol dependent needs to be rigorously tested. Methyl-β-cyclodextrin is frequently employed to extract cholesterol from membranes and thus disrupt microdomains such as rafts and caveolae[448]. Therefore, one option would be to determine whether this reagent disrupts the association of CLICs with membranes and whether activation of the CLIC5A signaling cascade can be inhibited by cholesterol depletion. Another method of cholesterol depletion is to incubate cells in cholesterol-free medium followed by incubation with a statin, which are specific inhibitors of HMG-CoA reductase, a key enzyme in the cholesterol synthetic pathway. We propose to analyze GFP-tagged CLICs by live-cell immunofluorescence imaging and observing the effect of cholesterol depletion on membrane association. If CLICs associate with the membrane in a cholesterol-dependent manner, cholesterol depletion would result in redistribution of CLICs from membranes to the cytosol, as demonstrated in a similar experiment using PLCγ activation in GFP-CLIC5A-transfected COS-7 cells by Al-Momany and colleagues[270]. Similarly, immunofluorescence staining can be used to determine whether

GFP-tagged CLICs co-localize with markers for membrane microdomains, most notably GPI-anchored proteins for rafts and caveolin for caveolae[432]. Lipid rafts and their related microdomains are controversial theories, so careful deliberation must be made to demonstrate this hypothesis. In addition, activation of Rac1 and ERM protein phosphorylation by CLIC5A in the presence and absence of cholesterol depletion would determine whether CLIC5A signaling is dependent on cholesterol-dependent membrane localization.

Based on a similarity to other cholesterol-binding consensus sequences and their conservation in CLICs, two putative cholesterol-binding motifs have been proposed in CLICs (Figure 7)[336]. Alone, these in silico observations are not sufficient to establish these sequences as definitive cholesterol-binding motifs. Therefore, it would be interesting to determine the effect of disrupting these sequences by site-directed mutagenesis, deletions, or insertions to concretely implicate these sequences in cholesterol-binding. For reasons not yet known, CLIC1 more readily associated to the fungal sterol analogue ergosterol than cholesterol *in vitro*[336]. In line with the possibility of CLICs to function as pore-forming proteins and given that several antimicrobial peptides share similarities with pore-forming proteins, these observations could implicate CLICs as interesting, endogenous anti-fungal molecules. Thus, exploring why CLIC1 has a high affinity for ergosterol remains an open question warranting investigation.

Determine whether CLIC5A is directly phosphorylated during membrane translocation and establish its biological relevance. The present study, while implicating a PKC in the translocation of CLIC5A to the membrane, did not establish that CLIC5A is directly phosphorylated or a direct PKC substrate. Though direct phosphorylation of CLIC5A seems highly probable based on our prediction analysis, direct phosphorylation of CLICs have not been established across the family. So far, only the phosphorylation of CLIC5B[275,359] and CLIC6[289] on their respective extended and non-conserved N-terminal domains have been proven *in vivo* along with a defined functional effect. To firmly establish whether CLIC5A is directly phosphorylated, and to determine whether direct phosphorylation induces translocation to the membrane, metabolic labeling with [γ-^{32}P]ATP would be a most important first step. The [γ-^{32}P]ATP would serve as the 32P donor for the putative CLIC5A substrate. Metabolic labeline would be performed in cells transfected with Flag-CLIC5A or vector,

followed by Calyculin A treatment with and without Staurosporine pre-treatment. CLIC5A would then be immunoprecipitated followed by SDS-PAGE and autoradiography of the blots. If this experiment is positive, site-directed mutagenesis of putative phosphorylation sites to phosphorylation resistant mutants would then be performed to determine which site supports the phosphorylation in cells. In addition, pure, recombinant CLIC5A protein and its site mutant(s) would be subjected to in vitro kinase assays to define which kinase supports the phosphorylation of each specific site. A staggering amount of phosphorylation sites were predicted using NetPhos (Table 5), though in combination with structural and proteomic data, we significantly narrowed down list of candidate phosphorylation sites. Based on their surface-exposure in homologous sites in CLIC1, as well as proteomic data for such sites in both CLIC1 and CLIC4 (Table 6), we propose Thr-154 and Thr-164 as the most likely phosphorylation sites in CLIC5A. Therefore, generating point mutants of these sites to Ala or phosphomimic mutants (Ser to Asp or Glu) and observing their localization in our fractionation assay would indicate the role of phosphorylation in membrane translocation. Finally, the functional effects of these mutations on Rac1 and Pak activation as well as ERM phosphorylation and actin-association would be evaluated using these mutants. If it was found that CLIC5A is indeed phosphorylated in living cells, and if the phosphorylation site(s) were identified, one would then proceed to produce antibodies that specifically recognize only the phosphorylated epitopes to study CLIC5A phosphorylation in living animals, *in vivo*.

Though the primary focus of the present study was on Ser/Thr phosphorylation, since the Calyculin A used in our investigations is a Ser/Thr phosphatase inhibitor, our prediction analysis showed that Tyr-101 in CLIC5A is surface-exposed and conserved among all CLICs (Figure 39). While Tyr kinases comprise ~10% of all kinase genes, less than 1% of all phosphoryl groups are conjugated to Tyr residues[449]. While this makes it unlikely that CLIC5A could be Tyr phosphorylated, CLIC5B was demonstrated to be Tyr phosphorylated by metabolic labeling[360], albeit on the *N*-terminal region not homologous with other CLICs, and CLICs contain consensus SH2 domains, which bind to phosphoTyr domains[264,307]. Therefore, Tyr phosphorylation and its effects on CLICs remains an open question and should be investigated. Our experiments on immunoprecipitated CLIC5A probed with anti-phosphoTyr antibodies in immunoblot analysis did not detect phosphoTyr (results not shown), though other methods should be employed to firmly exclude this possibility. Even if it was established that

CLIC5A is not Tyr phosphorylated, its putative SH2 domain could indicate some as-of-yet unexplored protein-protein interactions.

Determine whether phosphorylation or redox signaling is the biologically-relevant pathway translocating CLIC5A to membranes. Though we demonstrated for the first time in cells that H_2O_2 induces the translocation of CLIC1 and CLIC5A to membranes, our studies have limitations. First, the 100 μM treatment used, even if we account for the 100-fold decrease in intracellular concentration[447] to 1 μM, is still 100-fold greater than in oxidative eustress[332]. A simple corrective measure would be to repeat these experiments using lower H_2O_2 concentrations. Even if translocation were observed in such an instance, we would need to establish this as a biologically-relevant process. The findings of this thesis suggest either phosphorylation and/or redox as mechanisms that translocate CLICs to membranes but so far, they do not establish either pathway as actually operating in living systems. To explore these possibilities, it is first and foremost imperative to establish an interaction of CLICs with redox signaling molecules, such as the transcription factor NF-κB[332], by co-immunoprecipitation or similar assays. While convenient to perform these investigations in transfected cells, a demonstration of these protein interactions should be demonstrated in endogenous systems, such as in podocytes *in vivo* for CLIC5A, rather than by method of cell culture. *In vivo* validation using animal tissue would be an invaluable source of information validating the legitimacy of such interactions. Indeed, the same methods should be employed to establish the phosphorylation cascade as biologically relevant, perhaps by demonstrating interactions with CLIC5A and PKCα, as an example.

Relatively recent studies have revealed an enzymatic function for CLIC3[297], based on years of speculation on the relevance of the homology of CLICs to GSTΩs, that was contingent on the reactive cysteine situated in the conserved thioredoxin motif (Figure 7). To date, similar oxidoreductase activity has not been reported for other CLICs in a biologically-relevant context, though proteomic studies indicate that CLIC1, CLIC4, and CLIC5A are all reactive to a cysteine-labeling reagent[334]. Given that these proteins respond in some way to H_2O_2 in living cells, it would remain interesting to determine if they share oxidoreductase activity too.

6.3 Closing Words

CLICs are a unique family of proteins. Given that CLICs are metamorphic proteins differentially targeted to multiple subcellular locales, it is perhaps not surprising that early studies concluding that they are traditional ion channels were never translated into the *in vivo* situation even two decades after their discovery. In many ways, the study of CLICs are reminiscent of the ClCA family of proteins that were first believed to be ion channels, but are now known to have completely different functions. Even today, studies by groups unfamiliar with the peculiarity of CLICs still frame them as classical ion channels[361,362], which no doubt stems from the mis-classification and mis-naming of this gene family. Yet those who realized that CLICs are more than ion channels paved the way to understanding the hidden nature of these proteins. If CLICs were only framed as ion channels, revelations like the involvement of CLICs in shaping cell architecture, in diet-induced obesity[450], metastatic oxidoreductase behaviour[451], or as potential biomarkers for metastatic severity[302,356] and as antifungal agents[336]—just to name a few—may have never surfaced. Indeed, much more remains to be investigated about not just CLIC5A, but all other CLICs.

Literature Cited

1. Singer, S.J.; Nicolson, G. L. The Fluid Mosaic Model of the Structure of Cell Membranes. *Science (80-.).* **175,** 720–731 (1972).

2. Vanderkooi, G. Molecular Architecture of Biological Membranes. *Ann. N. Y. Acad. Sci.* **195,** 6–15 (1972).

3. Capaldi, R. A. The Structure of Erythrocyte Membranes. A Partial Separation of Intrinsic and Extrinsic Membrane Proteins. *Eur. J. Biochem.* **29,** 74–79 (1972).

4. Singer, S. J. The Molecular Organization of Biological Membranes. in *Structure and Function of Biological Membranes* 145–222 (Elsevier, 1971). doi:10.1016/B978-0-12-598650-2.50009-0

5. Singer, S. J. The Molecular Organization of Membranes. *Annu. Rev. Biochem.* **43,** 805–833 (1974).

6. Wise, K. S. & Kim, M. F. Identification of intrinsic and extrinsic membrane proteins bearing surface epitopes of Mycoplasma hyopneumoniae. *Isr. J. Med. Sci.* **23,** 469–73 (1987).

7. Spector, A. *et al.* An extrinsic membrane polypeptide associated with high-molecular-weight protein aggregates in human cataract. *Science (80-.).* **204,** 1323–1326 (1979).

8. Wang, S.-C. & Hung, M.-C. Nuclear translocation of the epidermal growth factor receptor family membrane tyrosine kinase receptors. *Clin. Cancer Res.* **15,** 6484–9 (2009).

9. Wang, Y.-N. *et al.* Membrane-bound trafficking regulates nuclear transport of integral epidermal growth factor receptor (EGFR) and ErbB-2. *J. Biol. Chem.* **287,** 16869–79 (2012).

10. Whited, A. M. M. & Johs, A. The interactions of peripheral membrane proteins with biological membranes. *Chem. Phys. Lipids* **192,** 51–59 (2015).

11. Gennis, R. B. Characterization and Structural Principles of Membrane Proteins. in *Biomembranes : Molecular Structure and Function* 85–137 (Springer, New York, NY, 1989). doi:10.1007/978-1-4757-2065-5_3

12. Nicolson, G. L. The Fluid—Mosaic Model of Membrane Structure: Still relevant to understanding the structure, function and dynamics of biological membranes after more than 40 years. *Biochim. Biophys. Acta - Biomembr.* **1838,** 1451–1466 (2014).

13. Enqelman, D. M. Lipid Bilayer Structure in the Membrane of Mycoplasma laidlawii. *J. Mol. Biol.* **58,** 153–166 (1971).

14. Griffith, O. H., Dehlinger, P. J. & Van, S. P. Shape of the hydrophobic barrier of phospholipid bilayers (Evidence for water penetration in biological membranes). *J. Membr. Biol.* **15,** 159–192 (1974).

15. Wiener, M. C. & White, S. H. Structure of a fluid dioleoylphosphatidylcholine bilayer

determined by joint refinement of x-ray and neutron diffraction data. II. Distribution and packing of terminal methyl groups. *Biophys. J.* **61,** 434–447 (1992).

16. Wiener, M. C., King, G. I. & White, S. H. Structure of a fluid dioleoylphosphatidylcholine bilayer determined by joint refinement of x-ray and neutron diffraction data. I. Scaling of neutron data and the distributions of double bonds and water. *Biophys. J.* **60,** 568–576 (1991).

17. Wiener, M. C. & White, S. H. Structure of a fluid dioleoylphosphatidylcholine bilayer determined by joint refinement of x-ray and neutron diffraction data. III. Complete structure. *Biophys. J.* **61,** 434–47 (1992).

18. Gawrisch, K. *et al.* Energetics of a hexagonal-lamellar-hexagonal-phase transition sequence in dioleoylphosphatidylethanolamine membranes. *Biochemistry* **31,** 2856–2864 (1992).

19. van den Brink-van der Laan, E., Antoinette Killian, J. & de Kruijff, B. Nonbilayer lipids affect peripheral and integral membrane proteins via changes in the lateral pressure profile. *Biochim. Biophys. Acta - Biomembr.* **1666,** 275–288 (2004).

20. Ding, W., Palaiokostas, M., Wang, W. & Orsi, M. Effects of Lipid Composition on Bilayer Membranes Quantified by All-Atom Molecular Dynamics. *J. Phys. Chem. B* **119,** 15263–15274 (2015).

21. Disalvo, E. A. *et al.* Structural and functional properties of hydration and confined water in membrane interfaces. *Biochim. Biophys. Acta - Biomembr.* **1778,** 2655–2670 (2008).

22. Hong, H. Toward understanding driving forces in membrane protein folding. *Arch. Biochem. Biophys.* **564,** 297–313 (2014).

23. Heerklotz, H. & Epand, R. M. The enthalpy of acyl chain packing and the apparent water-accessible apolar surface area of phospholipids. *Biophys. J.* **80,** 271–9 (2001).

24. Mukhin, S. I. & Baoukina, S. Analytical derivation of thermodynamic characteristics of lipid bilayer from a flexible string model. *Phys. Rev. E* **71,** 061918 (2005).

25. White, S. H. & Wimley, W. C. Hydrophobic interactions of peptides with membrane interfaces. *Biochimica et Biophysica Acta - Reviews on Biomembranes* **1376,** 339–352 (1998).

26. Warshaviak, D. T., Muellner, M. J. & Chachisvilis, M. Effect of membrane tension on the electric field and dipole potential of lipid bilayer membrane. *Biochim. Biophys. Acta - Biomembr.* **1808,** 2608–2617 (2011).

27. Charifson, P. S., Hiskey, R. G. & Pedersen, L. G. Construction and molecular modeling of phospholipid surfaces. *J. Comput. Chem.* **11,** 1181–1186 (1990).

28. Dill, K. A. Dominant Forces in Protein Folding. *Biochemistry* **29,** 7133–7155 (1990).

29. Henderson, R. The structure of the purple membrane from Halobacterium halobium: Analysis of the X-ray diffraction pattern. *J. Mol. Biol.* **93,** 123–138 (1975).

30. Kyte, J. & Doolittle, R. F. A Simple Method for Displaying the Hydropathic Character

of a Protein. *J. Mol. Biol* **157,** 105–132 (1982).

31. Wimley, W. C. & White, S. H. Experimentally determined hydrophobicity scale for proteins at membrane interfaces. *Nat. Struct. Mol. Biol.* **3,** 842–848 (1996).

32. Nilsson, J., Persson, B. & von Heijne, G. Comparative analysis of amino acid distributions in integral membrane proteins from 107 genomes. *Proteins Struct. Funct. Bioinforma.* **60,** 606–616 (2005).

33. Von Heijne, G. Membrane-protein topology. *Nature Reviews Molecular Cell Biology* **7,** 909–918 (2006).

34. Ulmschneider, M. B., Sansom, M. S. P. & Di Nola, A. Properties of integral membrane protein structures: Derivation of an implicit membrane potential. *Proteins Struct. Funct. Genet.* **59,** 252–265 (2005).

35. Andrushchenko, V. V., Aarabi, M. H., Nguyen, L. T., Prenner, E. J. & Vogel, H. J. Thermodynamics of the interactions of tryptophan-rich cathelicidin antimicrobial peptides with model and natural membranes. *Biochim. Biophys. Acta - Biomembr.* **1778,** 1004–1014 (2008).

36. Blondelle, S. E. & Houghten, R. A. Hemolytic and antimicrobial activities of the twenty-four individual omission analogs of melittin. *Biochemistry* **30,** 4671–4678 (1991).

37. Mcintosh, T. J. & Simon, S. A. Roles of Bilayer Material Properties in Function and Distribution of Membrane Proteins Rafts: transient microdomains in plasma or bilayer membranes thought to contain specific lipids and proteins. *Annu. Rev. Biophys. Biomol. Struct* **35,** 177–98 (2006).

38. Cantor, R. S. Lateral Pressures in Cell Membranes: A Mechanism for Modulation of Protein Function. *J. Phys. Chem. B* **101,** 1723–1725 (1997).

39. Baoukina, S., Marrink, S. J. & Tieleman, D. P. Lateral pressure profiles in lipid monolayers. *Faraday Discuss.* **144,** 393-409; discussion 445-481 (2010).

40. Winter, R. & Köhling, R. Static and time-resolved synchrotron small-angle x-ray scattering studies of lyotropic lipid mesophases, model biomembranes and proteins in solution. *J. Phys. Condens. Matter* **16,** (2004).

41. Wallin, E. & Heijne, G. Von. Genome-wide analysis of integral membrane proteins from eubacterial, archaean, and eukaryotic organisms. *Protein Sci.* **7,** 1029–1038 (2008).

42. Liu, J. & Rost, B. Comparing function and structure between entire proteomes. *Protein Sci.* **10,** 1970–1979 (2001).

43. Almén, M. S., Nordström, K. J. V, Fredriksson, R. & Schiöth, H. B. Mapping the human membrane proteome: A majority of the human membrane proteins can be classified according to function and evolutionary origin. *BMC Biol.* **7,** 50 (2009).

44. Krogh, A., Larsson, B., von Heijne, G. & Sonnhammer, E. L. . Predicting transmembrane protein topology with a hidden markov model: application to complete

genomes. *J. Mol. Biol.* **305,** 567–580 (2001).

45. Terstappen, G. C. & Reggiani, A. In silico research in drug discovery. *Trends Pharmacol. Sci.* **22,** 23–26 (2001).

46. Overington, J. P., Al-Lazikani, B. & Hopkins, A. L. How many drug targets are there? *Nat. Rev. Drug Discov.* **5,** 993–996 (2006).

47. Henderson, R. The Purple Membrane from Halobacterium Halobium. *Annu. Rev. Biophys. Bioeng.* **6,** 87–109 (1977).

48. Blobel, G. Intracellular protein topogenesis (protein translocation across membranes/protein integration into membranes/posttranslocational sorting/topogenic sequences/ phylogeny of membranes and compartments). *Cell Biol.* **77,** 1496–1500 (1980).

49. Engelman, D. M., Steitz, T. A. & Goldman, A. Identifying Nonpolar Transbilayer Helices in Amino Acid Sequences of Membrane Proteins. *Annu. Rev. Biophys. Biophys. Chem.* **15,** 321–353 (1986).

50. Lasters, I., Wodakt, S. J., Alard, P. & Cutsemt, E. Van. Structural principles of parallel beta-barrels in proteins. *Biochemistry* **85,** 3338–3342 (1988).

51. Schleiff, E. & Soll, J. Membrane protein insertion: mixing eukaryotic and prokaryotic concepts. *EMBO Rep.* **6,** 1023–7 (2005).

52. Killian, J. A. Hydrophobic mismatch between proteins and lipids in membranes. *Biochim. Biophys. Acta - Rev. Biomembr.* **1376,** 401–416 (1998).

53. Pogozheva, I. D. & Lomize, A. L. Evolution and adaptation of single-pass transmembrane proteins. *Biochim. Biophys. Acta - Biomembr.* **1860,** 364–377 (2018).

54. Bernsel, A. & Von Heijne, G. Improved membrane protein topology prediction by domain assignments. *Protein Sci.* **14,** 1723–1728 (2005).

55. Hubert, P. *et al.* Single-spanning transmembrane domains in cell growth and cell-cell interactions. *Cell Adh. Migr.* **4,** 313–324 (2010).

56. Binda, C., Hubálek, F., Li, M., Edmondson, D. E. & Mattevi, A. Crystal structure of human monoamine oxidase B, a drug target enzyme monotopically inserted into the mitochondrial outer membrane. *FEBS Lett.* **564,** 225–228 (2004).

57. Cosson, P., Perrin, J. & Bonifacino, J. S. Anchors aweigh: Protein localization and transport mediated by transmembrane domains. *Trends Cell Biol.* **23,** 511–517 (2013).

58. Langosch, D. & Arkin, I. T. Interaction and conformational dynamics of membrane-spanning protein helices. *Protein Sci.* **18,** 1343–1358 (2009).

59. Zickermann, V., Angerer, H., Ding, M. G., Nübel, E. & Brandt, U. Small single transmembrane domain (STMD) proteins organize the hydrophobic subunits of large membrane protein complexes. *FEBS Lett.* **584,** 2516–2525 (2010).

60. Alder, N. N. & Johnson, A. E. Cotranslational membrane protein biogenesis at the

endoplasmic reticulum. *Journal of Biological Chemistry* **279,** 22787–22790 (2004).

61. Rapoport, T. A., Goder, V., Heinrich, S. U. & Matlack, K. E. S. Membrane-protein integration and the role of the translocation channel. *Trends in Cell Biology* **14,** 568–575 (2004).

62. Skach, W. R. Cellular mechanisms of membrane protein folding. *Nat. Struct. Mol. Biol.* **16,** 606–612 (2009).

63. Shao, S. & Hegde, R. S. Membrane Protein Insertion at the Endoplasmic Reticulum. *Annu. Rev. Cell Dev. Biol.* **27,** 25–56 (2011).

64. Spencer Yost, C., Hedgpeth, J. & Lingappa, V. R. A stop transfer sequence confers predictable transmembrane orientation to a previously secreted protein in cell-free systems. *Cell* **34,** 759–766 (1983).

65. Guna, A., Volkmar, N., Christianson, J. C. & Hegde, R. S. The ER membrane protein complex is a transmembrane domain insertase. *Science (80-.).* **359,** 470–473 (2018).

66. Sharpe, H. J., Stevens, T. J. & Munro, S. A comprehensive comparison of transmembrane domains reveals organelle-specific properties. *Cell* **142,** 158–69 (2010).

67. Fry, M. Y. & Clemons, W. M. Complexity in targeting membrane proteins. *Science (80-.).* **359,** 390–391 (2018).

68. Seaton, B.A., Roberts, M. F. Peripheral Membrane Proteins. in *Biological Membranes: A Molecular Perspective from Computation and Experiment* (ed. MerzJr, K.M., Roux, B.) 355–403 (Birkhäuser Boston, 1996).

69. Murray, D. & Honig, B. Electrostatic control of the membrane targeting of C2 domains. *Mol. Cell* **9,** 145–154 (2002).

70. Cho, W. & Stahelin, R. V. Membrane-Protein Interactions in Cell Signaling and Membrane Trafficking. *Annu. Rev. Biophys. Biomol. Struct.* **34,** 119–151 (2005).

71. Won, D. H. *et al.* PI(3,4,5)P3 and PI(4,5)P2 lipids target proteins with polybasic clusters to the plasma membrane. *Science (80-.).* **314,** 1458–1461 (2006).

72. van Meer, G., Voelker, D. R. & Feigenson, G. W. Membrane lipids: where they are and how they behave. *Nat. Rev. Mol. Cell Biol.* **9,** 112–124 (2008).

73. Das, S., Dixon, J. E. & Cho, W. Membrane-binding and activation mechanism of PTEN. *Proc. Natl. Acad. Sci.* **100,** 7491–7496 (2003).

74. Thelen, M., Rosen, A., Nairn, A. C. & Aderem, A. Regulation by phosphorylation of reversible association of a myristoylated protein kinase C substrate with the plasma membrane. *Nature* **351,** 320–322 (1991).

75. Murray, D., Arbuzova, A., Honig, B. & McLaughlin, S. The Role of Electrostatic and Nonpolar Interactions in the Association of Peripheral Proteins with Membranes. *Curr. Top. Membr.* **52,** 277–307 (2002).

76. McCloskey, M. A. & Pop, M. Rates of Membrane-associated Reactions: Reduction of

Dimensionality Revisited. doi:10.1083/jcb.102.1.88

77. Mathias, R. T., Baldo, G. J., Manivannan, K. & Mclaughlin, S. Discrete Charges on Biological Membranes. in *Electrified Interfaces in Physics, Chemistry and Biology* 473–490 (Springer Netherlands, 1992). doi:10.1007/978-94-011-2566-6_19

78. Das, S., Rafter, J. D., Kim, K. P., Gygi, S. P. & Cho, W. Mechanism of Group IVA Cytosolic Phospholipase A2 Activation by Phosphorylation. *J. Biol. Chem.* **278,** 41431–41442 (2003).

79. Stahelin, R. V. Lipid binding domains: more than simple lipid effectors. *J. Lipid Res.* **50 Suppl,** S299-304 (2009).

80. Cho, W. Membrane Targeting by C1 and C2 Domains. *Journal of Biological Chemistry* **276,** 32407–32410 (2001).

81. Ferguson, K. M. *et al.* Structural basis for discrimination of 3-phosphoinositides by pleckstrin homology domains. *Mol. Cell* **6,** 373–384 (2000).

82. Stahelin, R. V *et al.* Phosphatidylinositol 3-phosphate induces the membrane penetration of the FYVE domains of Vps27p and Hrs. *J. Biol. Chem.* **277,** 26379–26388 (2002).

83. Xu, Y., Seet, L. F., Hanson, B. & Hong, W. The Phox homology (PX) domain, a new player in phosphoinositide signalling. *Biochem. J.* **360,** 513–530 (2001).

84. De Camilli, P. *et al.* The ENTH domain. *FEBS Letters* **513,** 11–18 (2002).

85. Stahelin, R. V *et al.* Contrasting membrane interaction mechanisms of AP180 N-terminal homology (ANTH) and epsin N-terminal homology (ENTH) domains. *J. Biol. Chem.* **278,** 28993–28999 (2003).

86. Bretscher, A., Edwards, K. & Fehon, R. G. ERM proteins and merlin: Integrators at the cell cortex. *Nature Reviews Molecular Cell Biology* **3,** 586–599 (2002).

87. Blood, P. D. & Voth, G. A. Direct observation of Bin/amphiphysin/Rvs (BAR) domain-induced membrane curvature by means of molecular dynamics simulations. *Proc. Natl. Acad. Sci.* **103,** 15068–15072 (2006).

88. Carroll, K., Gomez, C. & Shapiro, L. Tubby proteins: the plot thickens. *Nat. Rev. Mol. Cell Biol.* **5,** 55–64 (2004).

89. Zhang, G., Kazanietz, M. G., Blumberg, P. M. & Hurley, J. H. Crystal structure of the cys2 activator-binding domain of protein kinase C delta in complex with phorbol ester. *Cell* **81,** 917–24 (1995).

90. Anderluh, G. & Lakey, J. H. Disparate proteins use similar architectures to damage membranes. *Trends Biochem. Sci.* **33,** 482–490 (2008).

91. Bittova, L., Stahelin, R. V. & Cho, W. Roles of Ionic Residues of the C1 Domain in Protein Kinase C-α Activation and the Origin of Phosphatidylserine Specificity. *J. Biol. Chem.* **276,** 4218–4226 (2001).

92. Das, J. & Rahman, G. M. C1 Domains: Structure and Ligand-Binding Properties. *Chem. Rev.* **114,** 12108–12131 (2014).

93. Singh, S. M. & Murray, D. Molecular modeling of the membrane targeting of phospholipase C pleckstrin homology domains. *Protein Sci.* **12,** 1934–1953 (2003).

94. Rebecchi, M., Peterson, A. & McLaughlin, S. Phosphoinositide-Specific Phospholipase C-Δ1 Binds with High Affinity to Phospholipid Vesicles Containing Phosphatidylinositol 4, 5-Bisphosphate. *Biochemistry* **31,** 12742–12747 (1992).

95. Kavran, J. M. *et al.* Specificity and promiscuity in phosphoinositide binding by pleckstrin homology domains. *J. Biol. Chem.* **273,** 30497–30508 (1998).

96. de Kruijff, B., Cullis, P. R. & Verkleij, A. J. Non-bilayer lipid structures in model and biological membranes. *Trends Biochem. Sci.* **5,** 79–81 (1980).

97. Karathanassis, D. *et al.* Binding of the PX domain of p47(phox) to phosphatidylinositol 3,4-bisphosphate and phosphatidic acid is masked by an intramolecular interaction. *EMBO J.* **21,** 5057–68 (2002).

98. Ago, T. *et al.* Phosphorylation of p47phox directs phox homology domain from SH3 domain toward phosphoinositides, leading to phagocyte NADPH oxidase activation. *Proc. Natl. Acad. Sci.* **100,** 4474–4479 (2003).

99. Resh, M. D. Covalent lipid modifications of proteins. *Curr. Biol.* **23,** R431–R435 (2013).

100. Baumann, N.A., Menon, A. K. Lipid Modifications of Proteins. in *Biochemistry of Lipids, Lipoproteins and Membranes (4th Ed.)* (ed. Vance, D.E., Vance, J. E.) 37–54 (Elsevier Science B.V., 2002). doi:10.1016/B978-0-444-53219-0.50004-0

101. Levental, I., Grzybek, M. & Simons, K. Greasing their way: Lipid modifications determine protein association with membrane rafts. *Biochemistry* **49,** 6305–6316 (2010).

102. Peitzsch, R. M. & McLaughlin, S. Binding of acylated peptides and fatty acids to phospholipid vesicles: Pertinence to myristoylated proteins. *Biochemistry* **32,** 10436–10443 (1993).

103. Hanakam, F., Gerisch, G., Lotz, S., Alt, T. & Seelig, A. Binding of hisactophilin I and II to lipid membranes is controlled by a pH-dependent myristoyl-histidine switch. *Biochemistry* **35,** 11036–11044 (1996).

104. Goldberg, J. Structural basis for activation of ARF GTPase: mechanisms of guanine nucleotide exchange and GTP-myristoyl switching. *Cell* **95,** 237–48 (1998).

105. Hermida-Matsumoto, L. & Resh, M. D. Localization of human immunodeficiency virus type 1 Gag and Env at the plasma membrane by confocal imaging. *J. Virol.* **74,** 8670–9 (2000).

106. Shahinian, S. & Silvius, J. R. Doubly-lipid-modified protein sequence motifs exhibit long-lived anchorage to lipid bilayer membranes. *Biochemistry* **34,** 3813–3822 (1995).

107. Paulick, M. G. & Bertozzi, C. R. The glycosylphosphatidylinositol anchor: a complex membrane-anchoring structure for proteins. *Biochemistry* **47,** 6991–7000 (2008).

108. Udenfriend, S. & Kodukula, K. How Glycosyl-Phosphatidylinositol-Anchored Membrane Proteins are Made. *Annu. Rev. Biochem.* **64,** 563–591 (1995).

109. Burn, P. Amphitropic proteins: a new class of membrane proteins. *Trends Biochem Sci* **13,** 79–83 (1988).

110. Goñi, F. M., Lix, F. Â. & Gon, M. Non-permanent proteins in membranes: when proteins come as visitors (Review). *Mol. Membr. Biol.* **19,** 237–245 (2002).

111. Johnson, J. E. & Cornell, R. B. Amphitropic proteins: regulation by reversible membrane interactions (Review). *Mol. Membr. Biol.* **16,** 217–235 (1999).

112. Wirtz, K. W. Phospholipid transfer proteins revisited. *Biochem. J.* **324 (Pt 2,** 353–60 (1997).

113. Jenkins, G. M. & Frohman, M. A. Phospholipase D: a lipid centric review. *Cell. Mol. Life Sci.* **62,** 2305–2316 (2005).

114. Márquez, M. G., Del Carmen Fernández-Tome, M., Favale, N. O., Pescio, L. G. & Sterin-Speziale, N. B. Bradykinin modulates focal adhesions and induces stress fiber remodeling in renal papillary collecting duct cells. *Am. J. Physiol. Renal Physiol.* **294,** 603–613 (2008).

115. Fehon, R. G., McClatchey, A. I. & Bretscher, A. Organizing the cell cortex: The role of ERM proteins. *Nat. Rev. Mol. Cell Biol.* **11,** 276–287 (2010).

116. Alouf, J. E. Pore-forming bacterial protein toxins: an overview. *Curr. Top. Microbiol. Immunol.* **257,** 1–14 (2001).

117. Ames, J. B., Tanaka, T., Stryer, L. & Ikura, M. Portrait of a myristoyl switch protein. *Curr. Opin. Struct. Biol.* **6,** 432–438 (1996).

118. Gaffarogullari, E.C., Masterson, L.R., Metcalfe, E.E., Traaseth, N.J., Balatri, E., Musa, M.M., Mullen, D., Distefano, M.D., Veglia, G. *et al.* A Myristoyl/Phosphoserine Switch Controls cAMP-dependent protein kinase association to membranes. *J. Mol. Biol.* **411,** 823–836 (2011).

119. Petosa, C., Collier, R. J., Klimpel, K. R., Leppla, S. H. & Liddington, R. C. Crystal structure of the anthrax toxin protective antigen. *Nature* **385,** 833–838 (1997).

120. DiNitto, J. P., Cronin, T. C. & Lambright, D. G. Membrane Recognition and Targeting by Lipid-Binding Domains. *Sci. Signal.* **2003,** re16-re16 (2003).

121. Mizuno, N. & Itoh, H. Functions and Regulatory Mechanisms of Gq-Signaling Pathways. *Neurosignals* **17,** 42–54 (2009).

122. Hannun, Y. A. & Obeid, L. M. Principles of bioactive lipid signalling: lessons from sphingolipids. *Nat. Rev. Mol. Cell Biol.* **9,** 139–150 (2008).

123. Bevers, E. M., Comfurius, P. & Zwaal, R. F. Changes in membrane phospholipid

distribution during platelet activation. *Biochim. Biophys. Acta* **736,** 57–66 (1983).

124. Marsh, D. Lateral pressure profile, spontaneous curvature frustration, and the incorporation and conformation of proteins in membranes. *Biophysical Journal* **93,** 3884–3899 (2007).

125. Dennis, M. K., Taneva, S. G. & Cornell, R. B. The intrinsically disordered nuclear localization signal and phosphorylation segments distinguish the membrane affinity of two cytidylyltransferase isoforms. *J. Biol. Chem.* **286,** 12349–12360 (2011).

126. Cornell, R. B. How cytidylyltransferase uses an amphipathic helix to sense membrane phospholipid composition. *Biochem. Soc. Trans.* **26,** 539–44 (1998).

127. Putta, P. *et al.* Phosphatidic acid binding proteins display differential binding as a function of membrane curvature stress and chemical properties. *Biochim. Biophys. Acta - Biomembr.* **1858,** 2709–2716 (2016).

128. Jékely, G. Did the last common ancestor have a biological membrane? *Biol. Direct* **1,** 35 (2006).

129. Deamer, D., Dworkin, J. P., Sandford, S. A., Bernstein, M. P. & Allamandola, L. J. The First Cell Membranes. *Astrobiology* **2,** 371–381 (2002).

130. Hilario, E. & Gogarten, J. P. The prokaryote-to-eukaryote transition reflected in the evolution of the V/F/A-ATPase catalytic and proteolipid subunits. *J. Mol. Evol.* **46,** 703–15 (1998).

131. Cao, T. B. & Saier, M. H. The general protein secretory pathway: phylogenetic analyses leading to evolutionary conclusions. *Biochim. Biophys. Acta - Biomembr.* **1609,** 115–125 (2003).

132. Isenbarger, T. A. *et al.* The Most Conserved Genome Segments for Life Detection on Earth and Other Planets. *Orig. Life Evol. Biosph.* **38,** 517–533 (2008).

133. Saier, M. H. A Functional-Phylogenetic Classification System for Transmembrane Solute Transporters. *Microbiol. Mol. Biol. Rev.* **64,** 354–411 (2000).

134. Borst, P., Evers, R., Kool, M. & Wijnholds, J. A Family of Drug Transporters: the Multidrug Resistance-Associated Proteins. *J. Natl. Cancer Inst.* **92,** 1295–1302 (2000).

135. Burton, B. & Dubnau, D. Membrane-associated DNA transport machines. *Cold Spring Harb. Perspect. Biol.* **2,** a000406 (2010).

136. Mitchell, P. Chemiosmotic coupling in oxidative and photosynthetic phosphorylation. *Biochim. Biophys. Acta - Bioenerg.* **1807,** 1507–1538 (2011).

137. Bean, B. P. The action potential in mammalian central neurons. *Nat. Rev. Neurosci.* **8,** 451–465 (2007).

138. Korsmeyer, S. J. *et al.* Pro-apoptotic cascade activates BID, which oligomerizes BAK or BAX into pores that result in the release of cytochrome c. *Cell Death Differ.* **7,** 1166–1173 (2000).

139. West, I. C. Ligand conduction and the gated-pore mechanism of transmembrane transport. *Biochim. Biophys. Acta - Rev. Biomembr.* **1331,** 213–234 (1997).

140. Pietropaolo, A., Pierri, C. L., Palmieri, F. & Klingenberg, M. The switching mechanism of the mitochondrial ADP/ATP carrier explored by free-energy landscapes. *Biochim. Biophys. Acta - Bioenerg.* **1857,** 772–781 (2016).

141. Pebay-Peyroula, E. *et al.* Structure of mitochondrial ADP/ATP carrier in complex with carboxyatractyloside. *Nature* **426,** 39–44 (2003).

142. Fiel, S.C., Polekhina, G., Gorman, M.A., Parker, M. W. Introduction. in *Proteins: Membrane Binding and Pore Formation introduction* 1–13 (2010).

143. Hutchison, M. L., Tester, M. A. & Gross, D. C. Role of biosurfactant and ion channel-forming activities of syringomycin in transmembrane ion flux: a model for the mechanism of action in the plant-pathogen interaction. *Mol. Plant-Microbe Interact.* **8,** 610–20

144. Rainey, P. B., Brodey, C. L. & Johnstone, K. Biological properties and spectrum of activity of tolaasin, a lipodepsipeptide toxin produced by the mushroom pathogen Pseudomonas tolaasii. *Physiol. Mol. Plant Pathol.* **39,** 57–70 (1991).

145. Singer, S. J. Molecular Biology of Cellular Membranes with Applications to Immunology. *Adv. Immunol.* **19,** 1–66 (1974).

146. MacKinnon, R. Pore loops: an emerging theme in ion channel structure. *Neuron* **14,** 889–92 (1995).

147. Minor, D. L. An Overview of Ion Channel Structure. in *Handbook of Cell Signaling* 201–207 (Elsevier, 2010). doi:10.1016/B978-0-12-374145-5.00030-9

148. Gouaux, E. & Mackinnon, R. Principles of Selective Ion Transport in Channels and Pumps. *Science (80-.).* **310,** 1461–1465 (2005).

149. Kovacs, J. A., Baker, K. A., Altenberg, G. A., Abagyan, R. & Yeager, M. Molecular modeling and mutagenesis of gap junction channels. *Progress in Biophysics and Molecular Biology* **94,** 15–28 (2007).

150. Dutzler, R., Campbell, E. B., Cadene, M., Chait, B. T. & MacKinnon, R. X-ray structure of a ClC chloride channel at 3.0 Å reveals the molecular basis of anion selectivity. *Nature* **415,** 287–294 (2002).

151. Jentsch, T. J. Cell biology: Chloride channels are different. *Nature* **415,** 276–277 (2002).

152. Haggie, P. M. & Verkman, A. S. Monomeric CFTR in plasma membranes in live cells revealed by single molecule fluorescence imaging. *J. Biol. Chem.* **283,** 23510–23513 (2008).

153. Liu, F., Zhang, Z., Csanády, L., Gadsby, D. C. & Chen, J. Molecular Structure of the Human CFTR Ion Channel. *Cell* **169,** 85–95.e8 (2017).

154. Kennedey, S. J. Structures of membrane proteins. *J. Membr. Biol.* **42,** 265–279 (1978).

155. Singer, S. J. Some Early History of Membrane Molecular Biology. *Annu. Rev. Physiol.* **66,** 1–27 (2004).

156. Jap, B. K. Molecular design of PhoE porin and its functional consequences. *J. Mol. Biol.* **205,** 407–419 (1989).

157. Weiss, M. S., Wacker, T., Weckesser, J., Welte, W. & Schulz, G. E. The three-dimensional structure of porin from Rhodobacter capsulatus at 3 A resolution. *FEBS Lett.* **267,** 268–72 (1990).

158. Cowan, S. *et al.* The structure of OmpF porin in a tetragonal crystal form. *Structure* **3,** 1041–1050 (1995).

159. Tamm, L. K., Hong, H. & Liang, B. Folding and assembly of β-barrel membrane proteins. *Biochim. Biophys. Acta - Biomembr.* **1666,** 250–263 (2004).

160. Okada, T. *et al.* Molecular and functional characterization of a novel mouse transient receptor potential protein homologue TRP7. Ca(2+)-permeable cation channel that is constitutively activated and enhanced by stimulation of G protein-coupled receptor. *J. Biol. Chem.* **274,** 27359–70 (1999).

161. Zitt, C. *et al.* Expression of TRPC3 in Chinese hamster ovary cells results in calcium-activated cation currents not related to store depletion. *J. Cell Biol.* **138,** 1333–41 (1997).

162. Plested, A. J. R. Structural mechanisms of activation and desensitization in neurotransmitter-gated ion channels. *Nat. Struct. Mol. Biol.* **23,** 494–502 (2016).

163. Boscardin, E., Alijevic, O., Hummler, E., Frateschi, S. & Kellenberger, S. The function and regulation of acid-sensing ion channels (ASICs) and the epithelial Na+channel (ENaC): IUPHAR Review 19. *British Journal of Pharmacology* **173,** 2671–2701 (2016).

164. Cuello, L. G., Cortes, D. M., Jogini, V., Sompornpisut, A. & Perozo, E. A molecular mechanism for proton-dependent gating in KcsA. *FEBS Lett.* **584,** 1126–1132 (2010).

165. Goldschen-Ohm, M. P. & Chanda, B. SnapShot: Channel Gating Mechanisms. (2017). doi:10.1016/j.cell.2017.07.019

166. Palovcak, E., Delemotte, L., Klein, M. L. & Carnevale, V. Evolutionary imprint of activation: The design principles of VSDs. *J. Gen. Physiol.* **143,** 145–156 (2014).

167. Schewe, M. *et al.* A Non-canonical Voltage-Sensing Mechanism Controls Gating in K2P K+ Channels. *Cell* **164,** 937–949 (2016).

168. Unwin, N. Acetylcholine receptor channel imaged in the open state. *Nature* **373,** 37–43 (1995).

169. Jiang, Y. *et al.* The open pore conformation of potassium channels. *Nature* **417,** 523–526 (2002).

170. Zhou, M. & MacKinnon, R. A Mutant KcsA K+ Channel with Altered Conduction Properties and Selectivity Filter Ion Distribution. *J. Mol. Biol.* **338,** 839–846 (2004).

171. Guy, H. R. & Seetharamulu, P. Molecular model of the action potential sodium channel. *Proc. Natl. Acad. Sci. U. S. A.* **83,** 508–12 (1986).

172. Schulz, G. E. Bacterial porins: structure and function. *Curr. Opin. Cell Biol.* **5,** 701–707 (1993).

173. Zeth, K., Diederichs, K., Welte, W. & Engelhardt, H. Crystal structure of Omp32, the anion-selective porin from Comamonas acidovorans, in complex with a periplasmic peptide at 2.1 Å resolution. *Structure* **8,** 981–992 (2000).

174. Roux, B. Ion channels and ion selectivity. *Essays Biochem.* **61,** 201–209 (2017).

175. Zhou, Y., Morais-Cabral, J. H., Kaufman, A. & MacKinnon, R. Chemistry of ion coordination and hydration revealed by a K+ channel-Fab complex at 2.0 A resolution. *Nature* **414,** 43–48 (2001).

176. Bernèche, S. & Roux, B. A microscopic view of ion conduction through the K+ channel. *Proc. Natl. Acad. Sci. U. S. A.* **100,** 8644–8 (2003).

177. Bernèche, S. & Roux, B. Energetics of ion conduction through the K^+ channel. *Nature* **414,** 73–77 (2001).

178. Ing, C. & Pomès, R. Simulation Studies of Ion Permeation and Selectivity in Voltage-Gated Sodium Channels. *Curr. Top. Membr.* **78,** 215–260 (2016).

179. Iacovache, I., van der Goot, F. G. & Pernot, L. Pore formation: An ancient yet complex form of attack. *Biochim. Biophys. Acta - Biomembr.* **1778,** 1611–1623 (2008).

180. Pipkin, M. E. & Lieberman, J. Delivering the kiss of death: progress on understanding how perforin works. *Curr. Opin. Immunol.* **19,** 301–308 (2007).

181. Kroemer, G., Galluzzi, L. & Brenner, C. Mitochondrial Membrane Permeabilization in Cell Death. *Physiol. Rev.* **87,** 99–163 (2007).

182. Bischofberger, M., Gonzalez, M. R. & van der Goot, F. G. Membrane injury by pore-forming proteins. *Curr. Opin. Cell Biol.* **21,** 589–595 (2009).

183. Iacovache, I., Bischofberger, M. & van der Goot, F. G. Structure and assembly of pore-forming proteins. *Curr. Opin. Struct. Biol.* **20,** 241–246 (2010).

184. Lesieur, C., Abrami, L., Fivaz, M. & Gisou van der Goot, F. Membrane insertion: the strategies of toxins (Review). *Mol. Membr. Biol.* **14,** 45–64 (1997).

185. Montecucco, C., Papini, E. & Schiavo, G. Bacterial protein toxins penetrate cells via a four-step mechanism. *FEBS Lett.* **346,** 92–98 (1994).

186. Mueller, M., Grauschopf, U., Maier, T., Glockshuber, R. & Ban, N. The structure of a cytolytic α-helical toxin pore reveals its assembly mechanism. *Nature* **459,** 726–730 (2009).

187. Ramachandran, R., Tweten, R. K. & Johnson, A. E. The domains of a cholesterol-dependent cytolysin undergo a major FRET-detected rearrangement during pore formation. *Proc. Natl. Acad. Sci. U. S. A.* **102,** 7139–44 (2005).

188. Czajkowsky, D. M., Hotze, E. M., Shao, Z. & Tweten, R. K. Vertical collapse of a cytolysin prepore moves its transmembrane β-hairpins to the membrane. *EMBO J.* **23,** 3206–3215 (2004).

189. Dang, T. X., Hotze, E. M., Rouiller, I., Tweten, R. K. & Wilson-Kubalek, E. M. Prepore to pore transition of a cholesterol-dependent cytolysin visualized by electron microscopy. *J. Struct. Biol.* **150,** 100–108 (2005).

190. Rosado, C. J. *et al.* A Common Fold Mediates Vertebrate Defense and Bacterial Attack. *Science (80-.).* **317,** 1548–1551 (2007).

191. Turner, J., Cho, Y., Dinh, N. N., Waring, A. J. & Lehrer, R. I. Activities of LL-37, a cathelin-associated antimicrobial peptide of human neutrophils. *Antimicrob. Agents Chemother.* **42,** 2206–14 (1998).

192. Lee, C.-C., Sun, Y., Qian, S. & Huang, H. W. Transmembrane pores formed by human antimicrobial peptide LL-37. *Biophys. J.* **100,** 1688–96 (2011).

193. Lella, M. & Mahalakshmi, R. Metamorphic Proteins: Emergence of Dual Protein Folds from One Primary Sequence. *Biochemistry* **56,** 2971–2984 (2017).

194. Husler, T., Lockert, D. H., Kaufman, K. M., Sodetz, J. M. & Sims, P. J. Chimeras of human complement C9 reveal the site recognized by complement regulatory protein CD59. *J. Biol. Chem.* **270,** 3483–3486 (1995).

195. Huang, Y., Qiao, F., Abagyan, R., Hazard, S. & Tomlinson, S. Defining the CD59-C9 binding interaction. *J. Biol. Chem.* **281,** 27398–27404 (2006).

196. Keen, J. H., Maxfieldt, F. R., Hardegree, M. C. & Habigt, W. H. Receptor-mediated endocytosis of diphtheria toxin by cells in culture (clustering/fluorescence/video intensification microscopy/clathrin-coated pits). *Cell Biol.* **79,** 2912–2916 (1982).

197. Gilbert, R. J. C. Cholesterol-dependent cytolysins. *Adv. Exp. Med. Biol.* **677,** 56–66 (2010).

198. Polzien, L. *et al.* Identification of novel in vivo phosphorylation sites of the human proapoptotic protein BAD: pore-forming activity of BAD is regulated by phosphorylation. *J. Biol. Chem.* **284,** 28004–20 (2009).

199. van der Goot, F. G., González-Mañas, J. M., Lakey, J. H. & Pattus, F. A 'molten-globule' membrane-insertion intermediate of the pore-forming domain of colicin A. *Nature* **354,** 408–410 (1991).

200. Ohgushi, M. & Wada, A. 'Molten-globule state': a compact form of globular proteins with mobile side-chains. *FEBS Lett.* **164,** 21–24 (1983).

201. Thuduppathy, G. R. & Hill, R. B. Acid destabilization of the solution conformation of Bcl-xL does not drive its pH-dependent insertion into membranes. *Protein Sci.* **15,** 248–257 (2006).

202. Wimley, W. C. Energetics of Peptide and Protein Binding to Lipid Membranes. in *Proteins: Membrane Binding and Pore Formation* (ed. Anderluh, G. L. J.) 14–23 (Springer, New York, NY, 2010). doi:10.1007/978-1-4419-6327-7_2

203. Thøgersen, L., Schiøtt, B., Vosegaard, T., Nielsen, N. C. & Tajkhorshid, E. Peptide aggregation and pore formation in a lipid bilayer: A combined coarse-grained and all atom molecular dynamics study. *Biophys. J.* **95,** 4337–4347 (2008).

204. Song, L. *et al.* Structure of staphylococcal alpha-hemolysin, a heptameric transmembrane pore. *Science (80-.).* **274,** 1859–1866 (1996).

205. Tweten, R. K. Cholesterol-dependent cytolysins, a family of versatile pore-forming toxins. *Infection and Immunity* **73,** 6199–6209 (2005).

206. Tilley, S. J., Orlova, E. V., Gilbert, R. J. C., Andrew, P. W. & Saibil, H. R. Structural Basis of Pore Formation by the Bacterial Toxin Pneumolysin. *Cell* **121,** 247–256 (2005).

207. Jentsch, T. J. J., Stein, V., Weinreich, F., a.a. Zdebik & Zdebik, A. a. Molecular structure and physiological function of chloride channels. *Physiol. Rev.* **82,** 503 (2002).

208. Alexander et al. Chloride channels. *Br. J. Pharmacol.* **158,** S130–S134 (2009).

209. Forte, M. & Blachly-Dyson, E. VDAC Channels. *IUBMB Life (International Union Biochem. Mol. Biol. Life)* **52,** 113–118 (2001).

210. Koetters, P. J., Chou, H. F. & Jonas, A. J. Lysosomal sulfate transport: inhibitor studies. *Biochim. Biophys. Acta* **1235,** 79–84 (1995).

211. Ballarin, C. & Sorgato, M. C. An electrophysiological study of yeast mitochondria. Evidence for two inner membrane anion channels sensitive to ATP. *J. Biol. Chem.* **270,** 19262–8 (1995).

212. Demaurex, N., Furuya, W., D'Souza, S., Bonifacino, J. S. & Grinstein, S. Mechanism of acidification of the trans-Golgi network (TGN). In situ measurements of pH using retrieval of TGN38 and furin from the cell surface. *J. Biol. Chem.* **273,** 2044–51 (1998).

213. Sheppard, D. N. & Welsh, M. J. Structure and function of the CFTR chloride channel. *Physiol. Rev.* **79,** S23–S45 (1999).

214. Alexander, S., Mathie, A. & Peters, J. Ion Channels. *Br. J. Pharmacol.* **164,** S137–S174 (2011).

215. Dutzler, R. The ClC family of chloride channels and transporters. *Curr. Opin. Struct. Biol.* **16,** 439–446 (2006).

216. Kornak, U. *et al.* Loss of the ClC-7 chloride channel leads to osteopetrosis in mice and man. *Cell* **104,** 205–15 (2001).

217. Picollo, A. & Pusch, M. Chloride/proton antiporter activity of mammalian CLC proteins ClC-4 and ClC-5. *Nature* **436,** 420–423 (2005).

218. Accardi, A. & Picollo, A. CLC channels and transporters: Proteins with borderline personalities. *Biochim. Biophys. Acta - Biomembr.* **1798,** 1457–1464 (2010).

219. Jentsch, T. J., Günther, W., Pusch, M. & Schwappach, B. Properties of voltage-gated chloride channels of the ClC gene family. *J. Physiol.* **482,** 19S–25S (1995).

220. Nguitragool, W. & Miller, C. Uncoupling of a CLC Cl−/H+ Exchange Transporter by Polyatomic Anions. *J. Mol. Biol.* **362,** 682–690 (2006).

221. Accardi, A., Kolmakova-Partensky, L., Williams, C. & Miller, C. Ionic Currents Mediated by a Prokaryotic Homologue of CLC Cl − Channels. *J. Gen. Physiol.* **123,** 109–119 (2004).

222. Ludewig, U., Pusch, M. & Jentsch, T. J. Independent gating of single pores in CLC-0 chloride channels. *Biophys. J.* **73,** 789–797 (1997).

223. Miyazaki, H. *et al.* CLC anion channel regulatory phosphorylation and conserved signal transduction domains. *Biophys. J.* **103,** 1706–18 (2012).

224. Yamada, T., Bhate, M. P. & Strange, K. Regulatory phosphorylation induces extracellular conformational changes in a CLC anion channel. *Biophys. J.* **104,** 1893–904 (2013).

225. Okkenhaug, H. *et al.* The human ClC-4 protein, a member of the CLC chloride channel/transporter family, is localized to the endoplasmic reticulum by its N-terminus. *FASEB J.* **20,** 2390–2 (2006).

226. Ran, S. & Benos, D. J. Isolation and functional reconstitution of a 38-kDa chloride channel protein from bovine tracheal membranes. *J. Biol. Chem.* **266,** 4782–8 (1991).

227. Guo, Y., Su, M., McNutt, M. A. & Gu, J. Expression and Distribution of Cystic Fibrosis Transmembrane Conductance Regulator in Neurons of the Human Brain. *J. Histochem. Cytochem.* **57,** 1113–1120 (2009).

228. Schwiebert, E. M., Benos, D. J., Egan, M. E., Stutts, M. J. & Guggino, W. B. CFTR is a conductance regulator as well as a chloride channel. *Physiol. Rev.* **79,** S145–S166 (1999).

229. Anderson, M. *et al.* Demonstration that CFTR is a chloride channel by alteration of its anion selectivity. *Science (80-.).* **253,** 202–205 (1991).

230. Linsdell, P. Architecture and functional properties of the CFTR channel pore. *Cellular and Molecular Life Sciences* **74,** 67–83 (2017).

231. Ikuma, M. & Welsh, M. J. Regulation of CFTR Cl- channel gating by ATP binding and hydrolysis. *Proc. Natl. Acad. Sci. U. S. A.* **97,** 8675–80 (2000).

232. Cheng, S. H. *et al.* Phosphorylation of the R domain by cAMP-dependent protein kinase regulates the CFTR chloride channel. *Cell* **66,** 1027–36 (1991).

233. Skach, W. R. Defects in processing and trafficking of the cystic fibrosis transmembrane conductance regulator. *Kidney Int.* **57,** 825–831 (2000).

234. Lu, Y. *et al.* Co- and posttranslational translocation mechanisms direct cystic fibrosis transmembrane conductance regulator N terminus transmembrane assembly. *J. Biol. Chem.* **273,** 568–76 (1998).

235. Sine, S. M. & Engel, A. G. Recent advances in Cys-loop receptor structure and function. *Nature* **440,** 448–455 (2006).

236. Betz, H. Ligand-gated ion channels in the brain: the amino acid receptor superfamily. *Neuron* **5,** 383–92 (1990).

237. Schofield, P. R., Pritchett, D. B., Sontheimer, H., Kettenmann, H. & Seeburg, P. H. Sequence and expression of human GABAA receptor alpha 1 and beta 1 subunits. *FEBS Lett.* **244,** 361–4 (1989).

238. Kaupmann, K. *et al.* Expression cloning of GABAB receptors uncovers similarity to metabotropic glutamate receptors. *Nature* **386,** 239–246 (1997).

239. Miller, P. S. & Smart, T. G. Binding, activation and modulation of Cys-loop receptors. *Trends Pharmacol. Sci.* **31,** 161–174 (2010).

240. Grenningloh, G. *et al.* Alpha subunit variants of the human glycine receptor: primary structures, functional expression and chromosomal localization of the corresponding genes. *EMBO J.* **9,** 771–6 (1990).

241. Sardini, A. *et al.* Cell volume regulation and swelling-activated chloride channels. in *Biochimica et Biophysica Acta - Biomembranes* **1618,** 153–162 (Elsevier, 2003).

242. Ran, S. & Benos, D. J. Immunopurification and structural analysis of a putative epithelial Cl- channel protein isolated from bovine trachea. *J. Biol. Chem.* **267,** 3618–25 (1992).

243. Ran, S., Fuller, C. M., Arrate, M. P., Latorre, R. & Benos, D. J. Functional reconstitution of a chloride channel protein from bovine trachea. *J. Biol. Chem.* **267,** 20630–7 (1992).

244. Fuller, C. M., Ismailov, I. I., Keeton, D. A. & Benos, D. J. Phosphorylation and activation of a bovine tracheal anion channel by Ca2+ /Calmodulin-dependent protein kinase II. *J. Biol. Chem.* **269,** 26642–26650 (1994).

245. Zhu, D. Z., Cheng, C. F. & Pauli, B. U. Mediation of lung metastasis of murine melanomas by a lung-specific endothelial cell adhesion molecule. *Proc. Natl. Acad. Sci. U. S. A.* **88,** 9568–72 (1991).

246. Cunningham, S. A. *et al.* Cloning of an epithelial chloride channel from bovine trachea. *J. Biol. Chem.* **270,** 31016–26 (1995).

247. Abdel-Ghany, M. *et al.* The interacting binding domains of the beta(4) integrin and calcium-activated chloride channels (CLCAs) in metastasis. *J. Biol. Chem.* **278,** 49406–16 (2003).

248. Gruber, A. D., Elble, R. C. & Pauli, B. U. Discovery and cloning of the CLCA gene family. *Curr. Top. Membr.* **53,** 367–387 (2002).

249. Loewen, M. E. & Forsyth, G. W. Structure and Function of CLCA Proteins. *Physiol. Rev.* **85,** 1061–1092 (2005).

250. Gandhi, R. *et al.* Molecular and functional characterization of a calcium-sensitive chloride channel from mouse lung. *J. Biol. Chem.* **273,** 32096–101 (1998).

251. Gruber, A. D. *et al.* Genomic Cloning, Molecular Characterization, and Functional Analysis of Human CLCA1, the First Human Member of the Family of Ca2+-Activated

Cl−Channel Proteins. *Genomics* **54,** 200–214 (1998).

252. Gruber, A. D., Schreur, K. D., Ji, H.-L., Fuller, C. M. & Pauli, B. U. Molecular cloning and transmembrane structure of hCLCA2 from human lung, trachea, and mammary gland. *Am. J. Physiol. Physiol.* **276,** C1261–C1270 (1999).

253. Gruber, A. D. & Pauli, B. U. Molecular cloning and biochemical characterization of a truncated, secreted member of the human family of Ca2+-activated Cl− channels. *Biochim. Biophys. Acta - Gene Struct. Expr.* **1444,** 418–423 (1999).

254. Whittaker, C. A. Distribution and Evolution of von Willebrand/Integrin A Domains: Widely Dispersed Domains with Roles in Cell Adhesion and Elsewhere. *Mol. Biol. Cell* **13,** 3369–3387 (2002).

255. Patel, A. C., Brett, T. J. & Holtzman, M. J. The role of CLCA proteins in inflammatory airway disease. *Annu. Rev. Physiol.* **71,** 425–449 (2009).

256. Devi, L. Consensus sequence for processing of peptide precursors at monobasic sites. *FEBS Lett.* **280,** 189–194 (1991).

257. Bothe, M. K., Mundhenk, L., Beck, C. L., Kaup, M. & Gruber, A. D. Impaired autoproteolytic cleavage of mCLCA6, a murine integral membrane protein expressed in enterocytes, leads to cleavage at the plasma membrane instead of the endoplasmic reticulum. *Mol. Cells* **33,** 251–257 (2012).

258. Papassotiriou, J., Eggermont, J., Droogmans, G. & Nilius, B. Ca(2+)-activated Cl-channels in Ehrlich ascites tumor cells are distinct from mCLCA1, 2 and 3. *Pflugers Arch.* **442,** 273–9 (2001).

259. Romio, L. *et al.* Characterization of a murine gene homologous to the bovine CaCC chloride channel. *Gene* **228,** 181–8 (1999).

260. Mundhenk, L. *et al.* Both Cleavage Products of the mCLCA3 Protein Are Secreted Soluble Proteins. *J. Biol. Chem.* **281,** 30072–30080 (2006).

261. Gibson, A. *et al.* hCLCA1 and mCLCA3 are secreted non-integral membrane proteins and therefore are not ion channels. *J. Biol. Chem.* **280,** 27205–12 (2005).

262. Elble, R. C. *et al.* The Putative Chloride Channel hCLCA2 Has a Single C-terminal Transmembrane Segment. *J. Biol. Chem.* **281,** 29448–29454 (2006).

263. Bothe, M. K., Braun, J., Mundhenk, L. & Gruber, A. D. Murine mCLCA6 Is an Integral Apical Membrane Protein of Non-goblet Cell Enterocytes and Co-localizes With the Cystic Fibrosis Transmembrane Conductance Regulator. *J. Histochem. Cytochem.* **56,** 495–509 (2008).

264. Singh, H. Two decades with dimorphic Chloride Intracellular Channels (CLICs). *FEBS Lett.* **584,** 2112–2121 (2010).

265. Gururaja Rao, S. *et al.* Identification and Characterization of a Bacterial Homolog of Chloride Intracellular Channel (CLIC) Protein. *Sci. Rep.* **7,** 8500 (2017).

266. Cromer, B. A., Morton, C. J., Board, P. G. & Parker, M. W. From glutathione

transferase to pore in a CLIC. *Eur. Biophys. J.* **31,** 356–364 (2002).

267. Norman, J. & Zanivan, S. Chloride intracellular channel 3: A secreted pro-invasive oxidoreductase. *Cell Cycle* **16,** 1993–1994 (2017).

268. Valenzuela, S. M. *et al.* The nuclear chloride ion channel NCC27 is involved in regulation of the cell cycle. *J. Physiol.* **529 Pt 3,** 541–552 (2000).

269. Ulmasov, B., Bruno, J., Gordon, N., Hartnett, M. E. & Edwards, J. C. Chloride intracellular channel protein-4 functions in angiogenesis by supporting acidification of vacuoles along the intracellular tubulogenic pathway. *Am. J. Pathol.* **174,** 1084–1096 (2009).

270. Al-Momany, A., Li, L., Alexander, R. T. & Ballermann, B. J. Clustered PI(4,5)P2 accumulation and ezrin phosphorylation in response to CLIC5A. *J. Cell Sci.* **127,** 5164–5178 (2014).

271. Kim, K. H. *et al.* CRIg signals induce anti-intracellular bacterial phagosome activity in a chloride intracellular channel 3-dependent manner. *Eur. J. Immunol.* **43,** 667–678 (2013).

272. Money, T. T. *et al.* Expression and cellular localisation of chloride intracellular channel 3 in human placenta and fetal membranes. *Placenta* **28,** 429–36 (2007).

273. Suh, K. S. *et al.* The organellular chloride channel protein CLIC4/mtCLIC translocates to the nucleus in response to cellular stress and accelerates apoptosis. *J. Biol. Chem.* **279,** 4632–41 (2004).

274. Littler, D. R. *et al.* The enigma of the CLIC proteins: Ion channels, redox proteins, enzymes, scaffolding proteins? *FEBS Lett.* **584,** 2093–2101 (2010).

275. Landry, D. W., Reitman, M., Cragoe, E. J. & Al-Awqati, Q. Epithelial chloride channel. Development of inhibitory ligands. *J. Gen. Physiol.* **90,** 779–98 (1987).

276. Landry, D. W. *et al.* Purification and Reconstitution of Chloride Channels from Kidney and Trachea. *Science* **244,** 1469–1472 (1989).

277. Redhead, C. R., Edelman, A. E., Brown, D., Landry, D. W. & Al-Awqati, Q. A ubiquitous 64-kDa protein is a component of a chloride channel of plasma and intracellular membranes. *Proc. Natl. Acad. Sci. U. S. A.* **89,** 3716–20 (1992).

278. Landry, D. *et al.* Molecular cloning and characterization of p64, a chloride channel protein from kidney microsomes. *J. Biol. Chem.* **268,** 14948–14955 (1993).

279. Howell, S., Duncan, R. R. & Ashley, R. H. Identification and characterisation of a homologue of p64 in rat tissues. *FEBS Lett.* **390,** 207–210 (1996).

280. Duncan, R. R., Westwood, P. K., Boyd, A. & Ashley, R. H. Rat brain p64H1, expression of a new member of the p64 chloride channel protein family in endoplasmic reticulum. *J. Biol. Chem.* **272,** 23880–23886 (1997).

281. Valenzuela, S. M. *et al.* Molecular cloning and expression of a chloride ion channel of cell nuclei. *J. Biol. Chem.* **272,** 12575–82 (1997).

282. Heiss, N. S. & Poustka, A. Genomic Structure of a Novel Chloride Channel Gene, CLIC2, in Xq28. *Genomics* **45,** 224–228 (1997).

283. Qian, Z., Okuhara, D., Abe, M. K. & Rosner, M. R. Molecular cloning and characterization of a mitogen-activated protein kinase-associated intracellular chloride channel. *J. Biol. Chem.* **274,** 1621–7 (1999).

284. Chuang, J. Z., Milner, T. A., Zhu, M. & Sung, C. H. A 29 kDa intracellular chloride channel p64H1 is associated with large dense-core vesicles in rat hippocampal neurons. *J. Neurosci.* **19,** 2919–2928 (1999).

285. Suginta, W., Karoulias, N., Aitken, A. & Ashley, R. H. Chloride intracellular channel protein CLIC4 (p64H1) binds directly to brain dynamin I in a complex containing actin, tubulin and 14-3-3 isoforms. *Biochem. J.* **359,** 55–64 (2001).

286. Fernández-Salas, E., Sagar, M., Cheng, C., Yuspa, S. H. & Weinberg, W. C. p53 and tumor necrosis factor alpha regulate the expression of a mitochondrial chloride channel protein. *J. Biol. Chem.* **274,** 36488–97 (1999).

287. Berryman, M. & Bretscher, A. Identification of a Novel Member of the Chloride Intracellular Channel Gene Family (CLIC5) That Associates with the Actin Cytoskeleton of Placental Microvilli. *Mol. Biol. Cell* **11,** 1509–1521 (2000).

288. Urushidani, D. Chow, T. & Forte, J. G. Redistribution of a 120 kDa Phosphoprotein in the Parietal Cell Associated with Stimulation. *J. Membr. Biol.* **168,** 209–220 (1999).

289. Nishizawa, T., Nagao, T., Iwatsubo, T., Forte, J. G. & Urushidani, T. Molecular cloning and characterization of a novel chloride intracellular channel-related protein, parchorin, expressed in water-secreting cells. *J. Biol. Chem.* **275,** 11164–11173 (2000).

290. Friedli, M. *et al.* Identification of a novel member of the CLIC family, CLIC6, mapping to 21q22.12. *Gene* **320,** 31–40 (2003).

291. Littler, D. R. *et al.* Comparison of vertebrate and invertebrate CLIC proteins: The crystal structures of Caenorhabditis elegans EXC-4 and Drosophila melanogaster DmCLIC. *Proteins Struct. Funct. Bioinforma.* **71,** 364–378 (2008).

292. Berry, K. L., Bülow, H. E., Hall, D. H. & Hobert, O. A C. elegans CLIC-like Protein Required for Intracellular Tube Formation and Maintenance. *Science (80-.).* **302,** 2134–2137 (2003).

293. Bateman, A. *et al.* UniProt: the universal protein knowledgebase. *Nucleic Acids Res.* **45,** D158–D169 (2017).

294. Ulmasov, B., Bruno, J., Woost, P. G. & Edwards, J. C. Tissue and subcellular distribution of CLIC1. *BMC Cell Biol.* **8,** 8 (2007).

295. Ponnalagu, D. *et al.* Data supporting characterization of CLIC1, CLIC4, CLIC5 and DmCLIC antibodies and localization of CLICs in endoplasmic reticulum of cardiomyocytes. *Data Br.* **7,** 1038–1044 (2016).

296. Lecat, S., Matthes, H. W. D., Pepperkok, R., Simpson, J. C. & Galzi, J.-L. A Fluorescent Live Imaging Screening Assay Based on Translocation Criteria Identifies Novel

Cytoplasmic Proteins Implicated in G Protein-coupled Receptor Signaling Pathways. *Mol. Cell. Proteomics* **14,** 1385–1399 (2015).

297. Hernandez-Fernaud, J. R. *et al.* Secreted CLIC3 drives cancer progression through its glutathione-dependent oxidoreductase activity. *Nat. Commun.* **8,** 1–17 (2017).

298. Ponnalagu, D. *et al.* Molecular identity of cardiac mitochondrial chloride intracellular channel proteins. *Mitochondrion* **27,** 6–14 (2016).

299. Mark A. Berryman, J. R. G. CLIC4 is enriched at cell-cell junctions and colocalizes with AKAP350 at the centrosome and midbody of cultured mammalian cells. *Cell Motil. Cytoskeleton* **56,** 159–172 (2003).

300. Suh, K. S. *et al.* The organellular chloride channel protein CLIC4/mtCLIC translocates to the nucleus in response to cellular stress and accelerates apoptosis. *J. Biol. Chem.* **279,** 4632–41 (2004).

301. Suh, K. S. *et al.* CLIC4 mediates and is required for Ca2+-induced keratinocyte differentiation. *J. Cell Sci.* **120,** 2631–2640 (2007).

302. Flores-Téllez, T. N. J., Lopez, T. V., Vásquez Garzón, V. R. & Villa-Treviño, S. Co-expression of Ezrin-CLIC5-Podocalyxin is associated with migration and invasiveness in hepatocellular carcinoma. *PLoS One* **10,** e0131605 (2015).

303. Berryman, M., Bruno, J., Price, J. & Edwards, J. C. CLIC-5A functions as a chloride channel in vitro and associates with the cortical actin cytoskeleton in vitro and in vivo. *J. Biol. Chem.* **279,** 34794–34801 (2004).

304. Ponnalagu, D., Tafsirul Hussain, A., Gururaja Rao, S. & Singh, H. An Alternative Splice Variant of Chloride Intracellular Channel 5 Protein, (CLIC5B) Regulates Cardiac Mitochondrial Localization and Function of CLIC5. *Biophys. J.* **112,** 325a (2017).

305. Shanks, R. A. *et al.* AKAP350 at the Golgi apparatus. II. Association of AKAP350 with a novel chloride intracellular channel (CLIC) family member. *J. Biol. Chem.* **277,** 40973–80 (2002).

306. Griffon, N., Jeanneteau, F., Prieur, F., Diaz, J. & Sokoloff, P. CLIC6, a member of the intracellular chloride channel family, interacts with dopamine D2-like receptors. *Mol. Brain Res.* **117,** 47–57 (2003).

307. Ashley, R. H. Challenging accepted ion channel biology: p64 and the CLIC family of putative intracellular anion channel proteins (Review). *Mol. Membr. Biol.* **20,** 1–11 (2003).

308. Tulk, B. M., Schlesinger, P. H., Kapadia, S. A. & Edwards, J. C. CLIC-1 functions as a chloride channel when expressed and purified from bacteria. *J. Biol. Chem.* **275,** 26986–26993 (2000).

309. Harrop, S. J. *et al.* Crystal Structure of a Soluble Form of the Intracellular Chloride Ion Channel CLIC1 (NCC27) at 1.4-Å Resolution. *J. Biol. Chem.* **276,** 44993–45000 (2001).

310. Warton, K. *et al.* Recombinant CLIC1 (NCC27) assembles in lipid bilayers via a pH-

dependent two-state process to form chloride ion channels with identical characteristics to those observed in Chinese hamster ovary cells expressing CLIC1. *J. Biol. Chem.* **277,** 26003–11 (2002).

311. Singh, H. & Ashley, R. H. Redox regulation of CLIC1 by cysteine residues associated with the putative channel pore. *Biophys. J.* **90,** 1628–38 (2006).

312. Tulk, B. M., Kapadia, S. & Edwards, J. C. CLIC1 inserts from the aqueous phase into phospholipid membranes, where it functions as an anion channel. *Am. J. Physiol. Physiol.* **282,** C1103–C1112 (2002).

313. Yang, Y. & Sigworth, F. J. Single-channel properties of IKs potassium channels. *J. Gen. Physiol.* **112,** 665–78 (1998).

314. Singh, H. & Ashley, R. H. CLIC4 (p64H1) and its putative transmembrane domain form poorly selective, redox-regulated ion channels. *Mol. Membr. Biol.* **24,** 41–52 (2007).

315. Singh, H., Cousin, M. A. & Ashley, R. H. Functional reconstitution of mammalian 'chloride intracellular channels' CLIC1, CLIC4 and CLIC5 reveals differential regulation by cytoskeletal actin. *FEBS J.* **274,** 6306–6316 (2007).

316. Sasaki, S., Yui, N. & Noda, Y. Actin directly interacts with different membrane channel proteins and influences channel activities: AQP2 as a model. *Biochim. Biophys. Acta - Biomembr.* **1838,** 514–520 (2014).

317. Argenzio, E. & Moolenaar, W. H. Emerging biological roles of Cl ⁻ intracellular channel proteins. *J. Cell Sci.* **129,** 4165–4174 (2016).

318. Moorman, J. R. *et al.* Unitary anion currents through phospholemman channel molecules. *Nature* **377,** 737–740 (1995).

319. Dulhunty, A., Gage, P., Curtis, S., Chelvanayagam, G. & Board, P. The glutathione transferase structural family includes a nuclear chloride channel and a ryanodine receptor calcium release channel modulator. *J. Biol. Chem.* **276,** 3319–23 (2001).

320. Cromer, B. A. *et al.* Structure of the Janus Protein Human CLIC2. *J. Mol. Biol.* **374,** 719–731 (2007).

321. Littler, D. R., Brown, L. J., Breit, S. N., Perrakis, A. & Curmi, P. M. G. Structure of human CLIC3 at 2 Å resolution. *Proteins Struct. Funct. Bioinforma.* **78,** NA-NA (2010).

322. Li, Y., Li, D., Zeng, Z. & Wang, D. Trimeric structure of the wild soluble chloride intracellular ion channel CLIC4 observed in crystals. *Biochem. Biophys. Res. Commun.* **343,** 1272–1278 (2006).

323. Board, P. G. *et al.* Identification, characterization, and crystal structure of the Omega class glutathione transferases. *J. Biol. Chem.* **275,** 24798–806 (2000).

324. Tonini, R., Ferroni, A., Valenzuela, S.M., Warton, K., Campbell, T.J., Breit, S.N., Mazzanti, M. Functional characterization of the NCC27 nuclear protein in stable transfected CHO-K1 cells. *FASEB J.* **14,** 1171–1178 (2000).

325. Proutski, I., Karoulias, N. & Ashley, R. . Overexpressed chloride intracellular channel protein CLIC4 (p64H1) is an essential component of novel plasma membrane anion channels. *Biochem. Biophys. Res. Commun.* **297,** 317–322 (2002).

326. Hossain, K. R., Holt, S. A., Le Brun, A. P., Al Khamici, H. & Valenzuela, S. M. X-ray and Neutron Reflectivity Study Shows That CLIC1 Undergoes Cholesterol-Dependent Structural Reorganization in Lipid Monolayers. *Langmuir* **33,** 12497–12509 (2017).

327. Littler, D. R. *et al.* Crystal structure of the soluble form of the redox-regulated chloride ion channel protein CLIC4. *FEBS J.* **272,** 4996–5007 (2005).

328. Schlesinger, P. H., Blair, H. C., Teitelbaum, S. L. & Edwards, J. C. Characterization of the osteoclast ruffled border chloride channel and its role in bone resorption. *J. Biol. Chem.* **272,** 18636–43 (1997).

329. Wegner, B. *et al.* CLIC5A, a component of the ezrin-podocalyxin complex in glomeruli, is a determinant of podocyte integrity. *Am. J. Physiol. Physiol.* **298,** 1492–1503 (2010).

330. Fomenko, D. E. & Gladyshev, V. N. Identity and functions of CxxC-derived motifs. *Biochemistry* **42,** 11214–11225 (2003).

331. Littler, D. R. *et al.* The Intracellular Chloride Ion Channel Protein CLIC1 Undergoes a Redox-controlled Structural Transition. *J. Biol. Chem.* **279,** 9298–9305 (2004).

332. Sies, H. Hydrogen peroxide as a central redox signaling molecule in physiological oxidative stress: Oxidative eustress. *Redox Biol.* **11,** 613–619 (2017).

333. Goodchild, S. C. *et al.* Metamorphic response of the CLIC1 chloride intracellular ion channel protein upon membrane interaction. *Biochemistry* **49,** 5278–5289 (2010).

334. Weerapana, E., Simon, G. M. & Cravatt, B. F. Disparate proteome reactivity profiles of carbon electrophiles. *Nat. Chem. Biol.* **4,** 405–407 (2008).

335. Goodchild, S. C. *et al.* Oxidation promotes insertion of the CLIC1 chloride intracellular channel into the membrane. *Eur. Biophys. J.* **39,** 129–138 (2009).

336. Al Khamici, H., Hossain, K. R., Cornell, B. A. & Valenzuela, S. M. Investigating sterol and redox regulation of the ion channel activity of CLIC1 using tethered bilayer membranes. *Membranes (Basel).* **6,** 1–13 (2016).

337. Huang, W.-J., Zhang, X. & Chen, W.-W. Role of oxidative stress in Alzheimer's disease (Review). *Biomed. Reports* **4,** 519–522 (2016).

338. Milton, R. H. *et al.* CLIC1 function is required for beta-amyloid-induced generation of reactive oxygen species by microglia. *J. Neurosci.* **28,** 11488–11499 (2008).

339. Novarino, G. Involvement of the Intracellular Ion Channel CLIC1 in Microglia-Mediated -Amyloid-Induced Neurotoxicity. *J. Neurosci.* **24,** 5322–5330 (2004).

340. Al Khamici, H. *et al.* Members of the Chloride Intracellular Ion Channel Protein Family Demonstrate Glutaredoxin-Like Enzymatic Activity. *PLoS One* **10,** e115699 (2015).

341. Abais, J. M., Xia, M., Zhang, Y., Boini, K. M. & Li, P.-L. Redox Regulation of NLRP3

Inflammasomes: ROS as Trigger or Effector? *Antioxid. Redox Signal.* **22,** 1111–1129 (2015).

342. Tang, T. *et al.* CLICs-dependent chloride efflux is an essential and proximal upstream event for NLRP3 inflammasome activation. *Nat. Commun.* **8,** 202 (2017).

343. Gasteiger, E. *et al.* ExPASy: The proteomics server for in-depth protein knowledge and analysis. *Nucleic Acids Res.* **31,** 3784–3788 (2003).

344. Fanucchi, S., Adamson, R. J. & Dirr, H. W. Formation of an unfolding intermediate state of soluble chloride intracellular channel protein CLIC1 at acidic pH. *Biochemistry* **47,** 11674–11681 (2008).

345. Stoychev, S. H. *et al.* Structural Dynamics of Soluble Chloride Intracellular Channel Protein CLIC1 Examined by Amide Hydrogen-Deuterium Exchange Mass Spectrometry. *Biochemistry* **48,** 8413–8421 (2009).

346. Achilonu, I., Fanucchi, S., Cross, M., Fernandes, M. & Dirr, H. W. Role of individual histidines in the pH-dependent global stability of human Chloride intracellular channel 1. *Biochemistry* **51,** 995–1004 (2012).

347. Valenzuela, S. M. *et al.* Regulation of the Membrane Insertion and Conductance Activity of the Metamorphic Chloride Intracellular Channel Protein CLIC1 by Cholesterol. *PLoS One* **8,** e56948 (2013).

348. Hossain, K. R., Al Khamici, H., Holt, S. A. & Valenzuela, S. M. Cholesterol Promotes Interaction of the Protein CLIC1 with Phospholipid Monolayers at the Air-Water Interface. *Membranes (Basel).* **6,** (2016).

349. Barrett, P. J. *et al.* The Amyloid Precursor Protein Has a Flexible Transmembrane Domain and Binds Cholesterol. *Science (80-.).* **336,** 1168–1171 (2012).

350. Vishwanathan, S. A. *et al.* Hydrophobic substitutions in the first residue of the CRAC segment of the gp41 protein of HIV. *Biochemistry* **47,** 124–130 (2008).

351. Chen, J. I.-C. *et al.* Proteomic Characterization of Midproliferative and Midsecretory Human Endometrium. *J. Proteome Res.* **8,** 2032–2044 (2009).

352. Shukla, A. *et al.* TGF-β signalling is regulated by Schnurri-2-dependent nuclear translocation of CLIC4 and consequent stabilization of phospho-Smad2 and 3. *Nat. Cell Biol.* **11,** 777–784 (2009).

353. Ponnalagu, D. *et al.* Molecular identity of cardiac mitochondrial chloride intracellular channel proteins. *Mitochondrion* **27,** 6–14 (2016).

354. Mynott, A. V. *et al.* Crystal structure of importin-α bound to a peptide bearing the nuclear localisation signal from chloride intracellular channel protein 4. *FEBS J.* **278,** 1662–1675 (2011).

355. Edwards, J. C. The CLIC1 chloride channel is regulated by the cystic fibrosis transmembrane conductance regulator when expressed in Xenopus oocytes. *J. Membr. Biol.* **213,** 39–46 (2006).

356. Gurski, L.A., Knowles, LM., Basse, P.H., Maranchie, J.K., Watkins, S.C., Pilch, J. Relocation of CLIC1 Promotes Tumor Cell Invasion and Colonization of Fibrin Lisa. *Mol. Cancer Res.* **13,** 273–280 (2015).

357. Argenzio, E. *et al.* CLIC4 regulates cell adhesion and beta-1 integrin trafficking. *J. Cell Sci.* **127,** 5189–5203 (2014).

358. Malik, M. *et al.* Inducible NOS-induced chloride intracellular channel 4 (CLIC4) nuclear translocation regulates macrophage deactivation. *Proc. Natl. Acad. Sci.* **109,** 6130–6135 (2012).

359. Tamir, H., Piscopo, I.Liu, K.P., Adlersberg, M.Nicolaides, Al-Awqati, Q., Nunez, E.A., Gershon, M. D. Secretogogue-induced gating of chloride channels in the secretory vesicles of parafollicular cells. *Endocrinology* **135,** 2045–2057 (1994).

360. Edwards, J. C. & Kapadia, S. Regulation of the bovine kidney microsomal chloride channel p64 by p59fyn, a Src family tyrosine kinase. *J. Biol. Chem.* **275,** 31826–32 (2000).

361. Wagner, S. A. *et al.* Proteomic Analyses Reveal Divergent Ubiquitylation Site Patterns in Murine Tissues. *Mol. Cell. Proteomics* **11,** 1578–1585 (2012).

362. Fang, C. *et al.* Identification of Palmitoylated Transitional Endoplasmic Reticulum ATPase by Proteomic Technique and Pan Antipalmitoylation Antibody. *J. Proteome Res.* **15,** 956–962 (2016).

363. Anfinsen, C. B. Principles that Govern the Folding of Protein Chains. *Science (80-.).* **181,** 223–230 (1973).

364. Goodchild, S. C., Curmi, P. M. G. & Brown, L. J. Structural gymnastics of multifunctional metamorphic proteins. *Biophys. Rev.* **3,** 143 (2011).

365. Murzin, A. G. Metamorphic proteins. *Science (80-.).* **320,** 1725–1726 (2008).

366. Wasserman, H. & Saphire, E. O. More than Meets the Eye: Hidden Structures in the Proteome. *Annu. Rev. Virol.* **3,** 373–386 (2016).

367. Mezei, M. Chameleon sequences in the PDB. *Protein Eng.* **11,** 411–414 (1998).

368. Mallamace, F. *et al.* Energy landscape in protein folding and unfolding. *Proc. Natl. Acad. Sci.* **113,** 3159–3163 (2016).

369. Tyler, R. C., Murray, N. J., Peterson, F. C. & Volkman, B. F. Native-state interconversion of a metamorphic protein requires global unfolding. *Biochemistry* **50,** 7077–9 (2011).

370. Hoffmann, J., Wrabl, J. O. & Hilser, V. J. The role of negative selection in protein evolution revealed through the energetics of the native state ensemble. *Proteins Struct. Funct. Bioinforma.* **84,** 435–447 (2016).

371. Tanaka, K., Caaveiro, J. M. M. & Tsumoto, K. Bidirectional Transformation of a Metamorphic Protein between the Water-Soluble and Transmembrane Native States. *Biochemistry* **54,** 6863–6866 (2015).

372. Burmann, B. M. *et al.* An α Helix to β Barrel Domain Switch Transforms the Transcription Factor RfaH into a Translation Factor. *Cell* **150,** 291–303 (2012).

373. Landick, R. The regulatory roles and mechanism of transcriptional pausing. *Biochem. Soc. Trans.* **34,** 1062–1066 (2006).

374. Kuloğlu, E. S., McCaslin, D. R., Markley, J. L. & Volkman, B. F. Structural rearrangement of human lymphotactin, a C chemokine, under physiological solution conditions. *J. Biol. Chem.* **277,** 17863–70 (2002).

375. Fox, J. C. *et al.* Engineering Metamorphic Chemokine Lymphotactin/XCL1 into the GAG-Binding, HIV-Inhibitory Dimer Conformation. *ACS Chem. Biol.* **10,** 2580–2588 (2015).

376. Kosol, S., Contreras-Martos, S., Cedeño, C. & Tompa, P. Structural Characterization of Intrinsically Disordered Proteins by NMR Spectroscopy. *Molecules* **18,** 10802–10828 (2013).

377. Dyson, H. J. Expanding the proteome: disordered and alternatively-folded proteins. *Q. Rev. Biophys.* **44,** 467–518 (2012).

378. Andreeva, A., Howorth, D., Chothia, C., Kulesha, E. & Murzin, A. G. SCOP2 prototype: A new approach to protein structure mining. *Nucleic Acids Res.* **42,** D310-4 (2014).

379. Dai, Z., Tonelli, M. & Markley, J. L. Metamorphic protein IscU changes conformation by cis - Trans isomerizations of two peptidyl-prolyl peptide bonds. *Biochemistry* **51,** 9595–9602 (2012).

380. Nikolova, P. V *et al.* Semirational design of active tumor suppressor p53 DNA binding domain with enhanced stability. *Proc. Natl. Acad. Sci. U. S. A.* **95,** 14675–80 (1998).

381. Tuinstra, R. L. *et al.* Interconversion between two unrelated protein folds in the lymphotactin native state. *Proc. Natl. Acad. Sci.* **105,** 5057–5062 (2008).

382. Pirovano, W. & Heringa, J. Protein secondary structure prediction. *Methods in Molecular Biology* **609,** 327–348 (2010).

383. Gagnon, L. H. *et al.* The Chloride Intracellular Channel Protein CLIC5 Is Expressed at High Levels in Hair Cell Stereocilia and Is Essential for Normal Inner Ear Function. *J. Neurosci.* **26,** 10188–10198 (2006).

384. Pierchala, B. A., Mũoz, M. R. & Tsui, C. C. Proteomic analysis of the slit diaphragm complex: CLIC5 is a protein critical for podocyte morphology and function. *Kidney Int.* **78,** 868–882 (2010).

385. Gagnon, L. H. *et al.* The chloride intracellular channel protein CLIC5 is expressed at high levels in hair cell stereocilia and is essential for normal inner ear function. *J. Neurosci.* **26,** 10188–98 (2006).

386. Seco, C. Z. *et al.* Progressive hearing loss and vestibular dysfunction caused by a homozygous nonsense mutation in CLIC5. *Eur. J. Hum. Genet.* **23,** 189–194 (2015).

387. Velculescu, V.E., Zhang, L., Vogelstein, B., Kinzler, K. W. Serial analysis of gene expression. *Science (80-.).* **270,** 484–487 (1995).

388. Nyström, J., Fierlbeck, W., Granqvist, A., Kulak, S. C. & Ballermann, B. J. A human glomerular SAGE transcriptome database. *BMC Nephrol.* **10,** 13 (2009).

389. Fan, J. *et al.* The klotho-related protein KLPH (lctl) has preferred expression in lens and is essential for expression of clic5 and normal lens suture formation. *Exp. Eye Res.* **169,** 111–121 (2018).

390. Jiang, L. *et al.* CLIC proteins, ezrin, radixin, moesin and the coupling of membranes to the actin cytoskeleton: A smoking gun? *Biochim. Biophys. Acta - Biomembr.* **1838,** 643–657 (2014).

391. Ng, T. *et al.* Ezrin is a downstream effector of trafficking PKC-integrin complexes involved in the control of cell motility. *EMBO J.* **20,** 2723–2741 (2001).

392. Salles, F.T., Andrade, LR., Tanda, S., Grati, M., Plona, K.L., Gagnon, L.H., Johnson, K.R., Kachar, B., B. M. A. CLIC5 Stabilizes Membrane-Actin Filament Linkages at the Base of Hair Cell Stereocilia in a Molecular Complex with Radixin, Taperin, and Myosin VI. *Cytoskeleton* **71,** 61–78 (2014).

393. Tavasoli, M. *et al.* Both CLIC4 and CLIC5A activate ERM proteins in glomerular endothelium. *Am. J. Physiol. Physiol.* **311,** F945–F957 (2016).

394. Chuang, J.-Z., Chou, S.-Y. & Sung, C.-H. Chloride Intracellular Channel 4 Is Critical for the Epithelial Morphogenesis of RPE Cells and Retinal Attachment. *Mol. Biol. Cell* **21,** 3017–3028 (2010).

395. Ichimura, K., Kurihara, H. & Sakai, T. Actin Filament Organization of Foot Processes in Rat Podocytes. *J. Histochem. Cytochem.* **51,** 1589–1600 (2003).

396. Tavasoli, M. *et al.* The chloride intracellular channel 5A stimulates podocyte Rac1, protecting against hypertension-induced glomerular injury. *Kidney Int.* **89,** 833–847 (2016).

397. Tao, H. *et al.* Cyclic AMP prevents decrease of phosphorylated ezrin/radixin/moesin and chloride intracellular channel 5 expressions in injured podocytes. *Clin. Exp. Nephrol.* **19,** 1000–1006 (2015).

398. Andley, U. P., Tycksen, E., McGlasson-Naumann, B. N. & Hamilton, P. D. Probing the changes in gene expression due to α-crystallin mutations in mouse models of hereditary human cataract. *PLoS One* **13,** e0190817 (2018).

399. Jensen, F. & Girardi, A. Infection of human and simian tissue cultures with Rous sarcoma virus. *Proc. ...* **52,** 53–59 (1964).

400. Gluzman, Y. SV40-transformed simian cells support the replication of early SV40 mutants. *Cell* **23,** 175–82 (1981).

401. Hiller, Y., Gershoni, J. M., Bayer, E. A. & Wilchek, M. Biotin binding to avidin. Oligosaccharide side chain not required for ligand association. *Biochem. J.* **248,** 167–71 (1987).

402. Nguyen, M., Millar, D. G., Yong, V. W., Korsmeyer, S. J. & Shore, G. C. Targeting of Bcl-2 to the mitochondrial outer membrane by a COOH-terminal signal anchor sequence. *J. Biol. Chem.* **268,** 25265–8 (1993).

403. Nishikawa, M., Nojima, S., Akiyama, T., Sankawa, U. & Inoue, K. Interaction of digitonin and its analogs with membrane cholesterol. *J. Biochem.* **96,** 1231–1239 (1984).

404. Schulz, I. Permeabilizing cells: Some methods and applications for the study of intracellular processes. *Methods Enzymol.* **192,** 280–300 (1990).

405. Ramsby, M. & Makowski, G. Differential detergent fractionation of eukaryotic cells. *Cold Spring Harb. Protoc.* **2011,** prot5592 (2011).

406. Holden, P. & Horton, W. A. Crude subcellular fractionation of cultured mammalian cell lines. *BMC Res. Notes* **2,** 243 (2009).

407. Mooney, R. A. Use of digitonin-permeabilized adipocytes for cAMP studies. *Methods Enzymol.* **159,** 193–202 (1988).

408. Kato, Y. *et al.* Bioactive marine metabolites. Part 16. Calyculin A. A novel antitumor metabolite from the marine sponge Discodermia calyx. *J. Am. Chem. Soc.* **108,** 2780–2781 (1986).

409. Ishihara, H. *et al.* Calyculin A and okadaic acid: inhibitors of protein phosphatase activity. *Biochem. Biophys. Res. Commun.* **159,** 871–7 (1989).

410. Tamaoki, T. *et al.* Staurosporine, a potent inhibitor of phospholipidCa++dependent protein kinase. *Biochem. Biophys. Res. Commun.* **135,** 397–402 (1986).

411. Tamaoki, T. Use and specificity of staurosporine, UCN-01, and calphostin C as protein kinase inhibitors. *Methods in Enzymology* **201,** 340–347 (1991).

412. Chijiwa, T. *et al.* Inhibition of forskolin-induced neurite outgrowth and protein phosphorylation by a newly synthesized selective inhibitor of cyclic AMP-dependent protein kinase, N-[2-(p-bromocinnamylamino)ethyl]-5-isoquinolinesulfonamide (H-89), of PC12D pheochromocytoma . *J. Biol. Chem.* **265,** 5267–5272 (1990).

413. Deacon, S. W. *et al.* An Isoform-Selective, Small-Molecule Inhibitor Targets the Autoregulatory Mechanism of p21-Activated Kinase. *Chem. Biol.* **15,** 322–331 (2008).

414. Laemmli, U. K. Cleavage of structural proteins during the assembly of the head of bacteriophage T4. *Nature* **227,** 680–685 (1970).

415. Rueden, C. T. *et al.* ImageJ2: ImageJ for the next generation of scientific image data. *BMC Bioinformatics* **18,** 529 (2017).

416. Studier, F. W. & Moffatt, B. A. Use of bacteriophage T7 RNA polymerase to direct selective high-level expression of cloned genes. *J. Mol. Biol.* **189,** 113–130 (1986).

417. Hanahan, D. Studies on transformation of Escherichia coli with plasmids. *J. Mol. Biol.* **166,** 557–580 (1983).

418. Blom, N., Gammeltoft, S. & Brunak, S. Sequence and structure-based prediction of eukaryotic protein phosphorylation sites. *J. Mol. Biol.* **294,** 1351–1362 (1999).

419. Blom, N., Sicheritz-Pontén, T., Gupta, R., Gammeltoft, S. & Brunak, S. Prediction of post-translational glycosylation and phosphorylation of proteins from the amino acid sequence. *Proteomics* **4,** 1633–1649 (2004).

420. Goujon, M. *et al.* A new bioinformatics analysis tools framework at EMBL-EBI. *Nucleic Acids Res.* **38,** W695–W699 (2010).

421. DeLano, W. PyMOL: An open-source molecular graphics tool. *CCP4 Newsl. Protein Crystallogr.* **700,** (2002).

422. Pettersen, E. F. *et al.* UCSF Chimera--A visualization system for exploratory research and analysis. *J. Comput. Chem.* **25,** 1605–1612 (2004).

423. Hornbeck, P. V. *et al.* PhosphoSitePlus, 2014: mutations, PTMs and recalibrations. *Nucleic Acids Res.* **43,** D512–D520 (2015).

424. Littler, D. R. *et al.* The intracellular chloride ion channel protein CLIC1 undergoes a redox-controlled structural transition. *J. Biol. Chem.* **279,** 9298–305 (2004).

425. Wiedemann, C., Bellstedt, P. & Görlach, M. CAPITO—a web server-based analysis and plotting tool for circular dichroism data. *Bioinformatics* **29,** 1750–1757 (2013).

426. Moroni, A. *et al.* The short N-terminus is required for functional expression of the virus-encoded miniature K+ channel Kcv. *FEBS Lett.* **530,** 65–69 (2002).

427. Shapiro, L., Kwong, P. D., Fannon, A. M., Colman, D. R. & Hendrickson, W. A. Considerations on the folding topology and evolutionary origin of cadherin domains. *Proc. Natl. Acad. Sci. U. S. A.* **92,** 6793–6797 (1995).

428. Barber, R. D., Harmer, D. W., Coleman, R. A. & Clark, B. J. GAPDH as a housekeeping gene: analysis of GAPDH mRNA expression in a panel of 72 human tissues. *Physiol. Genomics* **21,** 389–395 (2005).

429. Cronan, J. E. Biotination of proteins in vivo: A post-translational modification to label, purify, and study proteins. *J. Biol. Chem.* **265,** 10327–10333 (1990).

430. McCarthy, F. M., Burgess, S. C., Van Den Berg, B. H. J., Koter, M. D. & Pharr, G. T. Differential detergent fractionation for non-electrophoretic eukaryote cell proteomics. *J. Proteome Res.* **4,** 316–324 (2005).

431. Simons, K. & Toomre, D. Lipid rafts and signal transduction. *Nat. Rev. Mol. Cell Biol.* **1,** 31–39 (2000).

432. Patel, H. H. & Insel, P. A. Lipid Rafts and Caveolae and Their Role in Compartmentation of Redox Signaling. *Antioxid. Redox Signal.* **11,** 1357–1372 (2009).

433. Severs, N. J. Plasma membrane cholesterol in myocardial muscle and capillary endothelial cells. Distribution of filipin-induced deformations in freeze-fracture. *Eur. J. Cell Biol.* **25,** 289–299 (1981).

434. Meder, D., Shevchenko, A., Simons, K. & Füllekrug, J. Gp135/podocalyxin and NHERF-2 participate in the formation of a preapical domain during polarization of MDCK cells. *J. Biol. Chem.* **168,** 303–13 (2005).

435. Yu, C.-Y. *et al.* A bipartite signal regulates the faithful delivery of apical domain marker podocalyxin/Gp135. *Mol. Biol. Cell* **18,** 1710–22 (2007).

436. Ghatak, S., Misra, S. & Toole, B. P. Hyaluronan Constitutively Regulates ErbB2 Phosphorylation and Signaling Complex Formation in Carcinoma Cells. *J. Biol. Chem.* **280,** 8875–8883 (2005).

437. Prag, S. *et al.* Activated Ezrin Promotes Cell Migration through Recruitment of the GEF Dbl to Lipid Rafts and Preferential Downstream Activation of Cdc42. *Mol. Biol. Cell* **18,** 2935–2948 (2007).

438. del Pozo, M. A. *et al.* Integrins Regulate Rac Targeting by Internalization of Membrane Domains. *Science (80-.).* **303,** 839–842 (2004).

439. Rüegg, U. T. & Gillian, B. Staurosporine, K-252 and UCN-01: potent but nonspecific inhibitors of protein kinases. *Trends Pharmacol. Sci.* **10,** 218–220 (1989).

440. Meggio, F. *et al.* Different Susceptibility of Protein Kinases to Staurosporine Inhibition: Kinetic Studies and Molecular Bases for the Resistance of Protein Kinase CK2. *Eur. J. Biochem.* **234,** 317–322 (1995).

441. Sauvanet, C., Wayt, J., Pelaseyed, T. & Bretscher, A. Structure, Regulation, and Functional Diversity of Microvilli on the Apical Domain of Epithelial Cells. *Annu. Rev. Cell Dev. Biol.* **31,** 593–621 (2015).

442. Vlastaridis, P. *et al.* Estimating the total number of phosphoproteins and phosphorylation sites in eukaryotic proteomes. *Gigascience* **6,** 1–11 (2017).

443. Di Meo, S., Reed, T. T., Venditti, P. & Victor, V. M. Role of ROS and RNS Sources in Physiological and Pathological Conditions. *Oxidative Medicine and Cellular Longevity* **2016,** 1–44 (2016).

444. Schieber, M. & Chandel, N. S. ROS function in redox signaling and oxidative stress. *Current Biology* **24,** R453-62 (2014).

445. Zorov, D. B., Juhaszova, M. & Sollott, S. J. Mitochondrial Reactive Oxygen Species (ROS) and ROS-Induced ROS Release. *Physiol. Rev.* **94,** 909–950 (2014).

446. Antunes, F. & Cadenas, E. Estimation of H2O2 gradients across biomembranes. *FEBS Lett.* **475,** 121–126 (2000).

447. Huang, B. K. & Sikes, H. D. Quantifying intracellular hydrogen peroxide perturbations in terms of concentration. *Redox Biol.* **2,** 955–962 (2014).

448. Rodal, S. K. *et al.* Extraction of Cholesterol with Methyl-beta -Cyclodextrin Perturbs Formation of Clathrin-coated Endocytic Vesicles. *Mol. Biol. Cell* **10,** 961–974 (1999).

449. Hunter, T. Tyrosine phosphorylation: thirty years and counting. *Current Opinion in Cell Biology* **21,** 140–146 (2009).

450. Bradford, E. M. *et al.* CLIC5 mutant mice are resistant to diet-induced obesity and exhibit gastric hemorrhaging and increased susceptibility to torpor. *Am. J. Physiol. Regul. Integr. Comp. Physiol.* **298,** R1531-42 (2010).

451. Norman, J. & Zanivan, S. Chloride intracellular channel 3: A secreted pro-invasive oxidoreductase. *Cell Cycle* **16,** 1993–1994 (2017).

Appendix

PDB ID Index

PDB ID	X-ray structure
1PTR	PKCδC1 in a complex with phorbol-13-acetate
1OKC	Mitochondrial ADP/ATP translocase
1E54	Omp32 complexed with a periplasmic peptide
7AHL	α-hemolysin from *Staphylococcus aureus*
1K0M	Human CLIC1
2R5G	Human CLIC2
3KJY	Human CLIC3
2D2Z	Human CLIC4
1YYV	*Yp*SspA from *Yersinia pestis*
2YV7	*Dm*CLIC from *Drosophila melanogaster*
2YV9	*Ce*EXC4 from *Caenorhabditis elegans*
1RK4	Human CLIC1, oxidized with 2 mM H_2O_2
3FY7	Human CLIC3, oxidized with 2 mM H_2O_2